



**HAL**  
open science

# Thermophysical analysis and engineering solutions towards cold chain sustainability

Kostadin Fikiin

► **To cite this version:**

Kostadin Fikiin. Thermophysical analysis and engineering solutions towards cold chain sustainability. Other. Nantes Université, 2023. English. NNT : 2023NANU4055 . tel-04632416

**HAL Id: tel-04632416**

**<https://theses.hal.science/tel-04632416>**

Submitted on 2 Jul 2024

**HAL** is a multi-disciplinary open access archive for the deposit and dissemination of scientific research documents, whether they are published or not. The documents may come from teaching and research institutions in France or abroad, or from public or private research centers.

L'archive ouverte pluridisciplinaire **HAL**, est destinée au dépôt et à la diffusion de documents scientifiques de niveau recherche, publiés ou non, émanant des établissements d'enseignement et de recherche français ou étrangers, des laboratoires publics ou privés.

# THESE DE DOCTORAT

NANTES UNIVERSITE

ECOLE DOCTORALE N° 602

*Sciences de l'Ingénierie et des Systèmes*

*Spécialité : Génie des Procédés et Bioprocédés*

Par

**Kostadin FIKIIN**

**Analyse thermophysique et solutions d'ingénierie vers la durabilité de la chaîne du froid**

**Thermophysical analysis and engineering solutions towards cold chain sustainability**

Thèse présentée et soutenue à ONIRIS, le 10 octobre 2023

Unité de recherche : GEPEA – UMR CNRS 6144

## **Rapporteurs avant soutenance :**

Laurence FOURNAISON, Directrice de Recherche, INRAE – Unité FRISE, 92 Anthony

Brice TREMEAC, Professeur au CNAM Paris, Directeur du Lafset, 75 Paris

## **Composition du Jury :**

Président : Brice TREMEAC, Professeur au CNAM Paris

Examineurs : Pascal LE BIDEAU, Maître de Conférences, Université de Bretagne Sud, Lorient

Jack LEGRAND, Professeur Emérite, Université de Nantes, UMR GEPEA Nantes

Corinne MIRAL, Vice-présidente déléguée aux affaires doctorales, Nantes Université

Dir. de thèse : Alain LE-BAIL, Professeur ONIRIS – UMR GEPEA, 6144 Nantes

## **Invités :**

Mathieu NOUHIN, Directeur des Produits et du management des applications, GEA – Nantes

## **ACKNOWLEDGEMENT**

The present thesis, within the mechanism of *Validation of Acquired Experience* (VAE), appears at a mature stage of my professional career, thereby covering research results from the last few decades. For this reason, I feel obliged to acknowledge many people, whose names cannot all be mentioned. First and foremost, I am grateful to my late parents, who instilled in me a taste and drive for scientific inquiry. Furthermore, I express my sincere gratitude to my professors and colleagues of the Technical University of Sofia and the Bulgarian Academy of Sciences, with whom I have had the good fortune to interact. It has been a unique chance and honour for me to collaborate closely with top academics and outstanding professionals around the globe, as part of renowned international organisations, scientific networks and many joint R&D projects and initiatives. I am deeply indebted to my dedicated thesis director and the experts from ONIRIS – Nantes, who encouraged and persuaded me to participate in this PhD procedure. Last but not least, I am thankful to the Academic Council of the Nantes University for their confidence, as well as to both highly helpful coaches from the doctoral school, who graciously guided me through this thrilling VAE exercise.

Kostadin FIKIIN

## TABLE OF CONTENTS

*(Click on the heading to locate the content)*

I. Introduction .....	2
I.1 Impact of artificial cold on human life and well-being .....	2
I.2 Refrigeration and global sustainability .....	4
I.3 Knowledge-based cold chain as a sustainability enabler .....	5
I.4 Existing cold-chain challenges and objectives of present VAE doctorate .....	10
II. Research chapters .....	15
II.1 Unsteady phase-change heat transfer in moisture-containing systems .....	15
II.2 Enthalpy and Kirchhoff transform method for food refrigeration heat transfer: finite-difference formulation .....	27
II.3 Enthalpy and Kirchhoff transform method for food refrigeration heat transfer: finite-element formulation .....	39
II.4 Predicting thermophysical properties and enthalpy of chilled and frozen foods .....	56
II.5 Immersion chilling and freezing by hydrofluidisation and ice slurries .....	65
II.6 Renewable refrigeration and smarter energy use for a sustainable cold chain .....	91
III. Summary of results and conclusion .....	146
III.1 Contributing developments .....	146
III.2 Technology outlook and research trends .....	149
Annex I – List of publications underlying the VAE thesis .....	153



## I. INTRODUCTION

### I.1 Impact of artificial cold on human life and well-being

Although heat and cold are of the same physical nature, they have played different roles in the history of human civilisation. Prometheus, the mythological hero who bestowed the divine fire of Olympus to mankind, is glorified in immortal works of art. On the contrary, to date the pioneers who created artificial cold and gave it to humanity have never been praised in a similar way as a token of gratitude (Fikiin, 2018).

For non-specialists, artificial cooling (called also refrigeration) is commonly associated with household refrigerators, refrigerated display cabinets in supermarkets, ice rinks or snow-making systems. However, such applications constitute just the small visible fragment of the refrigeration business taking part in countless sectors of the worldwide economy, ranging from food industry to air conditioning and playing a paramount role for healthcare, energy and the environment (Fikiin, 2017).

Today, refrigeration is a mega-sector of crosscutting nature (Table 1.1), which comprises: cold chain for refrigerated processing, storage, transport, distribution, retail and household handling of chilled and frozen food commodities, vaccines, medicines and pharmaceuticals; space cooling and air conditioning; blood and tissue banks; gene banks; keeping in-vitro materials and embryos; cryosurgery; cryotherapy; cold spray anaesthetics; cooling of medical diagnostic equipment; liquefaction and separation of gases (including liquid hydrogen for H<sub>2</sub>-based energy generation and LNG businesses); superconductivity; ice rinks, artificial ski runs, bobsleigh, luge and skeleton tracks, snowmaking machines; ice generators; cryogenics for powerful particle accelerators and thermonuclear reactors; cryogenic energy storage; cryorecycling; process cooling in brewery, chemical and metallurgical industries; cooling of electronic equipment and data centres, etc. (Fikiin & Coulomb, 2021).

A recent survey of the International Institute of Refrigeration (Dupont *et al.*, 2019; Fikiin, 2017) has revealed a rather impressive number of refrigerating systems currently in operation around the world. For instance, the domestic refrigerators and freezers exceed 2 billion; retail refrigeration

**Table 1.1:** Paramount role of refrigeration: facts and figures.

<input checked="" type="checkbox"/>	5+ billion refrigeration, air-conditioning and heat pump systems are operated worldwide.
<input checked="" type="checkbox"/>	Refrigeration spends 20% of the global electricity consumption, or 25-30% when heat pumps are included.
<input checked="" type="checkbox"/>	19+ new refrigerating appliances to be sold every second in the next 30 years.
<input checked="" type="checkbox"/>	Global annual sales of refrigeration, air-conditioning and heat-pump equipment reaches EUR 450 billion by 2030.
<input checked="" type="checkbox"/>	Refrigeration demands of the European building sector is expected to increase by 70% until 2030.
<input checked="" type="checkbox"/>	UK's Royal Society named refrigeration most significant invention in the history of food and drink.
<input checked="" type="checkbox"/>	Sociological polls always place the household fridge on the very top of the rankings for domestic appliances the today's people could not live without.
<input checked="" type="checkbox"/>	Nearly 50% of all food need refrigeration but less than 25% are effectively refrigerated.
<input checked="" type="checkbox"/>	All refrigerated foodstuffs around the world cost over EUR 3 trillion.
<input checked="" type="checkbox"/>	Up to 70% of food produced in EU27+UK is further chilled or frozen.
<input checked="" type="checkbox"/>	600+ million tonnes of food a year is lost between harvest and market for lacking cold chain.
<input checked="" type="checkbox"/>	Refrigeration-aided prevention of food losses and wastes could feed up to 950 million people.
<input checked="" type="checkbox"/>	40% of the world's vaccines spoil because of cold-chain absence or failures.
<input checked="" type="checkbox"/>	About 50% of a data centre's energy demand is to meet the cooling load.
<input checked="" type="checkbox"/>	Over 1.1 billion of people worldwide have no access to refrigeration.
<input checked="" type="checkbox"/>	Climate change is tending to cause 260,000 annual deaths from heath waves by 2050.
<input checked="" type="checkbox"/>	Carbon footprint of refrigeration accounts for 4.2 Gt CO <sub>2</sub> eq, or about 8% of global GHG emissions, against only 2% of the aviation.
<input checked="" type="checkbox"/>	Global energy for refrigeration is expected to exceed that for heating by 2050-2060.
<input checked="" type="checkbox"/>	Refrigeration systems and heat pumps are highly integrative of renewable energy.

systems (condensing units, stand-alone equipment and centralised systems) are over 120 million; while the worldwide refrigerated transport consists of over 5 million vehicles (vans, trucks, semi-trailers or trailers) and 1.2 million containers. Air conditioning systems of different types and capacities amount to over 1.6 billion, along with 1 billion mobile air-conditioning units on vehicles. Residential, commercial and industrial heat pumps (including reversible air conditioners) exceed 220 million, while the medical applications comprise, for example, more than 50,000 magnetic resonance imaging scanners. The global Liquefied Natural Gas (LNG) sector employs at least 126 LNG receiving and regasification terminals, along with an LNG tanker fleet of 525 vessels. Simultaneously, the refrigeration equipment for leisure and sports includes over 17,000 ice rinks worldwide. Refrigeration and cryogenic technologies play a crucial role for testing fundamental physical theories by using powerful particle accelerators, thermonuclear reactors, etc. Thus, the global annual sales of refrigeration, air-conditioning and heat-pump equipment appears to be roughly USD 500 billion or over EUR 450 billion.

The UK's Royal Society named refrigeration '*most significant invention in the history of food and drink*'. Sociological polls regularly place the household fridge on the very top of the rankings for domestic appliances the contemporary consumers could not live without (Fikiin, 2019).

## **1.2 Refrigeration and global sustainability**

The refrigeration sector (including air conditioning) accounts for about 20% of the worldwide electricity consumption, or 25-30% when heat pumps are taken into account (Fikiin & Coulomb, 2021, 2022). Thus, refrigeration determines to a large extent the sustainability of the global economy. The sector creates jobs for almost 15 million employees around the world (Dupont *et al.*, 2019). Some 37% of the global warming impact of refrigeration result from direct leaks of fluorocarbon refrigerants, while 63% are caused by indirect emissions due to the use of electricity generated by fossil fuels (Morlet *et al.*, 2017; Dupont *et al.*, 2019). Environmentally friendly natural refrigerants are increasingly employed, which also offer a means to capture and utilise industrially generated CO<sub>2</sub> as a refrigerant or to liquefy it for long-term storage (e.g., underground or underwater). Refrigeration and heat pump systems are easily prone to enhancing their environmental friendliness by integrating renewable energy sources (Fikiin, 2017).

Actually, the carbon footprint of refrigeration (4.2 Gt CO<sub>2</sub> eq.) represents about 8% of the global annual GHG emissions (Morlet *et al.*, 2017; Fikiin & Coulomb, 2021), thus exceeding four times the emission percentage coming from the aviation, as a comparative example. More specifically, the carbon footprint of food cold chains around the world amounts to approx. 1.3 Gt CO<sub>2</sub> eq. per annum (Sarr *et al.*, 2021; Fikiin & Coulomb, 2021).

Predictive studies (Henley, 2015) reveal that, by 2050-2060, the amount of energy used worldwide for cooling should overtake that used for heating (and will even prevail by some 60% by the end of the Century). Data of Eurostat shows that in 2019 about 75% of heating and cooling in Europe are generated from fossil fuels, while only 22% from renewable energy.

Energy diversification and clean transition from fossil-fuel-based to renewable technologies are vital prerequisites, which enable to achieve not only a carbon-neutral, but even a negative-emission economy of the future. Businesses, stakeholders and citizens should all be familiarised with the

energy, environmental and socio-economic impact of the low-temperature industrial technologies in terms of direct and indirect emissions, carbon footprint, environmental and climate change implications. Both cutting-edge and incremental innovations are actively launched around the world to meet the noble ambitions of the Paris Climate Agreement, the Katowice conference, the Kigali amendment to the Montreal Protocol, the UN's Sustainable Development Goals, the European Green Deal, the far-reaching 2030 Target Climate Plan, and REPowerEU (Fikiin & Coulomb, 2021).

In the above context, the UN Secretary-General António Guterres stated: *'We need all countries to develop National Cooling Action Plans to deliver efficient and sustainable cooling and bring essential life-preserving services like vaccines and safe food to all people. We are calling for concrete and enhanced actions from industry'*.

Along with affordable cold for the mass user around the globe, coordinated international actions on energy-efficient, climate-friendly refrigeration could bring substantial benefits to mankind, illustrated by a couple of figures (UNEP & IEA, 2020):

- ❄️ Only the reduced production and use of HFCs (as per the Kigali Agreement) could avoid 0.4 °C of global warming by 2100.
- ❄️ By efficiency measures and excluding harmful refrigerants, cumulative greenhouse emissions of 460 Gt CO<sub>2</sub> eq. could be avoided over the next four decades, equal to 8 years of global emissions at 2018 levels.

Such statistics refer to incremental innovations and routine actions only. Radical innovations might cause a dramatic change.

### **I.3 Knowledge-based cold chain as a sustainability enabler**

Given the indispensability of food for human life, the production of foods and beverages is among the most powerful industries worldwide. For instance, the European food and drink industry is one of the largest manufacturing sectors in Europe, which has an annual turnover of over EUR 1,121 billion, comprises some 294,000 companies, and employs over 4.6 million people across the enlarged EU (mostly in SMEs). The sector covers a market of 447 million consumers throughout the EU27 and enjoys a positive trade balance of EUR 73 billion, thereby consolidating the Europe's

position as the world's number one food exporter. Simultaneously, the EU food supply chain employs 21.5 million people (constituting a share of 11.1 % in the overall EU employment) and has a total turnover of EUR 3.6 trillion (FoodDrink Europe, 2022).

Refrigeration does not have a competitive alternative to maintain the nutritional resources of the planet. To provide safe and wholesome products, the continuous and ubiquitous impact of low temperatures must be ensured throughout the entire cold chain for perishable food commodities from producers to consumers (Figure 1.1). Nearly 50% of the today's global food output consists of

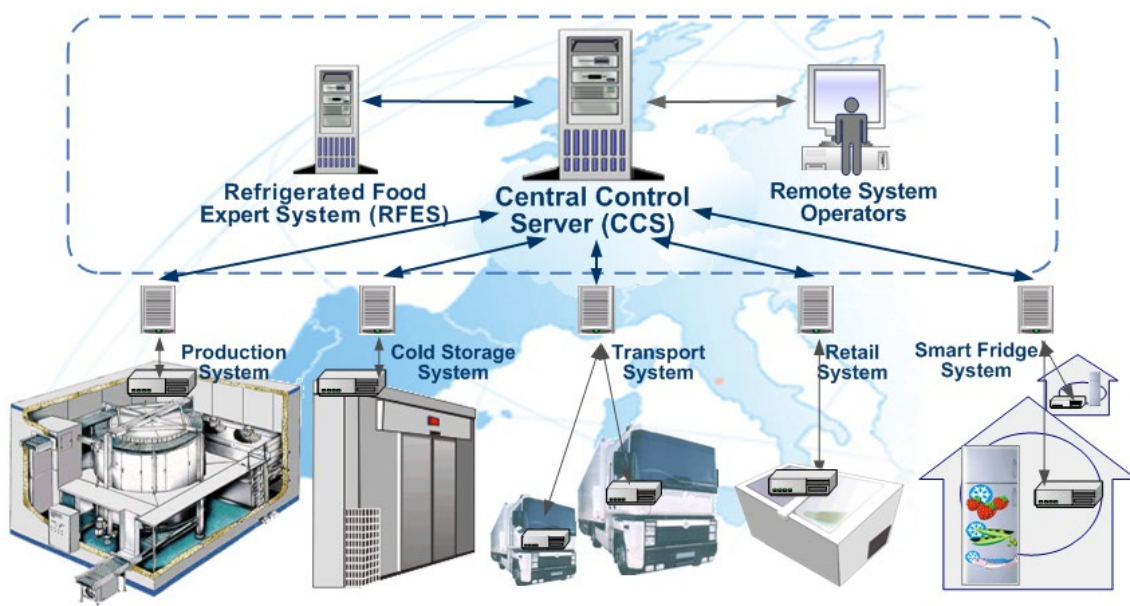


**Figure 1.1.** Continuous and ubiquitous remote monitoring and management of an uninterrupted and well-traceable food cold chain to ensure product quality, energy and environmental sustainability during production, storage and distribution.

perishable products which require refrigeration. For instance, as per the UN's Food and Agriculture Organization (FAO), in present days the world produces about 4 billion metric tons of food per year and, unfortunately, some 1.3 billion tons of them goes to waste. In the 2010s, 46 % of the total global food production required refrigerated processing, but only 47% of the latter amount was effectively preserved in chilled or frozen state (Dupont *et al.*, 2020). Nowadays, chilling is an indispensable element of almost all post-harvest or post-mortem techniques for handling food commodities of plant or animal origin, while freezing has been established as the paramount commercial method for long-term preservation of the natural quality attributes of perishable foods. In terms of money, the overall cost of all refrigerated foodstuffs around the world is estimated to

exceed USD 3 trillion (or 3.5 times the USA military budget). Some 616 million cubic meters in over 50,000 refrigerated food storage warehouses are available over the world. In the beginning of 2010s, the annual global production of various frozen foods was about 50 million tons (plus 20 million tons of ice creams and 30 million tons of fish), with a remarkable growth of 10 % every year (Fikiin, 2017; Dupont *et al.*, 2019). Estimated at USD 219.9 billion in 2018, the global frozen food market is going to reach USD 282.5 billion in 2023 (Dupont *et al.*, 2019), and it is projected to grow to USD 504.41 billion by 2030. FAO estimates that food production should increase globally by 70% to feed an additional 2.3 billion people by 2050, so that refrigeration has a vital role to play in this context (Fikiin, 2017).

In accordance with the universal definition established internationally, cold chain is a ‘*series of actions and equipment applied to maintain a product within a specified low-temperature range from harvest/production to consumption*’ (IIR, 2019; ASHRAE, 2019). An uninterrupted cold chain is a sequence of human activities during refrigerated production, storage and distribution, along with relevant equipment and logistics, which continuously and ubiquitously provide the desired low-temperatures, thereby keeping the safety, quality and shelf-life of perishable or temperature-sensitive products, such as foods and medicines. Proper cold chain management involves many interrelated aspects of organisation, engineering and logistics, requiring a comprehensive science-based approach, as illustrated in Figure 1.2.

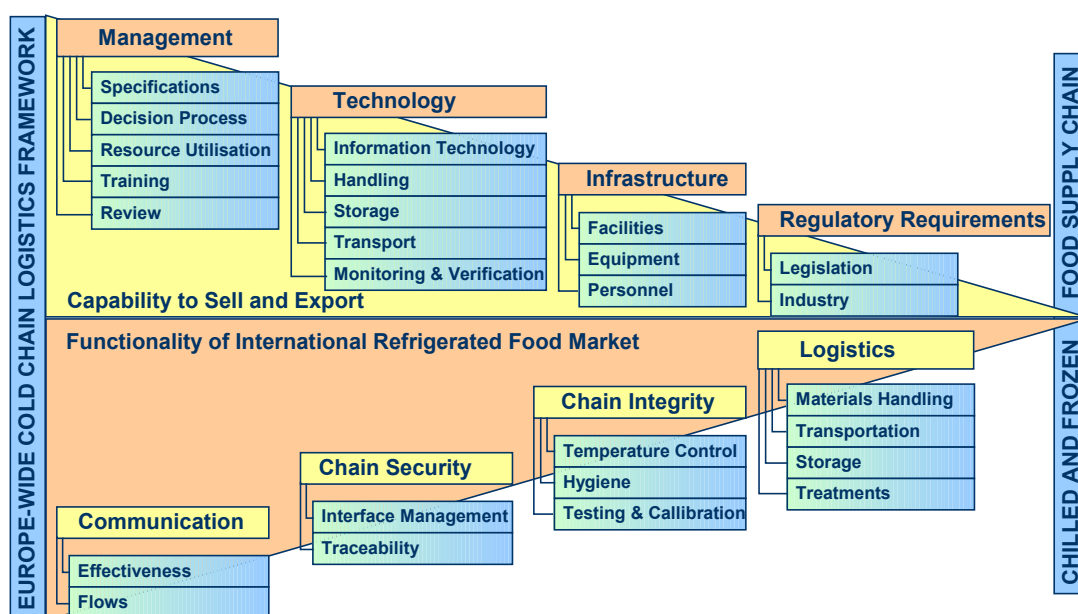


**Figure 1.2.** Schematics of a cold chain logistics framework.



Alongside the temperature, other refrigerating medium parameters affecting the useful shelf life of products under care, most often air humidity, velocity and composition, also need to be monitored and carefully controlled throughout the cold chain. Packaging, handling equipment and logistic systems play an essential role as well. To ensure optimal cold chain conditions, capable of overpowering the natural shelf-life constraints, contemporary achievements of digitalisation, information and communication technologies (involving expert and decision-support systems, artificial intelligence, automatic control and telematics) must adequately be harnessed (Figure 1.3).

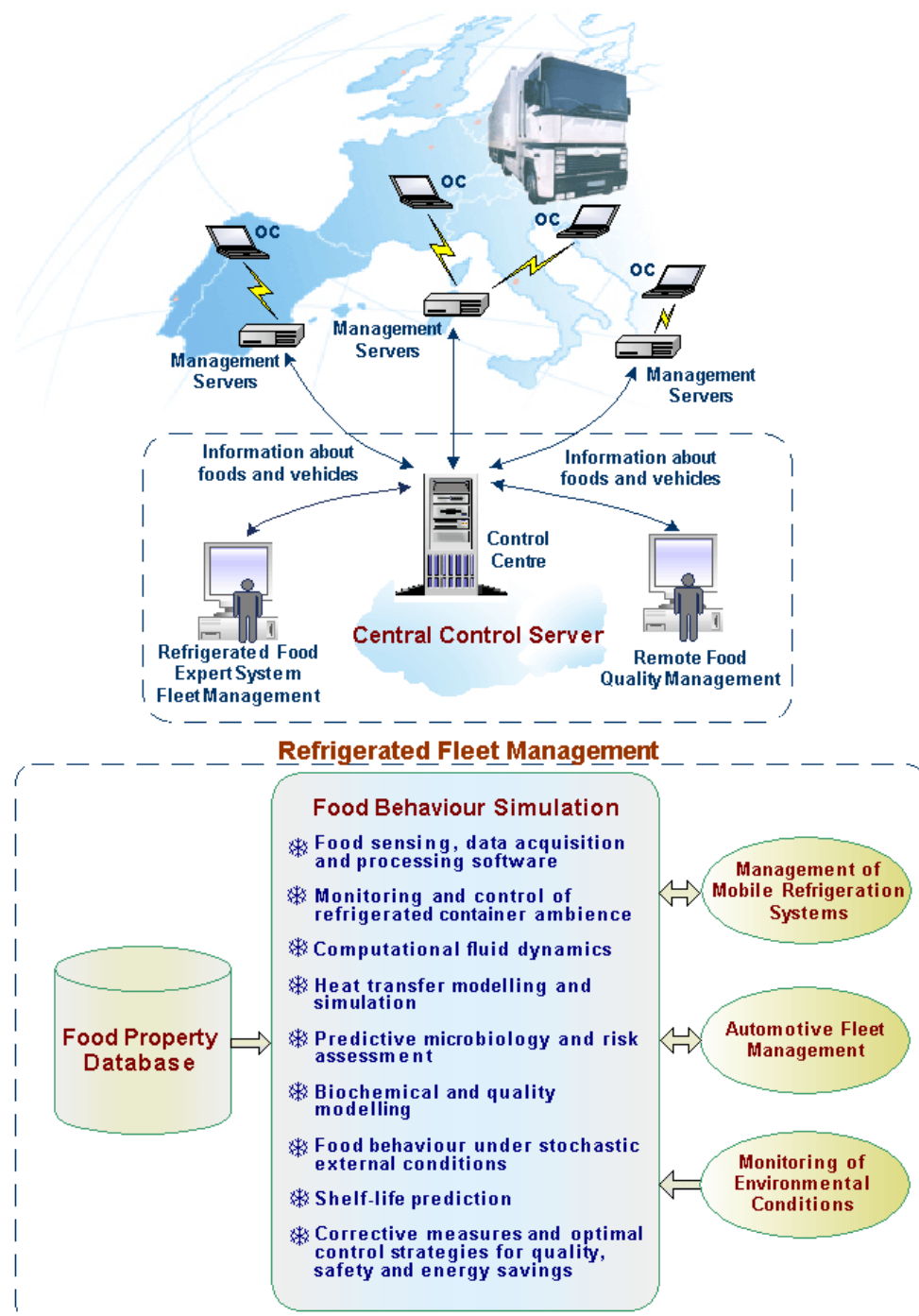


**Figure 1.3.** Architecture of a refrigerated food expert system controlling the transportation stage of cold chain (OC - Onboard Computer).

Unfortunately, the current cold-chain capacities are distributed quite unevenly across countries, and the conventional ones are typically energy intensive and polluting. Around 1/3 of the food produced for human consumption gets lost or wasted, costing the global economy USD 936 billion a year. Lack of effective cold chain results in the loss of 475 million tons, or 13 % of total food production. The latter amount is enough to feed around 950 million people in a planet where 690 million people suffer from malnourishment and 2 billion from food insecurity (Dupont *et al.*, 2020; Sayin & Peters, 2021). Thus, developing a sustainable cold-chain network around the globe is critical for human well-being, economic growth and socioeconomic development. A modelling study of IIR reveals that an improved global cold chain may nearly halve the carbon footprint of the existing cold chain (amounting to approx. 1.3 Gt CO<sub>2</sub> eq. per year), because the emissions saved from reduced food losses remarkably prevails over the increased emissions from cold-chain equipment (Sarr *et al.*, 2021).

Refrigerated warehouses (known also as cold stores) are the major industrial facilities for food preservation, constituting the core component of cold chain. That is why, the UK's Cold Chain Federation has developed a vision on how a modern and sustainable refrigerated warehouse should be arranged and operated, with a time horizon to 2050 (Figure 1.4).

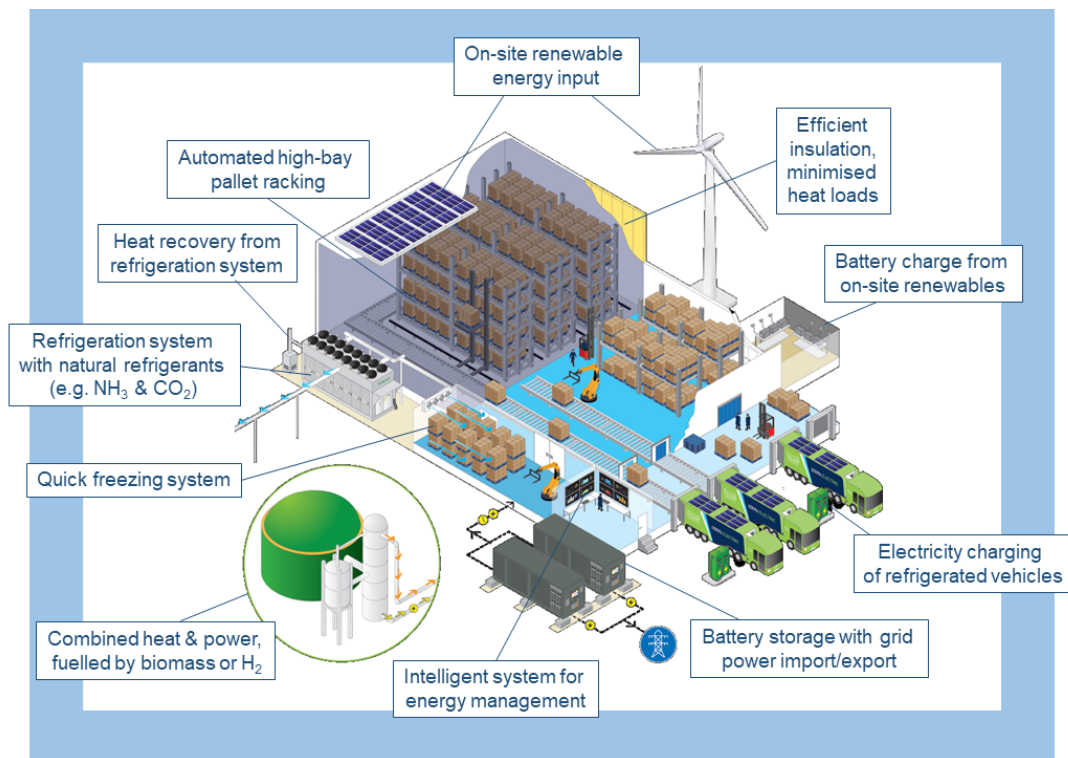


**Figure 1.4.** Efficient design and energy management of a sustainable refrigerated warehouse [Adapted from CCF (2022)].



In particular, in accordance with CCF (2022) the ‘cold store of 2050’ should possess the following features:

- ☑ Substantially improved energy efficiency reducing the power demand from the electrical grid or on-site generators, thereby cutting associated carbon emissions.
- ☑ Additional electrified infrastructure, such as electric chargers for refrigerated vans, trucks and trailers, to replace fossil-fuelled refrigerated transportation.
- ☑ Recovered waste heat from refrigeration equipment and/or integrated Combined Heat and Power (CHP) facilities to be operated synergistically with the district heating or cooling systems of neighbouring buildings.
- ☑ Harnessed potential of refrigerated warehouses as an active player on the energy marketplace through on-site energy production and export, demand management, energy storage, power peak shaving and resulting grid balancing.
- ☑ Eliminated high-GWP refrigerants and use of zero emission alternatives (such as NH<sub>3</sub> and CO<sub>2</sub>).

#### **1.4 Existing cold-chain challenges and objectives of present VAE doctorate**

Providing the security of regional, nation-wide and international food supplies and their extension to new markets and emerging economies around the world pose new **challenges for the cold chain sector** in the first quarter of 21<sup>st</sup> Century, which could briefly be outlined as follows:

- ❄ Cold chain equipment and logistics of many companies and SMEs are still based on low technologies, which suffer from low cooling rates, poor temperature control and resulting detrimental effects on the product throughput and quality. Conventional and novel food refrigeration techniques could substantially be optimised and refined by advanced modelling and experimental tools based on a deep theoretical understanding of underlying phenomena determining the intrinsic quality of chilled and frozen commodities.
- ❄ The manufacture of refrigerated commodities and the chain of their supply insufficiently employ advanced achievements of digitalisation and *hi-tech* branches (e.g., electronics, information and communication technologies, automatics, telematics, etc.). Thus, the sector and related scientific research are still insufficiently attractive for high-skilled experts and young specialists and this gap must be bridged in the best possible way.

- ✿ Although the recent emergence of several innovative food refrigeration technologies attracts the attention of researchers and industrialists, useful innovations are often deemed a high-risk venture and remain unimplemented in the common industrial practice. The EU cold chain should become much more competitive in terms of innovations in front of the dynamic economies of the USA, Far East, South-East Asia, BRICS, etc. For example, the EU is still behind the USA and Japan as regards the consumption of frozen foods per inhabitant and associated cold chain logistics for frozen commodities.
- ✿ The sector is still conservative, highly energy-intensive and does not take enough advantage of renewable energy technologies. Cold chain facilities are still simple energy consumers, although there exist many unused opportunities to interact with the energy market as an active player which integrate synergistically renewables, 'passive' or 'active' modes of energy storage, demand response, power peak shaving, grid balancing, on-site power generation and intelligent energy management. Furthermore, the cold chain sector is obliged to phase out harmful synthetic refrigerants (associated with ozone depletion and global warming) and to ensure exceptional precautions and strictest possible control when handling hazardous highly flammable working substances of natural origin.

This **VAE doctorate** makes a modest contribution to addressing some of the aforementioned challenges by focusing on **the following objectives**:

1. Theoretical and methodological contribution to the general principles for modelling of unsteady-state heat transfer with isothermal and non-isothermal phase change in moisture-containing systems during freezing or thawing.
2. Developing an improved and innovative enthalpy method for numerical solution of highly nonlinear problems of unsteady phase-change heat transfer during cooling and freezing of moisture-containing food materials. Approbation of the method's capabilities and performances when employing FDM- and FEM-based numerical techniques.
3. Elaborating a set of reliable, accurate and versatile analytical equations (with a broad scope of application) to predict thermophysical properties and enthalpy of chilled and frozen food materials.

4. Launching, deploying the thermophysical background and introducing to food engineering a novel method for rapid chilling and freezing of foods by hydrofluidisation using unfreezable liquids or pumpable ice slurries as fluidising agents.
5. Exploring and systematising various opportunities for integration of renewable energy resources of different nature (solar, wind, geothermal, biogas, etc.) in the energy supply of large refrigerated food storage facilities. Investigating intelligent engineering solutions and temperature control strategies for 'passive' thermal energy storage and smarter energy use in refrigerated warehouses.



**Figure 1.5.** Mapping between objectives and research chapters of the present VAE doctorate.

The interrelations between the structural components of this VAE doctorate in terms of objectives and constituting chapters, which follow hereafter, are illustrated in Figure 1.5.

## Acronyms

ASHRAE	American Society of Heating, Refrigerating and Air-conditioning Engineers	GWP	Global Warming Potential
		IEA	International Energy Agency
BRICS	Brazil, Russia, India, China & South Africa	IIR	International Institute of Refrigeration
CCF	Cold Chain Federation	LNG	Liquefied Natural Gas
CHP	Combined Heat and Power	OC	Onboard Computer
EU	European Union	SME	Small or Medium Enterprise
EUR	Euro (European Monetary Unit)	UK	United Kingdom
EU27	All 27 EU Member States	UN	United Nations
FAO	UN Food and Agriculture Organization	UNEP	United Nations Environment Programme
FDM	Finite Difference Method	USA	United State of America
FEM	Finite Element Method	USD	United States Dollar
GHG	Greenhouse Gas	VAE	Validation of Acquired Experience

## References

- ASHRAE (2019). *Terminology*. American Society of Heating, Refrigerating and Air Conditioning Engineers. <https://xp20.ashrae.org/terminology>
- CCF (2022). *Shaping the Cold chain of the Future: The Road to Net Zero Part 4 – Cold Store of 2050*. Cold Chain Federation. <https://lnkd.in/emvKWnqj>
- Dupont J.L., Domanski P., Lebrun P. & Ziegler F. (2019). The role of refrigeration in the global economy. *38<sup>th</sup> Informatory Note on Refrigeration Technologies*. International Institute of Refrigeration, <https://iifir.org/en/fridoc/142028>
- Dupont J.L., El Ahmar A. & Guilpart J. (2020). The role of refrigeration in worldwide nutrition. *6<sup>th</sup> Informatory Note on Refrigeration and Food*, International Institute of Refrigeration, <https://iifir.org/en/fridoc/142029>
- Fikiin K. (2019). Some order in the multiple definitions of refrigeration. *EurActiv.com – European media platform for policymaking*, 27 March 2019, <http://lnkd.in/dzpS6sh>
- Fikiin K. (2018). ‘World Refrigeration Day’ pays respect to the masters of artificial cold. *EurActiv.com – European media platform for policymaking*, 3 September 2018, <http://lnkd.in/dZZBDYr>
- Fikiin K. (2017). Cooling and refrigeration sector: the Cinderella of the EU energy system. *EurActiv.com – European media platform for policymaking*, 16 May 2017, <http://eurac.tv/8hE7>
- Fikiin K. & Coulomb D. (2021). Towards universal definitions of renewable cooling and renewable refrigeration in the context of international energy legislation. *International Journal of Refrigeration*, Vol. 129, pp. v-viii, <https://doi.org/10.1016/j.ijrefrig.2021.08.016>
- Fikiin K. & Coulomb D. (2022). The first of its kind EU legislation on renewable cooling: Status and challenges. *International Journal of Refrigeration*, Vol. 137, pp. 51-52, <https://doi.org/10.1016/j.ijrefrig.2022.02.016>
- FoodDrink Europe (2022). Data & Trends. EU Food and Drink Industry. <https://lnkd.in/dxnm8FWx>

- Henley J. (2015). World set to use more energy for cooling than heating. *The Guardian*, <https://lnkd.in/g2MWgs2>
- IIR (2019). *International Dictionary of Refrigeration*, <http://dictionary.iifiir.org>
- Morlet, V., Coulomb, D. & Dupont, J.-L. (2017). The impact of the refrigeration sector on climate change. *35<sup>th</sup> Informatory Note on Refrigeration Technologies*. International Institute of Refrigeration, <https://iifiir.org/en/fridoc/141135>
- Sarr J., Dupont J.L. & Guilpart J. (2021). *The Carbon Footprint of the Cold Chain. 7<sup>th</sup> Informatory Note on Refrigeration and Food*. International Institute of Refrigeration, <https://iifiir.org/en/fridoc/143457>
- Sayin L. & Peters, T. (2021). *Global Food Cold Chain Status Summary Briefing*. Cool Coalition, United Nations Environment Programme. <https://lnkd.in/dvxAHYtd>
- UNEP & IEA (2020). *Cooling Emissions and Policy Synthesis Report: Benefits of cooling efficiency and the Kigali Amendment*. United Nations Environment Programme & International Energy Agency, <https://lnkd.in/dQUpGAFf>

## **II. RESEARCH CHAPTERS**

### **CHAPTER 1**

**Unsteady phase-change heat transfer  
in moisture-containing systems**

## Chapter 1

is to set the scene by considering rigorously key theoretical principles of the mathematical modelling of unsteady-state heat transfer in moisture-containing systems undergoing isothermal and non-isothermal phase-changes in arbitrarily shaped regions. Thus, it plays a methodological role as regards the sustainability-improving heat transfer studies and engineering solutions reported in the following chapters.

Some considerations regarding the phase transition in real food materials are original and reported for the first time in the scientific literature. Particular attention is paid to the enthalpy methods for solving highly non-linear heat transfer problems by analytical and numerical techniques. A theoretical proof is presented that the classical Stefan problem with isothermal phase change and sharp moving interface appears to be an isolated case of the general enthalpy formulation of a nonlinear moving-boundary scenario formulated for the whole studied domain undergoing gradual phase change within a temperature range.

It is demonstrated how the enthalpy and Kirchhoff transforms permit to handle non-linearities of the governing heat conduction equation by transforming the equivalent specific heat capacity method to smarter formulations involving suitable relationships between enthalpy, temperature, Kirchhoff function and thermal diffusivity. Capabilities advantages and drawback of the resulting solution methodologies are discussed as well.

Since their publication, the results from Chapter 1 have been used by the research community (*click on the logo below to locate the users*):



Obviously, although theoretical, the presented heat transfer analysis facilitated the modelling and simulation of a variety of heat transfer situations of different nature (e.g. mushroom freezing, chilling and freezing of bakery products, freezing times of vegetables, frozen muscle food quality, freezing individual foods, freezing crab species, heat transfer in foods of irregular geometry, etc.). The results presented in this chapter have been used by both English- and Spanish-language researchers worldwide.



ISSN 1018-5593



SCIENCE  
RESEARCH  
DEVELOPMENT

EUROPEAN  
COMMISSION



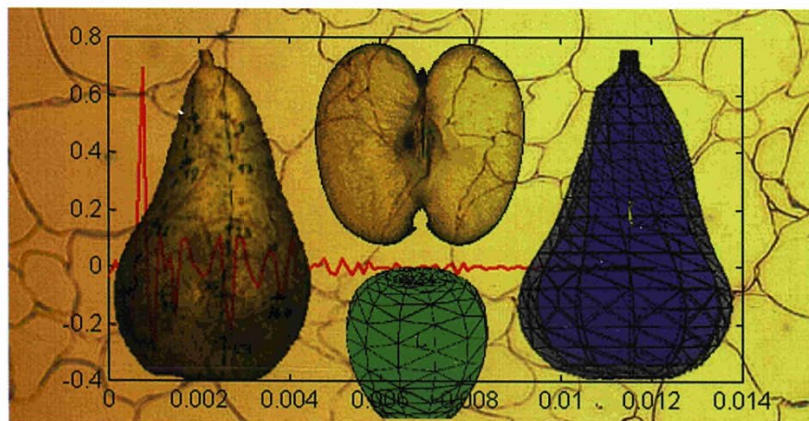
**COST Action 915**

**Consumer-oriented quality improvement of  
fruit and vegetable products**

# Food quality modelling

Edited by

Bart M. Nicolaï and Josse De Baerdemaeker



EUR 18183 EN

Luxembourg: Office for Official Publications of the European Communities, 1998

ISBN 92-828-3309-7

© European Communities, 1998

Reproduction is authorised provided the source is acknowledged.

*Printed in Belgium*



# SOME GENERAL PRINCIPLES IN MODELLING OF UNSTEADY HEAT TRANSFER IN TWO-PHASE MULTICOMPONENT AQUEOUS FOOD SYSTEMS FOR PRODUCT QUALITY IMPROVEMENT

Kostadin A. Fikiin

*Refrigeration Science and Technology Division, Technical University of Sofia, BG*

## ABSTRACT

The present paper considers some general aspects of the mathematical description of heat transfer in food objects of arbitrary configuration with or without internal phase transitions. Special attention is devoted to the analysis of unsteady heat conduction by solving a unified nonlinear moving boundary problem, formulated for the entire studied domain, as a contemporary tool for modelling of conduction phase-change processes. Abilities, advantages and drawbacks of different solution methods (including enthalpy techniques), applied to isothermal or non-isothermal phase changes, are discussed. For isothermal phase changes, a rigorous mathematical proof is presented for the identity between the enthalpy formulation and the classical Stefan problem. Practical recommendations are given for prediction of the unsteady temperature, enthalpy and phase-content fields and of the cooling and freezing (heating and thawing) times of foods in various heat transfer situations. Further promising trends in that area are outlined.

**Keywords:** unsteady-state heat transfer, phase change, foods, chilling, freezing, mathematical modelling.

## 1. INTRODUCTION

Food materials are extraordinary complicated solid capillary-porous or liquid biostructures and can be considered from different points of view simultaneously as solutions, suspensions, emulsions and other physico-colloidal formations where various physiological, biochemical, microbiological, heat and mass transfer processes develop continuously. Multicomponent aqueous foods can be analysed as two-phase and two-component systems of water and dry matter (in the presence of gaseous inclusions as three-phase ones). Below the initial freezing point they represent a dynamic complex of three fractions, continuously changing their quantitative ratios: dry substance, water and ice. Hence, the solid phase includes all dry substances (proteins, fats, carbohydrates, mineral salts, microelements, vitamins, etc.) and ice (if any), while the liquid phase consists of free water (in the form of solution).

Because all postharvest or post-mortem phenomena are highly temperature-dependent, the simulation of unsteady-state temperature distributions in foods is an integral part of the methodologies for modelling of food safety and quality. Moreover, the modelling of the space-time evolution of phase content has a direct value for quality assessment of frozen foods, in which the major water content should be quickly frozen in a fine-grain crystal structure.

Traditionally, the concept of solution of a partial differential equation, such as this of heat conduction, is based on the finding of a continuous function having continuous derivatives up to the order of the equation, which satisfies it at each point of an appropriate region. Since the time of Lagrange whenever discontinuous quantities arise, the studied regions are split into subregions excluding the discontinuities and then classical approaches can be employed. However, the majority of the contemporary computational techniques for solving highly nonlinear phase-change problems involve equivalent-specific-heat or enthalpy formulations and

suppose that a single quasi-linear heat conduction equation governs the thermal behaviour in the whole space-time region of integration, independently of the substance phase state in the different zones [1, 2, 5, 6]. Simultaneously, some basic aspects of these unified approaches have to be theoretically clarified with regard to their validity, limitations and capabilities. That is why, the present paper aims to outline and analyse, in the light of the above features, different mathematical formulations of the unsteady heat transfer in arbitrary-shaped aqueous food objects undergoing isothermal or non-isothermal phase transformations.

## 2. ISOTHERMAL AND NON-ISOTHERMAL PHASE CHANGES IN MOISTURE-CONTAINING SYSTEMS

Let an arbitrary fixed control volume,  $V$ , of a continuous water-containing medium is bounded by the closed surface  $S$  (Figure 1). The energy action of the material, external for  $V$ , includes heat inputs (points of type A) and heat outputs (points B), while sometimes there is no heat transfer across some areas of  $S$  (points C). This defines some distribution of the conductive heat flux vector  $\mathbf{q}$  on  $S$ . The *first principle of thermodynamics* for isobaric processes, applied to  $V$  for a small time interval  $d\tau$ , results directly in the following *energy conservation equation*:

$$\frac{d}{d\tau} \iiint_V \mathcal{H} dv = - \oiint_S \mathbf{q} \cdot \mathbf{n}' ds + \iiint_V \omega dv \quad (1)$$

where  $\mathcal{H}$  is the enthalpy per unit volume,  $\omega$  the volumetric rate of internal heat generation and  $\mathbf{n}'$  the unit vector of the outward normal to  $S$ . The above is valid without limitations, independently of the possible intersection of  $V$  by a sharp phase-change interface. It can be demonstrated that, for an isothermal phase transition, Eq.(1) is equivalent to the usual conservation equations for the frozen and unfrozen regions, as well as for the interface of transition.

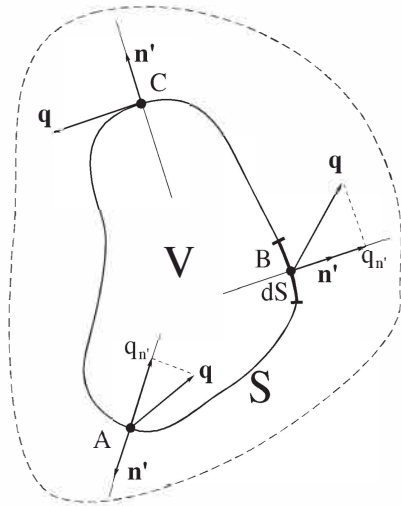


**Figure 1.** Control volume where phase changes are present or absent

In the **absence of sharp isothermal phase change**,  $\mathcal{H}$  and  $\mathbf{q}$  are continuous and smooth (or at least piecewise smooth) in the considered space-time domain. Hence, when there are no any phase transformations (the usually considered case in the literature) or there is a non-

isothermal phase change, it can be written

$$\frac{d}{d\tau} \iiint_V \mathcal{H} dv = \iiint_V \frac{\partial \mathcal{H}}{\partial \tau} dv \quad (2)$$

(for zero convective terms of the substantial derivative). Moreover, the Divergence Theorem of Gauss-Ostrogradskij

$$\oiint_S \mathbf{q} \cdot \mathbf{n}' ds = \iiint_V \operatorname{div} \mathbf{q} dv \quad (3)$$

can also be employed. It is obvious from Eqs (1), (2) and (3) that the following *enthalpy-heat-flux form* of the conservation equation is valid for every internal point of the region considered:

$$\frac{\partial \mathcal{H}}{\partial \tau} + \operatorname{div} \mathbf{q} - \omega = 0 \quad (4)$$

For solids  $c \equiv c_p = (1/\rho) (\partial \mathcal{H} / \partial t)_p \approx c_v = (1/\rho) (\partial U / \partial t)_v$ , and then we obtain the *temperature-heat-flux form* of the above equation:

$$c \rho \frac{\partial t}{\partial \tau} + \operatorname{div} \mathbf{q} - \omega = 0 \quad (5)$$

where  $c_p$  and  $c_v$  (both denoted by  $c$ ) are the mass specific heat capacities of the medium at constant pressure or volume, respectively;  $\rho$  is the substance density and  $t$  the temperature.

M. Planck expressed the *second principle of thermodynamics for heat conduction processes* as follows [4]:

$$\mathbf{q} \cdot \operatorname{grad} t < 0 \quad \text{or} \quad \frac{\pi}{2} < (\widehat{\mathbf{q}, \operatorname{grad} t}) < \frac{3\pi}{2} \quad (6)$$

In anisotropic media the vectors  $\mathbf{q}$  and  $\operatorname{grad} t$  can form an angle different from  $\pi$ , but for isotropic objects they are assumed collinear or  $(\widehat{\mathbf{q}, \operatorname{grad} t}) = \pi$ . Besides, in the general case the heat flux is a nonlinear function:

$$\mathbf{q} = \mathbf{q} \left[ M, \tau, t(M, \tau), \frac{\partial t(M, \tau)}{\partial n} \right] \quad (7)$$

If the considerations are restricted to the Fourier Hypothesis for a linear relationship between  $\mathbf{q}$  and  $\partial t / \partial n$ , i.e.

$$\mathbf{q} = -\lambda [M, \tau, t(M, \tau)] \frac{\partial t(M, \tau)}{\partial n} \cdot \mathbf{n} = -\lambda [M, \tau, t(M, \tau)] \operatorname{grad} t(M, \tau) \quad (8)$$

and simultaneously all thermal properties and  $\omega$  are assumed dependent on  $M$ ,  $\tau$  and the temperature  $t$  (but not on its derivatives), Eqs (5) and (8) will result in the *quasi-linear version of the nonlinear heat-conduction equation*:

$$\begin{aligned} c [M, \tau, t(M, \tau)] \cdot \rho [M, \tau, t(M, \tau)] \frac{\partial t(M, \tau)}{\partial \tau} = \\ = \operatorname{div} \{ \lambda [M, \tau, t(M, \tau)] \operatorname{grad} t(M, \tau) \} + \omega [M, \tau, t(M, \tau)] \end{aligned} \quad (9)$$

In Eqs (7), (8) and (9)  $M \in V$  denotes an arbitrary point with coordinates  $\xi, \eta, \zeta$  in some coordinate system;  $\lambda$  is the thermal conductivity,  $\mathbf{n}$  the unit normal to the isothermal surface in  $M$ , and  $\partial t / \partial n$  the derivative at  $M$  in the direction of  $\mathbf{n}$ . Frequently, in homogeneous media, the thermophysical characteristics and  $\omega$  are only temperature-dependent and hence

$$c [t(M, \tau)] \cdot \rho [t(M, \tau)] \frac{\partial t(M, \tau)}{\partial \tau} = \operatorname{div} \{ \lambda [t(M, \tau)] \operatorname{grad} t(M, \tau) \} + \omega [t(M, \tau)] \quad (10)$$

For constant thermophysical coefficients the energy conservation equation can be rewritten in a *vector form*:

$$\frac{1}{a} \frac{\partial \mathbf{q}}{\partial \tau} = \operatorname{grad} (\operatorname{div} \mathbf{q}) - \operatorname{grad} \omega \quad (11)$$

where  $a = \lambda / (c \cdot \rho)$  is the thermal diffusivity of the medium.

If the heat-flux function, Eq.(7), is specified by the Hypothesis of Vernotte and Cattaneo

$$\mathbf{q} = -\lambda \operatorname{grad} t - \tau_r \frac{\partial \mathbf{q}}{\partial \tau} \quad (12)$$

then, instead of the usual parabolic Eqs (9) and (10), we will obtain (for position-independent  $\tau_r$ ) the *nonlinear hyperbolic equation* describing the so-called “non-Fourier” heat conduction:

$$c \rho \frac{\partial t}{\partial \tau} + \tau_r \frac{\partial}{\partial \tau} \left( c \rho \frac{\partial t}{\partial \tau} \right) = \operatorname{div} (\lambda \operatorname{grad} t) + \omega + \tau_r \frac{\partial \omega}{\partial \tau} \quad (13)$$

where in Eqs (12) and (13)  $\tau_r$  is the time of heat relaxation.

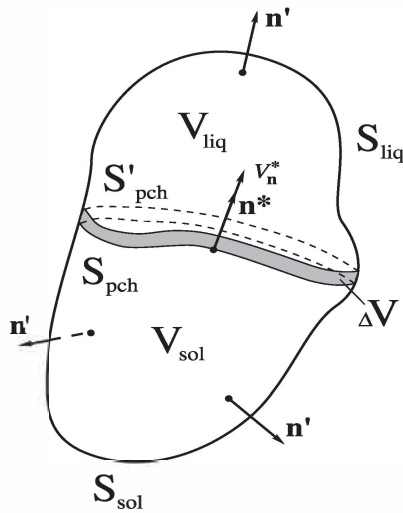


**Figure 2.** Phase-change interface moving in the control volume

In contrast to the non-isothermal phase transition in real food systems behaving as solutions, the **isothermal phase change** is inherent for pure substances. Then the heat transfer mechanism in the unfrozen zone (pure liquid) can be assumed conductive, provided that the liquid phase is highly viscous or incorporated in some suspension or other insoluble structure. For isothermal transition in the control volume,  $V$  (Figure 2), the functions  $\mathcal{H}$  and  $\mathbf{q}$  undergo first-kind (jump-type) discontinuities on the moving phase-change interface  $S_{pch}$ . Therefore, Eqs (2), (3) and (4) [respectively Eqs (5), (9) and (10)], containing undetermined terms of the type  $\partial\mathcal{H}/\partial\tau$  and  $\text{div } \mathbf{q}$ , become inapplicable. Consequently, the control volume is traversed by a *moving singular surface*, for which the energy conservation expression, Eq.(1), acquires a specific form.

According to Eqs (1) and (8) it can be written:

$$\frac{d}{d\tau} \iiint_V \mathcal{H} dv = \oint_S \lambda \text{grad } t \cdot \mathbf{n}' ds + \iiint_V \omega dv \quad (14)$$

At the instant  $\tau$  the phase-change interface,  $S_{pch}$ , subdivides the control volume,  $V$ , to a single-phase solid region,  $V_{sol}$ , and a liquid-phase-containing domain,  $V_{liq}$ . The element surface is also split into two areas  $S_{sol}$  and  $S_{liq}$ . After some small time increment  $\Delta\tau$  the phase-change front occupies a new position  $S'_{pch}$ . Besides,  $V_{sol}$  increases, while  $V_{liq}$  decreases with  $\Delta V$ .

For the instant  $\tau$  we have

$$\iiint_V \mathcal{H} dv = \iiint_{V_{sol}} \mathcal{H}_{sol} dv + \iiint_{V_{liq}} \mathcal{H}_{liq} dv = \iiint_{V_{sol}} \mathcal{H}_{sol} dv + \iiint_{V_{liq} - \Delta V} \mathcal{H}_{liq} dv + \iiint_{\Delta V} \mathcal{H}_{liq} dv \quad (15)$$

and for the instant  $\tau + \Delta\tau$

$$\iiint_V \mathcal{H} dv = \iiint_{V_{sol} + \Delta V} \mathcal{H}_{sol} dv + \iiint_{V_{liq} - \Delta V} \mathcal{H}_{liq} dv = \iiint_{V_{sol}} \mathcal{H}_{sol} dv + \iiint_{\Delta V} \mathcal{H}_{sol} dv + \iiint_{V_{liq} - \Delta V} \mathcal{H}_{liq} dv \quad (16)$$

By deducting Eq.(15) from Eq.(16) and dividing the result by  $\Delta\tau$ , the following expression is obtained when  $\Delta\tau \rightarrow 0$  (and  $V_{liq} - \Delta V \rightarrow V_{liq}$ ):

$$\frac{d}{d\tau} \iiint_V \mathcal{H} dv = \frac{d}{d\tau} \iiint_{V_{sol}} \mathcal{H}_{sol} dv + \frac{d}{d\tau} \iiint_{V_{liq}} \mathcal{H}_{liq} dv + \lim_{\Delta\tau \rightarrow 0} \iiint_{\Delta V} \frac{\mathcal{H}_{sol, \tau + \Delta\tau} - \mathcal{H}_{liq, \tau}}{\Delta\tau} dv \quad (17)$$

The last term in the right-hand side of Eq.(17) contains an integral over the volume,  $\Delta V$ , that comprise the interface,  $S_{pch}$ , as well. When  $\Delta\tau \rightarrow 0$  the ratio  $dv/\Delta\tau = (\Delta n^*/\Delta\tau) ds$  tends to  $(dn^*/d\tau) ds = v_n^* ds$ , where  $\Delta n^*$  and  $v_n^*$  are respectively the displacement and local velocity of the interface element  $ds$  along its normal directed to the unfrozen domain. Simultaneously the region of integration  $\Delta V$  shrinks to  $S_{pch}$ , and  $\mathcal{H}_{sol}$  and  $\mathcal{H}_{liq}$  tend to their saturation values  $\mathcal{H}_{sol}^*$  and  $\mathcal{H}_{liq}^*$ . Then

$$\frac{d}{d\tau} \iiint_V \mathcal{H} dv = \frac{d}{d\tau} \iiint_{V_{sol}} \mathcal{H}_{sol} dv + \frac{d}{d\tau} \iiint_{V_{liq}} \mathcal{H}_{liq} dv + \iint_{S_{pch}} (\mathcal{H}_{sol}^* - \mathcal{H}_{liq}^*) v_n^* ds \quad (18)$$

By using Eq.(14) for both regions  $V_{sol}$  and  $V_{liq}$  and assuming constant and mutually equal densities of the frozen and unfrozen zones,  $\mathcal{H}_{liq}^* - \mathcal{H}_{sol}^* = \rho L$ , the above relation, Eq.(18), yields:

$$\begin{aligned}
\frac{d}{d\tau} \iiint_V \mathcal{H} dv &= \iint_{S_{\text{sol}}+S_{\text{pch}}} \lambda \text{grad } t \cdot \mathbf{n}' ds + \iint_{S_{\text{liq}}+S_{\text{pch}}} \lambda \text{grad } t \cdot \mathbf{n}' ds + \\
&+ \iiint_{V_{\text{sol}}} \omega dv + \iiint_{V_{\text{liq}}} \omega dv - \iint_{S_{\text{pch}}} \rho L v_n^* ds
\end{aligned} \tag{19}$$

where  $L$  is the latent heat of solidification.

Obviously, the unit vector,  $\mathbf{n}'$ , of the outward normal to  $S_{\text{pch}}$  (regarding  $V_{\text{sol}}$  or  $V_{\text{liq}}$ ) is coinciding or opposite to the unit normal vector,  $\mathbf{n}^*$ , directed always towards the unfrozen region. Hence, for the first term in the right-hand side of Eq.(19)  $\mathbf{n}' \equiv \mathbf{n}^*$ , while for the second one  $\mathbf{n}' \equiv -\mathbf{n}^*$ . Then, Eq.(19) can be rewritten, as follows:

$$\begin{aligned}
\frac{d}{d\tau} \iiint_V \mathcal{H} dv &= \iint_S \lambda \text{grad } t \cdot \mathbf{n}' ds + \iiint_V \omega dv + \\
&+ \iint_{S_{\text{pch}}} \left[ \left( \lambda \frac{\partial t}{\partial n^*} \right)_{\text{sol}} - \left( \lambda \frac{\partial t}{\partial n^*} \right)_{\text{liq}} - \rho L v_n^* \right] ds = 0
\end{aligned} \tag{20}$$

where  $\partial t/\partial n^*$  is the derivative in the direction of  $\mathbf{n}^*$ .

The comparison of Eq.(20) with Eq.(14) shows right away that the integral over  $S_{\text{pch}}$  is equal to zero. Because  $S_{\text{pch}}$  is an arbitrary chosen area from the entire phase-change front, the following relationship should be satisfied for all interface points:

$$\left( \lambda \frac{\partial t}{\partial n^*} \right)_{\text{sol}} - \left( \lambda \frac{\partial t}{\partial n^*} \right)_{\text{liq}} - \rho L v_n^* = 0 \tag{21}$$

In essence, the isolated case deduced, Eq.(21), represents the well-known Stefan boundary condition valid for the singular surface moving inside the studied region.

### 3. ENTHALPY FORMULATIONS FOR SOLVING HIGHLY NONLINEAR PHASE-CHANGE PROBLEMS INVOLVING FREEZING AND THAWING

Contemporary numerical methods, based on finite differences (FDM) finite-elements (FEM), boundary elements (BEM), etc., do not have any reasonable alternative when solving nonlinear heat-conduction problems of food manufacture. A group of these computational approaches deals with some type of tracking of the moving phase-change boundary. Usually, too complicated schemes are employed for front location at every time step, which causes additional difficulties for the multidimensional geometries. The second main group comprises more flexible methods for solving the governing equation by comparatively simple fixed-grid techniques over the whole space-time domain of integration, where the physical state of the substance in the different zones and the latent heat effect are accounted for by temperature-dependent thermophysical coefficients [1-3, 6].

Fortunately, the phase change in the real moisture-containing foods is performed, like in diluted solutions, over a temperature interval and all differential forms of the conservation equation, namely Eqs (4), (5), (9) and (10), are generally valid. Let us consider for simplicity the homogeneous version of Eq.(10), where the existing nonlinearities are caused by the temperature dependence of the thermal properties:

$$c(t) \rho(t) \frac{\partial t}{\partial \tau} = \text{div} [ \lambda (t) \text{grad } t ] \tag{22}$$

Eq.(22) is based on the concept of equivalent (apparent) specific heat capacity (ESHC) that,



for non-isothermal phase change, is expressed as [2]:

$$c(t) = c_{\text{mat}}(t) - \varphi L(t) \frac{dw(t)}{dt} \quad (23)$$

while for isothermal transition:

$$c(t) = c_{\text{ps}}(t) + L \delta(t - t_{\text{pch}}) \quad (24)$$

In Eqs (23) and (24)  $c_{\text{mat}}$  and  $c_{\text{ps}}$  denote the specific heat capacities of the food material and pure substance (water), calculated for both frozen and unfrozen ranges by the well-known methods [2];  $L$  is the latent heat of water freezing,  $\varphi$  the relative moisture content of the unfrozen material,  $w$  the ice fraction with respect to the total water content,  $t_{\text{pch}}$  the phase-change temperature of the pure substance and  $\delta$  the Dirac function. For the isothermal case, in order to make the real computations possible and Eq.(22) valid for the whole studied domain, including the phase-change interface, a special smoothing of the ESHC, Eq.(24), should be performed. The Dirac function is replaced with a  $\delta$ -resembling function  $\delta(\Delta t_{\text{pch}}, t - t_{\text{pch}})$  that differs from zero within a small interval  $(t_{\text{pch}} - \Delta t_{\text{pch}}, t_{\text{pch}} + \Delta t_{\text{pch}})$  and satisfies the condition of normalisation:

$$\int_{t_{\text{pch}} - \Delta t_{\text{pch}}}^{t_{\text{pch}} + \Delta t_{\text{pch}}} \delta(\Delta t_{\text{pch}}, t - t_{\text{pch}}) dt = 1 \quad (25)$$

After smoothing  $c_{\text{ps}}(t)$  and  $\lambda(t)$  over the interval as well, the sharp phase-change interface is “spread” and the differential ESHC formulation, Eq.(22), becomes generally applicable.

When using the ESHC method a lot of care must be taken to avoid undesirable computational phenomena, such as ESHC peak “jumping” and “stable oscillations”. After the problem, defined in moving boundary regions, is brought to a fixed-domain thermal problem, the most natural and logical step is to use the enthalpy as a new dependent variable and an indivisible part of the solution methodology [1-3,6]. Recently, the Kirchhoff substitution [1-3,6] was also successfully employed for numerical solution of food freezing/thawing problems by incorporating all nonlinearities, due to the temperature-dependent thermophysical coefficients of the heat conduction equation, in a single relationship between the volumetric specific enthalpy and the Kirchhoff function [2].

The above-mentioned enthalpy and Kirchhoff transforms are:

$$\mathcal{H}(t) = \int_{t_{\text{ref}}}^t c(t) \rho(t) dt \quad (26)$$

$$E(t) = \int_{t_{\text{ref}}}^t \lambda(t) dt \quad (27)$$

where  $t_{\text{ref}}$  is a suitably chosen reference temperature corresponding to the zero values of  $\mathcal{H}$  and  $E$ . By means of these two transformations several useful formulations of the nonlinear problem, governed by Eq.(22), can be written:

$$\frac{\partial \mathcal{H}}{\partial \tau} = \text{div} [\lambda(t) \text{grad } t] \quad (28)$$

$$\frac{\partial \mathcal{H}}{\partial \tau} = \text{div} [\alpha(\mathcal{H}) \text{grad } \mathcal{H}] \quad (29)$$

$$\frac{\partial E}{\partial \tau} = \alpha(E) \nabla^2 E \quad (30)$$

$$\frac{\partial \mathcal{H}}{\partial \tau} = \nabla^2 E \quad (31)$$

Eqs (28) and (29) stay in the basis of the so-called “enthalpy-temperature” and “enthalpy diffusion” methods, respectively. Eq.(30) is represented only in terms of the Kirchhoff variable, while Eq.(31) combines both two transforms, Eqs (26) and (27).

The principal meaning of these changes of variables is to bring the existing nonlinearities from their initial (inconvenient) form to another more convenient one from a computational point of view. Figure 3 illustrates different types of nonlinearities that are handled by the above-mentioned formulations of the governing heat-conduction equation when solving food freezing/thawing problems.

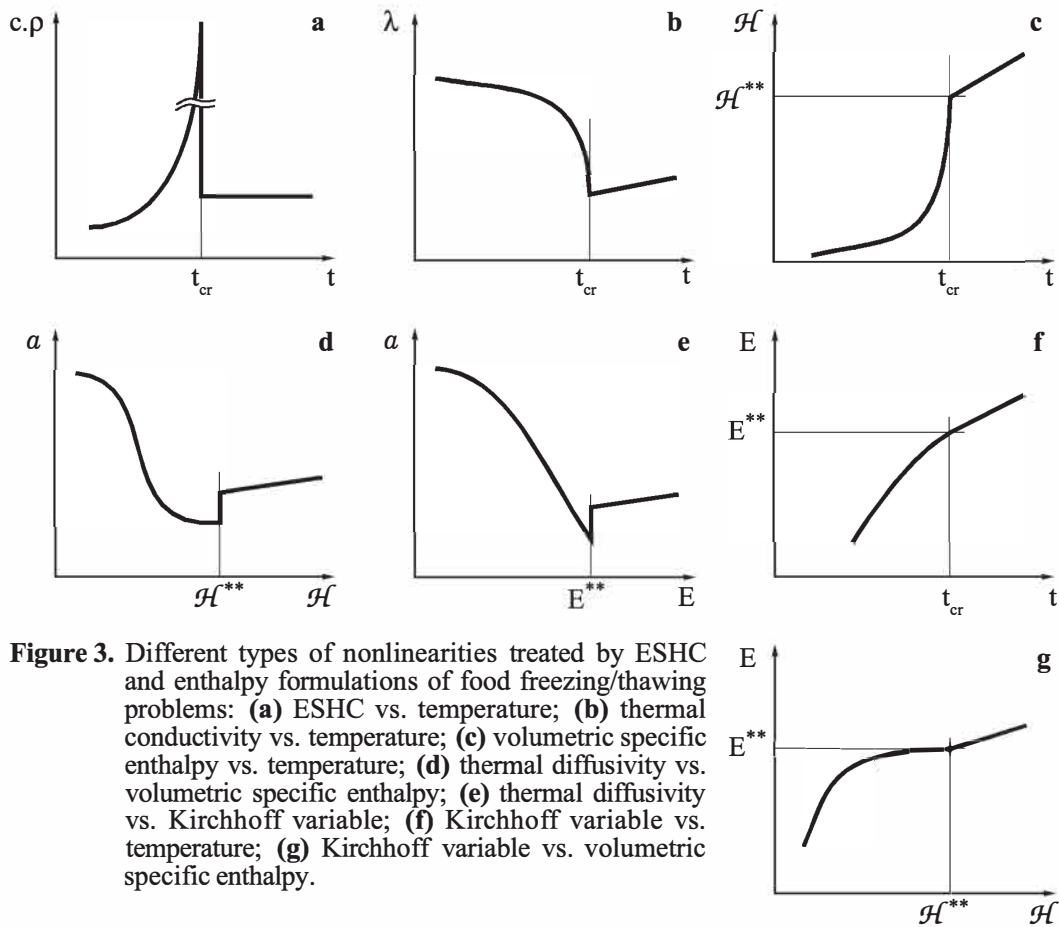


**Figure 3.** Different types of nonlinearities treated by ESHC and enthalpy formulations of food freezing/thawing problems: **(a)** ESHC vs. temperature; **(b)** thermal conductivity vs. temperature; **(c)** volumetric specific enthalpy vs. temperature; **(d)** thermal diffusivity vs. volumetric specific enthalpy; **(e)** thermal diffusivity vs. Kirchhoff variable; **(f)** Kirchhoff variable vs. temperature; **(g)** Kirchhoff variable vs. volumetric specific enthalpy.

Obviously, Eq.(22) is used with the relations  $c.p - t$  and  $\lambda - t$  (Figure 1a,b); Eq.(28) with  $\lambda - t$  and  $\mathcal{H} - t$  (Figure 1b,c); Eq.(29) with  $a - \mathcal{H}$  (Figure 1d); Eq.(30) with  $a - E$  (Figure 1e) and Eq.(32) with  $\mathcal{H} - t$  and  $E - t$  (Figure 1c,f) or with the direct relationship  $E - \mathcal{H}$  (Figure 1g).

There is no universal receipt for selection of the best approach among Eqs (22) and (28) – (31). The different methods can be compared and strictly evaluated only after a detailed analysis of the computational schemes themselves. However, some rough estimates could be drawn *a priori*. The traditional ESHC method, Eq.(22), seems to be less reliable, because of the large ESHC peak over a comparatively narrow interval and related complications. The enthalpy diffusion and Kirchhoff transform methods, Eq.(29) and (30), should be better, regardless the existence of an inverse diffusivity peak in Eq.(30) and discontinuities of  $a$ , since their relative jump size is many time smaller than that of the ESHC. The enthalpy-temperature and enthalpy-Kirchhoff transform methods, Eqs (28) and (31), are expected to be enough robust. Simultaneously, the application of the enthalpy-Kirchhoff transform approach leads to very economical computational algorithms and implies a series of advantages, especially when the  $E - \mathcal{H}$  relationship is directly used [2].

#### 4. CONCLUSIONS

Several mathematical formulations and their abilities for solving highly nonlinear phase-change problems were considered.

The integral form of the energy conservation relationship, Eqs (1) and (14), is always valid for both isothermal and non-isothermal phase changes, as well as for absence of phase transitions.

The differential form of the conservation equation is strictly valid for lack of phase changes or for non-isothermal transitions (arising in food materials). For isothermal transformation the differential form can be applied as usual to the frozen or unfrozen zones, while Eq.(21) has to be employed for the moving phase-change interface. The differential formulation in a fixed domain can become universal as well, provided that the sharp transition front is “spread” over a small temperature interval. Otherwise, such a differential equation can be generally used, over the whole studied region, in the framework of the Sobolev spaces involving the “weak” derivative and “weak” solution concepts.

The enthalpy numerical methods, and especially the enthalpy-Kirchhoff transform method, are very promising for wider future application in combination with various FDM, FEM and BEM computational techniques.

#### REFERENCES

1. **Comini, G., Nonino, C. and Saro, O. (1990)** Performance of enthalpy-based algorithms for isothermal phase change. *Advanced Computational Methods in Heat Transfer, 3: Phase Change and Combustion Simulation* (Eds: L. C. Wrobel *et. al.*) Computational Mechanics Publication, Southampton & Springer-Verlag, Berlin, 3-13
2. **Fikiin, K. A. (1996)** Generalized numerical modelling of unsteady heat transfer during cooling and freezing using an improved enthalpy method and quasi-one-dimensional formulation. *International Journal of Refrigeration, 19*: 132-140
3. **Kozdoba, L.A. (1975)** *Methods of Solving Nonlinear Heat Conduction Problems*. Science, Moscow, p. 228, in Russian
4. **Novikov, I. I. and Voskresenskij, K. D. (1961)** *Applied Thermodynamics and Heat Transfer*. Gosatomizdat, Moscow, p. 548, in Russian
5. **Shamsundar, N. and Sparrow, E.M. (1975)** Analysis of multidimensional conduction phase change via the enthalpy model. *Transactions of the ASME, Series C: Journal of Heat Transfer, 97*: 333-340
6. **Tikhonov, A. N. and Samarskij, A. A. (1972)** *Equations of Mathematical Physics*. Science, Moscow, p. 736, in Russian





## EUROPEAN COMMISSION

Édith CRESSON, Member of the Commission  
responsible for research, innovation, education, training and youth

DG XII/B.1 — RTD actions: Cooperation with non-member countries and  
international organisations — European Economic Area, COST, Eureka  
and international organisations

Contact: Ms Francisca Serra

Address: European Commission, rue de la Loi 200 (SDME 1/50)  
B-1049 Brussels — Tel. (32-2) 29-69591; fax (32-2) 29-64289

---

Price (excluding VAT) in Luxembourg: ECU 26.50

ISBN 92-828-3309-7



OFFICE FOR OFFICIAL PUBLICATIONS  
OF THE EUROPEAN COMMUNITIES

L-2985 Luxembourg



9 789282 833094

## **CHAPTER 2**

**Enthalpy and Kirchhoff transform method  
for food refrigeration heat transfer:  
*finite-difference formulation***

## Chapter 2

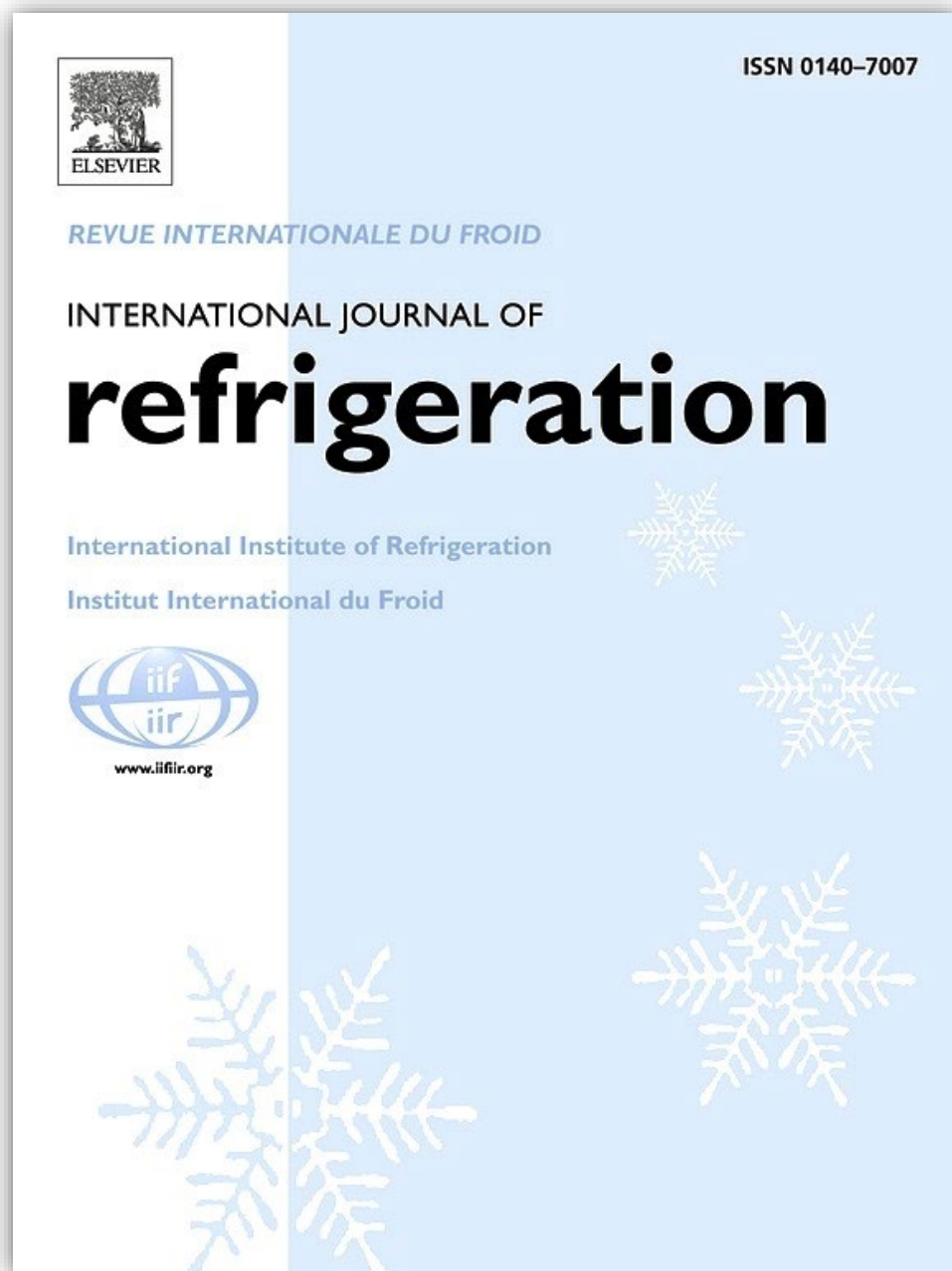
presents an efficient numerical solution for a generalised highly non-linear problem of unsteady-state heat transfer, comprising various industrial scenarios involving chilling and freezing (heating and thawing) of two-phase food systems with one freezable component. By using the methodologies in Chapter 1, an improved enthalpy method was introduced for the first time in food refrigeration, where gradual non-isothermal phase changes occur during freezing or thawing. The Goodman and Kirchhoff substitutions are simultaneously employed, thereby incorporating all non-linearities, caused by the temperature-dependent thermophysical characteristics, in a single functional relationship between the volumetric enthalpy and the Kirchhoff function.

A number of method's advantages are demonstrated when using finite differences to implement this numerical technique as a unified and robust tool for fixed-grid modelling, algorithmizing and computer simulation of phase-change heat conduction taking place in complex processes of food refrigeration. A quasi-one-dimensional approach was also applied, resorting to shape factors, which permit to handle 3D heat transfer scenarios by means of 1D solutions, with a satisfactory accuracy for engineering computations. Unsteady distributions of temperature, enthalpy, Kirchhoff variable and phase content could be determined at once, along with the cooling and freezing (heating and thawing) times of studied objects being refrigerated. The method's reliability was confirmed by experimental validation.

The originality and capabilities of the findings presented in Chapter 2 have been well appreciated by scientists around the globe (*click on the logos below to locate publications, which cite, use and/or recommend related results*):



The suggested enthalpy and Kirchhoff transform method has been used by many independent researchers for modelling and simulations of various processes and systems of food refrigeration and beyond (e.g. freezing of grounds for metro construction, plasma-sprayed coating, multi-type heat pumps, latent thermal energy storage, cooling by solid nitrogen, wood freezing, etc.). The citing publications that were noticed are in English, French, Spanish, Portuguese, Russian and Greek languages.



Reprinted from *International Journal of Refrigeration*, Vol. 19, No. 2, Fikiin K. Generalized numerical modelling of unsteady heat transfer during cooling and freezing using an improved enthalpy method and quasi-one-dimensional formulation, pp. 132-140, doi: [https://doi.org/10.1016/0140-7007\(95\)00055-0](https://doi.org/10.1016/0140-7007(95)00055-0), Copyright © 1996, with permission from Elsevier, License No. 5053150055153 of 20 April 2021.



## Generalized numerical modelling of unsteady heat transfer during cooling and freezing using an improved enthalpy method and quasi-one-dimensional formulation

K. A. Fikiin

Refrigeration Science and Technology Division, Technical University of Sofia,  
 95 Vassil Levski Blvd., 1000 Sofia, Bulgaria. Fax: + 35 92878774

Received 19 August 1994; revised 10 July 1995

A numerical solution of a generalized Stefan problem is presented. It covers a great variety of unsteady heat conduction cases accompanied by phase transformations. A mathematical model is developed for determination of the unsteady-state temperature and enthalpy fields (as well as the space–time evolution of the phase content) and of the cooling and freezing (heating and thawing) times of food materials and other bodies of various configuration (representing multicomponent two-phase systems having one freezable component). An improved enthalpy method is proposed by which all non-linearities, caused by the temperature dependence of the thermophysical coefficients, are introduced in a functional relationship between the volumetric specific enthalpy and the Kirchhoff function. Thus the non-linearities are eliminated as a factor making the solution difficult. The applied approach possesses great adaptivity and flexibility in solving complicated moving boundary problems: it is suitable for both isothermal and non-isothermal phase change, reaches a high degree of correspondence between the real physical phenomenon and its mathematical formalization, uses uniform and easy fixed-grid computational techniques, makes it possible to avoid complications and to eliminate possible errors caused by ‘jumping’ of the equivalent specific heat capacity peak at the maximum of the latent heat effect, etc. Efficient procedures and algorithms for computer simulation of complex refrigerating technological processes are created. Experimental verification demonstrating the applicability and accuracy of the model is carried out.

(Keywords: food chilling and freezing; phase change heat transfer; mathematical modelling; enthalpy method)

## Modélisation numérique généralisée du transfert de chaleur non-stationnaire pendant la réfrigération et la congélation par une méthode enthalpique améliorée et une formulation quasi-unidimensionnelle

*On présente une solution numérique d'un problème de Stefan généralisé. Elle couvre une grande variété de cas de conduction thermique accompagnée par des changements de phase. On a mis au point un modèle mathématique pour la détermination des champs de température et d'enthalpie (ainsi que l'évolution spatiale et temporaire du contenu de phases) en régime non-stationnaire et du temps de réfrigération et de congélation (ou de réchauffement et de décongélation) de matières alimentaires et d'autres corps de configuration variée (représentant des systèmes multicomposants biphasiques d'un composant congélatable). Une méthode enthalpique est proposée, par laquelle toutes les non-linéarités, causées par les coefficients thermophysiques dépendant de la température, sont introduites dans une relation fonctionnelle entre l'enthalpie volumique et la fonction de Kirchhoff. De cette façon, les non-linéarités sont éliminées comme facteur rendant la solution difficile. L'approche appliquée possède une grande adaptivité et flexibilité dans la résolution des problèmes compliqués aux limites mobiles: elle convient à la fois pour des changements de phase isothermes et non-isothermes, garantit un haut degré de correspondance entre le phénomène physique réel et sa formalisation mathématique, utilise des techniques de calcul faciles aux maillages fixes et uniformes, permet d'éviter des complications et d'éliminer les erreurs possibles provoquées par le 'saut au dessus' du pic de la capacité thermique équivalente, etc. Les procédés et algorithmes efficaces sont créés pour la simulation par ordinateur de processus complexes de la technologie frigorifique. Une vérification expérimentale est effectuée, démontrant l'applicabilité et la précision du modèle.*

(Mots clés: réfrigération et congélation d'aliments; transfert thermique; changement de phase; modélisation mathématique; méthode enthalpique)

## Nomenclature

$a$	Thermal diffusivity: $a = \lambda / (c \cdot \rho)$ ( $\text{m}^2 \text{s}^{-1}$ )
$c$	Specific heat capacity ( $\text{J kg}^{-1} \text{K}^{-1}$ )
$E$	Kirchhoff function ( $\text{W m}^{-1}$ )
$\mathcal{H}$	Enthalpy per unit volume ( $\text{J m}^{-3}$ )
$h$	Space increment on the axis $\xi$ in the finite-difference scheme: $h = R/n$ (m)
$L$	Latent heat of water solidification/fusion ( $\text{J kg}^{-1}$ )
$l$	Time step in the finite-difference scheme (s)
$n$	Number of discrete divisions in the dimension $R$
$R$	Half of the smallest characteristic body dimension (for <i>one-dimensional solids</i> : semi-thickness of slab, radius of cylinder or sphere; for <i>multidimensional solids</i> : semi-thickness of rectangular prism or parallelepiped, semi-minor diagonal of rhombus or octahedron, semi-minor axis of ellipse or ellipsoid, etc.) (m)
$r$	Spatial radial coordinate (m)
$S$	Heat transfer surface of the solid ( $\text{m}^2$ )
$t, T$	Temperature ( $^{\circ}\text{C}$ or $\text{K}$ )
$V$	Volume of the body ( $\text{m}^3$ )
$w$	Relative quantity of the frozen water (ice fraction) ( $\text{kg}_{\text{ice}}/\text{kg}_{\text{water}}$ )
$X_1, X_2, X_3$	Halves of the body characteristic dimensions (m)
$x$	Spatial Cartesian coordinate (m)

## Greek letters

$\alpha$	Surface heat transfer coefficient ( $\text{W m}^{-2} \text{K}^{-1}$ )
$\Gamma$	Geometric factor
$\delta$	Dirac function ( $\text{K}^{-1}$ in Equation (1.5))
$\lambda$	Thermal conductivity ( $\text{W m}^{-1} \text{K}^{-1}$ )
$\xi$	Generalized coordinate (m)
$\rho$	Substance density ( $\text{kg m}^{-3}$ )
$\tau$	Time (s; min)
$\Phi$	Shape coefficient of the solid: $\Phi = V / (S \cdot R)$
$\varphi$	Relative moisture content of the material ( $\text{kg}_{\text{water}}/\text{kg}_{\text{mat}}$ )
$\omega$	Volumetric rate of the internal heat generation ( $\text{W m}^{-3}$ )

## Subscripts

cr	Cryoscopic (initial freezing) point
ds	Dry substance
$i, k$	Indexes of a node in the finite-difference scheme based on position $\xi = ih$ and time $\tau = kl$ , respectively ( $i = 0, 1, 2, \dots, n$ and $k = 0, 1, 2, \dots$ )
in	Initial
mat	Material
o	Ambient
pch	Phase change
ps	Pure substance
wat	Water

Cooling and freezing are indivisible structural elements of the food cold chain. The accurate prediction of the unsteady-state temperature distribution in foods, enthalpy variation, phase content, process duration and energy consumption during cooling and freezing (heating and thawing), for a wide range of industrial heat transfer scenarios, has an extraordinary importance. It is necessary for the scientifically based design of refrigeration systems, for their cost-effective operation and control, for correct decision-making, and to ensure proper product safety and quality.

The traditional approach for solving the non-linear thermal problems involving freezing (thawing) of food materials assumes the presence of a sharp, clearly expressed phase-change interface and the existence of two well-outlined zones: frozen and unfrozen, each of them having constant thermophysical characteristics. In essence, these two domains are considered as individual bodies divided by a moving front of solidification (melting), where isothermally, at the cryoscopic temperature, the whole latent heat is removed. Mathematically, this is expressed by writing, for each separate layer, linear heat conduction equations conjugated by the classical Stefan boundary condition. On this basis approximate analytical solutions for one-dimensional solids with simple geometry, mainly with infinite slab shape, are deduced<sup>1</sup>.

Upon numerical solution of the Stefan problems, in the presence of a sharply outlined front of phase transformation, the difficulties are mainly connected

with the exact localization of the interface position. As a rule, the different front-tracking techniques are rather slow and lead to considerable complications in the multidimensional case. Similarly to the above-mentioned analytical results, they are precise only for pure substances, but not for multicomponent moisture-containing systems, such as food materials.

The analysis of unsteady heat conduction in systems of bodies with moving boundaries by solving a unified non-linear thermophysical problem, formulated for the entire studied domain, represents a qualitatively new stage in the modelling of conduction phase change processes. Within this approach a single quasi-linear heat conduction equation is written for the whole space–time region of integration, independent from the phase state of the substance in the different zones. The effects of phase transition are accounted for by their incorporation in temperature-dependent thermophysical characteristics. The phase-change front is not followed explicitly and its location is estimated indirectly – from the instantaneous position of the cryoscopic isothermal surfaces and of the zones situated within the temperature range of the transition. The Stefan boundary condition is eliminated and the impact of the released or absorbed latent heat is taken into account through an equivalent (apparent) specific heat capacity (ESHC). That is why this method of formalization is sometimes called the ESHC method<sup>2</sup> or a definition of a ‘zero latent heat’ problem<sup>3</sup>.

Useful ideas for numerical solution of phase change



problems reformulated in this manner are contained in the works of Tikhonov and Samarskij<sup>4</sup> and Samarskij<sup>5</sup>, where parabolic partial differential equations having coefficients with discontinuity points are considered. In refrigeration technology ESHC-based numerical models using invariable fixed grids were proposed for the first time by Bonacina and Comini<sup>6</sup>, and were developed further in a series of papers by Bonacina, Comini, Cleland, Earle, Hayakawa, Pham and others<sup>7–16</sup>. Moreover, these studies often use three time level integration methods, such as that of Lees<sup>17</sup>, for evaluation of the thermophysical properties directly at the intermediate time level without subsequent iterations. Simultaneously, in order to minimize the negative effects connected with the so-called latent heat peak ‘jumping’ (i.e. with possible missing of the ESHC maximum), usually special enthalpy techniques for volumetric or temporal averaging of the ESHC are employed<sup>2,11,12,18,19</sup>.

There are several transformations facilitating the integration of the Stefan problems: for example, those of Boltzmann, Friedman and Landau<sup>3,20</sup>. However, after the problem, defined in moving boundary regions, is brought by ESHC to a fixed domain thermal problem, the most natural and logical step is to apply the Goodman substitution<sup>20</sup>, by which the enthalpy is introduced as a new dependent variable and becomes an indivisible part of the solution methodology. This approach lies in the basis of one of the most promising and advanced areas in modelling of non-linear heat conduction – the enthalpy methods (EM)<sup>2,21–34</sup>. When the enthalpy substitution is performed only for the unsteady-state term of the heat conduction equation, the EM are called enthalpy–temperature methods (ETM), and if this variable change is applied to the entire equation they are called enthalpy–diffusion methods<sup>2</sup>. Shamsundar and Sparrow<sup>31</sup> demonstrated by rigorous considerations that the integral form of the enthalpy equation is equivalent to three differential equations representing the usual energy conservation equations for the liquid and the solid phases and for the solid–liquid interface, respectively. For the first time an enthalpy method making it possible to ‘avoid’ the non-linearities in a conduction problem was proposed by Eyres *et al.*<sup>25</sup>. A qualitative description of this type of techniques was initially given by Dusinberre<sup>24</sup> and a more detailed mathematical reasoning by Kamenomostskaja<sup>27</sup>. The earliest numerical methods combined with EM may be found in the works of Albasiny<sup>22</sup> and Rose<sup>30</sup>, followed later by those of Crowley<sup>23</sup>, Voller and Cross<sup>32</sup>, Voller *et al.*<sup>33</sup> and others. By means of an explicit version of the ETM, Mannaperuma and Singh<sup>28,29</sup> obtained rational numerical solutions of the first, second and third boundary value problems for the case of freezing or thawing of food objects with six typical configurations.

The simultaneous application of the ETM and the Kirchhoff transformation reveals great potential possibilities in the solution of moving boundary problems. On this basis, recently Hunter and Kuttler<sup>26</sup> examined a simple case of pure water freezing in an infinite slab shape. Even though some elements of such an approach could be found earlier, as means for analysis of non-linear conduction<sup>4,5</sup>, up to now there have not been observed any mathematical models (based on a similar

idea) for food freezing/thawing – processes whose description would demonstrate the full advantages of the method.

The aim of this paper is to propose a convenient enthalpy method for unified mathematical modelling and computer simulation of complicated cooling and freezing (heating and thawing) processes in multicomponent two-phase systems, such as food materials, and to cover with necessary completeness the diversity of their geometric and thermophysical characteristics, internal and boundary energy influences and the whole complex of factors determining the heat transfer.

### Problem formulation

In order to analyze the predominant part of the multitude of encountered physical situations, in this study the parameters governing the process are presented in a quite general form. Both classical one-dimensional and various and complex-shaped multidimensional objects, susceptible to quasi-one-dimensional interpretation, are considered. The initial temperature distributions and ambient fluid temperature are assumed as arbitrary functions of the space variable and time respectively. The thermophysical characteristics and the volumetric rate of internal heat generation may be arbitrary functions of temperature. The heat transfer coefficient can depend in an arbitrary way on the surface and ambient medium temperatures, i.e. many cases are covered simultaneously, including surface boiling, condensation, natural convection, forced streaming by fluids having highly temperature-dependent parameters, and radiative heat transfer reduced to convection.

In the above-mentioned physical statement the mathematical description of the heat transfer upon symmetric cooling/heating and freezing/thawing is based on the following non-linear and inhomogeneous heat conduction equation and the corresponding uniqueness conditions:

$$c(t)\rho(t)\frac{\partial t}{\partial \tau} = \frac{1}{\xi^\Gamma} \cdot \frac{\partial}{\partial \xi} \left[ \xi^\Gamma \lambda(t) \frac{\partial t}{\partial \xi} \right] + \omega(t) \quad (1)$$

$$(\tau > 0, 0 < \xi < R)$$

$$t(\xi, 0) = t_{in}(\xi) \quad (1.1)$$

$$-\left\{ \lambda(t) \frac{\partial t}{\partial \xi} \right\}_{\xi=R} = \alpha [t(R, \tau), t_o(\tau)] \cdot [t(R, \tau) - t_o(\tau)] \quad (1.2)$$

$$\left\{ \lambda(t) \frac{\partial t}{\partial \xi} \right\}_{\xi=0} = 0 \quad (1.3)$$

where  $\Gamma = 0$ ,  $\xi \equiv x$  for an infinite slab;  $\Gamma = 1$ ,  $\xi \equiv r$  for an infinite cylinder;  $\Gamma = 2$ ,  $\xi \equiv r$  for a sphere; Equation (1) is the governing differential equation unified for Cartesian, cylindrical and spherical coordinate systems; Equation (1.1) is the initial condition; Equation (1.2) represents the non-linear and inhomogeneous boundary condition of the third kind; Equation (1.3) is a second-kind boundary condition reflecting the temperature field symmetry. In the fixed domain problem, formulated in such a way, Equations (1)–(1.3), there simultaneously exist non-linearities of the first-, second- and third-kinds (according to the classification in ref. 20).

## Generalized numerical modelling of unsteady heat transfer during cooling and freezing

135

In the case of non-isothermal phase change, characteristic for multicomponent two-phase systems from the type of food materials, biological tissues, soils, etc., having one freezable (thawing) component, the ESHC, participating in Equation (1), may be presented in the following manner:

$$c(t) = c_{\text{mat}}(t) - L \varphi \frac{dw(t)}{dt} \quad (1.4)$$

The first term in the right-hand side of Equation (1.4) represents the pure specific heat capacity of the material, while the second takes into account the impact of the latent heat of phase transition on the ESHC. The temperature dependence of the ice fraction  $w = w(t)$  may be determined by some of the well-known methods<sup>34</sup>.

In the presence of isothermal phase change, typical for single-component substances, for example pure water ( $\varphi = 1$ ),  $w$  changes abruptly from 0 to 1 (or vice versa) and the generalized presentation, Equation (1.4), used in this study includes as an isolated case the known expression<sup>5</sup>

$$c(t) = c_{\text{ps}}(t) + L \delta(t - t_{\text{pch}}) \quad (1.5)$$

Food materials undergoing refrigeration treatment represent a complicated dynamic complex of three fractions, continuously changing their quantitative ratios: dry substance (proteins, lipids, carbohydrates and mineral salts), water and ice crystals. Both in the over-cryoscopic ( $w = 0$ ) and undercryoscopic ( $0 < w < 1$ ) temperature ranges the additive expression is valid:

$$c_{\text{mat}}(t) = (1 - \varphi) c_{\text{ds}}(t) + \varphi [1 - w(t)] c_{\text{wat}}(t) + \varphi w(t) c_{\text{ice}}(t) \quad (1.6)$$

The thermal conductivity is also a compound function of the temperature and, in contrast to the heat capacity, it cannot be expressed by strict theoretical means on the basis of the properties of the different constituents. However, the additive principle could be applied with a sufficient accuracy for engineering research. The density variation, caused mainly by the difference between the water and ice densities, is within relatively narrow limits, and therefore the volume and characteristic dimensions of the food objects may be considered as constants.

The temperature dependences of the volumetric ESHC and the thermal conductivity for one typical representative of moisture-containing materials, namely the Karlsruhe food simulator, representing a methyl-hydroxyethyl-cellulose water gel (23% Tylose MH 1000 and 77% water in mass), are shown in Figures 1 and 3. For the purposes of the present investigation they were evaluated more precisely and were additionally determined especially for low temperatures, including also part of the cryogenic range.

As was mentioned above, the use of the ESHC method causes many problems connected with ESHC peak 'jumping' and 'stable oscillations'. Numerous theoretical investigations have been devoted to the struggle with these undesirable phenomena. For example, in the multidimensional case, there have been different 'volumetric' or 'temporal' averaging techniques proposed for ESHC estimation, resorting to information for the

enthalpy and temperature gradients and minimizing the risk of missing the ESHC maximum<sup>2,11,12,18,19</sup>:

$$c_k = \frac{\text{grad } \mathcal{H}_k \cdot \text{grad } t_k}{\text{grad } t_k \cdot \text{grad } t_k} \quad (1.7)$$

$$c_k = \left( \frac{\text{grad } \mathcal{H}_k \cdot \text{grad } \mathcal{H}_k}{\text{grad } t_k \cdot \text{grad } t_k} \right)^{1/2} \quad (1.8)$$

$$c_k = \left( \frac{d\mathcal{H}}{dt} \right)_k = \left( \frac{\partial \mathcal{H}}{\partial \tau} / \frac{\partial t}{\partial \tau} \right)_k \approx \frac{\mathcal{H}_k - \mathcal{H}_{k-1}}{t_k - t_{k-1}} \quad (1.9)$$

To reformulate the posed generalized problem, Equations (1)–(1.3), the following substitutions are applied during our considerations:

$$E(t) = \int_{t'}^t \lambda(t) dt \quad (1.10)$$

$$\mathcal{H}(t) = \int_{t'}^t c(t) \rho(t) dt \quad (1.11)$$

where  $t^*$  is a suitably chosen reference temperature

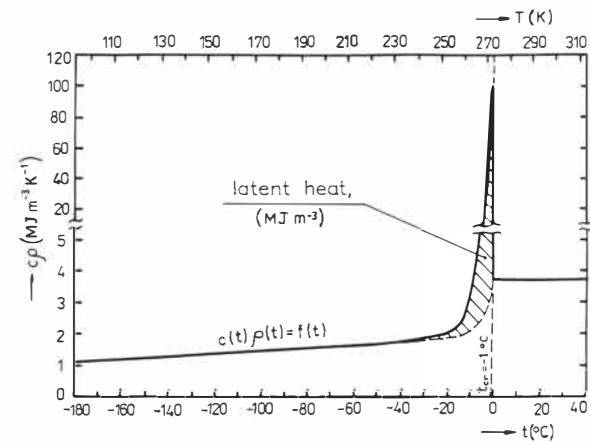


Figure 1 Volumetric specific heat capacity of the Karlsruhe test substance

Figure 1 Capacité thermique volumique de la substance d'épreuve de Karlsruhe

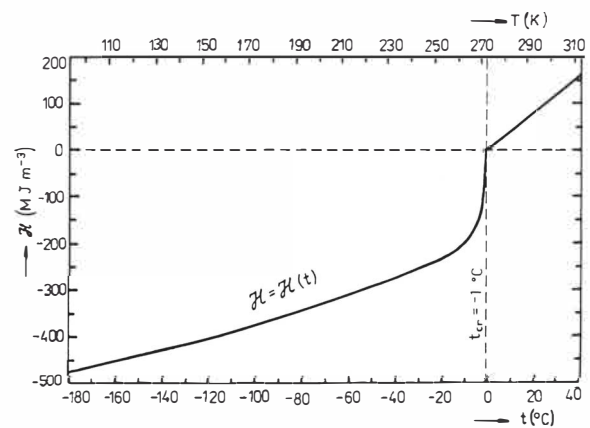


Figure 2 Volumetric specific enthalpy of the Karlsruhe test substance

Figure 2 Enthalpie volumique de la substance d'épreuve de Karlsruhe



corresponding to the zero values of  $E$  and  $\mathcal{H}$ . It is convenient to assume it equal to the cryoscopic temperature, i.e.  $t^* \equiv t_{cr}$ .

Equations (1.10) and (1.11) determine six relationships between the quantities  $E$ ,  $\mathcal{H}$  and  $t$ , namely direct ones:  $E(t)$  and  $\mathcal{H}(t)$  and inverse:  $t(E)$  and  $t(\mathcal{H})$  as well as  $E(\mathcal{H})$  and  $\mathcal{H}(E)$ . Since  $c$ ,  $\rho$  and  $\lambda$  are positive and limited, all these functions are strictly increasing and continuous, and consequently between the independent and dependent variables there exist one-to-one mappings. Only for isothermal phase change is there one singularity: if a special smoothing of the ESHC, expressed by Equation (1.5), is not applied (which is necessary for the differential form of the governing equation to be valid for the entire studied region<sup>31</sup>), the dependences  $\mathcal{H}(t)$  and  $\mathcal{H}(E)$  undergo an abrupt jump at the phase transition points (where  $c \rightarrow \infty$ ), but the inverse functions  $t(\mathcal{H})$  and  $E(\mathcal{H})$  are completely defined, continuous and monotonic. Figures 2 and 4 present the relations  $\mathcal{H}(t)$  and  $E(t)$  for the Karlsruhe test substance obtained by numerical integration of the volumetric ESHC and thermal conductivity functions.

As a result of this variable change the following transformed differential system is obtained:

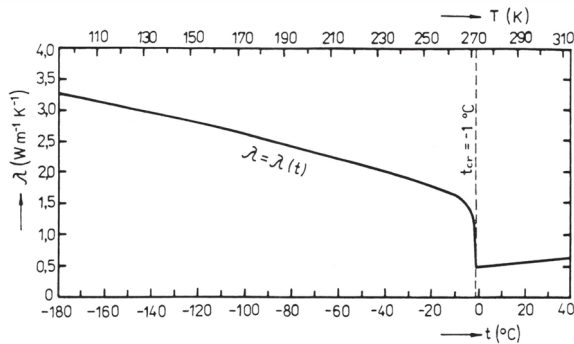


Figure 3 Thermal conductivity of the Karlsruhe test substance

Figure 3 Conductivité thermique de la substance d'épreuve de Karlsruhe

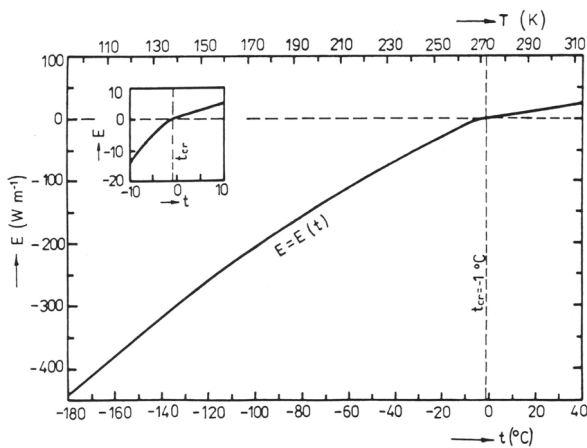


Figure 4 Kirchhoff function for the Karlsruhe test substance

Figure 4 Fonction de Kirchhoff pour la substance d'épreuve de Karlsruhe

$$\frac{\partial \mathcal{H}(E)}{\partial \tau} = \frac{\partial^2 E}{\partial \xi^2} + \frac{\Gamma}{\xi} \cdot \frac{\partial E}{\partial \xi} + \omega(E) \quad (2)$$

$$(\tau > 0, 0 < \xi < R)$$

$$E(\xi, 0) = E_{in}(\xi) \quad (2.1)$$

$$-\left\{ \frac{\partial E}{\partial \xi} \right\}_{\xi=R} = \alpha \{t[E(R, \tau)], t_o(\tau)\} \cdot \{t[E(R, \tau)] - t_o(\tau)\} \quad (2.2)$$

$$\left\{ \frac{\partial E}{\partial \xi} \right\}_{\xi=0} = 0 \quad (2.3)$$

In this way the modified problem, Equations (2)–(2.3), is defined by means of two new mutually related dependent variables: the volumetric specific enthalpy (the Goodman variable) and the Kirchhoff function. The correlation between them includes all the first-kind nonlinearities resulting from the temperature dependence of the thermophysical properties.

### Numerical solution

One of the commonly encountered faults in the analytical and numerical modelling of natural and industrial processes is the needless attack by powerful mathematical apparatus of inadequately posed (from a physical point of view) problems and, due to this, the groundless spending of enormous intellectual and machine resources. The valuable quality of the improved enthalpy method, proposed in the present work, is the high degree of conformity between the thermophysical phenomenon and its mathematical description. That is why, in order to show the advantages of this approach, upon the numerical solution of the reformulated problem, Equations (2)–(2.3), a very easy and convenient explicit non-iterative finite-difference scheme was used. The studied space–time domain is discretized by a fixed uniform rectangular grid. Naturally, within the framework of the method, it is possible to employ a wide range of versions of the methods of finite differences (FDM), finite elements (FEM), boundary elements (BEM), etc.

Following a methodology similar to the one used in previous publications of Fikiin<sup>35–39</sup>, the following recurrent formulae were obtained for determination of the specific enthalpy and, hence, of the temperature and the Kirchhoff function.

(a) For the internal nodes of the solids ( $i = 1, 2, 3, \dots, n-1$  and  $k = 0, 1, 2, \dots$ ):

$$\mathcal{H}_{i,k+1} = \psi_{i,k}^1 + \frac{l}{h^2} \left( 1 + \frac{\Gamma}{2i} \right) E_{i+1,k} + \frac{l}{h^2} \left( 1 - \frac{\Gamma}{2i} \right) E_{i-1,k} + l \omega_{i,k} \quad (3)$$

where

$$\psi_{i,k}^1 = \mathcal{H}_{i,k} - \frac{2l}{h^2} E_{i,k}$$

(b) For the middle plane of the slab, the cylinder axis

and the sphere centre ( $i = 0$  and  $k = 0, 1, 2, \dots$ ):

$$\mathcal{H}_{0,k+1} = \psi_{0,k}^2 + \frac{2l}{h^2}(\Gamma + 1)E_{1,k} + l\omega_{0,k} \quad (4)$$

where

$$\psi_{0,k}^2 = \mathcal{H}_{0,k} - \frac{2l}{h^2}(\Gamma + 1)E_{0,k}$$

(c) For the nodes on the body surface ( $i = n$  and  $k = 0, 1, 2, \dots$ ):

$$\mathcal{H}_{n,k+1} = \psi_{n,k}^3 + \frac{2l}{h^2}E_{n-1,k} + l\omega_{n,k} \quad (5)$$

where

$$\psi_{n,k}^3 = \mathcal{H}_{n,k} - \frac{2l}{h^2}E_{n,k} - \frac{2l}{h} \left(1 + \frac{\Gamma}{2n}\right) \alpha_{n,k} [t_{n,k} - t_o(kl)]$$

The computational process of time updating starts by the discrete presentation of the initial condition, Equation (2.1), i.e.  $E_{i,k} \equiv E_{i,0} = E_{in}(ih)$  for  $i = 0, 1, 2, \dots, n-1$  and  $k = 0$ . A number of authors have established that the direct application of this equality also to the case  $i = n$  does not ensure sufficiently good approximation upon calculation of the thermal state of the nodal points close to the surface of the body at small times<sup>1,24</sup>. That is why  $t_{n,0}$ , respectively  $E_{n,0}$  and  $\mathcal{H}_{n,0}$ , as in refs 35, 38 and 39, were determined additionally with the aid of an auxiliary analytical solution using a special iterative procedure<sup>37</sup>. Even though the computational relationships used are comparatively cumbersome, it does not make the solution difficult, since during the calculation it is applied only once.

The stability criterion of the finite-difference scheme, determined by the requirement  $d\psi^j(t)/dt \geq 0$  or  $d\psi^j(E)/dE \geq 0$ ,  $j = 1, 2, 3$ , for a given  $\alpha$ , is

$$l \leq \frac{h^2}{2a_{\max}} \cdot \min \left\{ (\Gamma + 1)^{-1}, \left[ \left(1 + h \frac{\alpha_{\max}}{\lambda_{\min}} \left(1 + \frac{\Gamma}{2n}\right)\right)^{-1} \right] \right\} \quad (6)$$

If the above condition turns out to be severe, i.e. the time step  $l$  is very small, the computations may be speeded by using a time non-uniform grid, where  $l$  is readjusted before going to a new time level on the basis of information for the current values of the thermo-physical parameters.

### Quasi-one-dimensional approach

Let it be assumed as sufficiently representative the class of all solids with central symmetry, limited by convex surfaces or planes. One introduces a rectangular coordinate system whose origin coincides with the body centre. The system is situated in such a manner that the coordinates of the intersection points of its axes with the body surface are equal to the halves of the characteristic dimensions of the solid  $X_1 \geq X_2 \geq X_3 \equiv R$ . Temperature or enthalpy distribution along the coordinate  $\xi$ , related to the half of the smallest characteristic body dimension  $X_3 \equiv R$ , represents the greatest interest for food engineering investigations.

The idea of the quasi-one-dimensional approach is

based on the possibility of finding, for such a defined multidimensional body, an interpolation parameter  $\Gamma$ , which, upon substitution into the governing Equation (2) and in the one-dimensional solution, Equations (3)–(6), ensures numerical results coinciding or satisfactorily close to those, obtained by solution of the corresponding multidimensional problem. Since the geometric factor chosen by this criterion guarantees the simultaneous (homochronic) development of the obtained (by one- or multidimensional techniques) temperature (or enthalpy) histories of the points along the axis  $\xi$ , it is called the 'homochronomy factor'. If these factors are equal for each  $\xi$ , they are global, while if they pertain only to a fixed  $\xi$  they are local.

In a number of cases with practical importance, by means of the shape coefficient  $\Phi$ , global or local homochronomy factors could easily be determined<sup>35–39</sup>:

$$\Gamma = \frac{1}{\Phi} - 1 = \frac{S \cdot R}{V} - 1 \quad (7)$$

while some situations require deduction of special relations for  $\Gamma$ <sup>37</sup>. As is well known, for classical one-dimensional bodies (an infinite slab, an infinite cylinder and a sphere),  $\Phi$  is equal to 1,  $\frac{1}{2}$  or  $\frac{1}{3}$  respectively. In refs 37 and 38, by using the linear quantities  $X_1$ ,  $X_2$  and  $X_3$ , analytical formulae are presented for determination of  $\Phi$  and of global and local  $\Gamma$ -values for two- and three-dimensional objects of diverse configurations (infinite rectangular prism; parallelepiped; infinite or finite rhombic prism, circular and elliptic cylinders; triplex-axis ellipsoid and octahedron; etc.). For irregular shapes, close to the defined above, which defy an exact mathematical description, the value of  $\Phi$  may be determined by statistical treatment of the experimental data<sup>38</sup>.

In this way the multidimensional problem is reduced to a one-dimensional one, and the range of applications of the obtained solution widens significantly, covering solids with various and complicated configuration. Moreover, such quasi-one-dimensional approximation allows the multidimensional bodies not to be treated by time- and computer-memory-wasting models with two or three spatial variables.

### Algorithmization

Algorithms for direct implementation of the created model as a computer program were developed. For their use the functions  $\mathcal{H} = \mathcal{H}(t)$ ,  $t = t(\mathcal{H})$  and  $E = E(t)$  must be determined on the basis of the input data for  $c(t)$ ,  $\rho(t)$  and  $\lambda(t)$ . A very effective computational procedure, allowing significant decrease in the required memory and drastic reduction of the computing time, may be fulfilled, if beforehand the relationship between the Kirchoff function and the volumetric specific enthalpy  $E = E(\mathcal{H})$  is constructed. For the Karlsruhe test substance this was determined by the author and is shown in Figure 5. In such a manner, after one determines also the function  $\omega(\mathcal{H})$ , the calculations may be carried out using quite an economical algorithm, by which one finds the enthalpy field and directly the field of  $E$ , without the compulsory recovery of the internal point temperatures for each new time level. The passage from  $\mathcal{H}$  to  $t$  may be performed only for those instants of

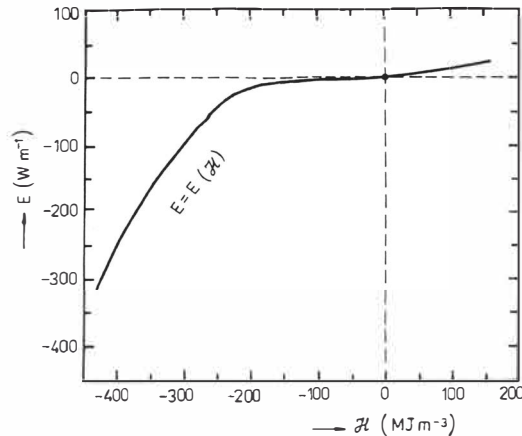


**Figure 5** Dependence between the Kirchhoff function and volumetric specific enthalpy for the Karlsruhe test substance

Figure 5 Dépendance entre la fonction de Kirchhoff et l'enthalpie volumique pour la substance d'épreuve de Karlsruhe

process development, at which the temperature distribution represents a special user interest.

### Experimental verification

For verification of the obtained numerical results some available analytical solutions were used<sup>40</sup>, which, however, refer to quite simplified idealized conditions and are not sufficient for testing of the model, especially for that variety of situations where it fully reveals its true advantages. That is why, in order to demonstrate to a maximum degree the model's abilities, a multichannel microcomputer cryosystem and its servicing software were created (Figure 6) for automated experimental determination of unsteady-state temperature fields in food materials and sample bodies from reference test substances. A series of investigations were effectuated on a great multitude of cooling and freezing regimes, resembling real industrial modes of refrigeration processing. Custom-made sample bodies from the Karlsruhe test substance with different shape (parallelepipeds, finite elliptic cylinders, triple-axis octahedrons, etc.) were used. The initial temperature state of the objects was very different, and during the process the temperature of refrigerating air medium was varied in a wide interval (down to  $-180^{\circ}\text{C}$ ) according to diverse patterns of change. In addition, experiments were accomplished by direct immersion in liquid nitrogen boiling at  $-195.8^{\circ}\text{C}$  – a case when the heat transfer coefficient strongly depends on the difference between the body surface and the ambient temperatures. The performed comparisons between the numerical and real experiments showed a very good coincidence of the results. As an illustration, Figure 7 shows a comparison between the theoretical and experimental time-temperature curves for one of the studied deep-freezing processes in air ambient<sup>37</sup>.

### Conclusions

The proposed enthalpy formulation and numerical solution have significant advantages in comparison

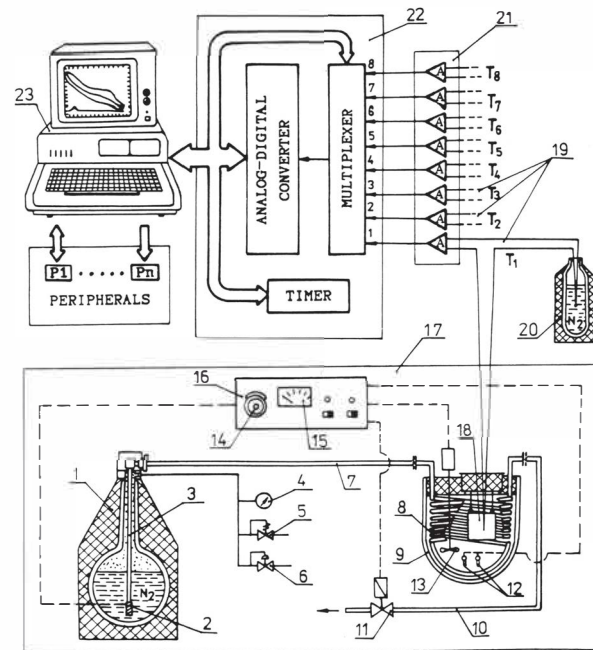


**Figure 6** Automated multichannel microcomputer cryosystem for experimental determination of unsteady-state temperature fields: 1, Dewar vessel with liquid nitrogen; 2, electric heater; 3, feed pipe; 4, manometer; 5 and 6, control and relief valves; 7, inlet pipe; 8, coiled tube evaporator of liquid nitrogen; 9, experimental cryocompartment with Dewar insulation; 10, outlet pipe; 11, solenoid valve; 12, platinum resistance thermosensors; 13, fan; 14, temperature regime regulator; 15, magnetic system with temperature scale; 16, control block; 17, Ultra-Cryostat type N180; 18, studied object; 19, thermocouples; 20, Dewar vessel with liquid nitrogen for the cold reference ends of the thermocouples; 21, multichannel analog input preamplifier; 22, device for input/output of information; 23, personal microcomputer

Figure 6 Cryosystème multicanal à microordinateur pour la détermination expérimentale automatisée des champs de température en régime non-stationnaire: 1, vase Dewar à azote liquide; 2, réchauffeur électrique; 3, tube d'alimentation; 4, manomètre; 5 et 6, robinets de réglage et de décharge; 7, tube d'entrée; 8, serpentins tubulaire-évaporateur d'azote liquide; 9, cryocompartiment d'expérience à isolation de Dewar; 10, tube de sortie; 11, robinet solénoïde; 12, thermosenseurs de platine à résistance; 13, ventilateur; 14, régulateur du régime de température; 15, système magnétique à échelle de température; 16, bloc de contrôle; 17, Ultra-Cryostat type N180; 18, objet étudié; 19, thermocouples; 20, vase Dewar à azote liquide pour les extrémités de référence froides des thermocouples; 21, préamplificateur d'entrée analogique multivoie; 22, module d'entrée-sortie d'information; 23, microordinateur personnel

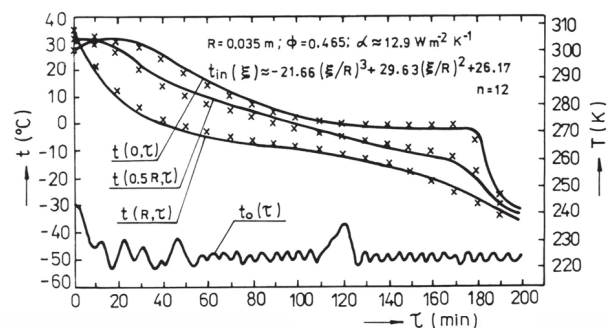


**Figure 7** Theoretical (x) and experimental (—) time-temperature curves during freezing of a finite elliptic cylinder from Karlsruhe test substance

Figure 7 Courbes temps-température théoriques (x) et expérimentales (—) pendant la congélation d'un cylindre elliptique fini de la substance d'épreuve de Karlsruhe



with other analytical and numerical approaches for determination of unsteady temperature fields in systems of bodies with moving boundaries and of the duration of freezing and thawing processes:

1. A greater degree of correspondence is achieved between the real physical phenomenon and its mathematical formalization. It is taken into account that the phase transformation of water, contained in the food substances, is not accomplished isothermally, but in the interval from cryoscopic to cryohydric temperature; that there is a 'spread', but not sharply outlined, phase-change front; and that the whole latent heat is not released or absorbed suddenly and at once on the moving cryoscopic isothermal interfaces, but in the entire phase transition region.

2. The numerical modelling is freed from the significant difficulties caused by the necessity to continuously trace the phase-change interface position. The processes of freezing/thawing are not treated by combining individual mathematical descriptions for their constituting periods and for the separate (being in a different physical state) regions, but through a single universal approach. Both the cooling/heating and freezing/thawing processes may be analysed by a unified method, and the numerical solution could be accomplished using single-type uniform finite-difference grids in the whole studied space-time domain.

3. It avoids the necessity of iteration cycles for evaluation of the thermophysical characteristics and heat transfer coefficient values after each time step together with the new moment temperatures, as well as of an averaging of the thermal conductivity for the current layers (space increments). The quite complicated highly non-linear problem is solved by a comparatively simple, explicit finite-difference scheme, that is non-iterative and linear in regards to enthalpy at the new time level.

4. The applied enthalpy formulation almost completely eliminates the possibility of 'jumping' of the latent heat-caused ESHC peak and of the appearance of oscillations in the solution. Therefore, the approach used in the present work makes unnecessary all complications of the type of Equations (1.7)–(1.9), whose application is connected with additional calculations and hence with error accumulation. Instead of functions  $c(t)\rho(t)$  and  $\lambda(t)$ , the first of which has a first kind (jump-type) discontinuity at the cryoscopic point and the second is not smooth in the whole temperature interval (Figures 1 and 3), one works with  $\mathcal{H}(t)$  and  $E(t)$ , representing continuous and smooth functions respectively (Figures 2 and 4). All this exerts a very beneficial influence on the computational properties of the finite-difference scheme.

5. Although the enthalpy method is the most powerful means for overcoming the 'jumping' effect, for highly moisture-containing objects (having a narrow temperature range of intensive phase transformation) a significant diminishing of the finite-difference grid sizes is required in all cases and therefore the main advantage of the implicit schemes – the possibility of large time steps – is lost to a considerable degree. The employed explicit non-iterative finite-difference scheme becomes comparable with them and fully competitive from the point of view of the computing time spent, especially if the  $E = E(\mathcal{H})$  relation is used directly (Figure 5).

6. Because the unsteady-state enthalpy fields  $\mathcal{H}(\xi, \tau)$  are handled directly, the energy analysis of the investigated technological processes is made significantly easier.

7. The developed generalized model possesses a high degree of universality. Some previous unified results of Fikiin<sup>35,38,39</sup>, as well as a number of solutions by other authors (see, for example, ref. 1), could be interpreted as its isolated cases. Moreover, to our knowledge, up to now there are no other numerical solutions of nonlinear problems, involving unsteady phase-change heat conduction in moisture containing food systems, performed by simultaneous application of Goodman and Kirchhoff type transforms and the quasi-one-dimensional approach.

Obviously, the presented enthalpy method is a reliable theoretical basis for description and prediction of complicated refrigeration and thermal processes, and therefore for the design, construction, optimization (according to the technological and energy criteria), control and effective operation of refrigeration systems in food and biotechnological industries. This gives reason to recommend its wider future application in combination with various FDM, FEM and BEM computational techniques.

#### Acknowledgement

The author is grateful to Associate Professor Dr Ratcho Ivanov from the Electronic Engineering Department, Technical University of Sofia, for his methodological help in the automation of the experimental set-up.

#### References

1. **Aliamovskij, I. G., Geintz, R. G., Golovkin, N. A., Loginov, L. I., Ushkov, P. P.** *Analytical Studies of Technological Processes of Meat Refrigeration Treatment* CNIITEI Press, Moscow (1970) (in Russian)
2. **Comini, G., Nonino, C., Saro, O.** Performance of enthalpy-based algorithms for isothermal phase change *Advanced Computational Methods in Heat Transfer*, Vol. 3: *Phase Change and Combustion Simulation*: L. C. Wrobel, C. A. Brebbia and A. J. Nowak (eds) Computational Mechanics Publications, Southampton & Springer-Verlag, Berlin (1990) 3–13
3. **Jarny, Y., Delaunay, D.** Numerical resolution of a phase change problem with zero latent heat *Numer Heat Transfer, Part B* (1989) **16** 125–141
4. **Tikhonov, A. N., Samarskij, A. A.** *Equations of Mathematical Physics* Science, Moscow (1972) (in Russian)
5. **Samarskij, A. A.** *Theory of Finite-Difference Schemes* Science, Moscow (1983) (in Russian)
6. **Bonacina, C., Comini, G.** On a numerical method for the solution of the unsteady state heat conduction equation with temperature dependent parameters *Proc XIII<sup>th</sup> Int Cong Refrigeration* Washington DC, USA (1971) **2** 329–336
7. **Bonacina, C., Comini, G., Fasano, A., Primicerio, M.** Numerical solution of phase-change problems *Int J Heat Mass Transfer* (1973) **16** 1825–1832
8. **Cleland, A. C., Earle, R. L.** Prediction of freezing times for foods in rectangular packages *Food Sci* (1979) **44** 964–970
9. **Cleland, D. J., Cleland, A. C.** An alternative direction, implicit finite difference scheme for heat conduction with phase change in finite cylinders *Proc XVIII<sup>th</sup> Int Cong Refrigeration* Montréal, Québec, Canada (1991) **4** 1855–1858
10. **Cleland, D. J., Cleland, A. C., Earle, R. L., Burne, S. J.** Prediction of rate of freezing, thawing and cooling in solids of arbitrary shape using the finite element method *Int J Refrig* (1984) **7** 6–13
11. **Comini, G., Saro, O.** Numerical modelling of freezing processes in foodstuffs *Computational Modelling of Free and Moving*

- Boundary Problems*, Vol. 2: *Heat Transfer*: L. C. Wrobel and C. A. Brebbia (eds), Computational Mechanics Publications, Southampton & Valter de Gruyter, Berlin (1991) 21–37
- 12 **Comini, G., Del Giudice, S., Saro, O.** A conservative algorithm for multidimensional conduction phase change *Int J Numer Methods Eng* (1990) **30** 697–709
- 13 **Hayakawa, K., Nonino, C., Succar, J., Comini, G., Del Giudice, S.** Two dimensional heat conduction in foods undergoing freezing: development of computerized model *J Food Sci* (1983) **48** 1849–1853
- 14 **Pham, Q. T.** The use of lumped capacitances in the finite-element solution of heat conduction with phase change *Int J Heat Mass Transfer* (1986) **29** 285–291
- 15 **Sheen, S., Hayakawa, K.** Finite difference simulation for heat conduction with phase change in an irregular food domain with volumetric change *Int J Heat Mass Transfer* (1991) **34** 1337–1346
- 16 **Wilson, H. A., Singh, R. P.** Numerical simulation of individual quick freezing of spherical foods *Int J Refrig* (1987) **10** 149–155
- 17 **Lees, M.** A linear three-level difference scheme for quasi-linear parabolic equations *Math Comput* (1966) **20** 516–522
- 18 **Comini, G., Del Giudice, S.** Thermal aspects of cryosurgery *Trans ASME, Ser C: J Heat Transfer* (1976) **98** 543–549
- 19 **Lewis, R. W., Morgan, K., Johnson, J. A., Smith, W. R. (eds)** *Computational Techniques in Heat Transfer* Pineridge Press, Swansea, UK (1985)
- 20 **Kozdoba, L. A.** *Methods for Solving Nonlinear Heat Conduction Problems* Science, Moscow (1975) (in Russian)
- 21 **Crank, J.** *Free and Moving Boundary Value Problems* Clarendon Press, Oxford (1984)
- 22 **Albasiny, E. L.** The solution of non-linear heat conduction problems on the pilot ACE *Proc IEE* (1956) **103(B)** 158–162
- 23 **Crowley, A. B.** Numerical solution of Stefan problems *Int J Heat Mass Transfer* (1978) **21** 215–219
- 24 **Dusinberre, G. M.** *Numerical Analysis of Heat Flow* McGraw-Hill Book Co., New York (1949)
- 25 **Eyres, N. R., Hartree, D. R., Ingham, J., Jackson, R., Sarjant, R. J., Wagstaffe, J. B.** The calculation of variable heat flow in solids *Phil Trans R Soc* (1946) **A 240** 1–57
- 26 **Hunter, L. W., Kuttler, J. R.** The enthalpy method for heat conduction problems with moving boundaries *Trans ASME Ser C: J Heat Transfer* (1989) **111** 239–242
- 27 **Kamenomostskaja, S. A.** On the Stefan problem *Mathematical Collection* (in Russian) (1961) **53/95** (4) 489–519
- 28 **Mannapperuma, J. D., Singh, R. P.** Prediction of freezing and thawing times of foods using a numerical method based on enthalpy formulation *J Food Sci* (1988) **53** 626–630
- 29 **Mannapperuma, J. D., Singh, R. P.** A computer-aided method for prediction of properties and freezing/thawing times of foods *J Food Eng* (1989) **9** 275–304
- 30 **Rose, M. E.** A method for calculating solutions of parabolic equations with a free boundary *Math Comput* (1960) **14** 249–256
- 31 **Shamsundar, N., Sparrow, E. M.** Analysis of multidimensional conduction phase change via the enthalpy model *Trans ASME, Ser C: J Heat Transfer* (1975) **97** 333–340
- 32 **Voller, V. R., Cross, M.** Accurate solutions of moving boundary problems using the enthalpy method *Int J Heat Mass Transfer* (1981) **24** 545–556
- 33 **Voller, V. R., Cross, M., Markatos, N. C.** An enthalpy method for convection/diffusion phase change *Int J Numer Methods Eng* (1987) **24** 271–284
- 34 **Fikiin, A. G.** *Refrigeration Technological Processes and Systems* “Technika” State Publishing Company, Sofia (1980) (in Bulgarian)
- 35 **Fikiin, K. A.** Solution numérique généralisée du problème de la conduction thermique dans les solides de diverse configuration lors d’un refroidissement convectif *Int J Refrig* (1992) **15** (4) 221–226
- 36 **Fikiin, K. A.** Nouvelles possibilités de détermination de la température moyenne et du changement d’enthalpie des solides de diverse configuration pendant leur refroidissement *Rev Gen Froid* (1991) (7) 58–64
- 37 **Fikiin, K. A.** Generalized physico-mathematical models of unsteady-state heat transfer during cooling and freezing of food materials and other solids. *Ph.D. Thesis* Bulgarian Academy of Sciences and Technical University, Sofia (1996)
- 38 **Fikiin, K. A., Fikiin, A. G.** Modèle numérique du refroidissement de matières alimentaires et d’autres corps solides de forme géométrique variée *Int J Refrig* (1989) **12** (4) 224–231
- 39 **Fikiin, K. A., Fikiin, A. G.** Dimensionless numerical model of refrigerating foodstuffs and other solid bodies. *Refriger Technol* (1989) (5) 28–34 (in Russian)
- 40 **Carslaw, H. S., Jaeger, J. C.** *Conduction of Heat in Solids* Clarendon Press, Oxford (1959)

## **CHAPTER 3**

**Enthalpy and Kirchhoff transform method  
for food refrigeration heat transfer:  
*finite-element formulation***

## Chapter 3

is a logical continuation of the previous Chapters 2 and 3. Analogously, the variables in the highly non-linear 3D heat transfer problem of food freezing or thawing are changed in a way that a single functional relationship between the volumetric specific enthalpy and the Kirchhoff function is further used to account for all non-linearities caused by the temperature-dependent thermophysical properties. Such a reformulation provides a convenient finite-element numerical solution, which eliminates the risk for missing the peak of apparent specific heat capacity and/or the abrupt change of thermal conductivity. Due to the linearisation of the transformed governing equation, the finite element matrices appear to be constant and have to be calculated only once.

This solution strategy saves substantial computational resources, as compared with the conventional FEM algorithms based on the original non-linear or enthalpy-transformed Fourier equation. A multi-optional FEM code was developed, comprising several automatic and fixed-step explicit and implicit time domain solvers, to predict the unsteady temperature and enthalpy distribution during freezing (thawing) of food materials of arbitrary 3D shape. Validating experiments with freezing Tylose (*Karlsruhe food simulator*) showed a good agreement with the model's predictions.

Findings reported in this chapter, which are a collective research endeavour with Belgian colleagues from the Catholic University of Leuven, were distinguished with the [Superior Paper Award 2001](#) of the *American Society of Agricultural and Biological Engineers (ASABE)*.

Achievements featured in Chapter 3 have also been used internationally (*click on the logos below to locate publications citing relevant results*):



Publications in English and Chinese languages, which cite Chapter 3, were detected. Both FDM and FEM algorithms, using the methodology in Chapters 1-3, demonstrate clear advantages over the conventional techniques employing an equivalent specific heat capacity or an enthalpy formulation alone. The enthalpy and Kirchhoff transform method permits to solve successfully a broad range of heat transfer problems for both food and non-food applications. Related contributions are original and unprecedented in the field of food engineering and food refrigeration in particular.





Reproduced from *Transactions of the ASAE*, Vol. 44, No. 2,  
Scheerlinck N., Verboven P., Fikiin K., De Baerdemaeker J. and Nicolai B.M.  
Finite-element computation of unsteady phase change heat transfer during  
freezing or thawing of food using a combined enthalpy and Kirchhoff  
transform method, pp. 429-438, doi: <https://doi.org/10.13031/2013.4671>,  
Copyright © 2001, with permission from the *American Society of Agricultural  
and Biological Engineers (ASABE)*

# FINITE ELEMENT COMPUTATION OF UNSTEADY PHASE CHANGE HEAT TRANSFER DURING FREEZING OR THAWING OF FOOD USING A COMBINED ENTHALPY AND KIRCHHOFF TRANSFORM METHOD

N. Scheerlinck, P. Verboven, K. A. Fikiin, J. De Baerdemaeker, B. M. Nicolai

**ABSTRACT.** *An improved finite element enthalpy method was developed and implemented for solving non-linear phase change heat transfer problems such as freezing or thawing of foods with arbitrary 3D geometries. By simultaneously applying the enthalpy and Kirchhoff transforms, all non-linearities caused by the temperature-dependent thermophysical properties were incorporated in a functional relationship between the volumetric specific enthalpy and the Kirchhoff function. Such a problem reformulation results in a much more convenient solution procedure and avoids the possibility of missing the apparent specific heat capacity peak and the abrupt thermal conductivity change. Algorithms for the finite element solution of the resulting transformed equation were developed and programmed in Matlab. As the transformed equation is linear, the finite element matrices are constant and have to be calculated only once. This greatly improves the execution speed of the code, as compared to traditional finite element algorithms based on the original non-linear or enthalpy-transformed Fourier equation. As a consequence, the method is well suited for computationally intensive applications, such as numerical optimization or Monte Carlo uncertainty propagation analysis, in which typically a large number of phase change heat transfer problems must be solved. As an illustration, the freezing of a cylinder filled with tylose was investigated. A good agreement between measurements and model predictions was obtained.*

**Keywords.** *Heat transfer, Phase changes, Finite element, Simulation, Enthalpy, Kirchhoff function.*

The numerical simulation of unsteady phase change heat transfer during freezing or thawing of foods has become a powerful tool for the proper management of the food cold chain. The accurate prediction of the instant temperature distribution in foods is an indispensable step to optimal control strategies and design of refrigeration systems, correct decision making, and improved product safety and quality. Because of the practical importance of these highly non-linear heat transfer problems, much research has been devoted to developing appropriate physical models and numerical techniques.

Heat conduction problems involving phase change — the so called “Stefan problems” — belong to a more general class of “free boundary” problems. A first group of numerical techniques for solving such Stefan problems is based on tracking the moving phase change boundary using complicated schemes for the localization of the interface

position at each time step (Crank, 1984). The different front tracking techniques are in general rather slow and lead to additional complications when multi-dimensional geometries are considered (Crank, 1984; Comini et al., 1990).

A second group of more flexible numerical techniques does not track directly the exact position of the moving phase change front. The effects of phase changes are incorporated in temperature-dependent thermophysical characteristics. Within this approach, the problem is reformulated and the governing equations, describing the thermophysical problem, are solved in a fixed domain. These techniques, involving an equivalent (apparent) specific heat capacity (ESHC), are in general advantageous in the development of reliable procedures for the solution of phase change problems (Bonacina and Comini, 1971; Tikhonov and Samarskij, 1972; Crank, 1984).

Numerical ESHC methods using invariable fixed grids were introduced for the first time in refrigeration technology by Bonacina and Comini (1971). The released or absorbed latent heat of phase change is there taken into account by an ESHC defined over a relatively small temperature range. This approach was further developed by various authors (Bonacina et al., 1973; Hayakawa et al., 1983; Pham, 1986; Comini et al., 1990; Cleland and Cleland, 1991; Comini and Saro, 1991). The space discretization of the resulting non-linear conduction heat transfer equation is usually performed by means of finite differences or finite elements, yielding a non-linear first-order differential system. Moreover, many special measures must be undertaken to avoid ESHC peak jumping and numerical oscillations.

The involvement of the enthalpy as a new dependent variable has been suggested by various authors to avoid the above problems (Tikhonov and Samarskij, 1972; Voller and Cross, 1981; Crank, 1984; Mannapperuma and Singh, 1988 and 1989). On the other hand, the whole governing heat equation may be reformulated in terms of the thermal

---

Article was submitted for review in January 1999; approved for publication by the Information & Electrical Technologies Division of ASAE October 2000. Presented at the 1997 ASAE Annual Meeting as Paper No. 97-6003.

The authors are **Nico Scheerlinck**, Graduate Research Assistant, Laboratory of Postharvest Technology, Dept. of Agro-Engineering and Economics, Katholieke Universiteit Leuven, Belgium; **Pieter Verboven**, Graduate Research Assistant, Laboratory of Postharvest Technology, Dept. of Agro-Engineering and Economics, Katholieke Universiteit Leuven, Belgium; **Kostadin A. Fikiin**, Research Assistant, Refrigeration Science and Technology Section, Technical University of Sofia, Bulgaria; **Josse De Baerdemaeker**, *ASAE Member Engineer*, Professor, Laboratory for Agro-Machinery and Processing, Department of Agro-Engineering and Economics, Katholieke Universiteit Leuven, Belgium; and **Bart Nicolai**, *ASAE Member Engineer*, Assistant Professor, Laboratory of Postharvest Technology, Department of Agro-Engineering and Economics, Katholieke Universiteit Leuven, Belgium **Corresponding author:** Nico Scheerlinck, Laboratory of Postharvest Technology, W. de Croylaan 42, B-3001 Leuven, Belgium; phone: +32-(0)16-322668; fax: +32-(0)16-322955; e-mail: nico.scheerlinck@agr.kuleuven.ac.be.

conductivity integral by means of the Kirchhoff function (Kamenomostskaja, 1961; Tikhonov and Samarskij, 1972). Several authors have combined the enthalpy and Kirchhoff transformations such that all non-linearities caused by the temperature dependent thermophysical properties are incorporated into a single functional relationship between the volumetric specific enthalpy and the thermal conductivity integral defined by the Kirchhoff function (Fikiin, 1996; Scheerlinck et al., 1997; Fikiin, 1998). In this method, inaccuracies caused by the jump of the thermal conductivity at the phase transition are avoided as well.

When the resulting transformed equation is numerically discretized by a finite element method, the resulting finite element matrices are constant. As a consequence, the execution speed can be enhanced considerably, which would be advantageous for applications which involve the consecutive solution of a large series of phase change problems, such as numerical optimization or Monte Carlo uncertainty propagation analysis of food freezing processes. However, so far these features have not been exploited in the literature. Further, other issues, such as the stability and accuracy of time discretization schemes for the enthalpy–Kirchhoff transformed Fourier equation, have not been addressed yet. As the resulting equations consist of one linear partial differential equation coupled to two non-linear algebraic equations, the numerical properties of the time discretization schemes are not necessarily equivalent compared to when they are applied to a linear or even non-linear spatially discretized Fourier equation, as is usually the case. Note that it has been pointed out that the selection of a transient solution algorithm for a non-linear thermal problem is not trivial (Huebner et al., 1995).

The objectives of the present work were:

- To develop and implement an efficient 3D finite element method to solve the enthalpy–Kirchhoff transformed heat conduction equation.
- To compare the execution speed of the code with that of the ESHC and enthalpy transform based code.
- To analyze the stability and accuracy of different time discretization schemes.
- To illustrate the applicability of the code to food freezing by means of a validated test case consisting of a cylindrical container filled with tylose.

## MATERIALS AND METHODS

### GOVERNING EQUATIONS AND CHANGE OF VARIABLES

Non-linear heat conduction problems involving phase changes with no internal heat generation can be described over some spatial domain  $\Omega$  by the heat equation:

$$\rho(T)c(T)\frac{\partial T}{\partial t} = \nabla \cdot [k(T)\nabla T] \quad (1)$$

where

- $\rho$  = density ( $\text{kg m}^{-3}$ )
- $c$  = apparent specific heat capacity ( $\text{J kg}^{-1} \text{ }^\circ\text{C}^{-1}$ )
- $k$  = thermal conductivity ( $\text{W m}^{-1} \text{ }^\circ\text{C}^{-1}$ )
- $T$  = temperature ( $^\circ\text{C}$ )
- $t$  = time (s)

The released or absorbed latent heat corresponding to the phase change is taken into account through the apparent specific heat capacity ( $c$ ). In this article, general three-dimensional geometries, defined in a 3D Cartesian coordinate system, are considered. The initial condition for equation 1 is:

$$T(x, y, z, t) = T_0(x, y, z) \quad \text{at } t = t_0 \quad (2)$$

where

$T_0$  = a known function

$t_0$  = initial time (s)

At the boundary surface of the freezing (thawing) object, convective boundary conditions are considered:

$$-k\frac{\partial T}{\partial n} = h_q(T - T_\infty) \quad \text{on } \Gamma_C \quad (3)$$

where

$T_\infty$  = ambient temperature ( $^\circ\text{C}$ )

$h_q$  = surface heat transfer coefficient ( $\text{W m}^{-2} \text{ }^\circ\text{C}^{-1}$ )

$n$  = outward normal to the surface

$\Gamma_C$  = convective boundary surface.

By performing a change of variables, the temperature-dependent density ( $\rho$ ) and apparent specific heat capacity ( $c$ ) in equation 1 can be removed through the introduction of the volumetric specific enthalpy ( $H$ ) (Comini et al., 1990):

$$H(T) = \int_{T^*}^T \rho(T) c(T) dT \quad (4)$$

where  $T^*$  is a suitably chosen reference temperature which corresponds to the zero value of  $H$ . Likewise, the temperature-dependent thermal conductivity ( $k$ ) can be removed through the thermal conductivity integral ( $E$ ) by using the Kirchhoff transformation (Comini et al., 1990; Saro et al., 1995; Fikiin, 1996):

$$E(T) = \int_{T^*}^T k(T) dT \quad (5)$$

Six relationships between the variables  $H$ ,  $E$ , and  $T$  are determined by equations 4 and 5:  $H(T)$ ,  $E(T)$ ,  $T(H)$ ,  $T(E)$ ,  $H(E)$ , and  $E(H)$ . All these functions are monotonic increasing and continuous because  $\rho$ ,  $c$ , and  $k$  are positive and bounded (Fikiin, 1996). Consequently, there exists a one-to-one mapping between the independent and dependent variables.

Substitution of equations 4 and 5 into equations 1, 2, and 3 results in a transformed partial differential system, in two mutually related dependent variables  $H$  and  $E$ :

$$\frac{\partial H}{\partial t} = \nabla^2 E \quad (6)$$

$$H(x, y, z, t) = H_0(x, y, z) \quad \text{at } t = t_0 \quad (7)$$

$$-\frac{\partial E}{\partial n} = h_q(T - T_\infty) \quad \text{on } \Gamma_C \quad (8)$$

where  $H_0 = H(T_0)$ . In this way, the non-linearities originating from the temperature-dependent thermophysical properties of the food material are removed from equations 1 through 3 and are incorporated in a functional relationship between the

volumetric specific enthalpy ( $H$ ) and the Kirchhoff function ( $E$ ).

**FINITE ELEMENT FORMULATION**

Because of the usual complicated shape of biological materials and the complex process conditions that can occur during refrigeration processing of foods, in general no analytical solutions are available for the partial differential system (eqs. 6–8). As a consequence, for most non-trivial phase change applications, numerical approximation techniques, such as the finite element method, are mandatory. Hereto, first a geometrical model of the food must be defined and subdivided into  $n_{el}$  elements of variable size and shape, which are interconnected in a finite number of nodes ( $n_{nod}$ ) (Zienkiewicz and Taylor, 1994). Subsequently, in every element the unknown functions  $H(x,y,z,t)$ ,  $E(x,y,z,t)$ , and  $T(x,y,z,t)$  are approximated by low-order interpolating polynomials. After applying the Galerkin weighted residual method, the following system is obtained:

$$C \frac{dh}{dt} + Ke + Fu = f \tag{9}$$

$$h(t = t_0) = h_0 \tag{10}$$

where

- $h, e,$  and  $u$  = vectors containing the nodal values of enthalpy, the Kirchhoff function, and temperature, respectively
- $C, K,$  and  $F$  = capacitance, conductance, and convection matrices, respectively
- $f$  = thermal load vector, which depends on the surface heat transfer coefficient and the ambient temperature.

It can be shown easily that, due to the simultaneous application of the enthalpy and the Kirchhoff transforms (eqs. 4 and 5), the non-linearities caused by the temperature-dependent thermophysical properties are eliminated from the capacitance and conductance matrices ( $C$  and  $K$ ). Consequently, these matrices remain constant and have to be calculated only once, which reduces the computer time significantly. If time-independent surface heat transfer coefficients are considered, the convection matrix ( $F$ ) also remains constant.

**TIME INTEGRATION**

The system of ordinary differential equations that results from the Galerkin finite element discretization of the Fourier equation is usually solved using an implicit or explicit Euler or trapezoidal finite difference scheme. The numerical properties of these schemes are well known. However, the time discretization of the enthalpy–Kirchhoff transformed Fourier equation leads to a vector differential equation (eqs. 9 and 10) in three unknowns ( $u, h,$  and  $e$ ), which are interrelated through non-linear algebraic functions. The corresponding algorithms are therefore more complicated, and their numerical properties have not been documented in the literature so far. Rather than limiting the analysis to the aforementioned finite difference schemes, three more general classes of time discretization, which include the above finite difference schemes, will be considered here.

The first class encompasses 1-step explicit Runge–Kutta methods of order  $r, r = 1$  to 4 [RK( $r$ )]:

$$h_{t+\Delta t} = h_t + \Delta t \sum_{i=1}^r \gamma_i z_i(t, h_t) \tag{11}$$

$$z_1(t, h) = -C^{-1} [Ke(h) + Fu(h) - f(t)] \tag{12}$$

$$i=2 \dots r \left\{ \begin{aligned} y_i(h) &= h + \Delta t \sum_{j=1}^{i-1} \beta_{i,j} z_j \\ z_i(t, h) &= -C^{-1} [Ke(y_i(h)) + Fu(y_i(h)) - f(t + \alpha_i \Delta t)] \end{aligned} \right. \tag{13}$$

where

- $\alpha_i, \beta_{i,j},$  and  $\gamma_i$  = coefficients related to a particular RK method (Lambert, 1991)
- $t$  = current time
- $\Delta t$  = time step.

The second class consists of the 1-step implicit trapezoidal rule of order 2 [TR(2)]:

$$\frac{C}{\Delta t} h_{t+\Delta t} =$$

$$\frac{C}{\Delta t} h_t - \frac{1}{2} [K(e_{t+\Delta t} + e_t) + F(u_{t+\Delta t} + u_t) - (f_{t+\Delta t} + f_t)] \tag{14}$$

The third class encompasses  $r$ -step implicit backward differentiation methods of order  $r, r = 1$  to 5 [BDF( $r$ )]:

$$\frac{C}{\beta_r \Delta t} h_{t+r\Delta t} =$$

$$-\frac{C}{\beta_r \Delta t} \left[ \sum_{i=0}^{r-1} \alpha_i h_{t+i\Delta t} \right] - Ke_{t+r\Delta t} - Fu_{t+r\Delta t} + f_{t+r\Delta t} \tag{15}$$

where  $\alpha_i$  and  $\beta_i$  are coefficients related to a particular BDF method (Lambert, 1991). Note that an  $r$ -step BDF method requires  $r$  starting values.

In this article, we will mainly focus on the general properties and performance of these schemes, when applied to equations 9 and 10. For a more rigorous treatment and theoretical considerations, refer to Lambert (1991).

For the explicit schemes (eqs. 11–13), the solution of an algebraic system at each time step can be avoided by lumping the capacitance matrix  $C$  to its diagonal form. From a computational point of view, the use of explicit schemes is then preferable, because only basic algebraic computations are needed to obtain a solution for  $h$ . The implicit schemes (eqs. 14 and 15), on the contrary, require more computational effort because at each time step a non-linear algebraic system has to be solved for the unknown  $h_{t+\Delta t}$  or  $h_{t+r\Delta t}$ . In this work, this is accomplished in an iterative way using a Newton–Raphson method (Lambert, 1991):

$$J^{[m]}(\Delta h)^{[m+1]} = -r^{[m]} \tag{16}$$

$$h_{t+s\Delta t}^{[0]} = h_{t+(s-1)\Delta t} \tag{17}$$



$$\mathbf{h}_{t+s\Delta t}^{[m+1]} = \mathbf{h}_{t+s\Delta t}^{[m]} + (\Delta \mathbf{h})^{[m+1]} \quad (18)$$

where  $[m]$  is the iteration step,  $s = 1$  for TR(2), and  $s = r$  for BDF( $r$ ). The Jacobian matrix ( $\mathbf{J}$ ) and the residual vector ( $\mathbf{r}$ ) for the TR(2) are computed as follows:

$$\mathbf{J} = \frac{\mathbf{C}}{\Delta t} + \frac{1}{2} \left[ \mathbf{K} \frac{\partial \mathbf{e}}{\partial \mathbf{h}} + \mathbf{F} \frac{\partial \mathbf{u}}{\partial \mathbf{h}} \right] \quad (19)$$

$$\mathbf{r} = \frac{\mathbf{C}}{\Delta t} (\mathbf{h}_{t+\Delta t} - \mathbf{h}_t) + \frac{1}{2} [\mathbf{K}(\mathbf{e}_{t+\Delta t} + \mathbf{e}_t) + \mathbf{F}(\mathbf{u}_{t+\Delta t} + \mathbf{u}_t) - (\mathbf{f}_{t+\Delta t} + \mathbf{f}_t)] \quad (20)$$

and for a BDF( $r$ ) method:

$$\mathbf{J} = \frac{\mathbf{C}}{\beta_r \Delta t} + \mathbf{K} \frac{\partial \mathbf{e}}{\partial \mathbf{h}} + \mathbf{F} \frac{\partial \mathbf{u}}{\partial \mathbf{h}} \quad (21)$$

$$\mathbf{r} = \frac{\mathbf{C}}{\beta_r \Delta t} \left[ \mathbf{h}_{t+r\Delta t} + \sum_{i=0}^{r-1} \alpha_i \mathbf{h}_{t+i\Delta t} \right] + \mathbf{K} \mathbf{e}_{t+r\Delta t} + \mathbf{F} \mathbf{u}_{t+r\Delta t} - \mathbf{f}_{t+r\Delta t} \quad (22)$$

The iterative process continues until a user-specified tolerance for  $\Delta \mathbf{h}$  is reached. In order to decrease the number of triangulations for solving the algebraic system (eq. 16) by means of a sparse Gaussian elimination algorithm, a modified Newton-Raphson method is used. This implies that the Jacobian matrix ( $\mathbf{J}$ ) is held constant within one or over several time step calculations. The computational effort related to the assembly of the Jacobian matrix ( $\mathbf{J}$ ) and the residual vector ( $\mathbf{r}$ ) can be minimized in an efficient way by exploiting the fact that  $\mathbf{K}$  and  $\mathbf{C}$  are constant and must only be assembled once.

To solve equations 11, 14, and 15 for the unknown nodal vector  $\mathbf{h}_{t+\Delta t}$  or  $\mathbf{h}_{t+r\Delta t}$ , the functional relationships between the volumetric specific enthalpy ( $H$ ), the Kirchhoff function ( $E$ ), and temperature ( $T$ ) are required. Based on the input data for  $c(T)$ ,  $\rho(T)$ , and  $k(T)$ , the functions  $H(T)$ ,  $E(T)$ , and  $T(H)$  can be calculated in advance by means of numerical integration techniques (Press et al., 1992). From these calculations, the functional relationship between  $H$  and  $E$  is deduced. The function  $T(H)$  is used to recover the temperature distribution. The derivatives of the functions  $E$  and  $T$  with respect to  $H$ , which are required to evaluate the Jacobian matrix ( $\mathbf{J}$ ), are computed by numerical differentiation (Press et al., 1992). The global algorithm for solving the finite element system (eqs. 9 and 10) can be summarized as follows:

**Global algorithm for solving non-linear heat transfer problems with phase changes using a finite element enthalpy method in combination with the Kirchhoff transform:**

**Step 1.** Compute  $H = H(T)$ ,  $E = E(T)$ ,  $E = E(H)$ ,  $T = T(H)$ ,  $\partial E / \partial H$ ,  $\partial T / \partial H$  based on the input data for  $\rho(T)$ ,  $c(T)$ , and  $k(T)$ .

**Step 2.** Compute the system matrices  $\mathbf{C}$ ,  $\mathbf{K}$ , and  $\mathbf{F}$ .

**Step 3.** Set the initial conditions (eq. 10) and choose an explicit or implicit method for solving the obtained finite element system (eqs. 9 and 10).

**Step 4a.** In case of Runge-Kutta methods: for each time step compute  $\mathbf{h}_{t+\Delta t}$  from equations 11–13.

**Step 4b.** In case of the Trapezoidal rule or BDF methods: for each time step compute  $\mathbf{J}(\mathbf{h})$  from equation 19 or 21, triangulate  $\mathbf{J}$ , and solve equations 16–18 until a user-specified tolerance for the absolute or relative norm of  $\Delta \mathbf{h}_{t+\Delta t}$  or  $\Delta \mathbf{h}_{t+r\Delta t}$  is reached.

**Step 5.** Calculate the temperatures from  $\mathbf{h}(t)$  and  $T(H)$  at the required time instances.

Whereas RK methods and the TR are self-starting, 1-step methods (no starting data beyond the given initial condition is needed), the BDF methods are not. An  $r$ -step BDF method is of order  $r$  but requires  $r$  starting values. These starting values are computed by using lower step BDF methods.

The choice of the time step is an important matter in any of the aforementioned finite difference schemes. The time step ( $\Delta t$ ) should not be too small, to avoid excessively many steps and corresponding round-off error accumulation. However,  $\Delta t$  should not be too large, either, to avoid a large truncation error per step and to ensure the stability of the computational process. It is known from linear stability theory that RK methods have very small and closed regions of absolute stability, which means that their use is highly restricted to the chosen time step (Lambert, 1991). The implicit TR and BDF methods, on the contrary, have stability regions that are spread out over the entire negative part of the complex plane and require no specific conditions for the time step. The BDF(1) method and TR(2) in particular are most preferable in terms of stability requirements combined with their accuracy and 1-step characteristic. Whether these properties can be extended to the solution in the time domain of the equations which result from applying the enthalpy method in combination with the Kirchhoff transform and subsequent finite element spatial discretization will be investigated below.

One fact that has clearly emerged from the extensive computational experience that has accumulated over the years is that the key to high efficiency in time-domain finite difference algorithms is the capacity to vary automatically not only the time step ( $\Delta t$ ), but also the order of the methods employed. Due to the high computational cost, automatic time-domain finite difference algorithms do not normally test to see whether the condition of absolute stability is satisfied for a given time step. These algorithms rely on the fact that if such a condition is not satisfied, then the error estimate will grow sharply, and the algorithm will then take appropriate action. In this work, the performance of five automatic time-domain finite difference algorithms (based on RK, TR, and BDF methods) for the solution of the non-linear system (eqs. 9 and 10) will be investigated and compared with the performance of the aforementioned fixed time step algorithms.

Efficient algorithms for general 3D, 2D, 2D-axisymmetric, and 1D non-linear heat transfer problems with phase changes, using the above-presented finite element enthalpy method and solution procedures, were developed and implemented in Matlab (The MathWorks, Inc., Natick, Massachusetts). A user-specified option for isoparametric

linear and quadratic lines, triangles, quadrilaterals, tetrahedrons, and hexahedrons was provided. Appropriate reordering algorithms were used to minimize the bandwidth of the sparsely structured finite element system matrices (Matlab, 1993). Automatic integration of the finite element system (eqs. 9 and 10) was performed by means of standard Matlab routines: ODE23, ODE45, ODE23t, and ODE15s (Dormand and Prince, 1980; Bogacki and Shampine, 1989; Shampine and Reichelt, 1997). All algorithms were programmed and executed on an HP-UX-9000 workstation.

### TEST MATERIAL

For the numerical simulations and the validation experiment, the freezing of a food model system consisting of the Karlsruhe test substance, a methyl-hydroxy-ethyl-cellulose water gel (23% Tylose MH 1000 and 77% water in mass) was considered. In the literature, several non-linear enthalpy-based heat transfer models have been validated successfully using this kind of food model substance (Cleland and Cleland, 1991; Fikiin, 1996). The temperature dependent thermophysical properties ( $\rho$ ,  $c$ , and  $k$ ) were obtained from Fikiin (1996). From these input data, the functions  $H = H(T)$ ,  $E = E(T)$ , and  $E = E(H)$  were computed using numerical integration schemes with a reference temperature ( $T^*$ ) of  $0^\circ\text{C}$ . As an illustration, the function  $E = E(H)$  is shown in figure 1. Note that the actual choice of the reference temperature is arbitrary.

## RESULTS AND DISCUSSION

### CODE VALIDATION

In a first stage, the finite element implementation was validated. Hereto, the numerical results for simple linear heat conduction problems (slab, cylinder, sphere, etc.) were compared favorably to analytical solutions (results not shown). Next, in order to validate the code for 3D phase change problems, the finite element code for non-linear heat transfer was tested for complex 3D geometries and process conditions by comparing the results with those obtained by means of a commercial finite element code, ANSYS (ANSYS, Inc., Canonsburg, Pennsylvania), which uses an enthalpy method without the Kirchhoff transformation approach. Hereto, the freezing of an ellipsoid made of tylose

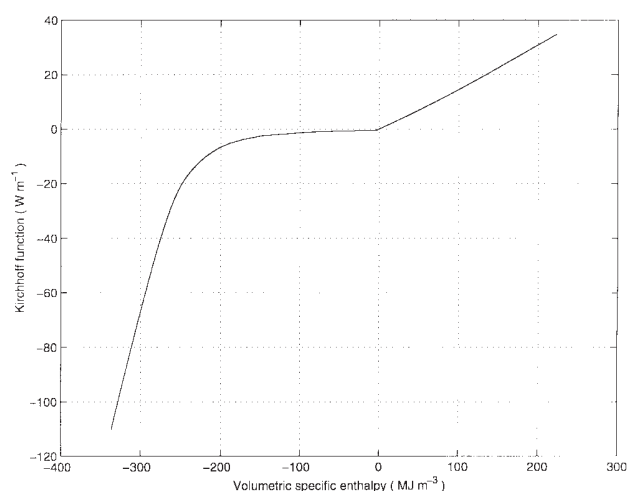


**Figure 1. Computed functional relationship between the Kirchhoff function and the volumetric specific enthalpy for the Karlsruhe test substance. Data for  $\rho c$  and  $k$  were obtained from Fikiin (1996).**

with major radii equal to 5 mm, 10 mm, and 15 mm was considered. The initial temperature was equal to  $24^\circ\text{C}$ , the temperature of the freezing medium was set at  $-16.5^\circ\text{C}$ , and the surface heat transfer coefficient was equal to  $250\text{ W m}^{-2}\text{C}^{-1}$ . The final time was equal to 10 minutes. The ellipsoid was meshed with linear tetrahedrons, and the resulting finite element mesh is shown in figure 2. The mesh consisted of 1,879 elements and 491 nodes. An automatic BDF(1) method was used to solve the finite element system in the time-domain.

The temperature course at three positions inside the ellipsoid along the smallest radius (5 mm) was calculated by means of the developed code and compared with that calculated using ANSYS. The results are shown in figure 3. It is clear that there is a very good agreement between the results obtained using both codes. The ANSYS code was executed on a RS-6000 node of an IBM-SP2 computer, and the CPU time for solving the non-linear heat transfer problem amounted to 1,122 s. The CPU time for solving the problem with our own code was 254 s. This indicates that the enthalpy method in combination with the Kirchhoff transformation approach (home made FEM code), executes much faster than when an enthalpy-only method is used (ANSYS code).

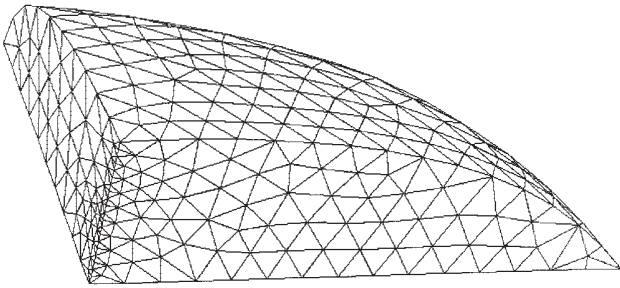


Figure 2. Finite element mesh for an ellipsoid made of tylose with major radii equal to 5 mm, 10 mm, and 15 mm (number of linear tetrahedral elements = 1,879; number of nodes = 491).

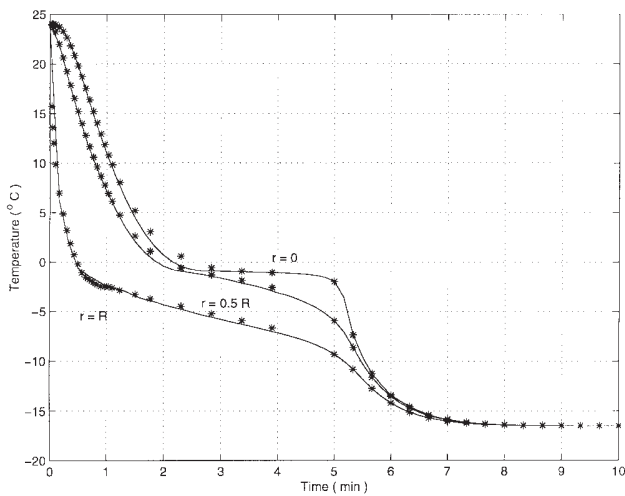


Figure 3. Simulation results for the freezing of an ellipsoid made of tylose: line = home made FEM code; \* = ANSYS code; R = smallest radius of ellipsoid.

VALIDATION EXPERIMENT

For the validation experiment a cylinder made of copper (inner radius 16.5 mm, inner height 32 mm) was filled with the Karlsruhe test substance. The latter was produced by mixing tylose (Hoechst Benelux Industry, Brussels, Belgium) with de-ionized water. The cylinder was submerged in a ternary refrigerant (15% glucose, 25% ethanol and 60% water) at a temperature of  $-16.5^{\circ}\text{C}$  in a Haake F6 cryostate (Gebrüder Haake GmbH, Karlsruhe, Germany). The freezing temperature of the Karlsruhe test substance was determined and found equal to  $-1.3^{\circ}\text{C}$ . This is sufficiently close to the freezing temperature of  $-1^{\circ}\text{C}$  reported in the literature (Fikiin, 1996), given the accuracy of the measurement setup ( $0.4^{\circ}\text{C}$ ). The experimental setup is shown in figure 4.

During freezing, the temperature was measured at several positions inside the cylinder, at the outer surface of the cylinder, and in the refrigerant around the cylinder. For this purpose, calibrated type-T Teflon-insulated thermocouples with a diameter of 0.2 mm (Omega Engineering, Inc., Stamford, Connecticut) were used. The thermocouples were connected to an HP 34970A data acquisition system, which was interfaced to a personal computer and controlled by

product-accompanied software. Inside the cylindrical container filled with tylose, the temperature was measured at positions along the diameter at the horizontal center of the cylinder (see figure 4).

Because of the axial symmetry, a 2D mesh of 400 linear quadrilateral elements with 441 nodes was used for the simulations. The final time was equal to 1,600 s, and the surface heat transfer coefficient was estimated by fitting measured to computed temperatures and found equal to  $250\text{ W m}^{-2}\text{ }^{\circ}\text{C}^{-1}$ . The measured and calculated temperatures are compared in figure 5. It is clear that the fit is excellent. The root mean squared error (RMSE) between the measured

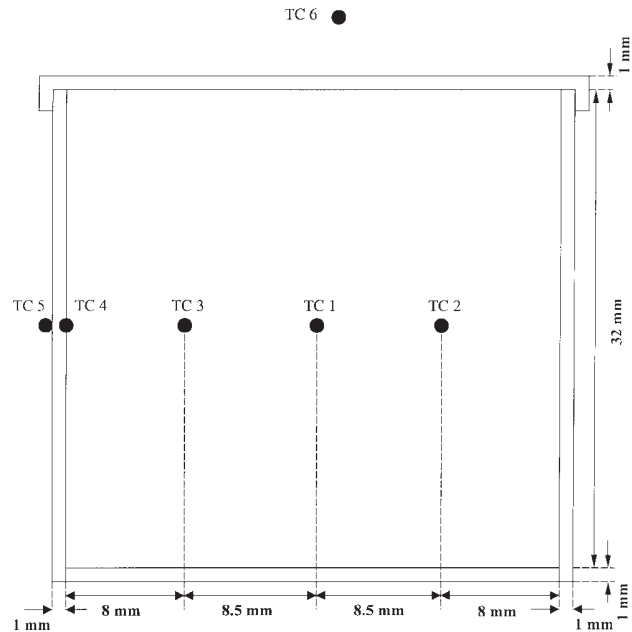


Figure 4. Experimental setup for the freezing of a copper container filled with tylose (TC = thermocouple).

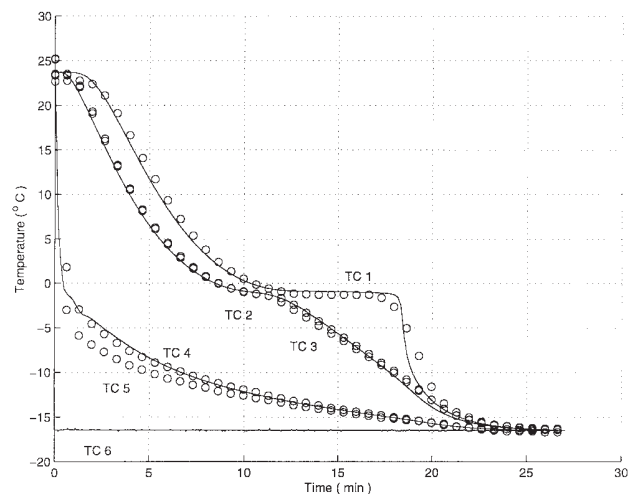


Figure 5. Measured and simulated temperatures at several positions in a copper container filled with tylose: line = simulation; circle = measurement; TC = position of thermocouple. RMSE =  $1.2^{\circ}\text{C}$ .



and calculated temperatures was 1.2°C, which is acceptable for this type of application and proves the validity of the heat transfer model.

**COMPARISON OF ALGORITHMS**

In order to compare the efficiency and accuracy of different algorithms (ESHC, enthalpy transform only, and combined enthalpy–Kirchhoff transform), a series of simulations based on the measurement setup used for the validation experiment was carried out. The mesh consisted of 400 quadrilateral elements with 441 nodes. For the ESHC and enthalpy transform methods, it was assumed that the thermophysical properties are constant in an element. In all algorithms, the time discretization was achieved by means of an automatic BDF algorithm of order 5. The temperature

course at the three different positions inside the cylinder is shown in figure 6 for the three algorithms. It can be observed that the enthalpy–only and the enthalpy–Kirchhoff transform algorithms give comparable results. However, at the early stage of the freezing process, the temperature at the boundary of the cylinder, as calculated by means of the ESHC method, is unstable and quite different from the temperature calculated with the other algorithms.

In table 1, the CPU time and the number of floating point operations (FLOPS) are compared for the different algorithms. It is clear that the combined enthalpy–Kirchhoff transform method is by far the most efficient algorithm. Observe that the CPU time is not always proportional to the number of FLOPS, which is due to the fact that user–programmed loops are executed very slowly in the Matlab environment. It is emphasized that the number of FLOPS is the most relevant measure of execution speed.

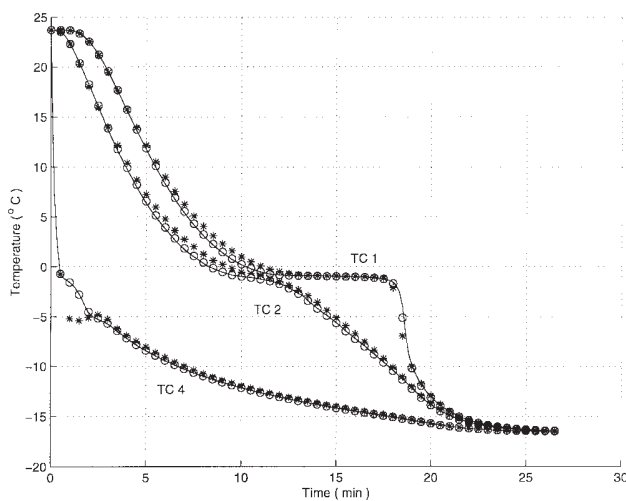


**Figure 6.** Simulation results for the freezing of a copper container filled with tylose using three different finite element methods. line = enthalpy–Kirchhoff transform method; circle = enthalpy transform method; \* = ESHC method.

**Table 1.** Computational effort for ESHC, enthalpy–only, and enthalpy–Kirchhoff methods applied to the freezing of a copper container filled with tylose<sup>[a]</sup>.

Method	NF	LU	Mega Flops	CPU
ESHC	4487	746	7557	22505
Enthalpy–only	4110	672	6840	20531
Enthalpy–Kirchhoff	3551	548	3936	880

<sup>[a]</sup> NF = Number of function evaluations  
 LU = Number of LU decompositions  
 Mega flops = Number of floating point operations (unit = 10<sup>6</sup>)  
 CPU = Computation time (in s).

**ANALYSIS OF TIME DISCRETIZATION SCHEMES**

The accuracy of the global finite element solution of equations 9 and 10 is a function of the accuracy of the finite element discretization as well as the accuracy obtained with the time–domain solver. In order to demonstrate the performance of the explicit and implicit finite difference schemes as described above, simulations were carried out for the finite element mesh of the copper container filled with tylose (CYLINDER) and the ellipsoid made of tylose (ELLIPSOID). The characteristics of the two finite element meshes and the parameters used to solve the heat transfer problems were the same as reported before.

Because in general no analytical solutions are available for the non–linear heat transfer problem with phase changes, an automatic BDF(5) method was used as a reference method for comparing different algorithms. The accuracy of a given method was estimated by computing the mean (ME) and root mean squared error (RMSE) of the error vector between the solutions obtained by means of the current method and the reference method. For implicit and automatic explicit schemes, the absolute and relative error tolerance for **h** was set to 10<sup>–4</sup>. The computational effort for the different automatic and fixed time step algorithms, which have been applied to solve the freezing problems CYLINDER and ELLIPSOID, are summarized in table 2. The timing results are shown in figure 7 and were normalized by dividing the actual CPU time by the time required to solve the problem with the reference time–domain method (automatic BDF(1)).

**Table 2.** Stability and computational effort of time discretization algorithms for the solution of the finite element differential system (eqs. 9–10)<sup>[a]</sup>.

Test Case	Method	Order	Δt	NF	LU	Stability	Mega Flops	ME	RMSE
C	BDF	1	Auto	9202	1903	Stable	12270	0.0075	0.0137
	BDF	5	Auto	3551	548	Stable	3936	Ref	Ref
Y	TR	2	Auto	2828	407	Stable	3035	0.0012	0.0023
L	RK	4–5	Auto	10033	0	Stable	260	0.0033	0.0062
I	RK	2–3	Auto	6505	0	Stable	152	0.0058	0.0116

N	BDF	1	2s	2232	1665	Stable	885	0.0235	0.0419
D	TR	2	2s	2077	1513	Stable	855	0.0031	0.0061
E	RK	4	2s	—	—	Unstable	—	—	—
R	BDF	1	10s	697	460	Stable	250	0.1233	0.1964
	TR	2	10s	654	654	Stable	251	0.0250	0.2372
	RK	4	10s	—	—	Unstable	—	—	—
E	BDF	1	Auto	623	97	Stable	1568	0.0545	0.0718
	BDF	5	Auto	502	79	Stable	1346	Ref	Ref
L	TR	2	Auto	471	83	Stable	1450	0.0079	0.0178
L	RK	4–5	Auto	—	—	Unstable	—	—	—
I	RK	2–3	Auto	—	—	Unstable	—	—	—
P	BDF	1	2s	1103	767	Stable	1651	0.0610	0.0850
S	TR	2	2s	1007	720	Stable	1583	0.0100	0.0198
O	RK	4	2s	—	—	Unstable	—	—	—
I	BDF	1	10s	320	320	Stable	673	0.3078	0.3807
D	TR	2	10s	349	349	Stable	751	0.0207	0.0387
	RK	4	10s	—	—	Unstable	—	—	—

[a] NF = Number of function evaluations  
 LU = Number of LU decompositions  
 Mega flops = Number of floating point operations (unit = 10<sup>6</sup>)  
 REF = Reference method  
 ME = Mean error  
 RMSE = Root mean squared error.

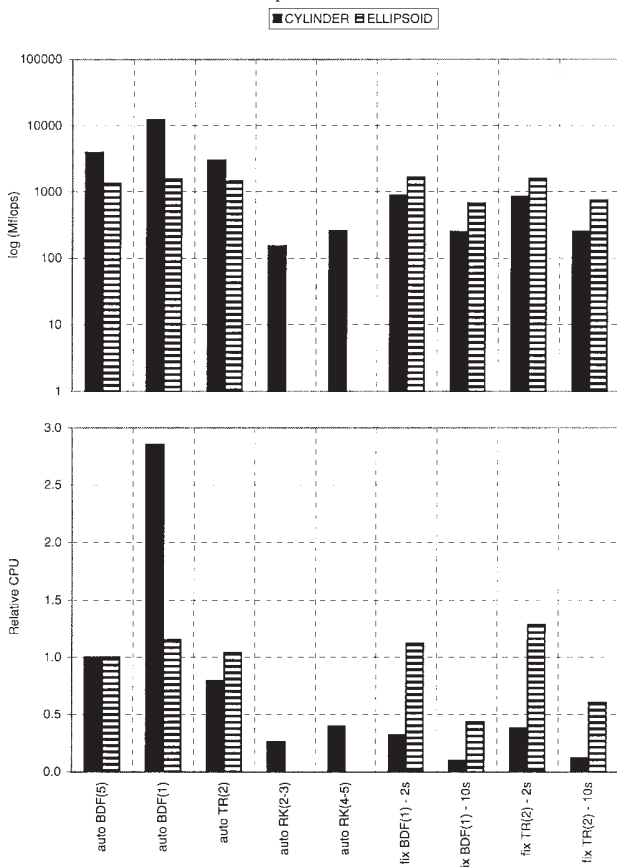


Figure 7. Relative CPU time and number of floating point operations for different time-domain finite difference schemes. The CPU time required for a simulation of the problem using the reference method is equal to unity.

For the CYLINDER test case involving automatic time-domain solvers, the RK methods are by far the fastest methods available. The computational effort related to an automatic BDF(1) is very large as compared to the other

automatic solvers, and the required CPU time is about three times larger than the automatic implicit schemes (BDF and TR). Among the tested solvers, the TR method is the most accurate scheme and performs better than the other implicit schemes in terms of execution speed. The fixed-step RK methods are unstable and are not useful for solving non-linear heat transfer problems. In contrast to the fixed-step RK methods, the fixed-step implicit methods are unconditionally stable, and hence, the use of much larger time steps is allowed. The fixed-step implicit schemes (BDF and TR) require computational efforts that are of the same order as for the automatic RK(4–5), but their execution speed is even faster than the speed of automatic RK solvers. For the CYLINDER test case, the automatic RK solvers are preferable in terms of computational performance; the fixed-step implicit schemes with larger time steps are competitive but are less accurate.

When automatic RK schemes are used for solving the ELLIPSOID test case, the solution becomes unstable in the early stages of integration, and the error controller is not able to perform appropriate actions to satisfy the stability requirements. This is because the degree of stiffness for the ELLIPSOID test case is much higher than for the CYLINDER test case. In general, non-linear heat transfer problems with phase changes are stiff problems, i.e., all eigenvalues of the Jacobian matrix of the finite element system (eq. 9) are negative, and the ratio of the maximum eigenvalue to the minimum eigenvalue is large. When the non-linear problem is of moderate stiffness, as in the case for the CYLINDER test case, automatic RK solvers seem capable of integrating the finite element system within the very hard stability conditions which are required, and their performance in terms of execution speed is much better than that of automatic solvers based on implicit algorithms.

For stiff problems, e.g., the ELLIPSOID test case, the computational efforts related to the automatic implicit algorithms are comparable. While the automatic TR is the most accurate method, the automatic BDF(5) performs slightly better in terms of computational effort and execution speed. The relative CPU time for the fixed-step implicit algorithms is much higher for stiff problems than for

problems of moderate stiffness, e.g., CYLINDER. This is because many more iterations are needed to meet the convergence criteria and stability requirements. Nevertheless, the fixed-step implicit solvers perform better than the automatic solvers when larger time steps are used. The use of fixed time step implicit solvers is recommended because the execution speed and computational effort can be reduced considerably, which is beneficial when the problem has to be solved many times, as is the case for design, optimization, and uncertainty propagation purposes.

## CONCLUSIONS

A multi-optional finite element code for non-linear heat transfer problems with phase changes using a functional relationship between the volumetric specific enthalpy and the Kirchhoff function was developed. The code incorporates several automatic and fixed-step explicit and implicit time domain solvers for predicting the unsteady temperature and enthalpy distribution during freezing (thawing) of food materials of arbitrary 3D shape.

The simultaneous application of the enthalpy and Kirchhoff transform methods is suitable for finite element computations because the non-linearities in the finite element system matrices can be eliminated. The constant properties and the sparse structure of these finite element system matrices are very useful from a computational point of view because they contribute to the development of very efficient algorithms. The resulting non-linear first-order differential system is then solved using the computed functional relationship between the volumetric specific enthalpy and the Kirchhoff function. It was shown that this solution strategy largely improves the execution speed compared to traditional finite element algorithms based on the original non-linear or enthalpy-transformed Fourier equation. To illustrate the applicability of the finite element enthalpy-Kirchhoff transform method to food freezing, the freezing of a cylinder filled with tylose was investigated. A good agreement between measurements and model predictions was obtained.

For the integration in the time domain, three classes of finite difference schemes were selected: explicit Runge-Kutta methods (RK), implicit backward differentiation methods (BDF), and the implicit trapezoidal rule (TR). Based on two test problems, it was shown that the stiffness of the problem determines the choice of automatic and fixed-step algorithms. When the non-linear heat transfer problem is of moderate stiffness, automatic RK methods perform much better in terms of computational effort and execution speed than automatic implicit schemes (BDF and TR). For stiff problems, the automatic RK solvers fail and become unstable. Combining accuracy, stability, and execution speed for time domain solvers, the BDF(5) and TR(2) in particular are most preferable for solving stiff non-linear transient finite element systems.

Although the computational cost is quite low, due to stability requirements the use of fixed-step explicit schemes (RK) is only possible with very small time steps. The performance of fixed-step implicit algorithms (BDF and TR) becomes very competitive and is even more beneficial over automatic solvers when the time step is fixed at relatively larger values. As a consequence, the finite element

enthalpy-Kirchhoff method in combination with fixed time step implicit solvers is well suited for computationally intensive applications, such as numerical optimization or Monte Carlo uncertainty propagation analysis, in which typically a large number of phase change heat transfer problems must be solved.

## ACKNOWLEDGEMENTS

The European Union (FAIR projects CT96-1192 and ERBIC15 CT98-0912, and PECO project CIPA CT93-0240) and the Flemish Minister of Science and Technology are gratefully acknowledged for their financial support. Author Nico Scheerlinck is Postdoctoral Fellow with the Research Fund of the Katholieke Universiteit Leuven. Author Pieter Verboven is Postdoctoral Fellow with the Flanders Fund for Scientific Research (F.W.O. Vlaanderen).

## REFERENCES

- Bogacki, P., and L. F. Shampine. 1989. A 3(2) pair of Runge-Kutta formulas. *Appl. Math. Letters* 2: 1-9.
- Bonacina, C., and G. Comini. 1971. On a numerical method for the solution of the unsteady state heat conduction equation with temperature dependent parameters. In *Proc. XIIIth Intl. Congress of Refrigeration*, 2: 329-336. Washington, D.C.: IIF/IIR.
- Bonacina, C., G. Comini, A. Fasano, and M. Primicerio. 1973. Numerical solution of phase-change problems. *Intl. J. Heat and Mass Transfer* 16: 1825-1832.
- Cleland, D. J., and A. C. Cleland. 1991. An alternating direction, implicit finite difference scheme for heat conduction with phase change in finite cylinders. In *Proc. XVIIIth Intl. Congress of Refrigeration* 4: 1855-1858. Montreal, Quebec: IIF/IIR.
- Comini, G., and O. Saro. 1991. Numerical modeling of freezing processes in foodstuffs. *Computational Modeling of Free and Moving Boundary Problems: Heat Transfer* 2: 21-37.
- Comini, G., C. Nonino, and O. Saro. 1990. Performance of enthalpy-based algorithms for isothermal phase change. *Advanced Computational Methods in Heat Transfer; Vol. 3: Phase Change and Combustion Simulation* 3: 3-13.
- Crank, J. 1984. *Free and Moving Boundary Value Problems*. Oxford, U.K.: Clarendon Press.
- Dormand, J. R., and P. J. Prince. 1980. A family of embedded Runge-Kutta formulae. *J. Computational and Appl. Math.* 6: 19-26.
- Fikiin, K. A. 1996. Generalized numerical modeling of unsteady heat transfer during cooling and freezing using an improved enthalpy method and quasi-one-dimensional formulation. *Intl. J. Refrigeration* 19(2): 132-140.
- \_\_\_\_\_. 1998. Some general principles in modeling of unsteady heat transfer in two-phase multi-component aqueous food systems for product quality improvement. In *Food Quality Modelling*, B. M. Nicolaï and J. De Baerdemaeker, eds., 179-186. Luxembourg: Office for Official Publications of the European Communities.
- Hayakawa, K., C. Nonino, J. Succar, G. Comini, and S. Del Giudice. 1983. Two dimensional heat conduction in foods undergoing freezing: Development of computerized model. *J. Food Sci.* 48: 1849-1853.
- Huebner, K. H., E. A. Thornton, and T. G. Byrom. 1995. *The Finite Element Method for Engineers*. 3rd ed. New York, N.Y.: John Wiley and Sons, Inc.
- Kamenomostskaja, S. A. 1961. On the Stefan problem. *Mathematical Collection* 53/95, No. 4: 489-519 (in Russian).
- Lambert, J. D. 1991. *Numerical Methods for Ordinary Differential Systems: The Initial Value Problem*. Chichester, U.K.: John Wiley and Sons, Ltd.

- Mannapperuma, J. D., and R. P. Singh 1988. Prediction of freezing and thawing times of foods using a numerical method based on enthalpy formulation. *J. Food Sci.* 53: 626–630.
- \_\_\_\_\_. 1989. A computer-aided method for prediction of properties and freezing/thawing times of foods. *J. Food Eng.* 9: 275–304.
- Matlab. 1993. *Matlab: High-Performance Numeric Computation and Visualization Software*. User's Guide. Natick, Mass.: The Math Works, Inc.
- Pham, Q. T. 1986. The use of lumped capacitances in the finite element solution of heat conduction with phase change. *Intl. J. Heat and Mass Transfer* 29: 285–291.
- Press, W. H., S. A. Teukolsky, W. T. Vetterling, and B. P. Flannery. 1992. *The Art of Scientific Computing, Vol. 3: Numerical Recipes in C*, 2nd ed. Cambridge, U.K.: Cambridge University Press.
- Saro, O., C. Nonino, and G. Comini. 1995. An enthalpy-based algorithm for the analysis of phase change in nonhomogeneous media. In *Computational Modelling of Free and Moving Boundary Problems III*, 127–134. L. C. Wrobel, B. Sarler, and C. A. Brebbia, eds. Southampton, U.K.: Computational Mechanics Publications.
- Scheerlinck, N., K. A. Fikiin, P. Verboven, J. DeBaerdemaeker, and B. M. Nicolai. 1997. Numerical solution of phase change heat transfer problems with moving boundaries using an improved finite element enthalpy method. In *Moving Boundaries IV: Computational Modelling of Free and Moving Boundary Problems*, R. Van Keer and C. A. Brebbia, eds., 75–85. Southampton, U.K.: Computational Mechanics Publications.
- Shampine, L. F., and M. W. Reichelt. 1997. The Matlab ODE suite. *SIAM J. Sci. Computing* 18(1): 1–22.
- Tikhonov, A. N., and A. A. Samarskij. 1972. *Equations of Mathematical Physics*. Moscow: (in Russian).
- Voller, V. R., and M. Cross. 1981. Accurate solutions of moving boundary problems using the enthalpy method. *J. Heat and Mass Transfer* 24: 545–556.
- Zienkiewicz, O. C., and R. L. Taylor. 1994. *The Finite Element Method, Vol. 1: Basic Formulation and Linear Problems*. 4th ed. Berkshire, U.K.: McGraw-Hill Europe.

**NOMENCLATURE**

BDF( <i>i</i> )	Backward differentiation method of order <i>i</i>	<i>k</i>	thermal conductivity ( $\text{W m}^{-1} \text{ }^\circ\text{C}^{-1}$ )
CPU	Computation time (s)	<b>K</b>	finite element conductance matrix
ESHC	Equivalent specific heat capacity	<i>m</i>	iteration step
FEM	Finite element method	<i>n</i>	outward normal to the surface
FLOPS	Floating point operations	<i>n<sub>el</sub></i>	number of finite elements
LU	Number of LU decompositions	<i>n<sub>nod</sub></i>	number of nodes
ME	Mean error	<i>r</i>	order of an explicit or implicit finite difference scheme
NF	Number of function evaluations	<b>r</b>	residual vector
RK( <i>i</i> )	Runge–Kutta method of order <i>i</i>	R	radius (mm)
RMSE	Root mean squared error	<i>s</i>	variable to denote the order of a method
TC	Thermocouple	<i>t</i>	time (s)
TR(2)	Trapezoidal rule (order 2)	<i>t<sub>0</sub></i>	initial time (s)
<i>c</i>	heat capacity ( $\text{J kg}^{-1} \text{ }^\circ\text{C}^{-1}$ )	<i>T<sub>∞</sub></i>	ambient temperature ( $^\circ\text{C}$ )
<b>C</b>	global finite element capacitance matrix	<i>T</i>	temperature ( $^\circ\text{C}$ )
<b>e</b>	nodal Kirchhoff function vector	<i>T<sub>0</sub></i>	initial temperature ( $^\circ\text{C}$ )
<i>E</i>	Kirchhoff function ( $\text{W m}^{-1}$ )	<i>T*</i>	reference temperature ( $^\circ\text{C}$ )
<b>f</b>	finite element thermal load vector	<b>u</b>	nodal temperature vector
<b>F</b>	finite element convection matrix	<i>x, y, z</i>	Cartesian coordinates (m)
<b>h</b>	nodal volumetric specific enthalpy vector	<i>y<sub>i</sub>, z<sub>i</sub></i>	auxiliary vectors used in RK method description
<b>h<sub>0</sub></b>	initial nodal volumetric specific enthalpy vector	$\alpha_i, \beta_i, \beta_{ij}, \gamma_i$	coefficients of explicit and implicit methods
<i>h<sub>q</sub></i>	surface heat transfer coefficient ( $\text{W m}^{-2} \text{ }^\circ\text{C}^{-1}$ )	$\Delta h$	unknown vector during the iterative process when implicit methods are used
<i>H</i>	volumetric specific enthalpy ( $\text{J m}^{-3}$ )	$\Delta t$	time step
<i>H<sub>0</sub></i>	initial volumetric specific enthalpy ( $\text{J m}^{-3}$ )	$\Gamma_C$	convective boundary surface
<b>J</b>	Jacobian matrix	$\rho$	density ( $\text{kg m}^{-3}$ )



EXAMPLES SOLVED BY THE ENTHALPY & KIRCHHOFF TRANSFORM FEM METHODOLOGY OF CHAPTER 3

(<https://doi.org/10.13031/2013.4671>, <https://lnkd.in/dDpFKMYr>)

1. Chilling of a sphere with thermal properties of strawberry

**Example Help**

**1D**

Username: Anonymous

Radius: 2.0 cm

Properties: Strawberry

Initial (uniform) temperature  $T_0$ : 30.0 °C (-20°C ≤  $T_0$  ≤ 40)

Ambient temperature  $T_\infty$ : 1.0 °C (-20°C ≤  $T_\infty$  ≤ 60)

Surface heat transfer coefficient  $h$ : 40.0 W/m<sup>2</sup>°C (5 ≤  $h$  ≤ 500)

Process Time  $t_f$ : 120.0 min

Compute Reset

Results

0.0	30.0	30.0
1.2	29.99901	23.1445
2.4	29.85366	20.49156
3.6	29.15518	18.5304
4.8	27.92016	16.92803
6.0	26.3859	15.55374
7.2	24.73989	14.34262
8.4	23.08944	13.25747
9.6	21.49296	12.27519
10.8	19.97825	11.38034
12.0	18.55662	10.56195
13.2	17.23108	9.811703
14.4	16.00041	9.122695
15.6	14.85988	8.488965
16.8	13.80424	7.906232
18.0	12.82814	7.369549
19.2	11.92599	6.875531
20.4	11.09208	6.420269
21.6	10.32203	6.001155

Show Table

Warning: Applet Window

2. Freezing of a sphere with thermal properties of strawberry

**Example Help**

**1D**

Username: Anonymous

Radius: 2.0 cm

Properties: Strawberry

Initial (uniform) temperature  $T_0$ : 30.0 °C (-20°C ≤  $T_0$  ≤ 40)

Ambient temperature  $T_\infty$ : -20.0 °C (-20°C ≤  $T_\infty$  ≤ 60)

Surface heat transfer coefficient  $h$ : 40.0 W/m<sup>2</sup>°C (5 ≤  $h$  ≤ 500)

Process Time  $t_f$ : 120.0 min

Compute Reset

Results


0.0	30.0	30.0
1.2	29.99835	18.13939
2.4	29.74965	13.54311
3.6	28.5577	10.14749
4.8	26.45533	7.376137
6.0	23.85087	5.004551
7.2	21.0585	2.917794
8.4	18.26077	1.051872
9.6	15.5542	-0.6381585
10.8	12.98461	-1.856122
12.0	10.5712	-2.186166
13.2	8.341167	-2.416727
14.4	6.360952	-2.616784
15.6	4.672015	-2.800016
16.8	3.271359	-2.972743
18.0	2.128499	-3.137393
19.2	1.207597	-3.296252
20.4	0.4751342	-3.450602
21.6	0.0000000	-3.601155

Show Table

Warning: Applet Window



### 3. Freezing of a cylinder with thermal properties of strawberry



Examples

**2D**

**Username:**

**Radius:**  cm

**Height:**  cm

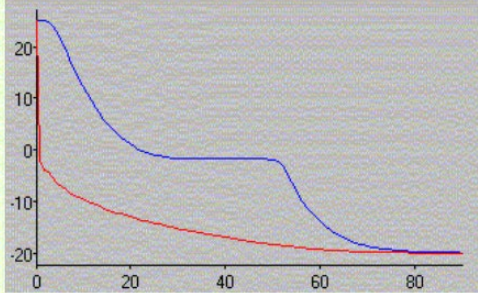
**Properties:**

**Initial (uniform) temperature  $T_0$ :**  °C (-20°C ≤  $T_0$  ≤ 40)

**Ambient temperature  $T_\infty$ :**  °C (-20°C ≤  $T_\infty$  ≤ 60)

**Surface heat transfer coefficient  $h$ :**  W/m<sup>2</sup>°C (5 ≤  $h$  ≤ 500)

**Process Time  $t_f$ :**  min




**Results**

0.0	25.0	25.0
0.9	24.9999	-1.841968
1.8	24.96748	-3.831439
2.7	24.67978	-4.381828
3.6	23.91802	-5.428616
4.5	22.69296	-6.46311
5.4	21.13329	-6.991064
6.3	19.39289	-7.567405
7.2	17.59325	-8.25876
8.1	15.80664	-8.813663
9.0	14.07884	-9.2101
9.9	12.44089	-9.575393
10.8	10.90642	-9.944327

Warning: Applet Window

### 4. Thawing of a mid-size strawberry



Examples

**3D**

**Username:**

**Strawberry shape:**

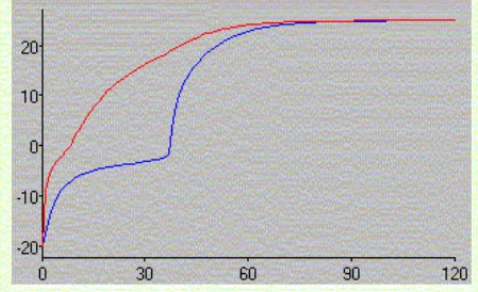
**Properties:**

**Initial (uniform) temperature  $T_0$ :**  °C

**Ambient temperature  $T_\infty$ :**  °C

**Surface heat transfer coefficient  $h$ :**  W/m<sup>2</sup>°C

**Process Time  $t_f$ :**  min



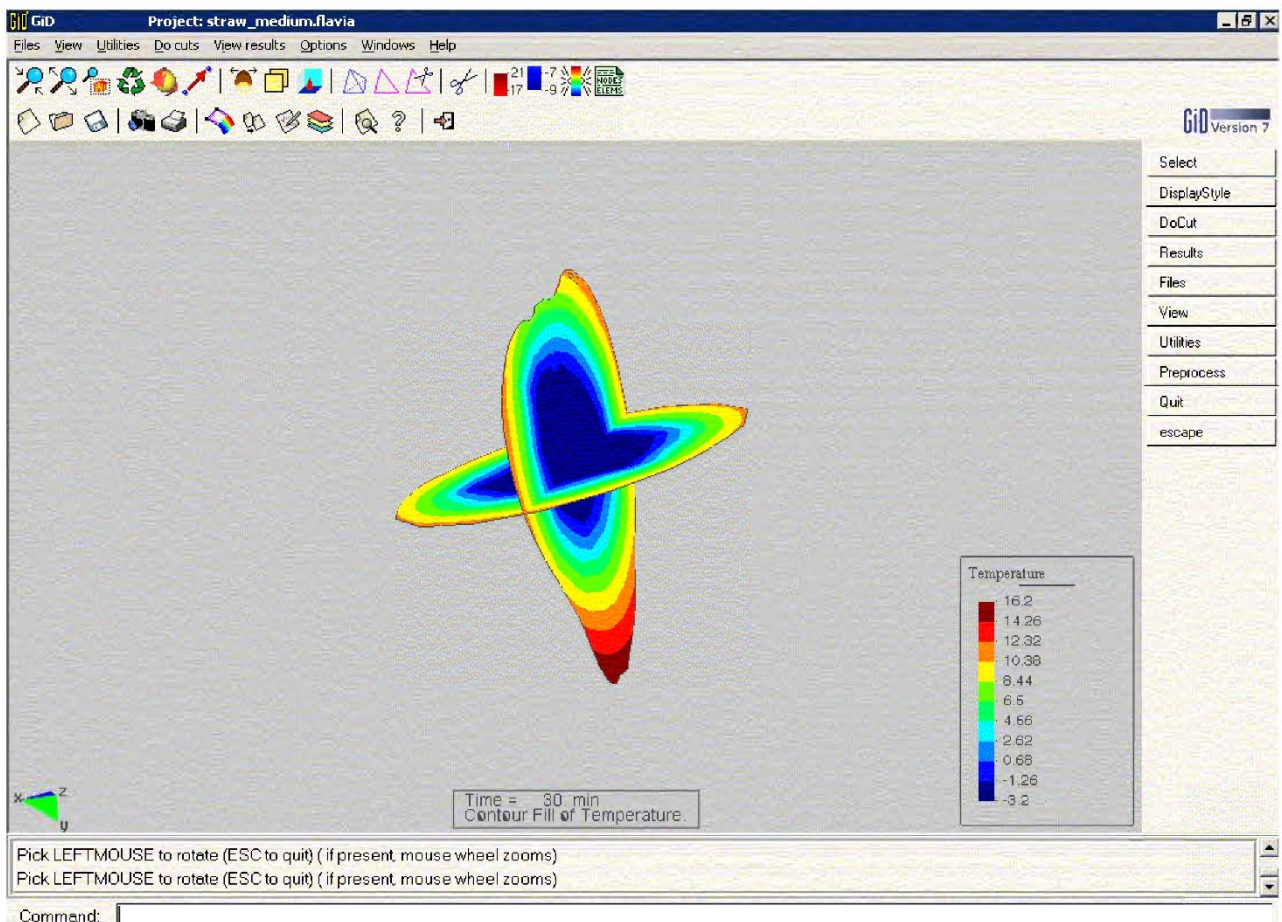
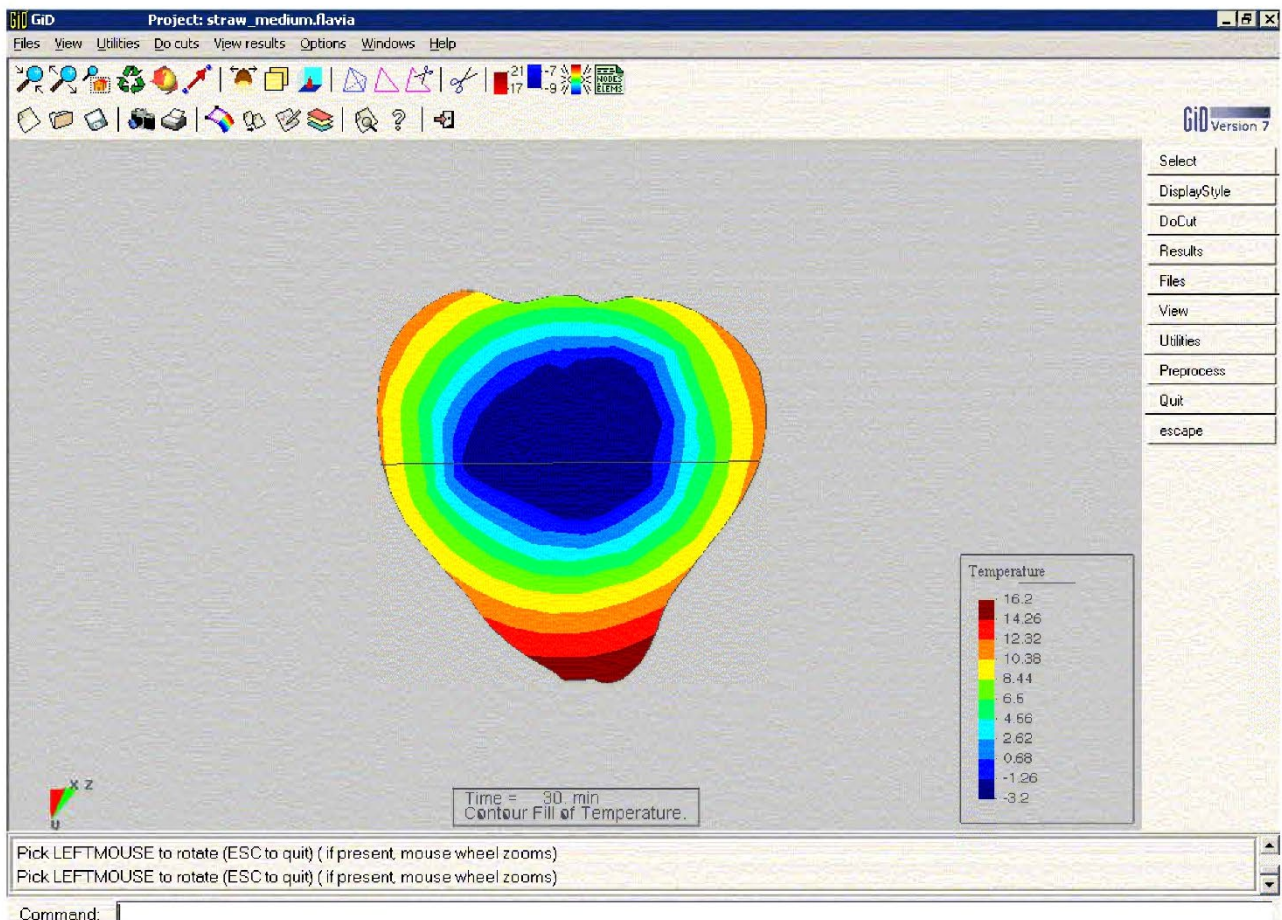
**Results**

0.0	-20.0	-20.0
1.2	-17.79064	-8.887961
2.4	-14.15105	-5.653305
3.6	-11.61674	-3.894949
4.8	-9.86381	-2.795147
6.0	-8.642299	-2.045305
7.2	-7.737464	-0.7364076
8.4	-7.044197	0.1379619
9.6	-6.496787	1.855999
10.8	-6.054539	3.061426
12.0	-5.689049	4.430969
13.2	-5.382276	5.766332
14.4	-5.11989	6.951857
15.6	-4.891039	8.141642
16.8	-4.688091	9.084717
18.0	-4.505253	10.04273
19.2	-4.339792	10.88677
20.4	-4.187874	11.60276
21.6	-4.048019	12.28283
22.8	-3.916435	12.97927
24.0	-3.791666	13.64903
25.2	-3.672412	14.22601
26.4	-3.557378	14.70998
27.6	-3.443512	15.19357

Warning: Applet Window



Temperature distribution in several cross-sections at 30 min from the process beginning.



## **CHAPTER 4**

**Predicting thermophysical properties and  
enthalpy of chilled and frozen foods**

## Chapter 4

addresses the elaboration of theoretical and applied means for determining reliable engineering characteristics, which are vital for studying the thermal behaviour of food systems throughout their refrigerated processing, preservation and distribution. The particular focus is on equations for predicting the thermophysical properties, enthalpy, Kirchhoff variable, etc. as a prerequisite for modelling, simulation, design and optimisation of cold chain processes and systems. The accurate prediction of the unsteady-state temperature distribution, process duration and energy consumption during cooling and freezing (heating and thawing) is a critical factor to guarantee both the product quality and the technological sustainability.

The task is rather challenging, given food materials are extraordinary complicated solid capillary-porous or liquid biostructures where various physiological, biochemical, microbiological, heat and mass transfer processes develop continuously. Multicomponent aqueous foods are analysed with sufficient accuracy as two-phase and two-component systems of water and dry matter. Below the initial freezing point, they are regarded as a dynamic complex of three fractions, continuously changing their quantitative ratios: dry substance, water and ice. The solid phase includes all dry substances (proteins, lipids, carbohydrates, minerals, microelements, vitamins, etc.) and ice, while the liquid phase consists of free water dissolving some of the constituents. Original unified equations for specific heat capacity, thermal conductivity, enthalpy and Kirchhoff functions are thus derived, along with a direct relationship between the enthalpy and the Kirchhoff variable.

The results presented in Chapter 4 have been well accepted and cited by the international professional community (*click on the logos below to locate citing publications*):



Equations and data from Chapter 4 are featured, used and/or recommended not only in research articles but also in a number of monographs and handbooks on food engineering, food preservation or on physical and engineering properties of foods. For example, our prediction methods were proposed as favourites in '*Food Freezing and Thawing Calculations*' (doi: 10.1007/978-1-4939-0557-7). These are referred to in publications in English, French, German, Russian, Chinese, Spanish and Portuguese languages and are often mentioned among the classical reference sources.





Reprinted from *Journal of Food Engineering*, Vol. 40, No. 1-2,  
Fikiin K. and Fikiin A. Predictive equations for thermophysical  
properties and enthalpy during cooling and freezing of food materials,  
pp. 1-6, doi: [https://doi.org/10.1016/S0260-8774\(99\)00026-6](https://doi.org/10.1016/S0260-8774(99)00026-6),  
Copyright © 1999 Elsevier, permitted for non-commercial purposes:  
<https://lnkd.in/d92jTrrY>



ELSEVIER

Journal of Food Engineering 40 (1999) 1–6

---



---

**JOURNAL OF  
FOOD  
ENGINEERING**


---



---

# Predictive equations for thermophysical properties and enthalpy during cooling and freezing of food materials

Kostadin A. Fikiin \*, Anguel G. Fikiin

Refrigeration Science and Technology Division, Technical University of Sofia, 95 Vassil Levski Blvd., 1000 Sofia, Bulgaria

Received 16 December 1996; accepted 20 December 1998

## Abstract

Good knowledge of thermophysical characteristics of a wide range of foodstuffs has a major importance for the accurate prediction of their unsteady-state temperature distribution, the process duration and energy consumption in cooling and freezing (heating and thawing). Such information is necessary to predict the microbiology and biochemistry of spoilage and to control the product safety and quality, as well as for the design, optimisation and efficient operation of refrigerating and thermal systems in the food and biotechnological industries. The purpose of this paper is to present reliable unified equations for determination of the specific heat capacity, enthalpy, thermal conductivity, Kirchhoff function, etc. on the basis of generalised parameters (moisture content, actual and initial freezing temperatures). The relationship between the volumetric specific enthalpy and the Kirchhoff function is also derived. The proposed formulae have large areas of application. They cover practically all industrially processed food materials except those consisting mainly of fats. The equations may easily be used for both simple and rapid engineering calculations and for implementation in more sophisticated mathematical models and computer software, including the cases in which advanced enthalpy methods for numerical heat transfer simulations are involved. © 1999 Elsevier Science Ltd. All rights reserved.

**Keywords:** Food refrigeration; Thermal properties; Enthalpy; Kirchhoff function; Heat transfer

## Nomenclature

$c$	Specific heat capacity ( $\text{J kg}^{-1} \text{K}^{-1}$ or $\text{kJ kg}^{-1} \text{K}^{-1}$ in Eqs. (23)–(29))
$E$	Kirchhoff function ( $\text{W m}^{-1}$ )
$f$	Correction factor (as in Eq. (15))
$H$	Enthalpy per unit mass ( $\text{J kg}^{-1}$ or $\text{kJ kg}^{-1}$ in Eqs. (23)–(29))
$\mathcal{H}$	Enthalpy per unit volume ( $\text{J m}^{-3}$ or $\text{kJ m}^{-3}$ in Eqs. (23)–(29))
$I_q$	Volumetric rate of the internal heat generations ( $\text{W m}^{-3}$ )
$L$	Latent heat of water freezing/thawing ( $\text{J kg}^{-1}$ or $\text{kJ kg}^{-1}$ in Eqs. (23)–(29))
$t$	Temperature ( $^{\circ}\text{C}$ )
$p$	Pressure (Pa)
<i>Greek letters</i>	
$\varepsilon$	Porosity ( $\text{m}_{\text{gas}}^3 \text{m}_{\text{m}}^{-3}$ )
$\lambda$	Thermal conductivity ( $\text{W m}^{-1} \text{K}^{-1}$ )
$\rho$	Substance density ( $\text{kg m}^{-3}$ )

$\tau$	Time (s)
$\phi$	Relative moisture content of the food material ( $\text{kg}_w \text{kg}_m^{-1}$ )
$\omega$	Relative quantity of the frozen water (ice fraction) ( $\text{kg}_w \text{kg}_w^{-1}$ )

## Subscripts

cr	Cryoscopic (initial freezing) point
d	Dry substance
fr	Frozen (in freezing/thawing process)
i	Ice
m	Material
p	At constant pressure
t	At constant temperature
un	Unfrozen
v	At constant volume
w	Water
$\varepsilon$	At given porosity
$\omega$	At constant ice content

## Acronyms

FMs	Food Materials
SHC	Specific Heat Capacity
TC	Thermal Conductivity
TPs	Thermophysical Properties

\* Corresponding author. Tel.: +359-2-884-816; fax: +359-2-884-816; e-mail: agf@vmei.acad.bg



## 1. Introduction

As is well known, the most complex form of the matter organisation in nature is the biological one. Food materials (FMs) are extraordinary complicated solid capillary-porous or liquid biostructures and can be considered from different points of view simultaneously as solutions, suspensions, emulsions and other physico-colloidal formations where various biochemical, microbiological, heat and mass transfer processes develop continuously. The FMs can be analysed as multicomponent two-phase systems (in the presence of gaseous inclusions as three-phase ones) which, below the initial freezing point, represent a complicated dynamic complex of three fractions, continuously changing their quantitative ratios: dry substance (proteins, lipids, carbohydrates, mineral salts, etc.), water and ice crystals. Although the separate FM components enter with each other into complex physico-chemical interactions, the FMs are usually considered as ideal mixtures in order to calculate their thermophysical properties (TPs) on the basis of the properties of the individual constituents. Unfortunately, the exact composition of the different foods is not always known. On the other hand, its variation for one and the same vegetable or animal product with the season, lot, variety, breed, etc. may be very significant and, therefore, published reference data on the chemical composition of these FMs cannot be considered as entirely reliable. Having in mind the negligible influence exerted on the food TPs by the differences in the thermophysical characteristics of the dry substance composite elements, the interpretation of the FMs as a two-component system of water (in solid and liquid phase) and dry matter is completely justified.

That is why, the aim of the present paper is to propose a set of unified predictive equations for determination of the TPs, enthalpy and Kirchhoff function during cooling and freezing (heating and thawing) of FMs on the basis of generalised indicators: moisture content, actual and initial freezing temperatures. For this purpose, the results of the authors' previous investigations (Fikiin, 1959; 1960a,b; 1961; 1964; 1974; 1980; 1981) were synthesised and further developed.

## 2. Theoretical background and some useful relationships

If the enthalpy of a two-phase aqueous food system is considered as a function of the temperature, pressure and ice fraction, i.e.  $H = H(t, p, \omega)$ , its total differential will be

$$dH = \left( \frac{\partial H}{\partial t} \right)_{p,\omega} dt + \left( \frac{\partial H}{\partial p} \right)_{t,\omega} dp + \left( \frac{\partial H}{\partial \omega} \right)_{t,p} d\omega$$

Hence the *specific heat capacity* (SHC) at constant pressure can be written as

$$c_p = \left( \frac{\partial H}{\partial t} \right)_p = \left( \frac{\partial H}{\partial t} \right)_{p,\omega} + \left( \frac{\partial H}{\partial \omega} \right)_{t,p} \left( \frac{\partial \omega}{\partial t} \right)_p \quad (1)$$

A detailed analysis of the pressure influence on the physical properties of frozen FMs is made by Miles and Morley (1978) and Miles (1991). Since the pressure is the weakest influencing factor and can practically be assumed as constant in the most food industry processes, this is usually ignored as a parameter, i.e.  $H = H[t, \omega(t)]$  and  $c \equiv c_p \approx c_v$ . Hence:

$$c(t) = \frac{dH(t)}{dt} = \left( \frac{\partial H}{\partial t} \right)_\omega + \left( \frac{\partial H}{\partial \omega} \right)_t \frac{d\omega(t)}{dt} \quad (2)$$

or

$$c(t) = c_m(t) - \varphi L(t) \frac{d\omega(t)}{dt} \quad (3)$$

where the first term in the right-hand side of Eq. (3),  $c_m(t) = (\partial H / \partial t)_\omega$ , represents the pure SHC of the material, i.e. the change of the enthalpy with temperature at constant ice fraction; while the second term (containing the change of the enthalpy with ice fraction at constant temperature  $(\partial H / \partial \omega)_t = -\varphi L(t)$ ) takes into account the impact of the latent heat of phase transition on the apparent SHC.

On the basis of the additive principle, the following three equivalent expressions for the SHC are valid:

$$c_m(t) = (1 - \varphi)c_d(t) + \varphi[1 - \omega(t)]c_w(t) + \varphi\omega(t)c_i(t) \quad (4)$$

$$c_m(t) = \varphi\{[c_w(t) - c_d(t)] - [c_w(t) - c_i(t)]\omega(t)\} + c_d(t) \quad (5)$$

or

$$c_m(t) = c_{un}(t) - \varphi\omega(t)[c_w(t) - c_i(t)] \quad (6)$$

where  $c_{un}(t) = (1 - \varphi)c_d(t) + \varphi c_w(t)$

The following thermodynamic relation exists between the water and ice SHCs and the latent heat of phase change:

$$c_w(t) - c_i(t) = \frac{dL(t)}{dt} \quad (7)$$

Although there are several experimental data for the unfrozen water SHC (Miles, van Beek & Veerkamp, 1983), the question of its determination is not fully clarified. For this purpose some authors (Mannapperuma & Singh, 1989) expressed  $c_w(t)$  by Eq. (7) for a given  $L(t)$ . Other (Latyshev, 1977; 1983) extrapolated  $c_w(t)$  for the super-cooled state and, on that basis, from Eq. (7) estimated  $L(t)$ . A number of equations exist in the literature for the function  $L(t)$ , often without fixed validity limits. This can lead to a loss of physical meaning for some temperature intervals (zero or negative  $L$ -values can occur at the lower temperatures).

From Eqs. (3), (4) and (7) we obtain:

$$c(t) = (1 - \varphi)c_d(t) + \varphi c_i(t) + \varphi \frac{d}{dt} \{ [1 - \omega(t)] L(t) \} \quad (8)$$

The substitution of Eq. (7) in Eq. (6) and of Eq. (6) in Eq. (3) yields

$$c(t) = c_{\text{un}}(t) - \varphi \frac{d[\omega(t)L(t)]}{dt} \quad (9)$$

According to Eq. (2) the *mass specific enthalpy* is

$$H(t) = \int_{t^*}^t c(t) dt$$

where  $t^*$  is a suitably chosen reference temperature corresponding to the zero value of  $H$ . It is convenient to accept this as equal to the initial freezing (cryoscopic) temperature, i.e.  $t^* \equiv t_{\text{cr}}$ . [The enthalpy  $\bar{H}$  for arbitrary other reference point  $t^{**}$  is  $\bar{H}(t) = H(t) - H(t^{**})$ .]

Then from Eqs. (8) and (9) it can be written:

$$H(t) = (1 - \varphi)H_d(t) + \varphi H_i(t) + \varphi \{ [1 - \omega(t)]L(t) - L(t_{\text{cr}}) \} \quad (10)$$

and

$$H(t) = H_{\text{un}}(t) - \varphi \omega(t)L(t) \quad (11)$$

The *thermal conductivity* (TC) prediction poses more problems in comparison with the SHC, since the TC is quite sensitive to the variations of the FM physico-chemical and histological structure, porosity, developing biochemical processes, formation of gaseous bubbles in the ice structure, etc. The TC is also a compound function of the temperature and unlike the SHC it cannot be expressed by strict theoretical means on the basis of the properties of the different constituents, but additive principles could be used with satisfactory precision for the engineering investigations (Miles et al., 1983; Schwartzberg, 1976). A number of adapted quasi-theoretical and empirical models exist for TC estimation. One of them is the so-called “parallel model” which can be represented by one of the following three equivalent forms:

$$\lambda(t) = \rho(t) \left[ \frac{1 - \varphi}{\rho_d(t)} \lambda_d(t) + \frac{\varphi[1 - \omega(t)]}{\rho_w(t)} \lambda_w(t) + \frac{\varphi\omega(t)}{\rho_i(t)} \lambda_i(t) \right] \quad (12)$$

$$\lambda(t) = \rho(t) \left\{ \varphi \left[ \left( \frac{\lambda_w(t)}{\rho_w(t)} - \frac{\lambda_d(t)}{\rho_d(t)} \right) + \left( \frac{\lambda_i(t)}{\rho_i(t)} - \frac{\lambda_w(t)}{\rho_w(t)} \right) \omega(t) \right] + \frac{\lambda_d(t)}{\rho_d(t)} \right\} \quad (13)$$

or

$$\lambda(t) = \rho(t) \left\{ \frac{\lambda_{\text{un}}(t)}{\rho_{\text{un}}(t)} - \varphi \omega(t) \left[ \frac{\lambda_i(t)}{\rho_i(t)} - \frac{\lambda_w(t)}{\rho_w(t)} \right] \right\} \quad (14)$$

where  $\lambda_{\text{un}}(t) = \rho_{\text{un}}(t)[(1 - \varphi)\lambda_d(t)/\rho_d(t) + \varphi\lambda_w(t)/\rho_w(t)]$

Eqs. (12)–(14) describe the character of the TC-temperature dependence, but do not always provide sufficiently accurate estimates. That is why, many researchers introduce various empirical corrections. For example Morley (Miles, 1991) proposed

$$\lambda(t) = \lambda_{\text{un}}(t) + f\varphi\omega(t)[\lambda_i(t) - \lambda_w(t)] \quad (15)$$

where  $f$  is a correction factor which for meat and fish varies from 0.61 to 0.77 and for comminuted products is about 0.7.

The question of the unfrozen water TC is not yet well clarified, but usually the available dependencies for  $\lambda_w(t)$  are extrapolated for the super-cooled state (Latyshev, 1977; 1983).

The TC of FMs with gaseous inclusions, having porosity  $\varepsilon$ , is  $\lambda_\varepsilon(t) = (1 - \varepsilon)\lambda_{\varepsilon=0}(t)$ .

The *density* of FMs, if they are considered as an ideal mixture of their constituents, will be

$$\rho(t) = \left\{ \frac{1 - \varphi}{\rho_d(t)} + \frac{\varphi[1 - \omega(t)]}{\rho_w(t)} + \frac{\varphi\omega(t)}{\rho_i(t)} \right\}^{-1} \quad (16)$$

or

$$\rho(t) = \left\{ \frac{1}{\rho_{\text{un}}(t)} + \varphi\omega(t) \left[ \frac{1}{\rho_i(t)} - \frac{1}{\rho_w(t)} \right] \right\}^{-1} \quad (17)$$

where  $\rho_{\text{un}}(t) = [(1 - \varphi)/\rho_d(t) + \varphi/\rho_w(t)]^{-1}$ . Besides  $\rho_\varepsilon(t) = (1 - \varepsilon)\rho_{\varepsilon=0}(t)$ . The density-temperature dependence, predetermined mainly by the small difference between the water and ice densities, is comparatively weakly expressed.

The *enthalpy methods* are one of the most promising and advanced fields in the simulation of non-linear heat conduction. In a previous work, Fikiin (1994; 1996) introduced a new concept for modelling of the unsteady-state heat transfer during cooling and freezing (heating and thawing) of aqueous food systems using an improved enthalpy method. This involves the integral transformations:

$$E(t) = \int_{t^*}^t \lambda(t) dt \quad (18)$$

and

$$\mathcal{H}(t) = \int_{t^*}^t c(t)\rho(t) dt \quad (19)$$

which permit the presentation of the differential equation of unsteady heat conduction

$$c(t)\rho(t) \frac{\partial t}{\partial \tau} = \text{div}[\lambda(t)\text{grad } t] + I_q(t) \quad (20)$$

in the following form

$$\frac{\partial \mathcal{H}(E)}{\partial \tau} = \nabla^2 E + I_q(E) \quad (21)$$

This approach has a series of advantages when solving complicated highly non-linear phase-change problems by numerical techniques (Fikiin, 1994; 1996; Comini, Nonino & Saro, 1990). It is convenient to assume in Eqs. (18) and (19) that  $t^* \equiv t_{\text{cr}}$ .

Eqs. (18) and (19) determine six relationships between the quantities  $E$ ,  $\mathcal{H}$  and  $t$ , namely, direct ones:  $E(t)$  and  $\mathcal{H}(t)$  and inverse:  $t(E)$  and  $t(\mathcal{H})$ , as well as  $E(\mathcal{H})$  and

4

K. A. Fikiin, A. G. Fikiin / Journal of Food Engineering 40 (1999) 1–6

$\mathcal{H}(E)$ . Since  $c$ ,  $\rho$  and  $\lambda$  of FMs are positive and limited, all these functions are strictly increasing and continuous and, consequently, between the independent and dependent variables there exist one-to-one mappings. In that way, after the transition from Eq. (20) to Eq. (21), all non-linearities, caused by the TP-temperature dependencies, are introduced in the functional relationship between the volumetric specific enthalpy  $\mathcal{H}$  and the Kirchhoff function  $E$  (Fikiin, 1994; 1996).

That is why, the determination of the *Kirchhoff function* along with all other thermophysical quantities acquires a great significance. The temperature dependence  $E = E(t)$  must be known and in addition it is very useful to find the direct relationship  $E = E(\mathcal{H})$  (Fikiin, 1994; 1996).

From Eqs. (15) and (18) it can be seen that:

$$E(t) = E_{\text{un}}(t) + f\varphi \int_{t_{\text{cr}}}^t [\lambda_i(t) - \lambda_w(t)]\omega(t) dt \quad (22)$$

In fact, the above-mentioned expressions, Eqs. (1)–(17) and (22), are applicable both below [ $0 < \omega(t) < 1$ ] and above ( $\omega = 0$  and  $L = 0$ ) the initial freezing point. It must be observed that when  $t \geq t_{\text{cr}}$ , according to Eq. (7), in Eqs. (8) and (10)  $c_i(t)$  and  $H_i(t)$  become  $c_w(t)$  and  $H_w(t)$ , respectively. Although for  $t \geq t_{\text{cr}}$  the functions  $c_{\text{un}}(t)$ ,  $H_{\text{un}}(t)$ ,  $\lambda_{\text{un}}(t)$ ,  $\rho_{\text{un}}(t)$  and  $E_{\text{un}}(t)$  represent parameters of the unfrozen product, it is obvious that in Eqs. (6), (9), (11), (14), (15), (17) and (22) they can have also arguments  $t < t_{\text{cr}}$ .

Often in engineering computations, instead of the involvement of appropriate TP-temperature dependencies, both the TPs of the separate constituents and  $L$  are assumed constant (although the last is in formal contradiction of Eq. (7)). This can provide a fully sufficient accuracy for reasonably wide temperature intervals. Simultaneously, the most precise  $L$ -temperature dependencies available must be employed when using Eqs. (8)–(11).

### 3. Unified predictive formulae

Using the ice content prediction method of Tchigeov (1979), on the basis of Eqs. (3) and (5) and some simplifying assumptions, Fikiin (1959; 1960a,b; 1961; 1964; 1974; 1980; 1981) proposed the following *unified formulae for the specific heat capacity*:

$$c(t) = \begin{cases} c_{\text{un}} = 2.805\varphi + 1.382 & \text{for } t \geq t_{\text{cr}} \\ c_{\text{fr}} = 1.382 - \varphi \left[ \frac{2.286}{1 + (0.7138/\ln(t_{\text{cr}} - t + 1))} - 2.805 \right] \\ \quad - \varphi L \frac{d\omega(t)}{dt} & \text{for } t < t_{\text{cr}} \end{cases} \quad (23)$$

where  $L \frac{d\omega(t)}{dt} = -264.231(t_{\text{cr}} - t + 1)^{-1} [\ln(t_{\text{cr}} - t + 1) + 0.7138]^{-2}$ . Besides  $-45 \leq t \leq 45^\circ\text{C}$  and  $-2 \leq t_{\text{cr}} \leq -0.4^\circ\text{C}$ .

The integration of Eq. (23) leads to the following relations for the *mass specific enthalpy* (with zero value at  $t_{\text{cr}}$ ):

$$H_{\text{un}}(t) = c_{\text{un}}(t - t_{\text{cr}}) \quad \text{for } t \geq t_{\text{cr}} \quad (24)$$

$$H_{\text{fr}}(t) = (A\varphi + B)(t - t_{\text{cr}}) - C\varphi \left\{ \ln [D \ln(t_{\text{cr}} - t + 1) + 1] + \sum_{k=1}^{\infty} \frac{[\ln(t_{\text{cr}} - t + 1) + E]^k - E^k}{k \cdot k!} \right\} - L\varphi\omega(t) \quad \text{for } t < t_{\text{cr}} \quad (25)$$

where  $A = 0.519$ ;  $B = 1.382$ ;  $C = 0.799$ ;  $D = 1.401$ ;  $E = 1/D = 0.7138$ ;

$$\omega(t) = 1.105/[1 + 0.7138/\ln(t_{\text{cr}} - t + 1)]$$

and  $L \approx 335$  kJ/kg

The numerical results, obtained by Eq. (25), coincide with an accuracy of the order of hundredths of a percent with the data from the *Universal Enthalpy Tables* of Fikiin (1959; 1960b; 1964), found earlier by numerical integration of Eq. (23).

Very good results may also be obtained by Eq. (11), i.e.:

$$H_{\text{fr}}(t) = c_{\text{un}}(t - t_{\text{cr}}) - \varphi\omega(t)L(t) \quad \text{for } t < t_{\text{cr}}$$

where  $c_{\text{un}}$  and  $\omega(t)$  are as in Eqs. (23) and (25); while  $L$  may be estimated through the expression  $L(t) = 334.2 + 2.12t + 0.0042t^2$ , as assumed by Tchigeov (1979).

The following equation (Fikiin, 1980; 1960b; 1964) fits in well (within 3%) with the most of the reliable literature values for enthalpy during freezing (or thawing) of foods:

$$H_{\text{fr}}(t) = -a(\varphi)(t_{\text{cr}} - t)^{b(\varphi)} \quad \text{for } t < t_{\text{cr}} \quad (26)$$

where

$$a(\varphi) = 225.25\varphi - 13.105 \quad \text{and} \quad b(\varphi) = 0.046/\varphi + 0.122.$$

From Eqs. (24) and (26) the *function*  $t = t(\mathcal{H})$  can be found, whose knowing, as indicated above, is very useful for the numerical modelling of unsteady heat transfer:

$$t(\mathcal{H}) = \begin{cases} t_{\text{cr}} + \mathcal{H}/(c_{\text{un}}\rho_{\text{un}}) & \text{for } \mathcal{H} \geq 0 \\ t_{\text{cr}} - [-\mathcal{H}/(\rho_{\text{fr}}a(\varphi))]^{1/b(\varphi)} & \text{for } \mathcal{H} < 0 \end{cases} \quad (27)$$

where  $a(\varphi)$  and  $b(\varphi)$  are as in Eq. (26) and the exact temperature dependence of  $\rho$  is neglected for simplicity, i.e.  $\rho_{\text{un}}$  and  $\rho_{\text{fr}}$  are average values above and below the initial freezing point, respectively.

From Eqs. (15) and (22), after some simplifications and application of the Raoult's Law-based method for ice content prediction (Fikiin, 1980; Miles, 1991; Miles

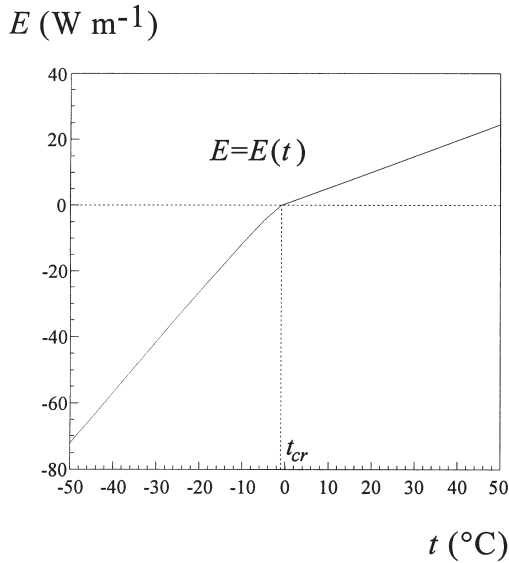


Fig. 1. Kirchhoff function for lean beef.

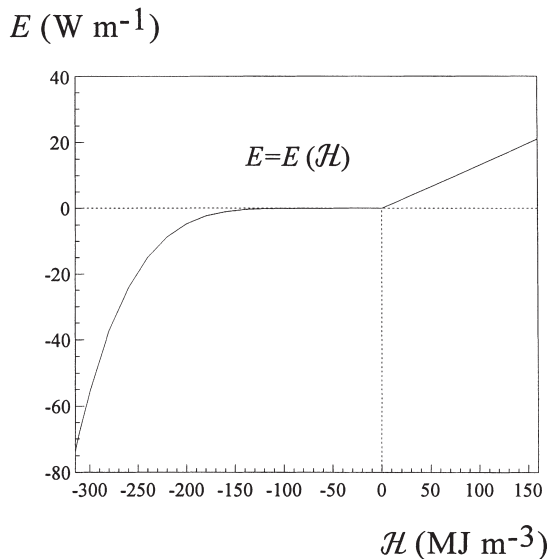


Fig. 2. Dependence between the Kirchhoff function and the volumetric specific enthalpy for lean beef.

et al., 1983), the following relation for the *Kirchhoff function* will be obtained:

$$E(t) = \begin{cases} E_{\text{un}}(t) = \lambda_{\text{un}}(t - t_{\text{cr}}) & \text{for } t \geq t_{\text{cr}} \\ E_{\text{fr}}(t) = (\lambda_{\text{un}} + 1.997f\varphi)(t - t_{\text{cr}}) \\ \quad - 1.997f\varphi t_{\text{cr}} \ln(t/t_{\text{cr}}) & \text{for } t < t_{\text{cr}} \end{cases} \quad (28)$$

Hence the *direct relationship between the volumetric specific enthalpy and the Kirchhoff function* will be:

$$E(\mathcal{H}) = \begin{cases} E_{\text{un}}(\mathcal{H}) = \frac{\lambda_{\text{un}}}{c_{\text{un}}\rho_{\text{un}}}\mathcal{H} & \text{for } \mathcal{H} \geq 0 \\ E_{\text{fr}}(\mathcal{H}) = -(\lambda_{\text{un}} + 1.997f\varphi) \left[ -\frac{\mathcal{H}}{\rho_{\text{fr}}a(\varphi)} \right]^{1/b(\varphi)} \\ \quad - 1.997f\varphi t_{\text{cr}} \ln \left\{ 1 - \frac{1}{t_{\text{cr}}} \left[ -\frac{\mathcal{H}}{\rho_{\text{fr}}a(\varphi)} \right]^{1/b(\varphi)} \right\} & \text{for } \mathcal{H} < 0 \end{cases} \quad (29)$$

where  $a(\varphi)$  and  $b(\varphi)$  are as in Eqs. (26) and (27). The presence of  $t_{\text{cr}}$  as a parameter in Eq. (29) is due to the method used for ice fraction determination. If the method of Tchigeov (1979) is employed for this purpose,  $t_{\text{cr}}$  will not participate in Eq. (29), but in return for this the computational relation would be much more cumbersome. Such a complication would not bring significant advantages, having in mind the resulting lower speed of the numerical simulations and the existing degree of uncertainty in the TC data.

It is interesting to note that, as demonstrated by Comini, Bonacina and Barina (1974) and Bonacina Comini, Fasano and Primicerio (1974), even a rough approximation of the TPs can turn out to be sufficiently good for the purposes of mathematical modelling and engineering calculations, dealing with highly non-linear phase change problems, provided that: (i) this fit does not lead to great changes in the true enthalpy-temperature dependence and (ii) the integral over the whole studied temperature interval of the absolute value of the difference between approximate and actual TCs is a sufficiently small quantity. In terms of our notation, the last means that the second acceptability criterion is the absence of significant changes in the original Kirchhoff function. All this confirms once again that, together with all TP relations, special attention should also be paid to the functions  $\mathcal{H}(t)$  and  $E(t)$ .

As an illustration, the  $E(t)$  and  $E(\mathcal{H})$  functions for lean beef ( $\varphi = 0.75$ ;  $t_{\text{cr}} = -1^\circ\text{C}$ ;  $\lambda_{\text{un}} \approx 0.48 \text{ W m}^{-1} \text{ K}^{-1}$ ;  $f = 0.72$ ;  $\rho_{\text{un}} \approx 1050 \text{ kg m}^{-3}$  and  $\rho_{\text{fr}} \approx 988 \text{ kg m}^{-3}$ ) are shown on Figs. 1 and 2.

#### 4. Concluding remarks

The set of predictive equations presented in this paper for determination of the thermophysical parameters of food materials during cooling and freezing (heating and thawing) has a wide range of application and aims to facilitate the professional activity of food scientists and technologists, refrigeration equipment designers as well as of mathematical and computer modellers.

#### Acknowledgements

This study was partly funded by the Commission of European Union under PECO Project CIPA CT93 0240.

## References

- Bonacina, C., Comini, G., Fasano, A., & Primicerio, M. (1974). On the estimation of thermophysical properties in nonlinear heat-conduction problems. *International Journal of Heat and Mass Transfer*, 17, 861–867.
- Comini, G., Bonacina, C., & Barina, S. (1974). Thermal properties of foodstuffs. In *Proceedings of the Meetings of IIR Commissions B1, C1 and C2 in Bressanone (Italy)* (pp. 163–172). Refrigeration Science and Technology, IIR-Paris (1974-3).
- Comini, G., Nonino, C., & Saro, O. (1990). Performance of enthalpy-based algorithms for isothermal phase change. In L. Wrobel et al (Eds.), *Advanced computational methods in heat transfer* (Vol. 3), (pp. 3–13). Southampton: Computational Mechanics Publications.
- Fikiin, A. (1959). Computational table for enthalpy of foods (pp. 104–107). *Communications of the USSR universities and ministry of higher education*, No. 5 (in Russian).
- Fikiin, A. (1960a). Universal diagram for food enthalpy determination. In: G. Tchigeov (Ed.), *Achievements and problems of refrigeration in USSR economics* (pp. 345–350). Moscow: LTIHP (in Russian).
- Fikiin, A. (1960b). Sur la relation entre l'enthalpie, la teneur en humidité et la température lors de la congélation des produits alimentaires. In *Proceedings of the Bulgarian Academy of Sciences* 13, 571–574.
- Fikiin, A. (1961). Relation entre la chaleur spécifique et la teneur en humidité des produits alimentaires. In *Proceedings of the Bulgarian Academy of Sciences*, 14(4), 373–376.
- Fikiin, A. (1964). Détermination de la quantité de froid dépensée au cours de la réfrigération et de la congélation des produits alimentaires. *Bulletin of the International Institute of Refrigeration – Paris*, 2, 1–15.
- Fikiin, A. (1974). Sur les paramètres thermophysiques des produits alimentaires congelés. In *Current studies on the thermophysical properties of foodstuffs – Proceedings of the Meetings of IIR Commissions B1, C1 and C2 in Bressanone (Italy)* (pp. 173–181). Refrigeration Science and Technology, IIR-Paris (1974-3).
- Fikiin, A. (1980). *Refrigeration technological processes and systems* (p. 512). Sofia: State Publishing Company Tehnika (in Bulgarian).
- Fikiin, A. (1981). *Fundamentals of the refrigeration science and technology* (p. 224). Sofia: State Publishing Company Tehnika (in Bulgarian).
- Fikiin, K. (1994). Generalised numerical modelling of unsteady heat transfer during cooling and freezing using an improved enthalpy method and quasi-one-dimensional formulation. In *New applications of refrigeration to fruit and vegetable processing – Proceedings of the Meeting of IIR Commissions C2, D1 and D2/3 in Istanbul (Turkey)* (pp. 343–360). Refrigeration Science and Technology, IIR-Paris (1994-3).
- Fikiin, K. (1996). Generalised numerical modelling of unsteady heat transfer during cooling and freezing using an improved enthalpy method and quasi-one-dimensional formulation. *International Journal of Refrigeration*, 19(2), 132–140.
- Latyshev, V. (1977). *Recommendations on calculations of thermophysical properties of foods* (p. 107). Moscow: VNIHI (in Russian).
- Latyshev, V. (1983). *Recommendations on calculations of thermophysical properties of foods* (p. 107). Moscow: VNIHI (in Russian).
- Mannapperuma, J., & Singh, R. (1989). A computer aided method for the prediction of properties and freezing/thawing times of foods. *Journal of Food Engineering*, 9, 275–304.
- Miles, C., & Morley, M. (1978). The effect of hydrostatic pressure on the physical properties of frozen foods. *Journal of Physics, D: Applied Physics*, 11, 201–207.
- Miles, C. (1991). The thermophysical properties of frozen foods. In W. Bald (Ed.), *Food freezing: today and tomorrow* (pp. 45–65). London: Springer-Verlag.
- Miles, C., van Beek G., & Veerkamp, C. (1983). Calculation of the thermophysical properties of foods. In: R. Jowitt et al. (Eds.), *Physical properties of foods* (pp. 269–312). London: Applied Science Publishers.
- Schwartzberg, H. (1976). Effective heat capacities for the freezing and thawing of foods. *Journal of Food Science*, 41, 152–156.
- Tchigeov, G. (1979). *Thermophysical processes in food refrigeration technology* (pp. 272). Moscow: Food Industry (in Russian).



## **CHAPTER 5**

**Immersion chilling and freezing by  
hydrofluidisation and ice slurries**

## Chapter 5

is dedicated to immersion methods for fast chilling and freezing of foods and more specifically to the emerging *HydroFluidisation Method* (HFM), we have introduced for the first time in food engineering (<http://doi.org/10.13140/RG.2.1.3901.1283/1>) to overcome the drawbacks and to bring together the advantages of both air fluidisation and immersion food freezing techniques. The HFM uses a circulating system that pumps the refrigerating medium, through orifices or nozzles, in a refrigerating vessel, thereby creating agitating jets. These form a fluidised bed of highly turbulent liquid and moving products, and thus evoke extremely high surface heat transfer coefficients.

Employing unfreezable liquids as fluidising agents demonstrates a much higher chilling or freezing rate as compared with other techniques for individual quick chilling and freezing. In addition, we have launched the idea to enhance further the advantages of the hydrofluidisation by employing two-phase ice suspensions (known as *FLO-ICE*, *BINARY ICE*, *Slurry-ICE*, *Liquid ICE*, *Pumpable ICE* or *Fluid ICE*) as fluidising media. Such ice slurries reveal a great energy potential as HFM refrigerating media whose minute ice particles absorb latent heat when thawing on the product surface. Hence, the ice slurry involvement provides an enormously high surface heat transfer coefficient, excessively short processing time and uniform temperature distribution in the whole volume of the refrigerating apparatus. Thus, the HFM freezing with ice slurries acquires a process rate approaching that of the cryogenic flash freezing modes.

Chapter 5 pays also attention to some conventional hydrocooling modes and specifically focuses on the advantages of immersion in ice-slurries over the traditional use of aqueous solutions or flake ice as a refrigerating medium.

Furthermore, Chapter 5 spotlights ice slurries based on sugar-ethanol aqueous solutions, which reveal a great potential as excellent refrigerating media when producing delicious dessert-type frozen fruits. Such immersion media provide high heat transfer rate and short freezing times, inhibit fruit enzymes and easily take up food additives (antioxidants, flavourings, aromas and micronutrients), which results in a better quality and extended shelf-life of the end product. Appropriate compositions of sugar-ethanol aqueous refrigerating media (single-phase liquids and two-phase ice slurries) are formulated and predictive equations are established for their thermophysical and rheological properties (density, viscosity, thermal conductivity and specific heat capacity).

HFM affords a sustainable engineering solution with low carbon footprint, as it provides surface heat transfer coefficients exceeding  $900 \text{ W m}^{-2} \text{ K}^{-1}$  (with unfreezable liquids) or of the order of  $1000\text{--}2000 \text{ W m}^{-2} \text{ K}^{-1}$  or more (with pumpable ice slurries), which results in short processing times at a relatively small temperature difference between product and cooling medium. For freezing, the evaporation temperature can be maintained much higher (at  $-25\text{--}-30 \text{ }^\circ\text{C}$ ) by a single-stage refrigerating machine with much higher COP and nearly half the CAPEX and OPEX, as compared with the conventional air fluidisation and air-blast freezing systems operated at  $-40\text{--}-50 \text{ }^\circ\text{C}$ .

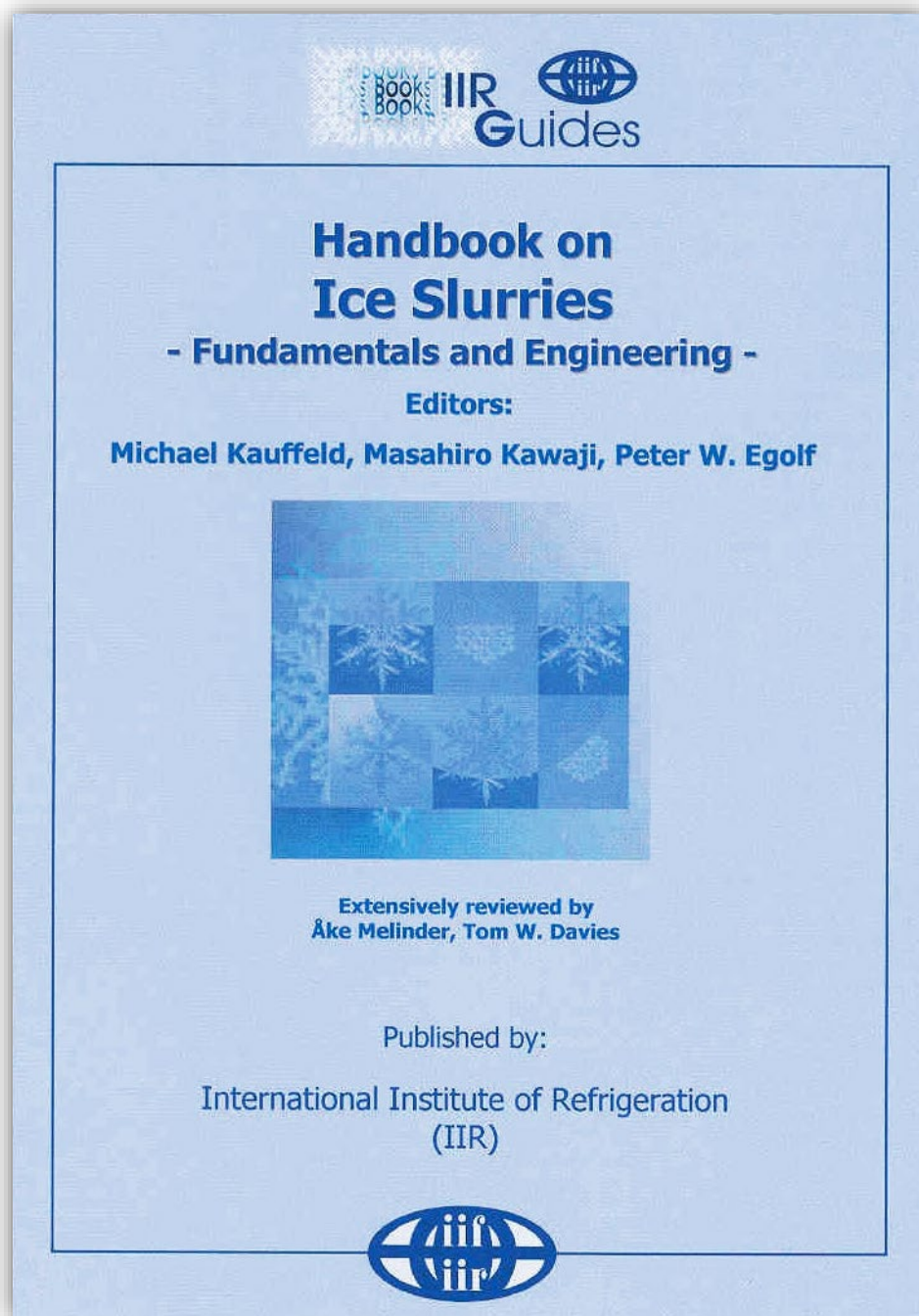
The HFM refrigerating media are environmentally friendly and easy-to-recycle secondary refrigerants (for instance, brine- or syrup-type aqueous solutions and ice slurries), while the primary refrigerant is closed in a small isolated system only, in contrast to the common industrial chilling and freezing systems circulating large quantities of synthetic or natural working substances, with resulting implications in terms of direct emissions to the atmosphere, which cause ozone depletion, global warming and/or safety hazards.

Contents of Chapter 5 have been cited in the scientific literature (*click on the logos below to locate citing publications*):



though some the chapter's reference sources about hydrofluidisation and novel modes of refrigerated processing, authored by the present VAE doctoral candidate, are even more popular.

The novel HFM, along with its combination with the high heat transfer efficiency of the ice-slurry-based refrigerating media, turned into a new interdisciplinary research field whose development advances essentially the refrigerated processing of foods. We have introduced the term '*hydrofluidisation*' for the first time in the scientific literature and an international research trend was created accordingly (mostly represented by R&D organisations in Bulgaria, Belgium, Russia, UK, Argentina and Poland). The HFM was widely publicised (in English, French, Spanish, Russian, Italian, Bulgarian, Hungarian and Persian languages). Research results on hydrofluidisation are demanded and actively sought by cold chain stakeholders.



Reproduced from *Handbook on Ice Slurries: Fundamentals and Engineering*, Fikiin K.A., Wang M.-J., Kauffeld M. and Hansen T.M. Direct contact chilling and freezing of foods in ice slurries – Chapter 9, pp. 251-271, <https://iifiir.org/en/fridoc/4122>, Copyright © 2005 International Institute of Refrigeration, permitted for non-commercial purposes.

## CHAPTER 9. DIRECT CONTACT CHILLING AND FREEZING OF FOODS IN ICE SLURRIES

*by Kostadin Fikiin, Ming-Jian Wang, Michael Kauffeld and Torben M. Hansen (see specific list of symbols in Appendix 3)*

Ice slurry has received increasing attention and demand for refrigeration processes in different industries because of the widespread concerns over product quality, process efficiency and environmental friendliness. This chapter deals with the application of ice slurry technologies to direct contact chilling and freezing of foods. As a rule, direct contact cooling in ice slurries improves the product quality. To date this technology has mainly been used in the fish industry (by employing sea-water-based ice slurry) but its recent applications to the fruit and vegetable processing sectors revealed a very promising potential as well. Both laboratory and industrial trials demonstrated convincingly the superiority of the ice-slurry-based immersion methods over conventional modes of food refrigeration.

Direct contact cooling by dried ice slurries has lately been applied in supermarket display cabinets. Ice slurry is thereby used similarly to flake ice, but the slurry handling is much easier because it can be pumped to the display cases and released via a hose, whereas the ice flakes have to be shovelled. Moreover, there are no traumatic effects on the food surface, which may occur when flakes are involved. Although the cooling ability of the ice slurry is very similar to that of flake ice in this particular application of dried ice slurry, ice slurry shows heat transfer benefits for the direct contact/immersion applications described below.

### 9.1. State of the art and conventional modes of food refrigeration

Let us, for instance, illustrate the ice slurry capabilities for food freezing applications as compared with the most common techniques known so far. In the early 1900s, many people were experimenting with mechanical and chemical methods to preserve food. As an industrial process, quick freezing began its history some 70 years ago when Clarence Birdseye found a way to flash-freeze foods and deliver it to the public – one of the most important steps forward ever taken in the food industry. During his stay in the Arctic, Birdseye observed that the combination of ice, wind and low temperature almost instantly froze just-caught fish. More importantly, he also found that when such quick-frozen fish were cooked and eaten, they were scarcely different from the fresh fish in taste and texture. After years of work, Birdseye invented a system that packed dressed fish, meat or vegetables into waxed-cardboard boxes, which were flash-frozen under pressure (US Patent No. 1,773,079, 1930). Then he turned to marketing and a number of ventures were initiated to manufacture, transport and sell frozen foods (e.g. construction of double-plate freezers and grocery display cases; lease of refrigerated boxcars for railway transport; and retail of frozen products in Springfield, Massachusetts, in 1930). These technological achievements constituted the world's first cold chain for frozen foods, which became shortly a legend (Fikiin, 2003).

Thus, quick freezing has further been adopted as a widespread commercial method for long-term preservation of perishable foods, which improved both the health and convenience of virtually everyone in the industrialised countries. Freezing rate affects strongly the quality of frozen foods, in which the predominant water content should quickly be frozen in a fine-grain crystal structure in order to prevent damages to the cellular tissues and to inhibit rapidly the spoiling microbiological and enzymatic processes.



Basic heat transfer considerations (Fikiin, 2003) clearly suggest that the desired shortening of freezing duration and a resulting high throughput of refrigerating equipment could be achieved by means of: (i) lower refrigerating medium temperature (which generally requires greater investment and running costs for the refrigeration machines to be employed), (ii) enhanced surface heat transfer coefficients (by increased refrigerating medium velocity and boundary layer turbulence, involvement of surface phase-change effects and less packaging), and (iii) reduced size of the refrigerated objects (by freezing small products individually or appropriately cutting the large ones into small pieces).

Air-blast and multiplate freezers are most widespread, while air fluidizing systems are used for individual quick freezing (IQF) of small products. The cryogenic IQF is still very restricted because of the high prices of the liquefied gases used.

### **Fluidized-bed freezing systems**

Air fluidization has been studied extensively and used commercially, with increasing popularity, over the last forty years (Fikiin et al., 1965, 1966, 1970; Fikiin, 1969, 1979, 1980). This freezing principle possesses many attractive features, including:

- High freezing rate due to the small sizes and thermal resistance of the IQF products, large overall heat transfer surface of the fluidized foods and high surface heat transfer coefficients.
- Good quality of the frozen products, that have an attractive appearance and do not stick together.
- Continuity and possibilities for complete automation of the freezing process.

In spite of these advantages, fluidization freezing by air has some drawbacks, such as:

- Necessity of two-stage refrigerating plants (often using large quantities of CFC-, HCFC- or HFC-based refrigerants with significant ozone depletion or global warming potentials) to hold an evaporation temperature of about  $-45^{\circ}\text{C}$ , which results in high investment and power costs.
- Lower surface heat transfer coefficients and freezing rates in comparison with the immersion methods described below.
- Need for a high speed and pressurized airflow, that results in large fan power consumption.
- Some moisture losses from the product surface and rapid frosting of the air coolers, caused by the large temperature difference between the products and the evaporating refrigerant.
- Excessive sensitivity of the process parameters to the product shape, mass and size, that requires careful control specific to every separate food commodity.

### **Freezing by immersion**

The immersion freezing in non-boiling liquid refrigerating media is a well-known method having several important advantages: high heat transfer rate, fine ice crystals in foods, high throughput, low investments and operational costs (Woolrich, 1966; Tressler, 1968; Fleshland and Magnussen, 1990; Lucas and Raoult-Wack, 1998). The immersion applications have been limited because of the uncontrolled solute uptake by the refrigerated products and operational problems with the immersion liquids (high viscosity at low temperatures, difficulty in maintaining the medium at a definite constant concentration and free from organic contaminants). Recent achievements in heat and mass transfer, physical chemistry, fluid dynamics and automatic process control make it possible to solve these problems and to

develop advanced immersion individual quick freezing (immersion IQF) systems (Fikiin and Fikiin, 1998, 1999a, 2002, 2003a,b; Fikiin, 2003).

## **9.2. Unfreezable liquids and pumpable ice slurries as refrigerating media and fluidizing agents**

The *Hydro Fluidization Method* (HFM) for fast freezing of foods was suggested and patented recently to overcome the drawbacks and to bring together the advantages of both air fluidization and immersion food freezing techniques (Fikiin, 1985, 1992, 1994). The HFM uses a circulating system that pumps the refrigerating liquid upwards, through orifices or nozzles, in a refrigerating vessel, thereby creating agitating jets. These form a fluidized bed of highly turbulent liquid and moving products, and thus evoke extremely high surface heat transfer coefficients. The principle of operation of an HFM freezing system is illustrated in *Figure 9.1*.

IIF-IIR – Handbook on Ice Slurries – 2005

## Hydrofluidisation

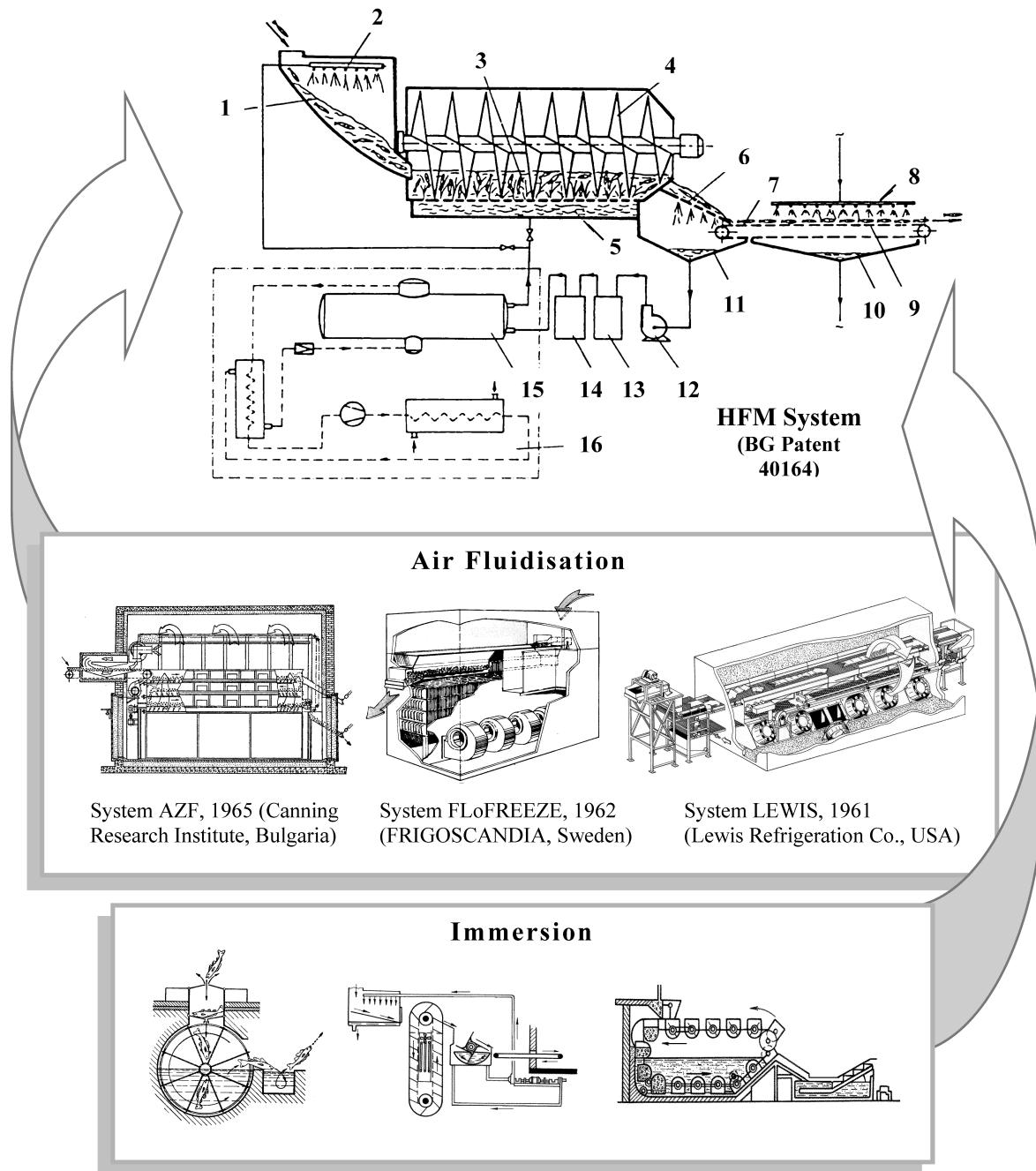


Figure 9.1. Possible arrangements of a HFM-based freezing system combining the advantages of both air fluidization and immersion food freezing techniques (Fikiin and Fikiin, 1998, 1999a): (1) charging funnel; (2) sprinkling tubular system; (3) refrigerating cylinder; (4) perforated screw; (5) double bottom; (6) perforated grate for draining; (8) sprinkling device for glazing; (7 and 9) netlike conveyor belt; (10 and 11) collector vats; (12) pump; (13 and 14) rough and fine filters; (15) cooler of refrigerating medium; (16) refrigeration plant

### Unfreezable liquid refrigerating media as fluidizing agents

Although various immersion techniques have been known for a long time, until now hydrofluidization principles have not been used for chilling and freezing of foods. Experiments on HFM freezing of small fish and some vegetables through an aqueous solution

of sodium chloride showed a much higher freezing rate when compared with other IQF techniques (Fikiin, 1992, 1994). The maximum surface heat transfer coefficient achieved exceeded  $900 \text{ W}/(\text{m}^2\text{K})$ , while this was  $378 \text{ W}/(\text{m}^2\text{K})$  when immersing in a flowing liquid,  $432 \text{ W}/(\text{m}^2\text{K})$  for sprinkling and  $475 \text{ W}/(\text{m}^2\text{K})$  for immersion with bubbling through (Fikiin and Pham, 1985). Even at a slight or moderate jet agitation and a comparatively high refrigerating medium temperature of about  $-16^\circ\text{C}$ , scad fish were frozen from  $25^\circ\text{C}$  down to  $-10^\circ\text{C}$  in the centre within 6-7 minutes, sprat fish and green beans within 3-4 minutes and green peas within 1-2 minutes. As an illustration *Figure 9.2* shows recorded temperature histories during hydrofluidization freezing of scad and sprat fish, green beans and peppers.

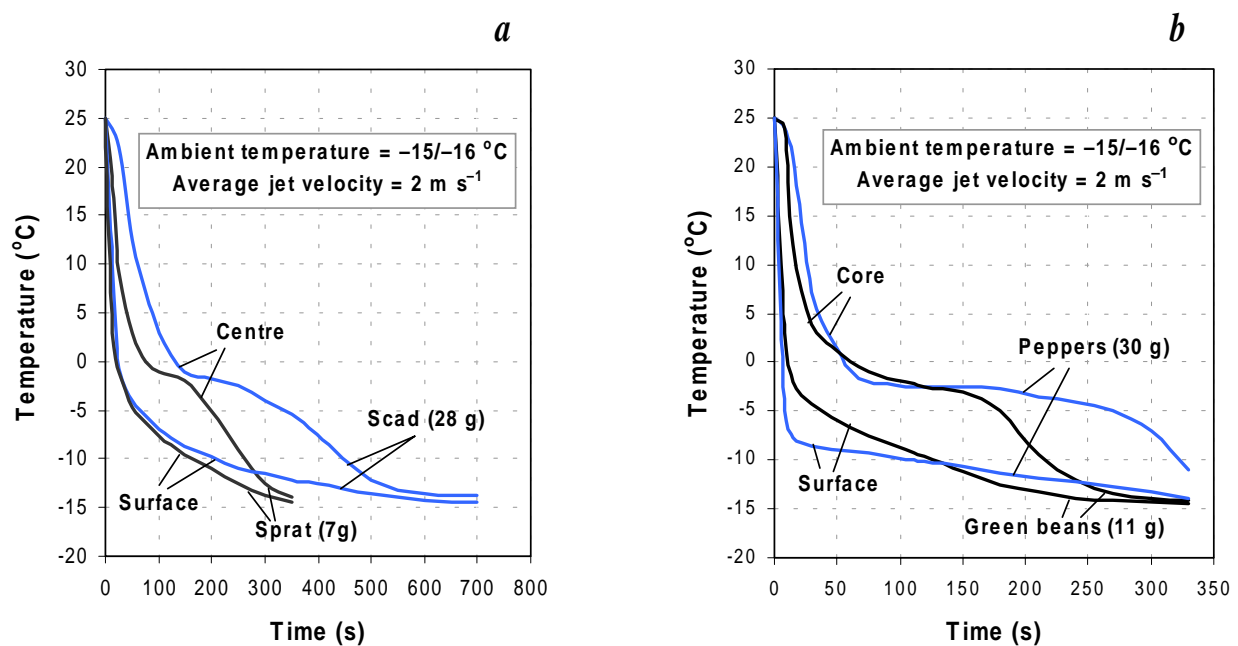


Figure 9.2. Experimental temperature histories during HFM freezing of some kinds of (a) fish and (b) vegetables, when using sodium chloride solution (without ice slurry) as a fluidizing agent (Fikiin, 1992; Fikiin and Fikiin, 1998, 1999a)

### Two-phase ice slurries as fluidizing agents

Pumpable ice slurries (known under different trade names, such as *FLO-ICE*, *BINARY ICE*, *Slurry-ICE*, *Liquid ICE*, *Pumpable ICE* or *Fluid ICE*) were proposed recently as environmentally benign secondary coolants circulated to the heat transfer equipment of refrigeration plants, instead of the traditional ozone-depleting CFC- or HCFC-based refrigerants (Paul, 1995; Ure, 1998; Egolf *et al.*, 1996; Bel and Lallemand, 1999; Pearson and Brown, 1998). Promising attempts to refrigerate foods by immersion in such slurries have already been carried out. As already discussed, fish chilling in sea water-based ice slurries has good potential to replace the traditional use of ice flakes (Fikiin *et al.*, 2002). A number of foods immersed in slurries with various ice contents are shown in *Figure 9.3*.

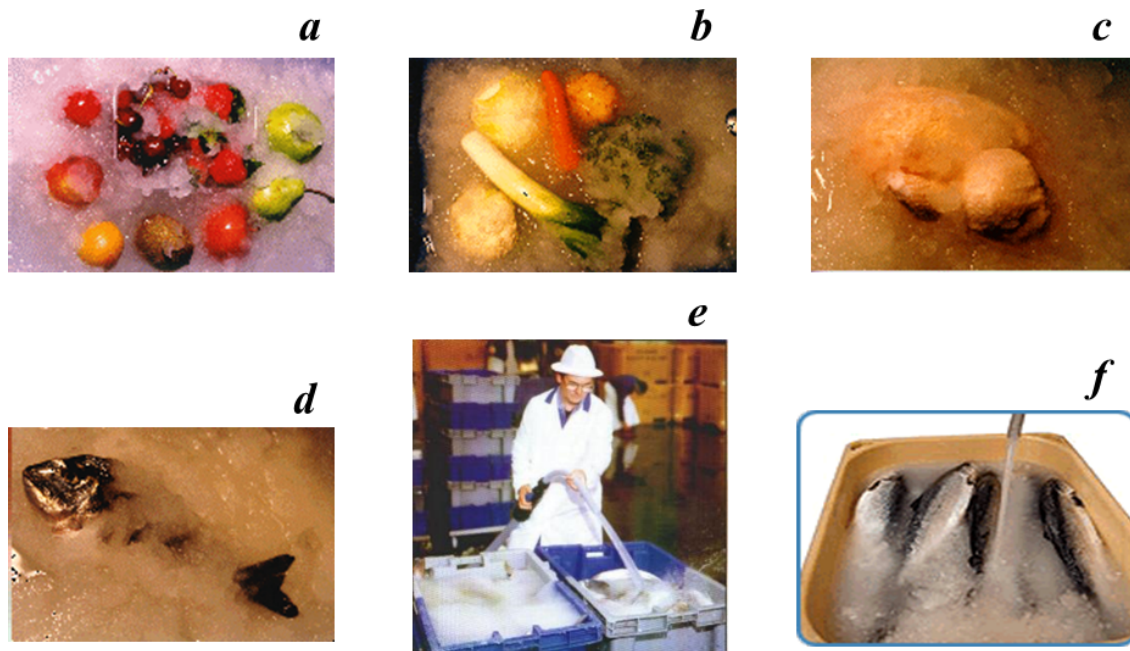


Figure 9.3. Different foods immersed in slurries with various ice concentrations: (a) fruits; (b) vegetables; (c) chickens; (d), (e) and (f) fish (Fikiin *et al.*, 2002)

Fikiin and Fikiin (1998, 1999a) launched, therefore, the idea to enhance the advantages of hydrofluidization (described above) by employing two-phase ice suspensions as fluidizing media. Ice slurries possess a large energy potential as HFM refrigerating media whose small ice particles absorb latent heat when thawing on the product surface. Hence, the goal of ice slurry usage is to provide a high surface heat transfer coefficient (of the order of 1000-2000 W/(m<sup>2</sup>K) or more), shortened freezing time and uniform temperature distribution in the whole volume of the freezing apparatus. The combination of the HFM with the high heat transfer efficiency of the ice-slurry-based refrigerating media represents a new interdisciplinary research field whose development would advance essentially the refrigerated processing of foods. The HFM freezing with ice slurries can acquire a process rate approaching that of the cryogenic flash freezing modes. For instance, at a refrigerating ice-slurry temperature of  $-25^{\circ}\text{C}$  and a heat transfer coefficient of 1000 W/(m<sup>2</sup>K), strawberries, apricots and plums can be frozen from  $25^{\circ}\text{C}$  down to an average final temperature of  $-18^{\circ}\text{C}$  within 8-9 minutes; raspberries, cherries and morellos within 1.5 to 3 minutes; and green peas, blueberries and cranberries within about 1 minute only. The general layout of an ice-slurry-based system for hydrofluidization freezing is shown in *Figure 9.4*.

#### Advantages of hydrofluidization freezing with ice slurries

As described above, the novelty of the hydrofluidization method lies in the involvement of unfreezable liquids or pumpable ice slurries as fluidizing agents. It is well-known that the immersion freezing history began with the use of brines to freeze fish, vegetables and meat. Binary or ternary aqueous solutions containing soluble carbohydrates (e.g. sucrose, invert sugar, glucose [dextrose], fructose and other mono- and disaccharides) with additions of ethanol, salts, glycerol, etc., have been studied as possible immersion media. There are practically unlimited possibilities to combine constituents and to formulate appropriate



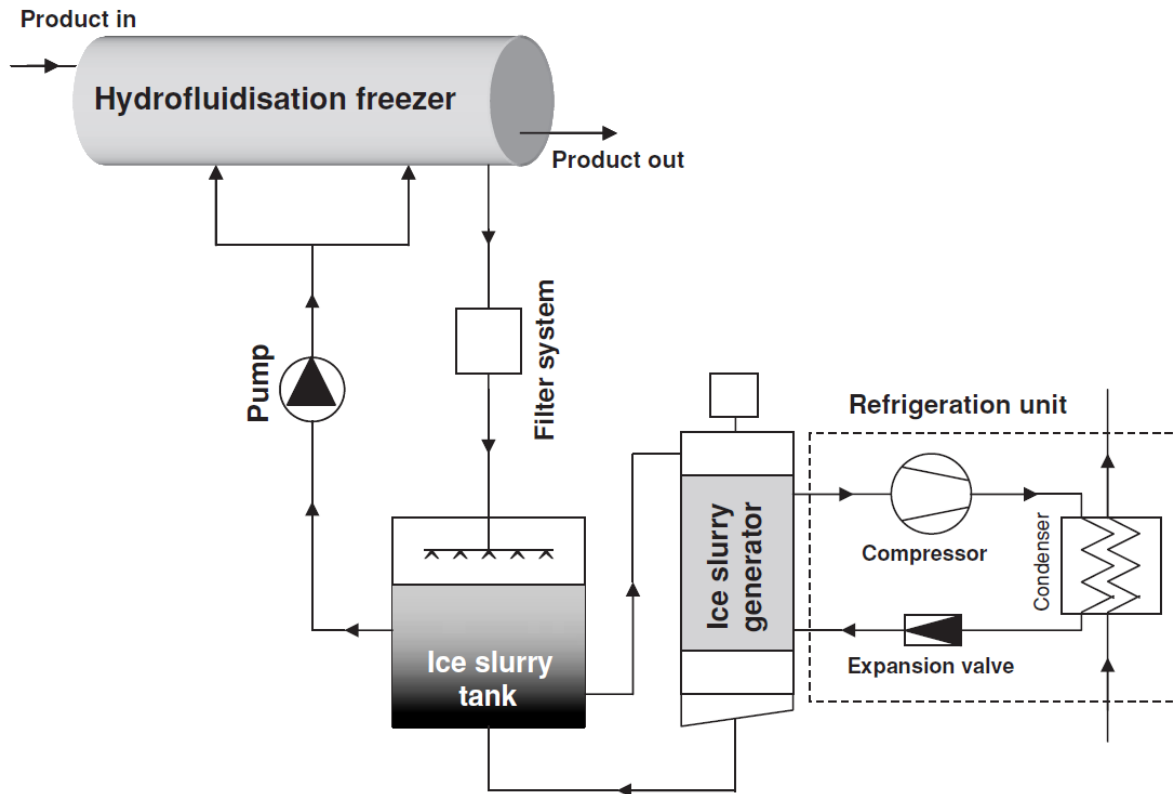


Figure 9.4. Schematic diagram of an ice-slurry-based hydrofluidization system *HyFloFreeze*<sup>®</sup> (Fikiin and Fikiin, 1998, 1999a)

multicomponent HFM refrigerating media based on single-phase liquids or two-phase ice slurries, which have to be both product- and environment-friendly and to possess a low enough viscosity in terms of pumpability and good hydrofluidization.

The main advantages of hydrofluidization over the conventional freezing modes can be summarized as follows:

- The HFM facilitates a very high heat transfer rate with a small temperature difference (product to cooling medium). The evaporation temperature can be maintained much higher (at  $-25/-30^{\circ}\text{C}$ ) achievable by a single-stage refrigerating machine with much higher COP and nearly half the investment and energy costs as compared with the conventional air fluidization. Cold dissipation through the freezer walls is subsequently also lower. The water flow rate or fan power consumption for cooling the condenser decreases as well, due to the reduced mechanical work of the refrigeration unit running at higher evaporation temperature.
- The critical zone of water crystallization (from  $-1$  to  $-8^{\circ}\text{C}$ ) is quickly passed through, which ensures a fine ice crystal structure in foods preventing the cellular tissues from perceptible damage.

- The product surface freezes immediately in a solid crust that hampers the osmotic transfer and gives an excellent appearance. The water losses tend to zero, while in air freezing tunnels the moisture losses are usually 2-3%.
- Delicious new products can easily be formulated by using some selected product-friendly HFM media (for example, fruits frozen in syrup-type sugar solutions turn into dessert products with beneficial effects on colour, flavour and texture). Such media can also include appropriate antioxidants, flavourings and micronutrients to extend the shelf life of the products and to improve their nutritional value and sensory properties.
- The HFM freezers use environmentally friendly secondary coolants (for instance, syrup-type aqueous solutions and ice slurries) and the primary refrigerant is closed in a small isolated system, in contrast to the common air fluidization freezers where large quantities of ozone depleting and/or high global warming potential CFCs, HCFCs or HFCs are circulated to remote evaporators with a much greater risk for emission to the environment.
- Fluidized state is acquired with low velocity and pressure of the fluid jets due to the Archimedes forces and buoyancy of the products, that lead to both energy savings and minimum mechanical action on the foods.
- The operation is continuous, easy to maintain, convenient for automation and the labour costs are substantially reduced. Further processing or packaging of the HFM-frozen products is considerably easier since they emerge from the freezer in a “free-flowing” state, i.e. do not stick together.
- Ice-slurry-based HFM agents may easily be integrated into systems for thermal energy storage, accumulating ice-slurry during the night at lower electricity costs.

The top view photos on *Figure 9.5* show how a hydrofluidized bed of highly turbulent ice slurry is formed inside the *HyFloFreeze*<sup>®</sup> prototype's freezing compartment.



Figure 9.5. *HyFloFreeze*<sup>®</sup> prototype: hydrofluidized bed of highly turbulent ice slurry (Fikiin, 2003).

### International research co-operation

Two main applications of the suggested HFM freezing technique can clearly be distinguished: (i) employment of unfreezable liquids as fluidizing agents and (ii) use of pumpable ice slurries as fluidizing media. This freezing principle provides an extremely high heat transfer rate, short freezing times, great throughput and better product quality at higher refrigerating temperatures. Thus, only about half the investment and power costs are necessary as compared with the popular individual quick freezing methods. Moreover, such

hydrofluidization freezing systems are less hazardous from an environmental viewpoint, since the primary refrigerant is limited to a small isolated circuit.

The emerging HFM technology has attracted the attention of a number of academics and industrialists. The identification of optimal design specifications for HFM freezing systems requires an interdisciplinary approach by researchers with complementary skills. The *HyFloFreeze* project was, therefore, funded by the European Commission and performed by an international research consortium of six participating organisations (four universities and two SMEs) from Belgium, Bulgaria, Russia and the UK (Fikiin, 2003).

### 9.3. Cooling of fish with ice slurries

The use of ice for extending the storage life of fish dates back many millennia. Up to the middle of the last century all ice used for fish cooling was from natural sources (winter snow or imported arctic ice). With the introduction of mechanical cold production, ice was and is produced in different forms, e.g. block, cube, tube or flake ice. Most of these forms need a certain degree of manual operation for transportation from one place to another, and have rather sharp edges capable of damaging the fish surface. Furthermore, they are usually quite coarse, resulting in poor heat transfer. The introduction of ice slurry for direct contact cooling of fish (*Figure 9.6*) presents several attractive features to the process operation over other forms of ice (Wang *et al.*, 2000).

For quality assurance it is essential that effective product cooling be provided throughout the entire production chain, from catch at sea, to storage, transportation, and processing. Cooling technologies employed often use refrigerated seawater and/or different types of fresh ice. Sea water systems placed on board large vessels maintain fish, by sea water circulation, at a mean temperature of about 2-4°C. Disadvantages of such systems are the volume taken up by the refrigeration machinery, difficult working conditions and salt uptake by the fish, especially in smaller species like sardine. Onboard smaller ships, fresh ice is normally loaded from harbour, stored and eventually mixed with the catch. The tendency of fresh ice to re-crystallize and agglomerate in many cases limits the quality of icing, since the ice has to be loosened by manual means before mixing. Often large blocks of ice mixed with the fish result in uneven cooling rates.

Bacterial growth is highly temperature-dependent. As a rule of thumb, the shelf life of fish kept at 0°C is more than doubled compared to +5°C; the closer to the freezing point of the fish, the better the product quality. Bearing in mind that bacterial growth rates can not be stopped, but only decelerated, it is also important to minimize the bacterial level by a rapid temperature drop in each part of the process. Possible freezing of the fish anticipated for chilling may result in decreased sensory perception (Sørensen, 1999) and should therefore be avoided. Intuitively, the use of ice slurry could improve cooling of fish by exploiting properties such as (Wang *et al.*, 2000):

- narrow approach to the freezing point of fish;
- close to isothermal heat exchange during melt-off;
- smooth surface preventing fish from damage;
- easy dosing, mixing, handling and pumping;
- possible drainage of salty water to minimize salt uptake.

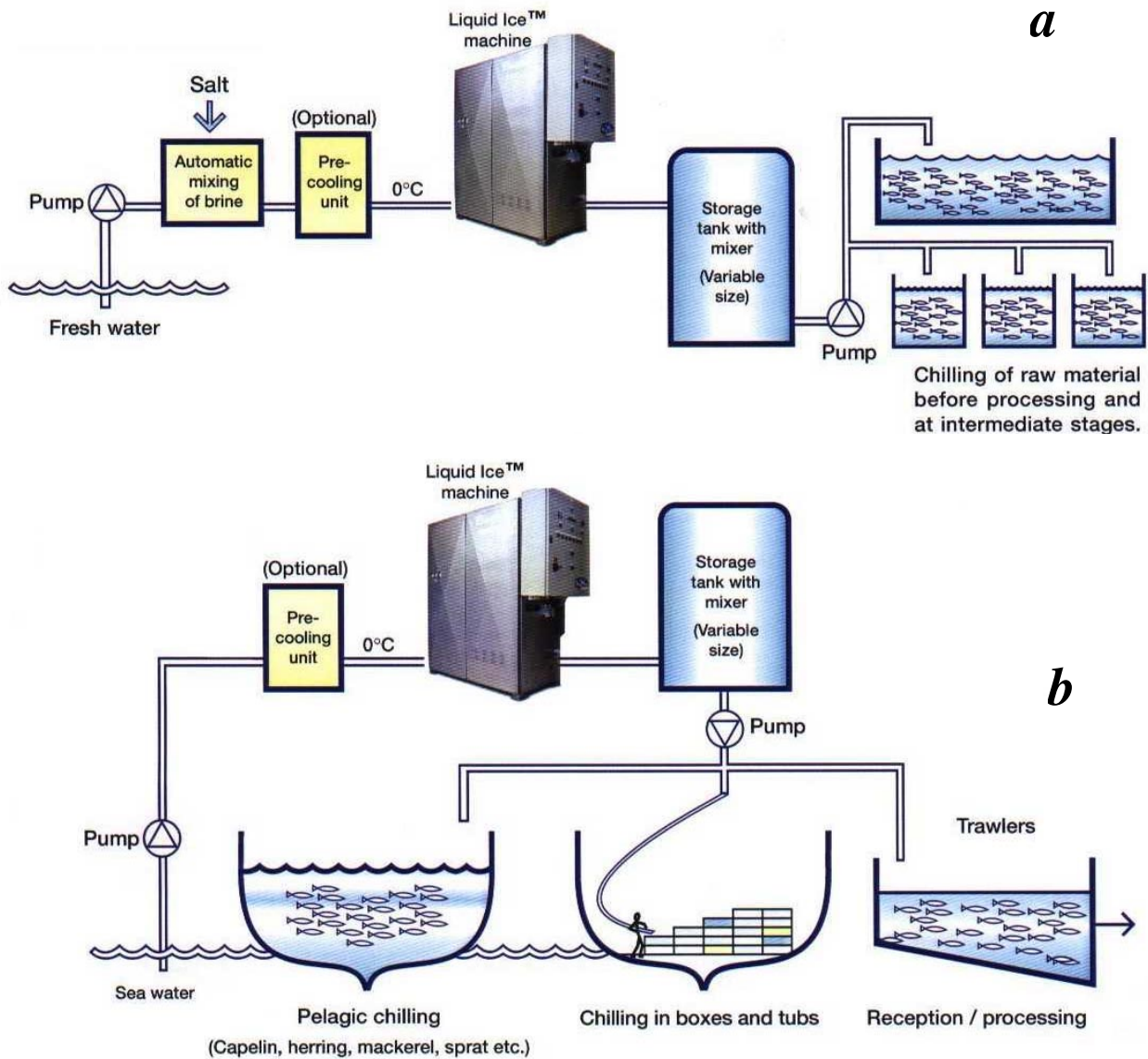


Figure 9.6. Fish chilling in ice slurry (Fikiin *et al.*, 2002): (a) land-based systems and (b) on-board systems (Liquid Ice™, Brontec, Iceland)

Because of its tiny ice crystals, ice slurry is soft and flexible for the chilled product. It effectively avoids any hot spots in the fish container, and provides excellent contact with fish without bruising. As fish are surrounded by numerous ice crystals, high cooling rate is achieved. This significantly retards bacterial growth and reduces fish tissue degradation.

#### Analysis of cooling methods and process simulation

Ice slurry for fish cooling and controlling temperature during storage can be implemented in different ways. In order to verify the aforementioned advantages of ice slurry a simulation model has been developed and related experiments have been carried out (Hansen *et al.*, 1999). To simulate the cooling process and to check whether freezing occurs near the fish

surface, a differential heat conduction equation was solved by using finite-element-based CFD software:

$$\text{div}(k \text{ grad } T) = \rho \cdot c_p \frac{\partial T}{\partial \tau} \quad (9.1)$$

Thermal properties are calculated by considering that phase change of water will occur over a wide temperature interval (see *Figure 9.7*). The majority of water (70-90%) is mechanically trapped in and between cells, and is relatively easy to freeze. During freezing the salt content increases, resulting in a temperature glide of phase change. Individual freezing curves may vary among species, although the characteristics remain the same, i.e. thermo-physical properties are strongly influenced down to a temperature of approximately  $-10^\circ\text{C}$ . The behaviour of phase change described has a large effect on the thermo-physical properties that vary with the temperature throughout a frozen fish. The composition of fish changes a lot among species and depends on the place and season of harvesting, which may also affect thermo-physical properties. White fish may be considered relatively stable containing about 80% water and 20% dry materials. For fatty fish like horse mackerel and sand eel, the content of dry materials may remain approximately 20% during the season whereas the oil content varies from 1 to 20%. Temperature-dependent thermo-physical properties for white fish (80% water) and fatty fish (70% water, 10% oil) are shown in *Figure 9.7*.

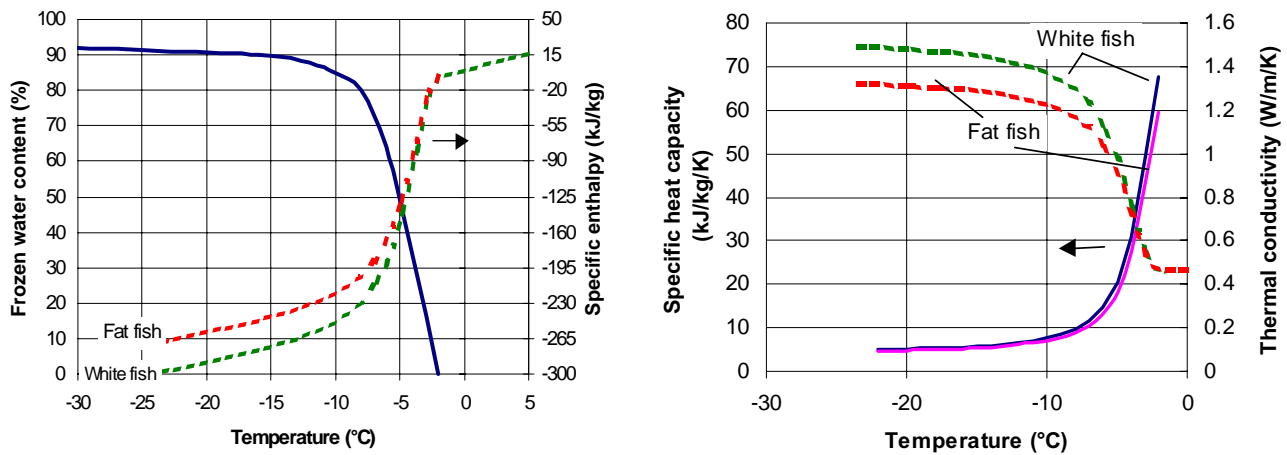


Figure 9.7. Enthalpy-temperature curve from differential scanning calorimetry of cod fillets (Sørensen and Spange, 1999) and calculated thermophysical properties

Based on the freezing curve, the enthalpy can be calculated as a function of temperature by assuming constant heat capacities of constituent substances. For fat fish neglecting the effect of oil on crystallization may cause some errors. The specific heat capacity of fish is calculated as follows:

$$\Delta h = \Delta T \cdot (X_d c_{p,d} + X_{oil} c_{p,oil} + (X_w - X_i) c_{p,w} + X_i c_{p,i}) + X_i L \quad (9.2)$$

$$c_p = \left( \frac{\partial h}{\partial T} \right)_p \quad (9.3)$$



The thermal conductivity,  $k$ , is determined by the assumption that the overall resistance to conduction is due to the resistance of parallel layers of each substance in parallel (=) or perpendicular ( $\perp$ ) to the heat flow direction. It is further assumed that both cases are equally represented, i.e.:

$$k = 1/2(k_{=} + k_{\perp}) \quad (9.4)$$

### Experiments with artificial and real fish samples

To eliminate biological and seasonal variation of fish properties when comparing cooling methods, artificial fish samples with thermophysical properties close to those of white fish have been made out of Karlsruhe food simulator (a mixture of methylcellulose, sodium chloride and water). The aim of the experiments was to compare cooling of fish in containers by using ice slurry or flake ice. The distribution of fish is assumed to be in perfect layers of fish and ice respectively. Three different cooling scenarios were set up, two of them representing an ideal distribution of either flake ice or ice slurry on top of each fish layer, and the third assuming larger re-crystallized/agglomerated blocks of ice covering only 25% of the total surface area, while liquid film heat transfer is present on the remaining surface.

Measurements were made for an artificial fish model with thermocouples placed internally. The fish was placed between artificial dummies in the middle of the container. A total of 20% pure ice was employed for each experiment. Results obtained were compared with the data for horse mackerel. For modelling purposes, fish were assumed to be cylinders of infinite length with adiabatic contact lines between fish. Temperatures of flake ice and ice slurry were set to 0 and  $-3^{\circ}\text{C}$ , respectively. The heat transfer coefficient between the ice particles and fish was estimated to be  $750 \text{ W}/(\text{m}^2\text{K})$ , a value affected by the resistance of the melting liquid layer between the fish surface and ice. Liquid film heat transfer coefficient was assumed to be  $50 \text{ W}/(\text{m}^2\text{K})$ .

*Figure 9.8* shows a reasonable agreement between calculated and measured temperature histories. However, it is also evident that a simple set of boundary conditions is not sufficient to describe the real situation in the container and some deviation may exist, especially for the time interval when almost all the ice has melted (1200 to 1600 seconds). Furthermore, it appears that the centre temperature decreases at a higher rate when using ice slurry at  $-3^{\circ}\text{C}$ . This is even more obvious at the surface. The calculated temperature histories indicate that freezing does not occur at the outer shell if the ice slurry is kept at above  $-3^{\circ}\text{C}$ . The final equilibrium temperature of the fish was approximately 1 K lower when using the same amount of ice slurry versus using flake ice. The difference is caused by the larger enthalpy change of the melting ice slurry.

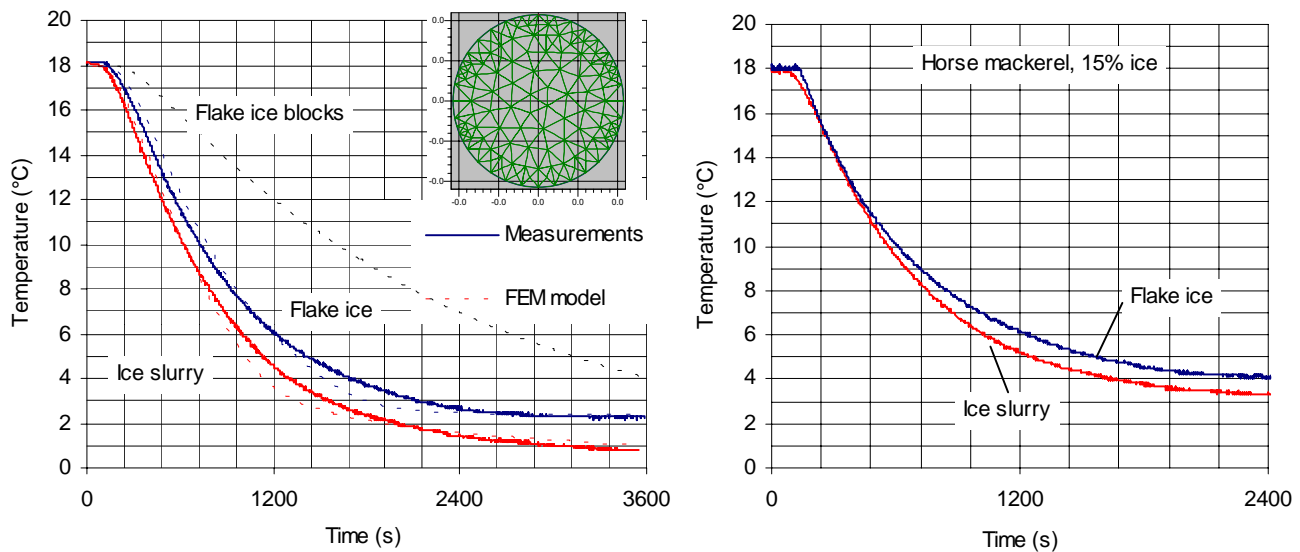


Figure 9.8. Variation in centre temperature (left graph) measured in an artificial fish model (43 mm diameter) cooled in a container with ice slurry at  $-3^{\circ}\text{C}$  and with flake ice at  $0^{\circ}\text{C}$ , together with calculated temperatures (initially 20% ice in the container). Temperature measurement (right graph) in horse mackerel cooled in a container with ice slurry and with flake ice (initially 15% ice in the container)

The results from the experiments with the artificial fish model were comparable with those with horse mackerel. A similar tendency was found, i.e., faster temperature drop and about 1 K lower final temperature when using ice slurry. The end cooling temperature was, however, different because of the smaller amount of ice. If the distribution of flake ice is not ideal because of re-crystallized blocks, *Figure 9.8* reveals that cooling with flake ice is less effective than with ice slurry.

Cooling experiments with a fish model immersed into a flowing stream of ice slurry with different velocities and ice concentrations were also conducted to identify any advantages of pre-cooling before container storage. Measurements were performed for flow velocities of 0.1 and 0.2 m/s and at ice concentrations of 10, 20 and 30 wt-%. Results showed that there is no major difference in terms of cooling time for different combinations of these parameters. Compared with the immersed fish model, no significant difference was detected when cooling a container with perfect distribution.

#### 9.4. Ice-slurry-based cooling of fruits and vegetables

The ice-slurry cooling method for fish can also be employed for fruit and vegetables, along with other food commodities to be chilled or frozen. In many cases the uncontrolled uptake of solutes (salt or alcohol) on the product surface is more undesirable than for fish (unless osmotic phenomena are exploited to give added value to the product). Similar to the fish cooling, much faster heat transfer rates can be obtained. Most notable is the improvement when comparing previously air cooled products versus ice slurry cooled products. For instance, the Danish Technological Institute investigated the chilling and freezing of pig

carcasses in ice slurry with good results, while a number of researchers around the world performed promising experiments with various fruits and vegetables.

When using suitable product-friendly media, the osmotic phenomena on the surface can be exploited to give added value to the products. In particular, by freezing of fruits in sugar-ethanol-based aqueous solutions or pumpable ice slurries new delicious dessert products can be formulated with beneficial effect on colour, flavour and texture due to the enzyme-inhibiting action of the sugar (Fikiin and Fikiin, 1998, 1999). In addition, the take-up of food additives (antioxidants, flavourings, aromas and micronutrients) is improved, which can result in a better quality and extended shelf-life of the end product. Nevertheless, the available data for the physical properties and the performance of such secondary fluids in food freezing equipment are still too scarce. A set of predictive equations for the density, viscosity, thermal conductivity and specific heat capacity of sugar-ethanol aqueous refrigerating media are given by Fikiin *et al.* (2001).

### Sugar-ethanol aqueous solutions and ice slurries suitable for immersion freezing of fruits

Several important criteria must be taken into consideration when selecting liqueur-type refrigerating liquids and ice-slurries pertinent for fruit freezing applications: (i) product friendliness with regard to the end product quality, (ii) environmental friendliness, (iii) suitable rheological properties in terms of good pumpability, and (iv) appropriate initial freezing temperature (Fikiin *et al.*, 2001). A number of test solutions were therefore prepared at the St. Petersburg State University of Refrigeration and Food Technologies by using distilled and deionized water, pure ethanol of food-admissible class and sugar (sucrose or glucose). Solution compositions and freezing points are presented in *Table 9.1*. The estimated uncertainty in the mass fraction data was  $\pm 0.1\%$ .

Table 9.1. Compositions and initial freezing temperatures of the studied solutions

Solution Number	Composition (mass fraction)			$t_f$ (°C)
	water, $x_w$	ethanol, $x_e$	sucrose, $x_s$	
1	0.55	0.25	0.20	-28.0
2	0.60	0.25	0.15	-25.0
3	0.65	0.25	0.10	-22.0
4	0.55	0.20	0.25	-26.5
5	0.60	0.20	0.20	-23.5
6	0.65	0.20	0.15	-19.5
7	0.55	0.15	0.30	-23.0
8	0.60	0.15	0.25	-20.0
9	0.65	0.15	0.20	-16.5
Solution No.	water, $x_w$	ethanol, $x_e$	glucose, $x_s$	$t_f$ (°C)
10	0.60	0.25	0.15	-24.5

An international taste panel considered that solutions No. 1, 2 and 10 possessed the best sensory and physical properties, but some other solutions (such as No. 4, 5 and 6) were also acceptable.

### Predictive equations for the thermophysical and rheological properties of sugar-ethanol aqueous solutions and ice slurries

A series of experiments were carried out and some theoretical approaches were employed to determine basic thermal and rheological properties of the studied single- and two-phase refrigerating media and to establish resulting regression relationships. The following assumptions were made when deriving the predictive equations: (i) water is the only freezable component of the solution (because, at atmospheric pressure, all the ethanol remains unfrozen above  $-114.5^{\circ}\text{C}$ ), (ii) the temperature-dependent properties of the liquid solution are extrapolated below the initial freezing point to estimate the unfrozen fraction properties, and (iii) the ice fraction variation with the temperature conforms with the Raoult's Law (Fikiin *et al.*, 2001).

#### Initial freezing temperature

Typical gradients of the time-temperature curves during slow freezing or thawing ( $\sim 0.5^{\circ}\text{C}/\text{min}$ ) were registered to measure the initial freezing points of the studied solutions (Table 9.1) and the following empirical equations were then established by a regression analysis:

$$t_f = a_0 + a_1 \cdot x_e + a_2 \cdot x_s + a_{12} \cdot x_e \cdot x_s \quad (9.4)$$

where  $0.15 \leq x_e \leq 0.25$ ,  $0.10 \leq x_s \leq 0.30$ , and  $a_0 = 10.9$ ,  $a_1 = -103.33$ ,  $a_2 = -51.67$  and  $a_{12} = -66.67$ .

#### Density

The liquid densities were determined by a piezometric technique, which was previously tested with reference liquids (water, ethanol and other well-investigated solutions). The resulting regression equation is:

$$\rho_l = (b_0 + b_1 x_e + b_2 x_s + b_{12} x_e x_s) + (c_0 + c_1 x_e + c_2 x_s + c_{12} x_e x_s) t \quad (9.5)$$

for  $t_f \leq t \leq 21^{\circ}\text{C}$ ,  $0.15 \leq x_e \leq 0.25$ ,  $0.10 \leq x_s \leq 0.30$  and coefficients are given in Table 9.2.

Table 9.2. Coefficients of Eq. (9.5)

$b_0$	$b_1$	$b_2$	$b_{12}$	$c_0$	$c_1$	$c_2$	$c_{12}$
981.8	-67.556	481.111	-255.556	0.30483	-3.10689	-2.06289	9.18444

Furthermore, the ice-slurry density can be expressed as follows:

$$\rho_{is} = [x_i / \rho_i + (1 - x_i) / \rho_l]^{-1} \quad (9.6)$$

where  $x_i$  is the mass fraction of ice, the ice density  $\rho_i = 916.8 (1 - 0.00015 t)$  and  $\rho_l$  is determined by Eq. (9.5) for  $x_s = x_s^{\text{in}} / [1 - (1 - t_f / t) x_w^{\text{in}}]$  and  $x_e = x_e^{\text{in}} / [1 - (1 - t_f / t) x_w^{\text{in}}]$ .

#### Viscosity

Measurements of the liquid viscosity were carried out by using glass capillary viscometers and the results obtained were approximated by the following equation:

$$\eta_l = D + E t + F t^2 \quad (9.7)$$

where:  $D = d_0 + d_1 x_e + d_2 x_s + d_{12} x_e x_s$ ,  $E = e_0 + e_1 x_e + e_2 x_s + e_{12} x_e x_s$ ,  $F = f_0 + f_1 x_e + f_2 x_s + f_{12} x_e x_s$ ,  $t_f \leq t \leq 21^\circ\text{C}$ ,  $0.15 \leq x_e \leq 0.25$  and  $0.10 \leq x_s \leq 0.30$ . The empirical coefficients are given in Table 9.3.

Table 9.3. Coefficients of Eq. (9.7)

$d_0$	-17.325	$e_0$	1.556	$f_0$	-0.04318
$d_1$	79.222	$e_1$	-6.162	$f_1$	0.15612
$d_2$	100.822	$e_2$	-7.486	$f_2$	0.18694
$d_{12}$	-181.778	$e_{12}$	15.611	$f_{12}$	-0.40644

The model of Thomas (1965), valid for ice particle diameters between 0.1 and 45  $\mu\text{m}$ , can further be employed to evaluate the apparent viscosity of the ice slurry (please refer to Chapter 3 for a detailed description of rheological ice slurry properties):

$$\eta_{is} = \eta_l [1 + 2.5 \varphi_i + 10.05 \varphi_i^2 + 0.00273 \exp(16.6 \varphi_i)] \quad (9.8)$$

where the volumetric ice fraction  $\varphi_i = x_i [x_i + (1 - x_i) (\rho_i / \rho_l)]^{-1}$  may vary between 0 and 0.625, while  $\eta_l$  is calculated by Eq. (9.7) for  $x_s = x_s^{\text{in}} / [1 - (1 - t_f/t) x_w^{\text{in}}]$  and  $x_e = x_e^{\text{in}} / [1 - (1 - t_f/t) x_w^{\text{in}}]$ .

### Thermal conductivity

As is well-known, the thermal conductivity of a ternary solution does not comply with the additive principle and cannot, therefore, be rigorously expressed through the properties of the different constituents. Nonetheless, by using a quasi-binary assumption the overall liquid conductivity could be considered as a compound function of the conductivities of ethanol and water-sugar system. It turned out that the liquid thermal conductivity predominantly depends on the ethanol content and could roughly be estimated on the basis of the ethanol fraction only:

$$k_l = (i_0 + i_1 x_e + i_2 x_e^2) + (l_0 + l_1 x_e + l_2 x_e^2) t \quad (9.9)$$

for  $t_f \leq t \leq 20^\circ\text{C}$ ,  $0.10 \leq x_e \leq 0.35$  and equation coefficients are shown in Table 9.4.

Table 9.4. Coefficients of Eq. (9.9)

$i_0$	$I_1$	$i_2$	$l_0$	$l_1$	$l_2$
0.50686	-0.573278	0.2401997	0.001347	-0.0028111	0.0011861

In accordance with the Maxwell model, the apparent thermal conductivity of the ice slurry could be written in the form of Jeffrey (1973):

$$k_{is} = k_l (1 + 3 \varphi_i \beta + 3 \varphi_i^2 \beta^2 \chi) \quad (9.10)$$

where  $\chi = 1 + 0.25 \beta + 0.1875 \beta [(\alpha + 2) / (2\alpha + 3)]$ ,  $\beta = (\alpha - 1) / (\alpha + 2)$ ,  $\alpha = k_i / k_l$ ,  $k_i = 2.22 (1 - 0.0015 t)$ ,  $\varphi_i$  is as in Eq. (9.8), and  $k_l$  is calculated by Eq. (9.9) for  $x_e = x_e^{\text{in}} / [1 - (1 - t_f/t) x_w^{\text{in}}]$ .



The dimensionless apparent ice-slurry viscosity,  $\eta^* = \eta_{is} / \eta_l$ , and thermal conductivity,  $k^* = k_{is} / k_l$ , determined by Eqs (9.8) and (9.10) as a function of the volumetric ice fraction,  $\phi_i$ , are shown in Figure 9.9.

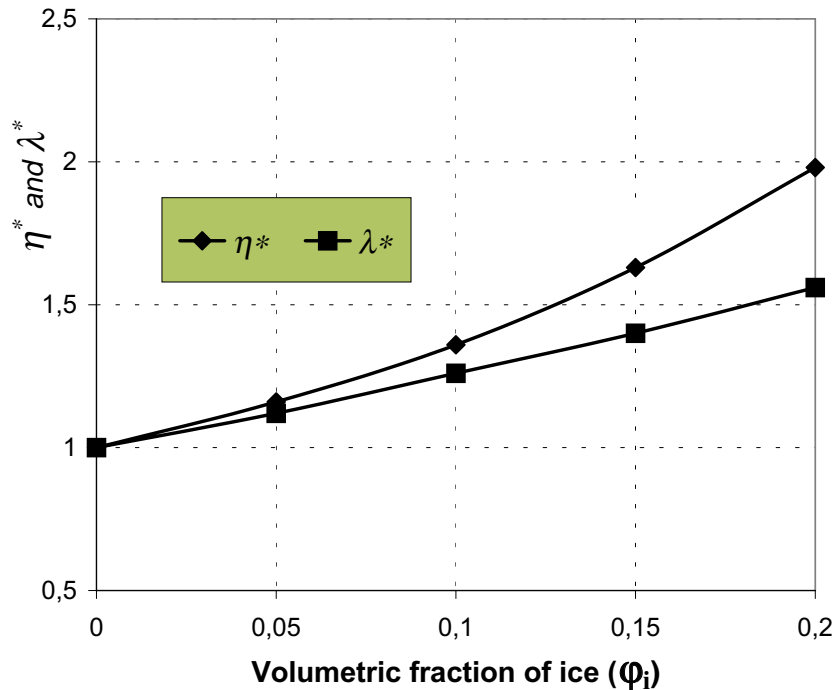


Figure 9.9. Dimensionless apparent viscosity,  $\eta^* = \eta_{is} / \eta_l$ , and thermal conductivity,  $k^* = k_{is} / k_l$ , versus  $\phi_i$ . (The notation for thermal conductivity in the figure follows the symbol tradition of Continental Europe, i.e. “ $\lambda$ ” is used instead of “ $k$ ”)

### Specific heat capacity

General thermodynamic considerations make it possible to determine the specific heat capacity of ternary solutions on the basis of the heat capacities of the solution components. The data obtained for liquid sugar-alcohol aqueous solutions were fitted by the following regression equation:

$$c_{p,l} = (m_0 + m_1 x_e + m_2 x_s + m_{12} x_e x_s) + (n_0 + n_1 x_e + n_2 x_s + n_{12} x_e x_s) t \quad (9.11)$$

for  $t_f \leq t \leq 20^\circ\text{C}$ ,  $0.15 \leq x_e \leq 0.25$ ,  $0.10 \leq x_s \leq 0.30$  and empirical coefficients are presented in Table 9.5.

Table 9.5. Coefficients of Eq. (9.11)

$m_0$	$m_1$	$m_2$	$m_{12}$	$n_0$	$n_1$	$n_2$	$n_{12}$
4.192	-1.9272	-2.8172	0.0910	0.000020	0.005075	0.002675	0.000459

The apparent specific heat capacity of ice slurries and other water-containing systems can easily be evaluated as follows (Fikiin and Fikiin, 1999b):

$$c_{p,is} = c_{p,l} - d [x_i L] / d t \quad (9.12)$$

where  $L = 334.2 + 2.12 t + 0.0042 t^2$ ,  $x_i = x_w^{\text{in}} (1 - t_f / t)$  and  $c_l$  is determined through Eq. (9.11) for  $x_s = x_s^{\text{in}} / [1 - (1 - t_f / t) x_w^{\text{in}}]$  and  $x_e = x_e^{\text{in}} / [1 - (1 - t_f / t) x_w^{\text{in}}]$ .

It is obvious that  $t < t_f$  in all the ice-slurry related equations, Eqs (9.6), (9.8), (9.10) and (9.12).

A small-size prototype of HFM freezer for testing, demonstration and promotion of the HFM technology is under investigation at the Technical University of Sofia and Interobmen Ltd. – Plovdiv (Bulgaria). The hydrofluidization, conveyor and driving systems of the prototype are shown in *Figure 9.10*.

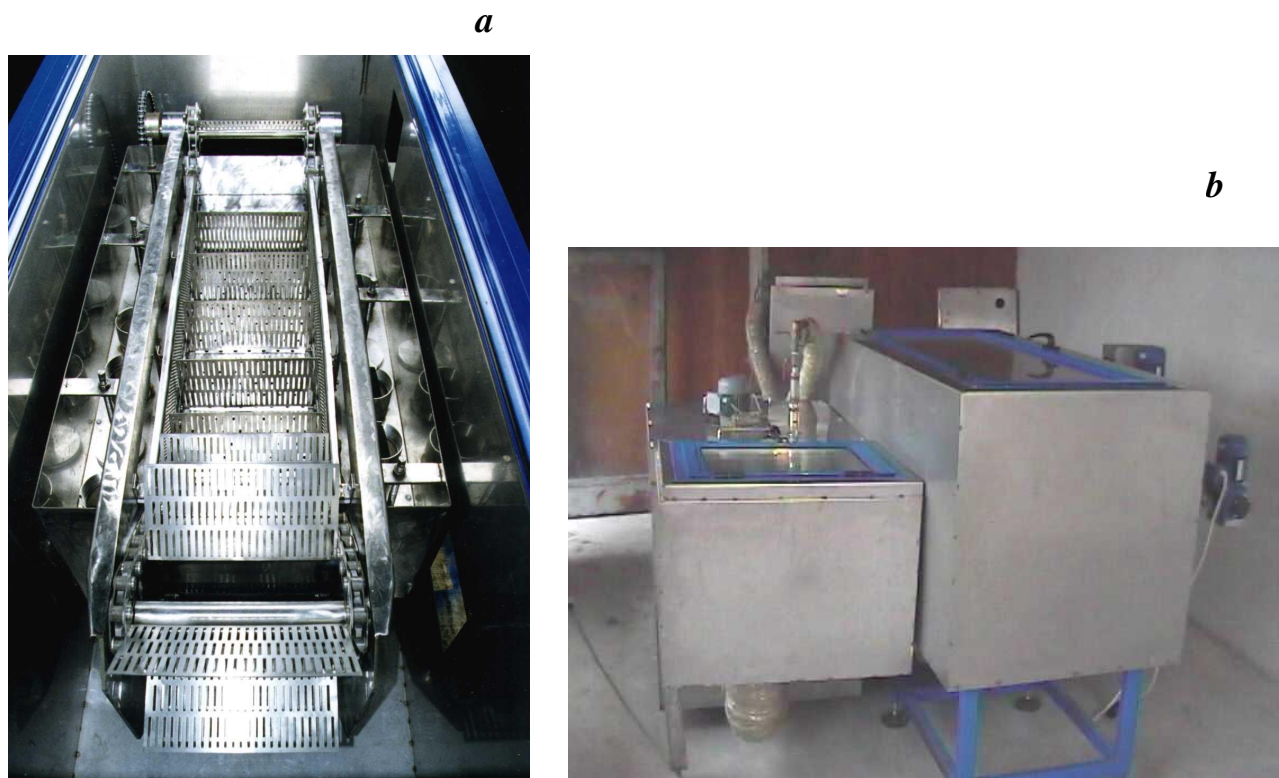


Figure 9.10. Hydrofluidization, conveyor and driving systems of the *HyFloFreeze*<sup>®</sup> prototype (Technical University of Sofia and Interobmen Ltd.): (a) top view, (b) overall view

The following initial design specifications were used when putting together the prototype freezer:

(i) *starting selection of fruits to be frozen*: strawberries, raspberries, plums, apricots, morellos, cherries, blueberries and cranberries; (ii) *refrigerating media*: unfreezable liquids or pumpable ice slurries based on sugar-ethanol aqueous solutions, (iii) *refrigerating medium temperature*:  $-25/-30^{\circ}\text{C}$ , (iv) *evaporation temperature of the refrigerant*:  $-30/-35^{\circ}\text{C}$ , (v) *throughput*: 20-50 kg per hour (depending on the product); (vi) *final temperature in the frozen food centre*:  $-12/-15^{\circ}\text{C}$ ; (vii) *final average temperature of the product*:  $-18/-20^{\circ}\text{C}$ ; (viii) *principle of operation*: enhanced hydrofluidization throughout the whole freezer by directed jets of fluidizing agent; and (ix) *conveyor system*: electronic regulation of the driving motor revolutions for smooth variation of the conveyor speed and product residence time depending on the individual freezing duration for each product.

The ice-slurry-based HFM technology possesses a series of advantages over the conventional IQF modes, which can be summarised as follows (Fikiin and Fikiin, 1998, 1999; Fikiin *et al.*, 2001):

- **Frozen fruit quality:** high freezing rate; fine-grain crystal structure; sharp reduction of the surface mass transfer; enzyme-inhibiting action of the sugar; easy incorporation of antioxidants, flavourings, aromas and micronutrients and formulation of delicious dessert-type frozen foods with extended shelf-life and improved nutritional value and sensory properties.
- **Energy and economic efficiency:** higher refrigerating and evaporation temperatures; possibility for single-stage refrigeration machine with reduced investment, maintenance and energy costs; easy connection with systems for thermal energy storage; high throughput and cost efficiency.
- **Environmental friendliness:** use of environmentally friendly secondary coolants (syrup-type solutions or ice-slurries) and primary refrigerant closed in a small isolated system.

At some temperatures and concentrations, the pumping of sugar-ethanol-based slurry through the hydraulic circuit and perforated bottom may be accompanied by intense foaming (*Figure 9.5*). Preliminary tests revealed that this adverse effect could be overcome by adding suitable antifoaming agents.

### Literature cited in chapter 9

1. Bel, O.; Lallemand, A. : Etude d'un fluide frigoporteur diphasique: 1 – Caractéristiques thermophysiques intrinsèques d'un coulis de glace; et 2 – Analyse expérimentale du comportement thermique et rhéologique. *Int. J. Refrig.*, Vol. 22, No. 3: pp. 164-187, 1999.
2. Egolf, P.W.; Brühlmeier, J.; Özvegyi, F.; Abächerli, F.; Renold, P.: Properties of ice slurry. *Proc. IIR Conf. Applications of Natural Refrigerants, Aarhus, Denmark 1996*, IIF/IIR: pp. 517-526, 1996.
3. Fikiin, A.G.: Congélation de fruits et de légumes par fluidisation. *Proc. Budapest Conf.*, IIF/IIR: pp. 197-203, 1969.
4. Fikiin, A.G. : Bases théoriques du procédé de fluidisation lors de l'intensification de la congélation des fruits et des légumes. *Proc. 15<sup>th</sup> Int. Congress Refrig.*, Venice, Vol. 4: pp. 221-230, 1979.
5. Fikiin, A.G.: Physical conditions of fluidized-bed freezing of fruits and vegetables. *Kholodilnaya Tekhnika/Refrig. Engng*, No. 7: pp. 59-61 (in Russian), 1980.
6. Fikiin, A.G.: Method and system for immersion cooling and freezing of foodstuffs by hydrofluidization. *Invention Certificate No. 40164*, Bulgarian Patent Agency INRA, 1985.
7. Fikiin, A.G.: New method and fluidized water system for intensive chilling and freezing of fish. *Food Control*, Vol. 3, No. 3: pp. 153-160, 1992.
8. Fikiin, A.G.: Quick freezing of vegetables by hydrofluidization. In *New Applications of Refrigeration to Fruit and Vegetables Processing – Proceedings of IIR Conference, Istanbul (Turkey), Refrigeration Science and Technology*, International Institute of Refrigeration, 1994-3: pp. 85-91, 1994.
9. Fikiin, A.G.; Pham, V.H.: System for examination of heat transfer regimes during hydrorefrigeration of foodstuffs. *Invention Certificate No. 39749*, Bulgarian Patent Agency INRA, 1985.

10. Fikiin, A.G.; Ditchev, S.P.; Fikiina, I.K.: Principal parameters characterising the fluidization of fruit and vegetable layers. *Kholodilnaya Tekhnika / Refrig. Engng*, No. 11, pp. 33-37 (in Russian), 1966.
11. Fikiin, A.G.; Ditchev, S.P.; Karagerov, D.I.: Fluidized bed freezing system for fruits and vegetables with various dimensions. *Invention Certificate No. 10967*, Bulgarian Patent Agency INRA, 1965.
12. Fikiin, A.G.; Ditchev, S.P.; Karagerov, D.I.: Fluidized bed freezing apparatus AZF. *Kholodilnaya Tekhnika / Refrig. Engng*, No. 7, pp. 55-58 (in Russian), 1970.
13. Fikiin K.A.: *Novelties of Food Freezing Research in Europe and Beyond*. Flair-Flow Europe Synthetic Brochure for SMEs No.10 (ISBN: 2-7380-1145-4), INRA: Institut National de la Recherche Agronomique, Paris (France), 55p., 2003.
14. Fikiin, K.A.; Fikiin, A.G.: Individual quick freezing of foods by hydrofluidization and pumpable ice slurries. In *Advances in the Refrigeration Systems, Food Technologies and Cold Chain*, Ed.: K. Fikiin, Proceedings of IIR Conference, Sofia (Bulgaria), *Refrigeration Science and Technology*, International Institute of Refrigeration, 1998-6: pp. 319-326 (published also in the *AIRAH Journal*, 2001, Vol. 55, No. 11, pp. 15-18), 1998.
15. Fikiin, K.A.; Fikiin, A.G.: Novel cost-effective ice-slurry-based technology for individual quick freezing of foods by hydrofluidization. *CD-Rom Proceedings of the 20<sup>th</sup> International Congress of Refrigeration*, Sydney (Australia), ICR Paper No. 271, 1999a.
16. Fikiin K.A.; Fikiin A.G.: Predictive equations for thermophysical properties and enthalpy during cooling and freezing of food materials. *Journal of Food Engineering*, Vol. 40, No. 1-2, pp. 1-6, 1999b.
17. Fikiin, K.A.; Fikiin A.G.: Congelación individual rápida de alimentos por hidrofluidificación y compuestos de hielo. *Frío, Calor y Aire Acondicionado* (Madrid), Vol. 30, No. 334, pp. 22-27, 2002.
18. Fikiin, K.A.; Fikiin A.G.: Quick freezing of foods by hydrofluidization and pumpable ice suspensions. *Kholodilnaya Tekhnika / Refrig. Engng*, No. 1, pp. 22-25 (in Russian), 2003a.
19. Fikiin K.A.; Fikiin A.G.: L'Ice Slurry (ghiaccio binario) per una surgelazione veloce degli alimenti – Surgelamento singolo degli alimenti mediante idrofluidizzazione. *Industria & Formazione per il Tecnico della Refrigerazione e Climatizzazione* (Milano), No. 3, pp. 36-39, 2003b.
20. Fikiin, K.A.; Kaloyanov, N.G.; Filatova, T.A.; Sokolov, V.N.: Fine-crystalline ice slurries as a basis of advanced industrial technologies: State of the art and future prospects. *Refrigeration Business* (Moscow), No. 7, pp. 4-11 (in Russian), 2002.
21. Fikiin, K.A.; Tsvetkov, O.B.; Laptev, Yu.A.; Fikiin, A.G.; Kolodyaznaya, V.S.: Thermophysical and engineering issues of the immersion freezing of fruits in ice slurries based on sugar-ethanol aqueous solutions. *Proceedings of the Third IIR Workshop on Ice Slurries*, Lucerne (Switzerland). International Institute of Refrigeration, pp.147-154, 2001. (published also in *EcoLibrium – Journal of AIRAH: Australian Institute of Refrigeration, Air Conditioning and Heating*, Vol. 2, No. 7, pp. 10-15, 2003.)
22. Fleshland, O.; Magnussen, O. M.: Chilling of farmed fish. *Proc. Aberdeen Conf.*, IIF/IIR, pp. 185-192, 1990.
23. Hansen, T.; Wang, M.J.; Kauffeld, M.; Christensen, K.G.; Goldstein, V.: Application of ice slurry technology in fishery. XXth Int. Cong. of Refr., Sydney, Australia, 19-24 September, 1999.

24. Jeffrey D.J.: Conduction through a random suspension of spheres, *Proceedings of the Royal Society London*, Vol. A 335: pp. 355-367, 1973.
25. Lucas, T.; Raoult-Wack, A.L.: Immersion chilling and freezing in aqueous refrigerating media: review and future trends. *Int. J. Refrig.*, Vol. 21, No. 6: pp. 419-429, 1998.
26. Paul, J.: Binary ice as a secondary refrigerant. *Proc. 19<sup>th</sup> Int. Congress Refrig.*, The Hague, Vol. 4b: pp. 947-954, 1995.
27. Pearson, S.F.; Brown J.: Use of pumpable ice to minimise salt uptake during immersion freezing. *Proc. Oslo Conf.*, IIF/IIR: pp. 712-722, 1998.
28. Sokolov, V.N.; Fikiin K.A.; Kaloyanov, N.G.: Advantages, production and applications of pumpable ice slurries as secondary refrigerants. *BulkToMM Machine Mechanics*, Vol. 44, pp. 26-31 (in Russian), 2002.
29. Sørensen, B.S.: Resultater fra brug af kvalitetsindikatorer i modelforsøg, Workshop i kvalitetsindikatorer, Danish Institute for Fisheries Research, 1999.
30. Thomas, D.G.: Transport characteristics of suspension – VIII: A note on the viscosity of Newtonian suspension of uniform spherical particles, *Journal of Colloid Science*, Vol. 20: pp. 267-277, 1965.
31. Tressler, D.K.: Food freezing systems. In: Tressler, D.K., Van Arsdel, W.B., Copley, M.J. *The Freezing Preservation of Foods*, Vol. 1, The AVI Publishing Co., Westport, Connecticut: pp. 120-152, 1968.
32. Ure, Z.: Slurry-ice based cooling systems. *Proc. Sofia Conf.*, IIF/IIR: pp. 172-179, 1998.
33. Woolrich, W.R.: *Handbook of Refrigerating Engineering*, Vol. 2: *Applications*. The Avi Publishing Co., Westport, Connecticut, 434 , 1966.
34. Wang, M.J.; Hansen, T.M.; Kauffeld, M.; Goldstein, V.: Slurry Ice in Fish Preservation. *Infofish International 2*, pp. 42-46, 2000.



**List of symbols Chapter 9**

$c$	Specific heat capacity ( $\text{kJ kg}^{-1} \text{K}^{-1}$ )
$D$	Diameter of ice particles ( $\mu\text{m}$ )
$x, X$	Mass fraction ( $\text{kg kg}^{-1}$ )
$h$	Enthalpy per unit mass ( $\text{kJ kg}^{-1}$ )
$k$	Thermal conductivity ( $\text{W m}^{-1} \text{K}^{-1}$ )
$L$	Latent heat of water freezing/thawing ( $\text{kJ kg}^{-1}$ )
$t, T$	Temperature ( $^{\circ}\text{C}$ or $\text{K}$ )
$t_f$	Initial freezing temperature ( $^{\circ}\text{C}$ )

*Subscripts*

e	ethanol
d	dry matters
i	ice
is	ice slurry
l	liquid solution
oil	fat matters (oil)
p	at constant pressure
s	sugar
w	water

*Greek letters*

$\eta$	Dynamic viscosity ( $\text{mPa s}$ )
$\lambda$	Thermal conductivity ( $\text{W m}^{-1} \text{K}^{-1}$ )
$\rho$	Density ( $\text{kg m}^{-3}$ )
$\tau$	Time ( $\text{s}$ )
$\varphi$	Volumetric fraction ( $\text{m}^3 \text{m}^{-3}$ )

*Superscripts*

in	initial
----	---------

*Acronyms*

CFC	ChloroFluoroCarbon	HFC	HydroFluoroCarbon
COP	Coefficient of Performance	HFM	HydroFluidisation Method
HCFC	HydroChloroFluoroCarbon	IQF	Individual Quick Freezing

**ISBN n° 2-913149-42-1**

**Copyright and Disclaimer**

“The information provided in this document is based on the current state of art and is designed to assist engineers, scientists, companies and other organizations. It is a preliminary source of information that will need to be complemented prior to any detailed application or project. Whilst all possible care has been taken in the production of this document, the IIR, its employees, officers and experts cannot accept any liability for the accuracy or correctness of the information provided nor for the consequences of its use or misuse.

For full or partial reproduction of anything published in this document, proper acknowledgement should be made to the original source and its author(s). No parts of the book may be commercially reproduced, recorded and stored in a retrieval system or transmitted in any form or by any means (mechanical, electrostatic, magnetic, optic photographic, multimedia, Internet-based or otherwise) without permission in writing from the IIR.

© Copyright 2005 International Institute of Refrigeration

## **CHAPTER 6**

**Renewable refrigeration and smarter energy use  
for a sustainable cold chain**

## Chapter 6

concentrates on sustainability-enhancing engineering solutions for decarbonising and ‘greening’ the cold chain industry as one of the most energy-intensive sectors of contemporary economy. The agri-food sector currently consumes 30 % of the global energy demand and is mostly powered by fossil fuels. Moreover, in accordance with [UNEP’s data](#), the energy demands and F-gas emissions of cold chain technologies, along with the food loss and waste due to lack of refrigeration, are responsible for 4 % of global greenhouse gas emissions.

Cooling often remains under the shadow of its heating counterpart, while it needs a tailored set of dedicated actions to ensure its climate-neutrality. The newly adopted [cooling provisions of the EU Renewable Energy Directive](#) addresses space cooling in buildings or districts, leaving food refrigeration outside the scope. The latter appears to be a still unexplored R&D field as far as renewable energy is concerned. Both radical and incremental innovations are vital to implement the noble and far-reaching ambitions of the Paris Climate Agreement, the United Nations’ Sustainable Development Goals, the European Green Deal and the REPowerEU plan.

Refrigerated warehouses for chilled and frozen commodities are large energy consumers and account for a significant portion of the global energy demand. However, the opportunity to integrate renewable energy sources (RES) in the energy supply of large cold storage facilities is often overlooked. In that context, the present Chapter 6 features, conceptualises and systematises a number of smart engineering solutions and control strategies to exploit renewables of different nature (solar, wind, geothermal, biogas, etc.) in the food storage sector, raising also the awareness of specialised knowledge that is not yet sufficiently popular among cold chain operators.

Intermittent supply is a major obstacle to the renewable power market. Renewables are fickle sources, prone to overproducing when demand is low and failing to meet requirements when demand peaks. RES-based technologies are therefore unfeasible without reliable energy storage. Integration of solar, wind and other distributed RES in the power grid is challenging, especially for traditional centralised grids with top-down structure. Thus, the so-called ‘*smart grids*’ shift from the traditional centralised top-down approach of power supply to more sophisticated decentralised (distributed, controllable, flexible and interactive) systems for electricity generation, storage, transmission, distribution and consumption. In this context, the RES-assisted warehouses should logically become interactive players within the modern smart grid networks.

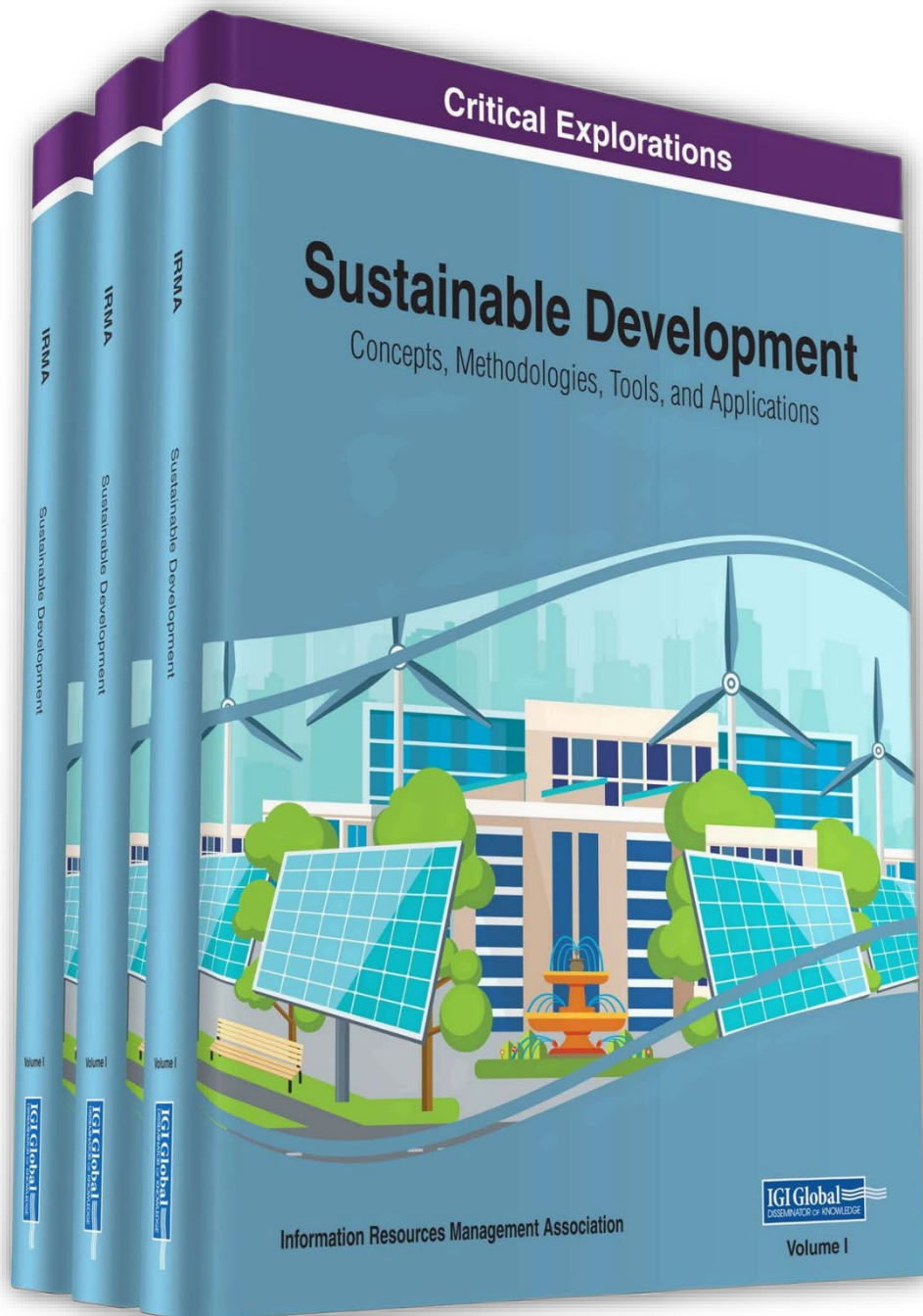
Suitable integration of RES in refrigerated food preservation facilities helps to achieve two important goals: (i) reducing the overall electricity usage from the power grid, and (ii) unloading the peak power consumption, thereby balancing the power supply and mitigating the environmental footprint of food refrigeration.

Chapter 6 pays special attention to a demand-response strategy (named '*Night Wind*') for managing the storage of renewable energy by smart load shifting in refrigerated warehouses. Distributed RES (such as wind and solar energy) have a substantial potential for reducing CO<sub>2</sub> emissions but are difficult to integrate because of their intermittent contribution. The existing mismatch between the power demand and supply is balanced by permitting the temperature of stored frozen products to vary within a small temperature range, thereby turning the warehouses to a powerful '*virtual battery*' on the grid. Thus, the frozen produce itself serves as a phase-change medium for latent thermal energy storage, while the cold chain operator is converted from a simple user to an active actor on the energy marketplace.

While balancing the power grid by burning fossil fuels is inefficient and polluting, storing renewable energy in a large refrigerated warehouse (to shave the peak power demands by temporarily turning off the refrigeration plant) is an environmentally friendly and cost-effective alternative, which reduces the running costs for cold chain operators. The '*Night Wind*' system for smart automated control is based on actual and forecast data for: (i) warehouse performance and energy demand, (ii) environmental conditions and RES availability, and (iii) variation of electricity price (depending on tariff plans negotiated and/or fluctuations on the stock market).

Another point of attention is the refrigerated food quality as affected by temperature fluctuations and freeze-thaw cycles, caused by the employed '*Night Wind*' control mode. Experimental tests are carried out and '*Night Wind*'-tolerable products are determined accordingly.

Results presented in Chapter 6 are reported by the author at several conference events around the world (e.g. organised by the *European Federation of Food Science and Technology* – EFFoST, *International Commission of Agricultural Engineering* – CIGR, *International Institute of Refrigeration* – IIR, etc.), while our relevant publication is referenced in monographs on geothermal heat pump systems (doi: [10.1007/978-3-031-24524-4](https://doi.org/10.1007/978-3-031-24524-4)) and on energy services (doi: [10.1016/C2018-0-04950-6](https://doi.org/10.1016/C2018-0-04950-6)).



Reproduced from *Sustainable Development: Concepts, Methodologies, Tools, and Applications*, Fikiin K. and Stankov B. Integration of renewable energy in refrigerated warehouses – Chapter 33, pp. 721-770, doi: <https://doi.org/10.4018/978-1-5225-3817-2.ch033>, Copyright © 2018, with permission from IGI Global.



# Chapter 33

## Integration of Renewable Energy in Refrigerated Warehouses

**Kostadin Fikiin**

*Technical University of Sofia, Bulgaria*

**Borislav Stankov**

*Technical University of Sofia, Bulgaria*

### ABSTRACT

*Refrigerated warehouses are large energy consumers and account for a significant portion of the global energy demand. Nevertheless the opportunity for integration of renewable resources in the energy supply of large cold storage facilities is very often unjustifiably neglected, whereas the employment of renewable energy for many other industrial and comfort applications is actively promoted and explored. In that context, the purpose of this chapter is to bridge the existing gap by raising the public awareness of stakeholders, researchers, practicing engineers and policy makers about the availability of a number of smart engineering solutions and control strategies to exploit renewables of different nature (solar, wind, geothermal, biogas, etc.) in the food storage sector, as well as by calling the readers' attention to the specialised knowledge in the matter, which has been published so far.*

### INTRODUCTION

On 5 June 2014 the UN Secretary-General launched the “UN Decade of Sustainable Energy for All”, urging leaders from around the world to “deliver new and expanded commitments and partnerships that will transform the global energy landscape” (“UN Secretary-General”, 2014). Increasing the integration of renewable energy sources (RES) in the global energy supply chain is one of the key aspects of sustainable development. Hence, one of the goals of the Sustainable Energy for All (SE4ALL) initiative is doubling the share of renewable energy in the global energy mix by 2030. As the International Energy Agency (2007) states, renewable sources are “essential contributors to the energy supply portfolio as they contribute to world energy supply security, reducing dependency on fossil fuel resources, and provide opportunities for mitigating greenhouse gases”.

DOI: 10.4018/978-1-5225-3817-2.ch033

### **Integration of Renewable Energy in Refrigerated Warehouses**

According to Coulomb (2006) and the International Institute of Refrigeration (2007, 2015), refrigeration (including air-conditioning) currently accounts for about 17% of worldwide electricity use, while over 80% of the global warming impact of refrigeration systems is due to this electricity use. Industrial refrigeration, comprising over 550 million m<sup>3</sup> of cold storage space worldwide (International Institute of Refrigeration, 2015), is a major consumer of about 8% of the electrical power on a global scale (consistent with the circumstance that approximately 40% of the global food output require refrigeration). In the context of sustainable development, designing or retrofitting of a cold store refrigeration plant should consider the possibility of using RES to provide at least a portion of the required energy input.

Although there are a number of RES-assisted technologies for different refrigeration applications, many of these tools are still at rudimentary stages of development, either not commercially viable or only applicable for relatively small-scale systems. However, integration of RES in refrigerated food storage facilities might provide a cost-efficient way of: (i) reducing electricity consumption from the grid, and/or (ii) shifting refrigeration loads from peak to low consumption periods, thereby contributing to the overall balance of the power supply system and minimizing the environmental footprint of the cold store. While many of the today's engineering solutions are not yet cost efficient by themselves, various governmental policies in support of renewable energy developments and integration are carried out around the world, which can substantially enhance the economic feasibility of RES-powered installations.

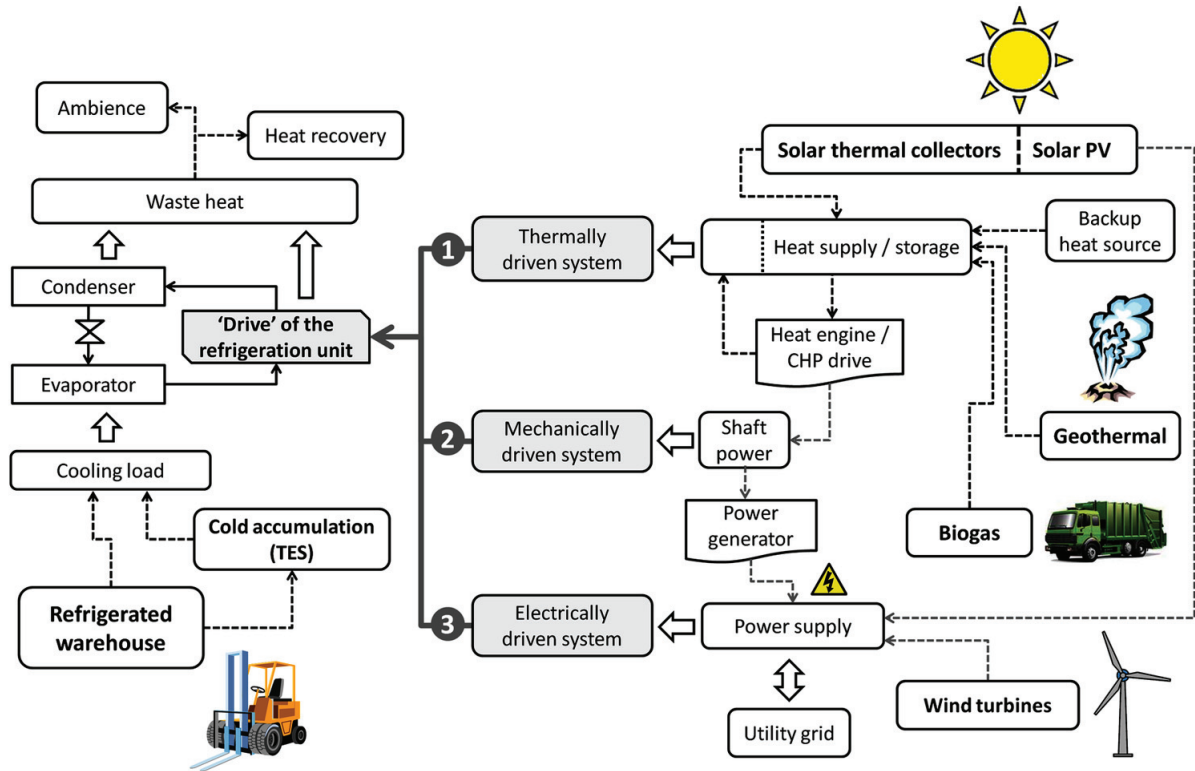
The objective of this chapter is to familiarise the readers with: (i) state-of-the-art RES-based technologies applicable to refrigeration systems, including their technical and economic performance, (ii) different strategies to integrate these technologies in the energy supply of refrigerated warehouses in an efficient way, (iii) practical examples, pilot projects and on-going research involving RES utilization for cold storage facilities, and (iv) government incentives which can facilitate investment in RES projects. The material is primarily intended to serve as guidance for cold store operators and refrigeration stakeholders, who are still unaware of the latest RES technologies and the opportunities to employ them in the food refrigeration industry. As the chapter has no ambition to analyse in-depth any of the concerned technologies, the readers are advised to examine additional literature in order to gain more comprehensive knowledge on the particular topics of interest (e.g., see the list of references as a starting point).

## **BACKGROUND**

Integration of renewables in the energy supply of cold storage facilities can be accomplished in a variety of ways, as illustrated in Figure 1. Solar photovoltaic cells and wind turbines can be used for on-site power generation, while solar thermal collectors, geothermal sources and biogas combustion can serve as a heat source for thermally driven refrigeration systems. In addition, thermal sources can be used to drive cogeneration or trigeneration systems, thereby simultaneously producing electricity, heating and refrigerating output. Thermal energy storage for heat and cold accumulation can be integrated in the system to shift energy supply and/or demand as to permit better overall utilization of renewable energy. Provided that proper interaction is established between the cold store operator and the electric utility, on-site RES-generated power can be fed to the utility grid, which permits to sell excessive energy at attractive prices (especially in the presence of convenient government policies). The latter and the inclusion of thermal energy storage can overcome a major inconvenience of many RES technologies, i.e. the intermittent energy supply due to the fluctuating availability of the energy resource.

### Integration of Renewable Energy in Refrigerated Warehouses

Figure 1. Various options to integrate renewable sources in the energy supply of refrigeration systems for cold storage facilities



Cold store operators can consider and evaluate different alternatives for RES integration in order to screen out the best option in terms of both technical and economic performance. Several metrics exist, which can be used to compare diverse alternatives. One of the main parameters, employed to evaluate the overall performance of refrigeration systems driven by renewable energy, is the overall system efficiency ( $OSE$ ) defined as:

$$OSE = \frac{\text{Refrigerating capacity}}{\text{Capacity of the renewable source}} = \frac{Q_E}{E_R} = \frac{Q_E}{E_S} \cdot \frac{E_S}{E_R} = COP \cdot \eta_{es} \quad (1)$$

$$COP = \frac{\text{Refrigerating capacity (useful output)}}{\text{Supplied input capacity (required input)}} = \frac{Q_E}{E_S} \quad (2)$$

where  $COP$  is the coefficient of performance of the refrigeration system and  $\eta_{es} = E_S/E_R$  is the energy conversion efficiency of the energy supply system utilizing RES (which is a product of the efficiencies of each consecutive stage of energy conversion prior to the refrigeration system, beginning from the device that captures the renewable resource).

**Integration of Renewable Energy in Refrigerated Warehouses**

As a measure of performance, *COP* can be used not only to compare different refrigeration systems, but also to define system efficiency in comparison with the theoretically possible maximum. Thermodynamically the maximum possible efficiency of a refrigeration cycle operating between two temperatures ( $T_A$  – temperature of the heat sink, e.g. ambient temperature, and  $T_L$  – temperature of the refrigerated space, both in K) is the Carnot efficiency defined as:

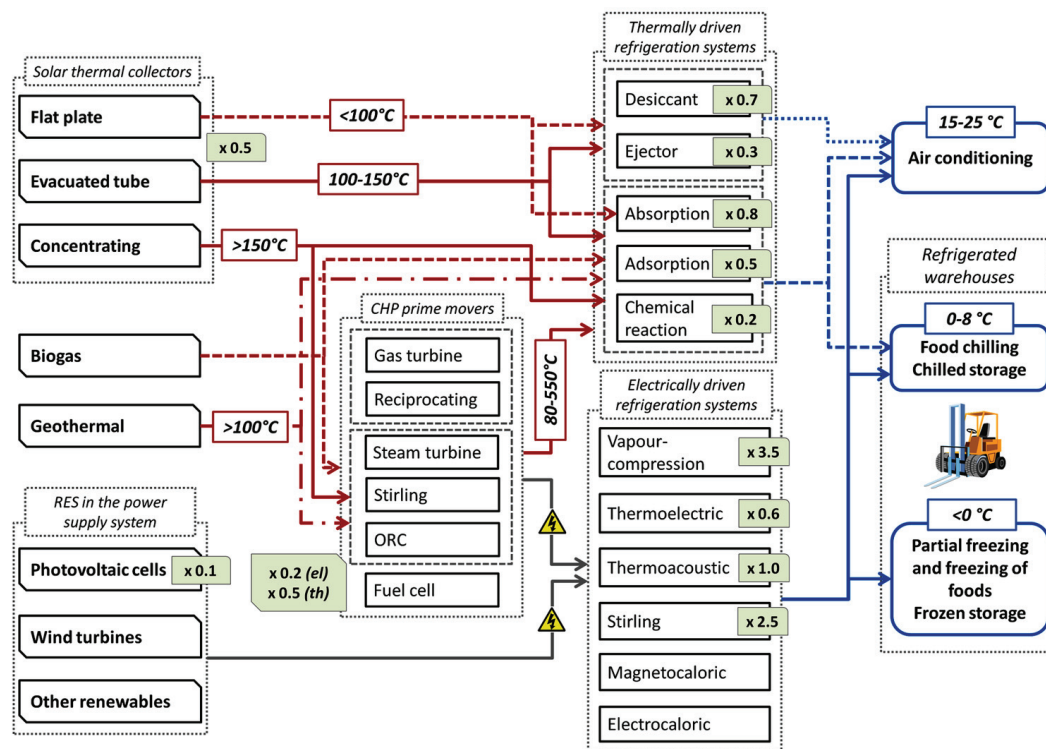
$$\eta_{C,rc} = \frac{T_L}{T_A - T_L} \tag{3}$$

The actual efficiency of the real refrigeration cycle, i.e. *COP*, can be represented as a product of the Carnot efficiency and the anticipated fraction,  $\alpha_r$ , of the Carnot efficiency that the cycle is expected to achieve:

$$COP = \alpha_r \cdot \eta_{C,rc} \tag{4}$$

Various possible configurations of RES-driven refrigeration systems based on different physical principles and indicative values of the respective efficiencies, for the consecutive stages of energy conversion, are shown in Figure 2.

Figure 2. Applications and indicative energy conversion efficiencies of refrigeration systems powered by renewable energy sources



### Integration of Renewable Energy in Refrigerated Warehouses

Many of the configurations shown in Figure 2 are commercially viable, while a number of these technologies (involving thermoelectric, thermoacoustic, magnetocaloric and electrocaloric principles of refrigeration) are still in an immature R&D phase of their elaboration. Part of the indicated configurations (e.g. those involving solar-driven desiccant and ejector refrigeration systems) are only feasible for air-conditioning applications and included just for completeness. Nevertheless, this chapter focusses on RES technologies and engineering solutions which are applicable for large-scale refrigeration systems suitable for cold storage facilities.

While technically feasible, some configurations may not be economically efficient. Several metrics can be used to assess the economic performance of different RES technologies. In some cases the installed cost per peak useful output is used, e.g. \$/W or €/W. Depending on the context, useful output can be the refrigeration capacity or the output capacity of the energy supply system (which represents the required input capacity for the refrigeration system). Another relevant metric, used to evaluate the economic efficiency of RES, is the levelized cost of energy (*LCOE*), i.e. the ratio of the lifecycle cost of the system to the energy produced over its operational lifetime (Intergovernmental Panel on Climate Change, 2014):

$$LCOE = \frac{\text{Present value of total costs}(\$)}{\text{Lifetime energy production}(MWh)} = \frac{CRF \cdot I + OM + F}{E_s} \quad (5)$$

$$F = FC \cdot \frac{E_s \cdot FLH}{\eta_{es}} \quad (6)$$

where  $I$  is the total investment costs, including initial costs, construction costs and decommissioning costs,  $OM$  is the net annual operation and maintenance (O&M) costs,  $FC$  is the fuel costs per unit of energy input and  $FLH$  is the number of annual equivalent full-load hours. The capital recovery factor is calculated as:

$$CRF = \frac{r}{1 - (1 + r)^{-L_T}} \quad (7)$$

where  $r$  is the weighted average cost of capital (e.g. 5 or 10%) and  $L_T$  is the project duration, i.e. operational lifetime of the system (Intergovernmental Panel on Climate Change, 2014). *LCOE* is a particularly popular metric for RES power generation systems.

### Opportunities for Integration of Renewables in Cold Stores

Various opportunities for RES integration in refrigerated warehouses are grouped and outlined hereafter in three sections of this chapter, entitled as follows: (i) “*Thermally Driven Refrigeration*” (which reviews the possibilities of using heat derived from RES to drive sorption refrigeration systems); (ii) “*Refrigeration through On-site Power Generation*” (which discusses distributed generation of electricity through RES technologies, including the use of cogeneration), and (iii) “*Integration of Renewables Involving*



### *Integration of Renewable Energy in Refrigerated Warehouses*

*Thermal Energy Storage*” (which examines engineering solutions for cold accumulation to utilize RES more efficiently in the context of the smart power grid).

## **THERMALLY DRIVEN REFRIGERATION**

### **Solar Thermal Collectors**

Solar thermal collectors are devices that capture solar radiation to heat a solid, liquid or gaseous substance. Collectors used for heating liquids (typically water or a glycol solution) are reviewed in this chapter.

While solar energy is an intuitive source for heating applications, its use for refrigeration is not so obvious, although there is usually a good match between the peaks of solar irradiation and cooling loads (in terms of both time and geographic location). In developing countries with no or unreliable power supply, where conventional fuels are difficult or too expensive to obtain, a number of solar refrigeration applications (e.g. vaccine storage or fish and milk preservation) have been known for decades. In industrialized countries, characterized with reliable supply of electricity from the grid, comparatively little interest has been shown in using solar energy as a driving source for refrigeration systems, because a number of technical and market barriers have led market actors to perceive these technologies as uneconomical.

The high initial cost of a solar system, whose largest portion is usually taken up by solar collectors, is one of the main obstacles. Solar radiation, however, is the primary source of energy for the planet and the potential of converting this energy for powering different processes, including refrigeration, is certainly huge. It is estimated that while 376,680,000 TWh of solar energy are dissipated into surface heating each year, only about 266 TWh are captured by solar collectors, of which 74% by thermal collectors, 24% by photovoltaic (PV) collectors and 2% by concentrated solar power (CSP) systems (Infante Ferreira & Kim, 2014). Since this energy is free whenever available, the only necessity is to find appropriate energy conversion technologies which can make utilization of this energy source technically and economically feasible.

One of the main inconveniences, common for all solar systems, is the fluctuating availability of solar radiation. Although this availability has more or less predictable annual and daily cycles, the solar energy to be captured is also determined by weather conditions, which are quite difficult to predict. Even in the presence of dedicated systems for thermal or electrical storage, it is very challenging to manage a system that relies solely on solar energy. Hence, efforts are to be concentrated on integrating the solar system with another energy source (primary or supplementary) in the most efficient manner, taking into account local climatic conditions and energy costs.

The design of a solar thermal system should be optimized to capture the largest possible amount of solar radiation through the smallest possible collector area in an economically efficient manner. Solar collectors can be installed at a fixed tilt, the optimum of which depends on location and season, e.g. for summer the optimal tilt is usually considered to be equal to the site latitude minus 10°. Alternatively, a movable sun tracking system can be used to automatically tilt the collector depending on the position of the sun – single-axis and two-axis trackers are available for this purpose. Tracking systems are necessary for concentrating solar collectors, but their involvement increases the complexity and cost of the system.

Flat plate and evacuated tube collectors are most common, because of the design simplicity and reasonable cost. Concentrating solar collectors use geometric optics to enhance collector efficiency, but this works effectively only for direct (i.e. beam) solar radiation and not for diffuse radiation, which in

### Integration of Renewable Energy in Refrigerated Warehouses

some locations may represent the greater share of total solar radiation. Hence, concentrating collectors are beneficial mainly for sunny locations relatively closer to the equator, which receive high amounts of direct solar radiation. Table 1 summarises different types of solar collectors and the range of temperatures they are expected to provide to the circulating heat transfer fluid. Weiss and Rommel (2008) compiled a detailed survey of recent advances in the design and optimisation of solar thermal collectors for a wide range of operating temperatures between 80°C and 250°C.

The efficiency of a solar thermal collector is defined as the ratio between the heat supplied to the heated substance,  $Q_{sol}$ , and the total amount of solar radiation reaching the surface of the collector, i.e. the product of the solar irradiance  $I_{\beta}$  (W/m<sup>2</sup>) and the surface area of the solar collector  $A_s$  (m<sup>2</sup>):

$$\eta_{sc} = \frac{Q_{sol}}{I_{\beta} \cdot A_s} \quad (8)$$

This efficiency depends on operating temperatures (i.e.  $T_A$  – the ambient air temperature and  $T_M$  – the mean temperature of the heat transfer fluid) and can be defined as Lazzarin (2014):

$$\eta_{sc} = \eta_0 - a_1 \cdot x - a_2 \cdot x^2 \quad (9)$$

$$x = \frac{T_M - T_A}{I_{\beta}} \quad (10)$$

The three coefficients:  $a_1$ ,  $a_2$  and  $\eta_0$  can vary significantly depending on collector types and constructions, and are normally determined by the manufacturer. Example values for four of the most commonly used solar collector types are shown in Table 2, along with indicative figures for the installed cost per unit area of the collector. The values given in Table 2 are derived from two different sources, i.e. the works of Infante Ferreira & Kim (2014), above, and Lazzarin (2014), below (shown in parentheses).

Table 1. Types of solar thermal collectors (Adapted from Kalogirou, 2009)

Collector Type	Sun Tracking	Absorber Geometry	Concentration Ratio	Indicative Temperature Range
Flat plate	No	Flat	1	30-80°C
Evacuated tube	No	Tubular	1	50-200°C
Compound parabolic	No	Tubular	1-5	60-240°C
	Single-axis	Tubular	5-15	60-300°C
Linear Fresnel	Single-axis	Tubular	10-40	60-250°C
Cylindrical trough	Single-axis	Tubular	15-50	60-300°C
Parabolic trough	Single-axis	Tubular	10-85	60-400°C
Parabolic dish	Two-axis	Point	600-2000	100-1500°C
Heliostat	Two-axis	Point	300-1500	150-2000°C

### Integration of Renewable Energy in Refrigerated Warehouses

Table 2. Examples of zero-loss collector efficiency, heat loss coefficients and installed cost for different types of solar thermal collectors

Collector Type	$\eta_0$	$a_1$	$a_2$	Installed Cost
Flat plate	0.8 (0.79)	3.02 (3.94)	0.0113 (0.012)	€371/m <sup>2</sup> (€350/m <sup>2</sup> )
Evacuated tube	0.84 (0.71)	2.02 (0.974)	0.0046 (0.005)	€750/m <sup>2</sup> (€650/m <sup>2</sup> )
Parabolic trough	0.76 (0.52)	0.22 (0.475)	0 (0.0031)	€540/m <sup>2</sup> (€450/m <sup>2</sup> )
Parabolic dish	0.82	0.22	0	€270/m <sup>2</sup>

## Solar Sorption Refrigeration

Sorption refrigeration machines are based on either the absorption or adsorption principle, which utilize physical or chemical attraction between a pair of substances to produce the required refrigeration output. In both cases heat, which can be supplied by solar thermal collectors, is used to regenerate the sorbent, while only small amounts of electricity are required to drive circulation pumps. The *COP* of sorption refrigeration systems is the ratio of the refrigerating capacity,  $Q_E$ , to the sum of the required input heat capacity, i.e. heat provided by the solar system,  $Q_S$ , and the power capacity of circulation pumps,  $P_P$  (which is usually negligible):

$$COP = \frac{Q_E}{Q_S + P_P} \approx \frac{Q_E}{Q_S} \quad (11)$$

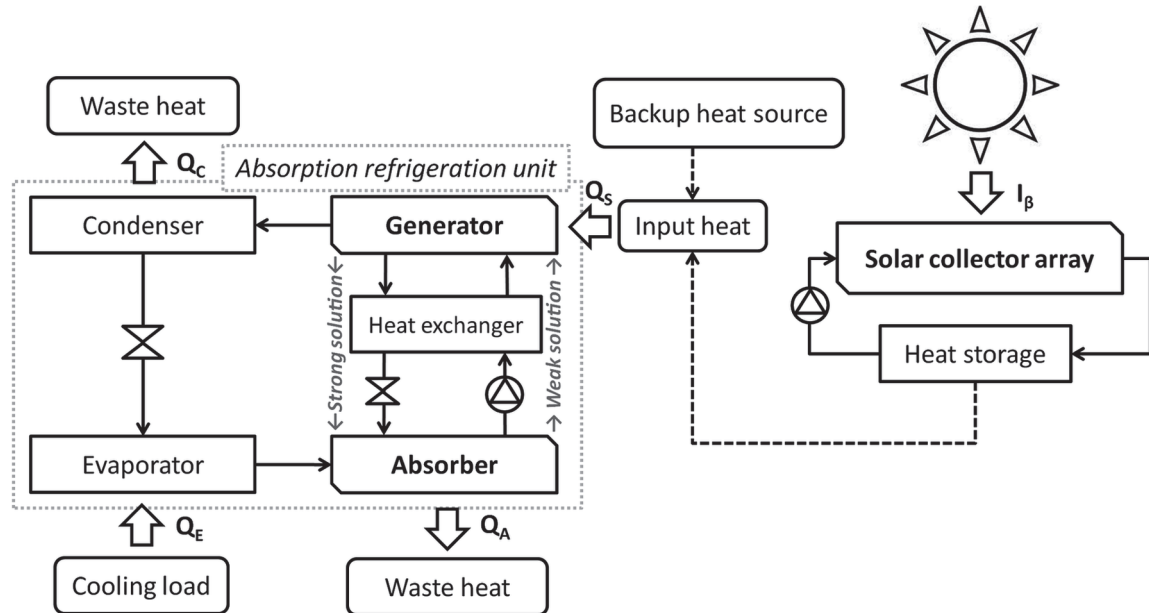
In an absorption machine, the sorption effect takes place in an absorber and desorption occurs in a generator which utilizes heat,  $Q_S$ , to regenerate the sorbent. The refrigerant vapour generated in this process condenses in the condenser, rejecting heat,  $Q_C$ , to the ambience and flows back through the expansion valve to the evaporator. After evaporating and removing heat from the refrigeration load at the evaporator,  $Q_E$ , the refrigerant is absorbed by the substance used as sorbent, while sorption heat generated during this process is rejected to the ambience,  $Q_A$ . The process is illustrated in Figure 3.

Typically, the refrigerant-sorbent working pair of absorption refrigeration systems is either water-LiBr (lithium bromide) or ammonia-water. Ammonia-water systems require higher mass circulation rates and higher operating pressures than water-LiBr systems (ASHRAE, 2009). While water-LiBr absorption chillers are popular for air-conditioning applications, ammonia-water systems can operate at sufficiently low temperatures down to  $-60^\circ\text{C}$  (Rutz, Mergner, & Janssen, 2012), which makes them suitable for food refrigeration purposes.

A solar-driven single-stage absorption refrigeration system is depicted in Figure 3. Multistage cycles are also available with one or more of the four basic heat exchangers (generator, absorber, condenser, evaporator) present at two or more places in the cycle, at different pressures or concentrations (ASHRAE, 2009). Several types of two-stage cycles have been developed, including double-effect and triple-effect cycles. These advanced configurations can provide better performance than single-stage systems, but also add complexity and increase unit costs. Typical *COPs* are in the range of 0.65-0.8 for single-effect

### Integration of Renewable Energy in Refrigerated Warehouses

Figure 3. Single-stage ammonia-water absorption refrigeration system powered by solar energy



and 0.9-1.2 for double-effect absorption systems (Rutz *et al.*, 2012). Advanced ammonia-water systems have comparable efficiencies with water-LiBr systems, e.g. the basic GAX (generator-absorber-heat exchanger) cycle has comparable performance with a single-effect water-LiBr system, the branched GAX cycle has comparable performance with a double-effect water-LiBr system and the vapour exchange GAX cycle would yield the same performance as a triple-effect water-LiBr system (ASHRAE, 2009).

Absorption refrigeration is in fact one of the oldest industrial refrigeration techniques, preceding vapour-compression refrigeration. Industrial absorption refrigeration units were developed in the mid 19<sup>th</sup> century by the Carre brothers in France and have been used during the American Civil War in the gunpowder production industry (ASHRAE, 2014). Another reported 19<sup>th</sup> century application is for ice production via wood-fired absorption systems (Briley, 2004). The concept of solar refrigeration is also not new. Augustin Mouchot demonstrated an absorption refrigeration machine driven by a concentrating solar collector at the Exposition Universelle of 1878 in Paris (Podesser *et al.*, 2010). The main reason for the modest market penetration in more recent years, as compared with the vapour-compression technology, is the high investment costs of absorption units. One of the causes is that while all components of vapour-compression systems are mass produced by different manufacturers, sorption refrigeration machines are usually manufactured as a whole unit by a single producer (Podesser *et al.*, 2010). Moreover the number of manufacturers of absorption refrigeration units is relatively small.

Solar-driven absorption refrigeration units have been applied and tested mainly for air-conditioning applications. Experience with cold storage facilities is limited and more research is needed to provide optimized solutions for larger scale systems. Experimental solar-driven absorption systems, which refrigerate small-scale cold storage compartments, have been investigated within the EU-funded SOL-ERA Project. In Freiburg, Germany, a linear Fresnel collector with a total aperture (mirror) area of 132 m<sup>2</sup> has been used to drive two ammonia-water absorption refrigeration units with a total refrigeration capacity of 24 kW. Weber *et al.* (2014) reported that such collectors have been operated at an efficiency

### Integration of Renewable Energy in Refrigerated Warehouses

of 50-60%, providing heat at 100-205°C to the absorption units, whose *COP* has been in the range of 0.4-0.8 and refrigerating temperatures down to -12°C have been achieved (enough for storing ice with a thermal capacity of about 110 kWh). In a very similar configuration in Umkirch, Germany, a linear Fresnel collector with aperture area of 88 m<sup>2</sup> (Figure 4) is used to drive an ammonia-water absorption unit with nominal refrigerating capacity of 12 kW and *COP* of 0.6, which is tested for a 32 m<sup>2</sup> cold storage space. The absorption unit cools a water-glycol mixture to -5°C and charges an ice storage system with a thermal capacity of about 52 kWh (Döll, Bentaher, & Morgenstern, 2014).

Vasilescu & Infante Ferreira (2014) carried out a theoretical study of a large-scale system featuring a double-effect ammonia-lithium nitrate absorption unit with a refrigeration capacity of 343 kW (when cooling a fluid to -20°C, with input heat at 195°C and inlet cooling water temperature of 30°C), driven by a parabolic trough collector with an aperture area of 1,000 m<sup>2</sup>. The study showed that for the climatic conditions of Naples, Italy the solar collectors can provide 50% of the heat required to cover the refrigeration demand of 600 kW in a food processing facility.

Instead of liquid absorbents, adsorption refrigeration systems utilize solid sorption materials with highly porous structure. Classical working pairs (refrigerant-adsorbent) for adsorption refrigeration are water-zeolite, water-silica gel and methanol-activated carbon (Podesser *et al.*, 2010). When saturated, the adsorbent can be regenerated with heat provided by a solar thermal system or another renewable source. Chemical adsorbents, e.g. metal hydrides, can also be used. Chemical adsorption is characterized with stronger bonds between the refrigerant and adsorbent, but it is more difficult to reverse and therefore more heat is required to drive the cycle (Pridasawas, 2006).

Unlike absorption systems, solid sorbents cannot be circulated and adsorption and desorption have to occur at the same solid adsorbent bed. The process is therefore intermittent and multiple adsorbent beds

Figure 4. Linear Fresnel collector used to drive an absorption refrigeration system at Umkirch, Germany. (© 2012, suncooling GmbH, a member of the KRAMER GROUP, Germany. Used with permission.)





### Integration of Renewable Energy in Refrigerated Warehouses

are required to permit continuous operation of the system (Kim & Infante Ferreira, 2008). Advanced adsorption cycles (e.g. heat recovery cycle, mass recovery cycle and thermal wave adsorption cycle) have been developed to cope with this issue (Lewis, Chaer, & Tassou, 2007). Schematic of a thermal wave cycle adsorption system driven by solar energy is presented in Figure 5.

Adsorption refrigeration systems offer several advantages as compared with absorption systems, including less corrosion issues when working at higher temperatures and the possibility of being activated by lower temperatures – as low as 50°C, as compared with 90°C for absorption systems (Wang & Vineyard, 2011). Additional advantage of adsorption systems is that they involve few moving parts, which means reduced noise and vibrations. This can also decrease maintenance efforts, but the external hydraulic circuits have to be carefully designed (Podesser *et al.*, 2010). However, the *COP* of adsorption machines is typically lower, e.g. 0.2-0.5, with  $\alpha_r$  in the range of 0.04-0.33 (Infante Ferreira & Kim, 2014). Chemical reaction systems have much lower *COPs* in the range of 0.1-0.2 (Pridasawas, 2006).

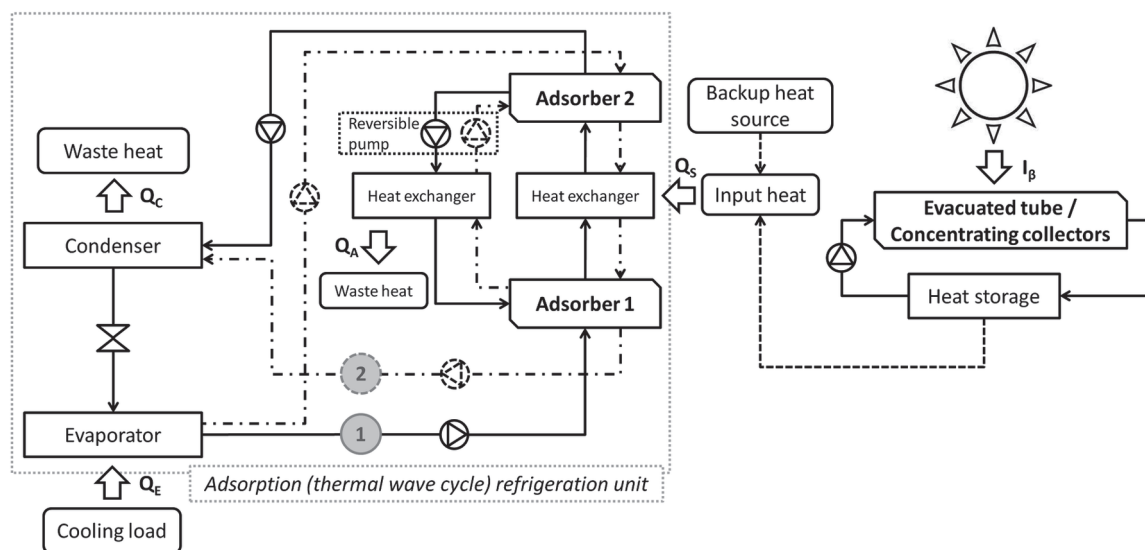
The number of manufacturers of adsorption systems is even lower than that of absorption systems. Commercially available large-scale units (larger than 100 kW) are manufactured by the Japanese company Mayekawa, while small-scale units (less than 15 kW) are produced by the German companies Invensor and SorTech (Podesser *et al.*, 2010). Commercial adsorption systems are still limited to mostly air-conditioning applications, while low-temperature adsorption refrigeration systems, potentially applicable to industrial facilities for cold storage, are still in a R&D stage (Lewis *et al.*, 2007).

The overall system efficiency of solar sorption refrigeration systems can be defined as:

$$OSE = \frac{Q_E}{I_\beta \cdot A_s} = \frac{Q_E}{Q_S} \cdot \frac{Q_S}{Q_{sol}} \cdot \frac{Q_{sol}}{I_\beta \cdot A_s} = COP \cdot \eta_{hd} \cdot \eta_{sc} \quad (12)$$

where  $\eta_{hd}$  is the efficiency of the heat distribution system and  $\eta_{sc}$  is the efficiency of the solar collector. *OSE* is typically low for solar refrigeration systems. Lazzarin (2014) estimated an *OSE* of 45% for a

Figure 5. Thermal wave cycle adsorption refrigeration system powered by solar energy



### **Integration of Renewable Energy in Refrigerated Warehouses**

single-effect absorption system driven by evacuated tube collectors and 40% for a double-effect absorption system driven by a parabolic trough collector. Comparing the prices of sorption refrigeration units, Kim & Infante Ferreira (2008) showed that the investment cost per refrigerating capacity (€/kW) of adsorption systems is in the range of €500-855/kW, as compared with €210-400/kW for single-effect and €300-855/kW for double-effect absorption systems.

#### **Other Renewables as a Heat Source**

Thermally driven refrigeration systems can operate with heat acquired from other renewables (e.g. via combustion of biofuels or geothermal sources). Holdmann (2008) reported a geothermally driven absorption system with a refrigeration capacity of about 180,000 BTU per hour (or approx. 53 kW), developed for the Ice Museum of Chena Hot Springs Resort in Alaska. Small-scale biofuel-driven or geothermally driven sorption refrigeration systems are available, but for large-scale applications combined heat and power (CHP) generation can be a more feasible option. Such systems are discussed further in this chapter.

## **REFRIGERATION THROUGH ON-SITE POWER GENERATION**

### **Solar Photovoltaic Systems**

Photovoltaic (PV) modules are solid-state semiconductor devices which employ the photoelectric effect to convert solar radiation into direct current (DC). This DC power can subsequently be used directly or converted to alternating current (AC) to run electrically driven refrigeration systems. If an appropriate interaction is established between the cold store operator and the electric utility, PV-generated power can also be sold to the utility grid.

Due to the reduced prices and increased efficiencies of PV systems, whose use is continuously fostered by various government incentive programs, total global operating capacity of solar photovoltaic systems has grown rapidly since the beginning of the new millennium – from 1.8 GW in 2001 to 100 GW in 2012, with the top markets currently being Germany, Italy, China, the United States, and Japan (REN21, 2013). According to the U.S. Department of Energy (2012), prices of PV modules have declined by 95% between 1976 and 2010 and as of 2010 the installed cost of a commercial PV system (including the price of the modules, power electronics and BOS costs) per peak power capacity was roughly \$/W. According to Lazzarin (2014) the unit cost of a PV module on per area basis is on the average €650/m<sup>2</sup>.

The most common types of PV cells are based on the monocrystalline and polycrystalline silicon technologies, which currently hold 85% of the PV market share. Another major type employs thin-film PV cells, which are about 100 times thinner than crystalline silicon cells. Thin-film cells most commonly use cadmium telluride (CdTe) as a semiconductor material, amorphous silicon and alloys of copper indium gallium diselenide (CIGS). Among thin-film technologies, CdTe-based PV modules have experienced the highest market growth during the last decade (U.S. Department of Energy, 2012). Concentrating PV systems are also available, but their market share is still small (REN21, 2013). Typical lifetime of solar PV modules is in the range of 20-25 years.

The efficiency of PV modules is defined as the ratio of generated electrical power to the product of solar panel surface area and incident solar radiation:

### Integration of Renewable Energy in Refrigerated Warehouses

$$\eta_{PV} = \frac{P_G}{I_\beta \cdot A_s} \quad (13)$$

This efficiency depends on the module type and design. According to the U.S. Department of Energy (2012), crystalline silicon modules currently have efficiencies in the range of 14-16%, non-standard high-quality designs achieve module efficiencies of about 17-21%, while thin-film modules have lower efficiencies in the range of 6-14%. Manufacturers provide reference values for  $\eta_{PV}$  determined under standard conditions, but the actual efficiency of PV modules varies according to ambient conditions. Lazzarin (2014) proposes the following equation to calculate the operating efficiency of PV modules as a function of ambient air temperature and solar irradiation:

$$\eta_{PV} = \eta_{PV,R} \cdot \left[ 1 - \beta \cdot (T_A - T_{Ref}) - \frac{\beta \cdot \tau\alpha \cdot I_\beta}{U_L} \right] \quad (14)$$

where  $T_{Ref}$  is the reference temperature at which the reference efficiency  $\eta_{PV,R}$  is evaluated (e.g. 25°C);  $\beta$  is a temperature coefficient of the PV cell (e.g. 0.004 K<sup>-1</sup> for monocrystalline cells);  $\tau\alpha$  is the product of glass transmissivity and cell absorptance (typical value is 0.95) and  $U_L$  is the overall heat loss coefficient of the PV cell (e.g. 20 Wm<sup>-2</sup>K<sup>-1</sup>). This equation shows that the operating efficiency decreases when ambient air temperature and solar irradiation are higher. Apart from the efficiency of the PV module itself, the efficiencies of the other components of the PV system have to be taken into account.

The overall efficiency of a refrigeration system driven by a PV system can be defined as:

$$OSE = \frac{Q_E}{I_\beta \cdot A_s} = \frac{Q_E}{P_S} \cdot \frac{P_S}{P_G} \cdot \frac{P_G}{I_\beta \cdot A_s} = COP \cdot \eta_{pd} \cdot \eta_{PV} \quad (15)$$

where  $P_S$  is the power supplied to the refrigeration system and  $\eta_{pd}$  is the efficiency of the power distribution system. A conservative estimate for *OSE* of a vapour-compression refrigeration unit driven by a photovoltaic system, using indicative values as shown in Figure 2 ( $\eta=0.1$  and  $EER=3.5$ ), would be 35%. If the system involves energy storage then this value would be somewhat lower. The *LCOE* of PV systems can vary significantly depending on local conditions. Comparing several situations, the U.S. Department of Energy (2012) estimated indicative values of *LCOE* for commercial systems in the range of \$120-340/MWh.

PV systems can serve as a primary or supplementary energy source for any of the electrically driven refrigeration cycles, as depicted in Figure 2. Photovoltaics, among other solar systems, have varying energy production as a result of the varying availability of incident solar radiation. The power supply of the refrigeration system must therefore be designed to cope with this varying electricity production rate. For smaller scale systems DC power generated by the PV modules can be used to directly operate the DC motor of a compressor in a vapour-compression system. In that case a major consideration is to appropriately match the electrical characteristics of the motor driving the compressor with the available current and voltage being produced by the PV array (Klein & Reindl, 2005). Electric batteries can serve as a buffer between the PV system and the load, providing electrical storage. If the PV system

### Integration of Renewable Energy in Refrigerated Warehouses

is connected to the utility grid, a proper energy management system (EMS) can provide the means for shifting power supply from/to the grid depending on the variation of the PV power supply and the power demand of the cold storage facility. The overall performance of the EMS can be enhanced through the thermal energy storage (TES) strategies described further in this chapter.

The relatively low energy conversion efficiencies, varying power production and high prices have traditionally been a barrier for wider implementation of solar PV systems. For many applications they are not economically viable or the associated payoff periods are too long, which often deters investments. Traditional cold storage applications of PV modules have been primarily for milk, fish and vaccine preservation in developing countries, especially in areas with no or unreliable power supply, but these are usually small-scale storage compartments with refrigeration capacities in the range of a few kilowatts. In developed countries with reliable power grids the use of PV systems for refrigerated warehousing has been limited until recently.

Large flat roofs of refrigerated warehouses are, however, a very convenient location for PV systems because of the presence of both a large unoccupied area for placing of PV modules and a substantial consumer of energy at the site of its generation. In addition, peak power demand in cold stores tends to coincide with the time when the intensity of solar radiation is at its highest, although higher temperatures and solar irradiation decrease the efficiency of PV modules. Similarly to all power generating systems, roof-mounted PV systems should be carefully designed and safely maintained in order to prevent fire hazards. Government incentives are among the most important drivers which enhance market penetration of PV-based technologies. Such measures are described in more detail in the section “*Policy instruments in support of renewable energy integration*”. The ease of demonstration, visibility and publicity of such PV projects promote public interest and stakeholders’ confidence in renewable energy technologies as a whole.

Promising prospects are revealed today for a sound integration of PV systems in refrigerated warehouses. A number of state-of-the-art engineering solutions around the world employ large PV arrays (including some in the megawatt range) capable of meeting a significant portion of the power demand of the cold storage facilities they serve. Some of these recent developments are summarised in Table 3.

Top-view photographs of three of the facilities listed in Table 3 are shown in Figures 6, 7 and 8.

### Solar Thermo-Mechanical Systems

Solar thermal collectors can provide energy to a heat engine for conversion of heat into mechanical work. This mechanical work can be used to drive the compressor of a vapour-compression refrigeration machine (Figure 9). In a basic configuration, the collector utilizes solar radiation incident on its surface to heat a fluid, which is usually water being converted to steam supplied to the heat engine,  $Q_S$ , which converts it to mechanical work,  $W$ , and rejects waste heat to the ambience,  $Q_A$ . The mechanical work, in turn, drives the compressor of the refrigeration machine, to remove heat from the evaporator,  $Q_E$ . Waste heat of the refrigeration cycle is rejected to the ambience at the condenser,  $Q_C$ . A storage tank can be included to provide some high temperature storage and serve as a buffer between the solar collectors and the heat engine.

The overall system efficiency of a solar thermo-mechanical refrigeration system can be defined as:

### Integration of Renewable Energy in Refrigerated Warehouses

Table 3. Some recent installations of large-scale solar PV systems at refrigerated warehouses

Location/Source	Technical Features	Cost / Economic Benefits
Refrigerated warehouse at the Gloucester Marine Terminal in New Jersey (Holt Logistics Corp., 2014)	<ul style="list-style-type: none"> <li>• 27,528 roof-mounted modules (102,200 m<sup>2</sup>)</li> <li>• 9 MW installed capacity</li> <li>• Capable of producing 11 GWh per year (meeting 80% of facility power demand)</li> <li>• 3-4 MW expansion is planned</li> </ul>	<ul style="list-style-type: none"> <li>• Investment of \$42 million</li> <li>• \$11 million in federal tax credit</li> <li>• Continued support of solar renewable energy credits (RECs) through the New Jersey renewable portfolio standards (RPS) scheme</li> <li>• Expected return on investment in 10 years or less</li> </ul>
Cold storage facilities in La Mirada and Livermore, California, and Phoenix, Arizona ("DeSolar Completes", 2011; US Foods, 2011a, 2011b, 2011c)	<ul style="list-style-type: none"> <li>• La Mirada: 4,998 modules with 1.15 MW installed capacity (annual production of approximately 1.65 GWh, 16% of power demand)</li> <li>• Livermore: 4,354 modules with 1.18 MW installed capacity (annual production of approximately 1.3 GWh, 40% of power demand during daylight hours)</li> <li>• Phoenix: 3,934 modules with 0.9 MW installed capacity (annual production of approximately 1.5 GWh, 15% of power demand)</li> </ul>	<ul style="list-style-type: none"> <li>• Facilities have earned Green Business Certification</li> <li>• The project in La Mirada has been partially funded through the California Solar Initiative program</li> <li>• Solar systems are leased from renewable energy providers</li> </ul>
Seven cold stores at various locations in England (Yearsley Group, 2012)	<ul style="list-style-type: none"> <li>• 8,997 roof-mounted modules</li> <li>• Capable of producing 1.753 GWh per year</li> </ul>	<ul style="list-style-type: none"> <li>• Investment of £3.5 million</li> <li>• The project is intended to meet carbon reduction commitments as part of ISO 14001 environmental certification</li> </ul>
Refrigerated warehouse and distribution centre at Goldthorpe near Barnsley, England (Bennett, 2014)	<ul style="list-style-type: none"> <li>• 6,000 roof-mounted modules (15,000 m<sup>2</sup>)</li> <li>• 1.5 MW installed capacity</li> <li>• Estimated to provide 1.2 GWh per year</li> </ul>	
Multi-purpose distribution center (including food storage facilities) in Heddeshheim, Germany (Wirsol, 2013)	<ul style="list-style-type: none"> <li>• 33,096 roof-mounted modules (110,000 m<sup>2</sup>)</li> <li>• 8.1 MW installed capacity</li> <li>• Capable of producing 7.9 GWh per year</li> </ul>	<ul style="list-style-type: none"> <li>• Pre-certified by the German Sustainable Building Council (DGNB) with gold certificate</li> </ul>
Three cold stores in New Jersey (EDF Renewable Energy, 2009; Milk, n.d.)	<ul style="list-style-type: none"> <li>• 30,000 roof-mounted PV modules of different technologies with total capacity of 3.2 MW</li> <li>• 21% reduction in grid power consumption</li> </ul>	<p>Part of the solar system is owned by the cold stores operator:</p> <ul style="list-style-type: none"> <li>• Investment of \$9 million</li> <li>• \$4.6 million in state and federal incentives, including 30% federal tax credit, a New Jersey state subsidy, and accelerated depreciation</li> </ul> <p>Part of the solar system is owned by a renewable energy provider:</p> <ul style="list-style-type: none"> <li>• Electricity production is fed to the cold stores at a fixed price under a power purchasing agreement (PPA)</li> </ul>
Cold storage facility in Wilmington, Los Angeles, California ("California Green Designs", 2011)	<ul style="list-style-type: none"> <li>• 7,500 roof-mounted modules with installed capacity of 1.49 MW</li> <li>• Capable of meeting 75% percent of facility power demand</li> </ul>	<ul style="list-style-type: none"> <li>• Average savings of between \$40,000 and \$42,000 per month on electricity costs</li> <li>• Benefits from government and utility incentives, including 30 percent federal grant, one-year accelerated bonus depreciation and rebate from the Los Angeles Department of Water &amp; Power</li> </ul>
Cold storage facility in San Diego, California ("ICE Cold Storage", 2009; Milk, n.d.)	<ul style="list-style-type: none"> <li>• Roof-mounted modules with 1.1 MW installed capacity</li> <li>• Capable of meeting 72% of facility power demand</li> <li>• Average production of 1,295 kWh per day during the winter months and 3,383 kWh per day in summer months</li> </ul>	<ul style="list-style-type: none"> <li>• Investors share renewable energy credits (RECs)</li> </ul> <p>Part of the solar system is owned by the power provider:</p> <ul style="list-style-type: none"> <li>• Part of San Diego Gas &amp; Electric Sustainable Communities Program that supports renewable energy initiatives</li> </ul> <p>Part of the solar system is owned by the cold store operator:</p> <ul style="list-style-type: none"> <li>• Investment of \$3.5 million before any subsidies</li> <li>• 40% reduction of the investment cost as a result of 30% federal tax credit and a five-year California refund (on a kWh basis)</li> </ul>
Refrigerated warehouse in West Sacramento, California (Milk, n.d.; "Tony's Goes Green", n.d.)	<ul style="list-style-type: none"> <li>• 5,700 roof-mounted modules with installed capacity of 1.2 MW</li> <li>• About 43% reduction of grid power consumption</li> </ul>	<ul style="list-style-type: none"> <li>• Investment of \$7.2 million before any subsidies</li> <li>• About 50% reduction of the investment cost as a result of federal tax credit and a \$3.5 million rebate from Pacific Gas &amp; Electric</li> <li>• In times of excessive production electricity is fed to the grid on a net metering basis</li> <li>• Average savings of \$22,000 per month on energy costs</li> </ul>

continued on following page



### Integration of Renewable Energy in Refrigerated Warehouses

Table 3. Continued

Location/Source	Technical Features	Cost / Economic Benefits
Refrigerated warehouse at the Port of Baltimore, Maryland (HelioSage, n.d.)	<ul style="list-style-type: none"> <li>• 3,136 roof-mounted modules with 736.9 kW installed capacity</li> <li>• Providing 824 MWh per year (capable of meeting 20% of facility power demand)</li> </ul>	<ul style="list-style-type: none"> <li>• Benefits from sale of solar renewable energy credits (SRECs)</li> <li>• Expected payback in less than six years</li> </ul>
Cold storage facility in Portland, Oregon (Henningsen Cold Storage Co., 2010)	<ul style="list-style-type: none"> <li>• 1,386 roof-mounted thin-film modules (3,017 m<sup>2</sup>)</li> <li>• 200 kW installed capacity</li> <li>• Capable of meeting 20% of facility power demand</li> </ul>	
Food Bank of Contra Costa & Solano, California (Food Bank of Contra Costa and Solano, n.d.)	<ul style="list-style-type: none"> <li>• 516 roof-mounted modules</li> </ul>	<ul style="list-style-type: none"> <li>• Investment of \$450,000</li> <li>• California Energy Commission rebate</li> </ul>
Cold storage and packing facility in San Joaquin Valley, California (REC Solar, 2014)	<ul style="list-style-type: none"> <li>• Ground-mounted system on a four acre field adjacent to the cold storage facility</li> <li>• 1.07 MW installed capacity</li> <li>• Capable of meeting 75% of facility power demand</li> </ul>	<ul style="list-style-type: none"> <li>• Local rebates</li> <li>• 30% federal investment tax credit and other tax incentives</li> <li>• Expected payback in five years</li> </ul>

Figure 6. Solar park on the roof of MTC Logistics' cold store at the Port of Baltimore. (© 2011, HelioSage. Used with permission)



$$OSE = \frac{Q_E}{I_\beta \cdot A_S} = \frac{Q_E}{W} \cdot \frac{W}{Q_S} \cdot \frac{Q_S}{Q_{sol}} \cdot \frac{Q_{sol}}{I_\beta \cdot A_S} = COP \cdot \eta_{he} \cdot \eta_{hd} \cdot \eta_{sc} \quad (16)$$

where  $\eta_{he}$  is the thermal efficiency (i.e. the ratio of the work output to the heat input) of the heat engine. The *OSE* of solar thermo-mechanical refrigeration is usually quite low (e.g. around 5%), which is unfavourable for the market penetration. According to Klein & Reindl (2005), such systems can be competitive if concentrating solar collectors with tracking systems are used to provide high temperatures for large-scale refrigeration applications (e.g. over approx. 3,500 kW).

### Integration of Renewable Energy in Refrigerated Warehouses

Figure 7. The Los Angeles' largest commercial solar installation on the rooftop of the Konoike-Pacific cold-storage warehouse in Wilmington. (© 2011, California Green Designs: [www.ca-green.com](http://www.ca-green.com). Used with permission)



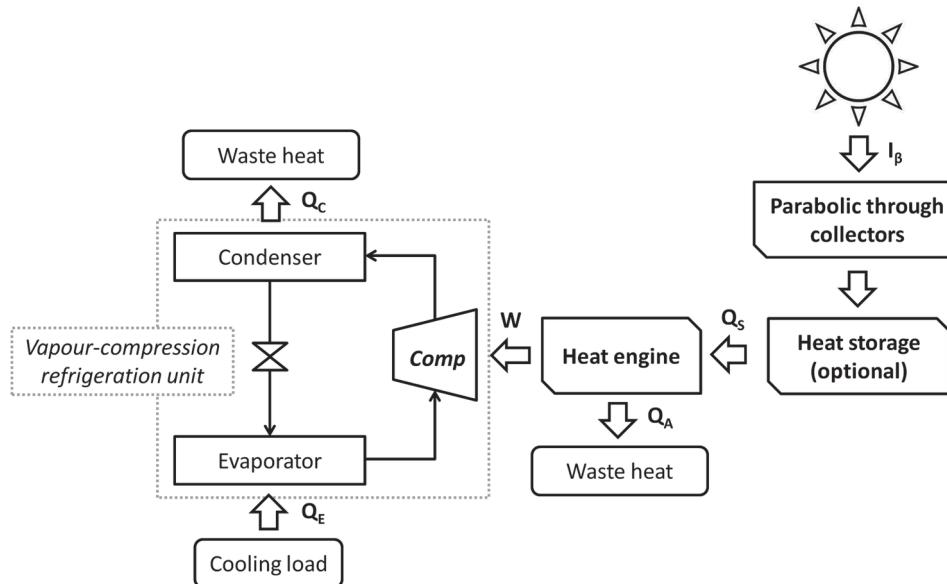
Figure 8. Solar park at the U.S. Foods' facility in La Mirada, California. (© 2011, Neo Solar Power Corporation. Used with permission)





### Integration of Renewable Energy in Refrigerated Warehouses

Figure 9. Solar thermo-mechanical refrigeration system



Rankine and Stirling engines are the main options as far as the heat engine for a solar thermo-mechanical system is concerned. Stirling engines can be used at very high temperatures (e.g. above  $750^\circ\text{C}$ ). These are therefore preferable when parabolic dish collectors are employed, while Rankine engines are applicable for lower temperatures and can be successfully combined with parabolic trough collectors (Infante Ferreira & Kim, 2014).

Applications of solar thermo-mechanical systems are limited and currently this technology is available only from a small number of large manufacturers (Podesser *et al.*, 2010). Another possibility is to use the heat engine for power generation. Aye *et al.* (2012) investigated the performance of a small-scale system with a solar-driven Organic Rankine cycle (ORC) engine, providing power for a vapour-compression refrigeration system, used for field storing of chilled blueberries at a storage temperature of  $4^\circ\text{C}$ . In addition, waste heat of the engine can be utilized for a thermally driven refrigeration system. Combined heat and power generation (CHP) systems using solar energy are discussed further in this chapter.

## Wind Turbines

Wind turbines are devices that convert the kinetic energy of wind into electrical power. There are two main types of wind turbines – horizontal-axis wind turbine (HAWT) and vertical-axis wind turbine (VAWT). The Darrieus and Savonius wind turbines are recognizable VAWT types, but in general HAWTs are more common. Different designs are available, but the main components of a typical HAWT include blades, rotor, pitch system that turns the blades and controls rotor speed, low-speed and high speed shafts, gearbox that connects the low-speed shaft of the rotor with the high speed shaft which drives the generator (converting mechanical energy into 50-60 Hz AC current) and control system (including an anemometer, windvane, controller, and brake) which switches the machine *on* or *off* depending on wind speed. Upwind positioned HAWTs also include a yaw drive to keep the rotor facing into the wind

### **Integration of Renewable Energy in Refrigerated Warehouses**

as the wind direction changes. Sizes and tower heights of wind turbines vary significantly. Some are available with small rotor diameters and capacity of only a few kilowatts, while the largest unit is 125 m tall, with a rotor diameter of 190 m and has a peak capacity of 10 MW. Like solar PV systems, wind turbines can be used as an off-grid energy source for electrically driven refrigeration systems or can be connected to the utility grid.

Wind has been used as an energy source since ancient times primarily for the purposes of grinding grain, pumping water and moving ships, while the use of wind turbines to generate electricity dates back to the late 19<sup>th</sup> century (Royal Academy of Engineering, 2014). Nowadays their use is growing rapidly and, according to REN21 (2013), global installed capacity of wind turbines reached 283 GW in 2012, up from 24 GW in 2001. Naturally, wind turbines are most beneficial in locations with steady winds, both onshore and offshore. The top markets of wind energy are currently the United States and China, followed by Germany, India and the United Kingdom (REN21, 2013).

Wind turbine prices reached their peak in 2008 and have been falling since then, before stabilizing in 2012, while the O&M costs have dropped significantly (REN21, 2013). A study by Tegen *et al.* (2013) on the economic performance of wind turbines in the United States indicates that as of 2011 the installed cost of onshore wind turbines varies in the range of \$1.4-2.9/W and LCOE varies in the range of \$60-100/MWh for operational lifetimes of 20-30 years. Both cost metrics have much higher values for offshore turbines (Tegen *et al.*, 2013). Comparison of the above metrics with those of solar PV systems indicates that wind turbines can be less expensive on a levelized basis, while the operational lifetime of both is similar. However wind turbines are usually more efficient for large-scale utility generation systems, while PV systems are more versatile and can be combined in smaller increments to produce varying capacities. The major consideration should be the availability of the energy resource, as wind and solar energy can have very diverging potentials in different locations.

Industrial examples for cold storage facilities featuring on-site wind turbines are already available. A landmark RES project is the Testa Produce's LEED Platinum-certified refrigerated food distribution facility in Chicago, Illinois, which features a 72 m high wind turbine with a capacity of 750 kW, along with PV modules and other sustainability oriented solutions, as visible in Figure 10 (Grover, 2011; Epstein, 2013). The wind turbine has an installed cost of \$1.6 million and is capable of meeting up to 40% of the facility's energy demand (Podmolik, 2011). The Walmart distribution center in Red Bluff, California also features a wind turbine (80 m in height, with a rotor diameter of 76 m), which has an installed capacity of 1 MW. The turbine has an estimated production of 200 MWh annually and is capable of meeting 15-20% of the facility's electricity demand ("Walmart unveils", 2012). Furthermore, Walmart Corp. (2014) reports that the company has renewable electricity generation capacities (in operation or under development) amounting to a total of 2,200 GWh per year.

### **Combined Heat and Power Generation**

Combined heat and power (CHP) generation, also known as cogeneration, is the simultaneous production of electricity and useful heat, whereas the heat is a by-product of the electricity generation process, i.e. waste heat, which would otherwise be discharged to the environment, is utilized as an energy source. Any system that simultaneously generates heat and electricity can be classified as a CHP system, but most commonly it involves a heat engine using the combustion of a carbon-based fuel to drive a power generator and the waste heat left is used as a thermal source for heating purposes or a thermally driven cycle. A thermally driven refrigeration system can be integrated with the CHP system to exploit this

### Integration of Renewable Energy in Refrigerated Warehouses

Figure 10. Testa Produce's LEED Platinum-certified refrigerated food distribution facility in Chicago, featuring a 750 kW wind turbine. (© 2013, Epstein. Used with permission)



waste heat as an energy source for refrigeration. Such configurations are often referred to as trigeneration systems. CHP systems have traditionally been used for district heating power plants and more recently for district cooling systems. They have also been used in places without reliable power supply. With the development of smart grids and increasing share of distributed power sources, linked to the utility grids, CHP systems are becoming more common, although they are still not a customary feature.

Various RES configurations can provide the primary energy for a CHP system. Different operable combinations of prime movers (heat engines) and renewables for CHP generation are shown in Table 4.

Biogas-fuelled and solar-driven systems are two of the more promising options for RES-driven trigeneration systems of refrigerated warehouses. Geothermal systems are also an interesting opportunity where Earth heat is plentiful. The power provided by the CHP unit can drive any of the known electrically-driven refrigeration systems, while the residual heat can run a thermally driven refrigeration system, depending on the temperature and amount of heat available.

### Solar-Driven CHP Systems

Solar energy can be used as a heat source for CHP systems when conditions are favourable for installing concentrating solar collectors that can provide sufficiently high temperatures for the heat engine (e.g. above 150°C). Stirling or Rankine cycle heat engines are most commonly used for solar-driven CHP systems. Rankine cycle systems using organic working fluids, i.e. organic Rankine cycle (ORC) systems,



### Integration of Renewable Energy in Refrigerated Warehouses

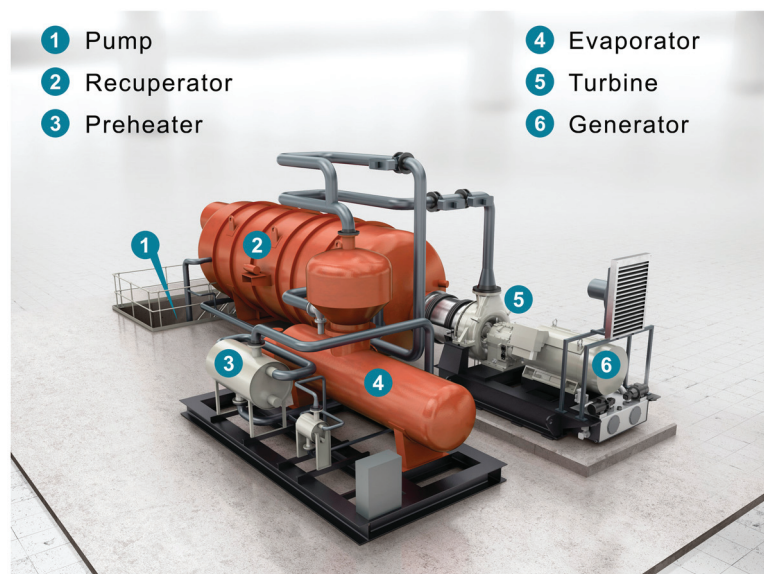
Table 4. Combinations of renewable sources and heat engines for CHP systems, which can be technically and economically feasible. (Adapted from Obersteiner et al., 2008).

Heat Engine \ Heat Source	Biogas	Liquid Biofuels	Solid Biomass	Geothermal	Solar Thermal
Gas turbine	✓	✓			
Reciprocating engine	✓	✓			
Steam turbine (Rankine cycle)	✓	✓	✓	✓	✓
Screw-type steam engine	✓	✓	✓	✓	✓
Stirling engine	✓	✓	✓	✓	✓
Organic Rankine cycle engine			✓	✓	✓

are arguably the most promising technology for solar-driven CHP systems, because they operate at lower temperatures, which can be achieved by concentrating solar collectors in smaller-scale systems. Stirling cycle engines typically require parabolic dish concentrating collectors, while ORC systems can also operate with parabolic trough collectors. Linear Fresnel concentrators are also a suitable choice for ORC systems (Quoilin, 2011). Both Stirling cycle and Rankine cycle heat engines, specifically designed for use with solar concentrating collectors, are available. Commercially available ORC systems with various capacities are reported to operate with heat source temperatures in the range of 74–350°C (Arvay, Muller, Ramdeen, & Cunningham, 2011). Figure 11 illustrates a commercially available 1 MW ORC module designed by Siemens (Siemens AG, 2014).

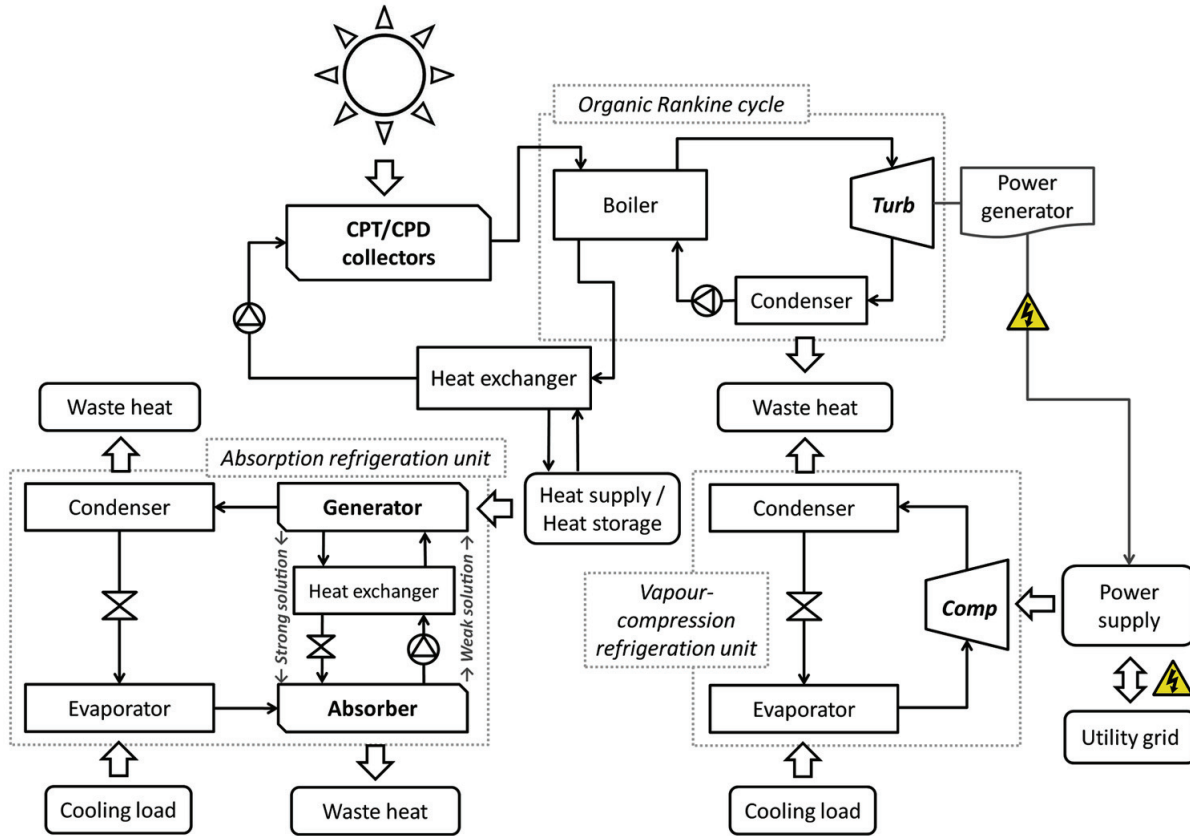
A possible configuration of trigeneration system with a solar-driven ORC engine, providing energy for both vapour-compression and absorption refrigeration units, is depicted in Figure 12.

Figure 11. A Siemens AG ORC module with a power output of up to 1 MW (© 2014, Siemens AG. Used with permission)



## Integration of Renewable Energy in Refrigerated Warehouses

Figure 12. Single-stage absorption and vapour-compression refrigeration systems powered by a solar-driven ORC engine



The electrical,  $\eta_{el,CHP}$ , and thermal,  $\eta_{th,CHP}$ , efficiencies of a solar-driven CHP system can be defined as:

$$\eta_{el,CHP} = \frac{P_G}{I_\beta \cdot A_S} = \frac{P_G}{W} \cdot \frac{W}{Q_S} \cdot \frac{Q_S}{Q_{sol}} \cdot \frac{Q_{sol}}{I_\beta \cdot A_s} = \eta_{pg} \cdot \eta_{he} \cdot \eta_{hd} \cdot \eta_{sc} \quad (17)$$

$$\eta_{th,CHP} = \frac{Q_R}{I_\beta \cdot A_S} = (1 - \eta_{he}) \cdot \eta_t \cdot \eta_{hd} \cdot \eta_{sc} \quad (18)$$

where  $P_G$  is the generated power [W],  $Q_R$  is the recovered (utilized) residual heat [W],  $\eta_{pg}$  is the efficiency of the power generator,  $\eta_{he}$  is the thermal efficiency (i.e. the ratio of the work output to the heat input) of the heat engine,  $\eta_{sc}$  is the efficiency of the concentrating solar collector and  $\eta_t$  is the fraction of the waste heat utilized. The overall efficiency of the solar-driven CHP system is therefore:

### Integration of Renewable Energy in Refrigerated Warehouses

$$\eta_{CHP} = \frac{P_G + Q_R}{I_{\beta} \cdot A_S} = \eta_{el,CHP} + \eta_{th,CHP} \quad (19)$$

This overall CHP system efficiency does not account for the individual efficiencies of the refrigeration systems which use the energy. According to Müller-Steinhagen & Trieb (2004), annual electrical efficiencies of solar-driven CHP systems can be expected in the range of 8-25% depending on technology (e.g. 10-15% for systems using parabolic trough collectors). For electrical efficiencies of over 20%, a solar tracking system is required, but this increases cost and decreases reliability, which is particularly undesirable for smaller-scale distributed generation systems (Norwood, 2011). The overall thermal efficiency of a Rankine cycle heat engine, driven by a variety of solar collector configurations, can be expected to reach more than 50% (Norwood, 2011). Thus, the overall efficiency of a solar-driven CHP system can reasonably be expected to exceed 60%, given the global average efficiency of CHP units is 58%, while state-of-the-art CHP systems can achieve overall efficiencies of over 85% (Intergovernmental Panel on Climate Change, 2014).

Indicative figures for the installed cost of a solar-driven ORC CHP system (per peak electrical and thermal capacities) are \$3.2/W<sub>el</sub> and \$0.4/W<sub>th</sub> (Norwood, 2011). According to the Intergovernmental Panel on Climate Change (2014), the *LCOE* of concentrated solar power systems is generally in the range of \$100-480/MWh (median of \$150-320/MWh) for plant lifetime of 20 years, but this does not account for the benefit from the recovered heat. Norwood & Kammen (2012) performed life-cycle analysis (LCA) of a solar-driven CHP system for air cooling in Oakland, California (which uses a single solar dish collector and a Rankine cycle) and predicted a levelized cost of \$250/MWh (electricity) and \$30/MWh (heat).

### Geothermal CHP Systems

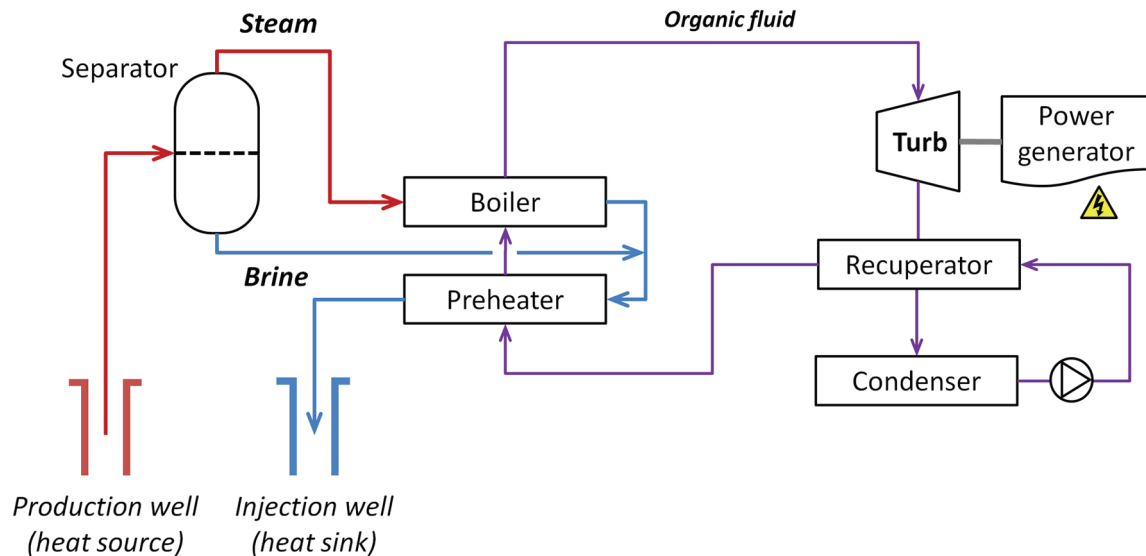
The comparatively lower heat source temperatures, needed to run the organic Rankine cycle engines, makes geothermal energy another viable option for implementing ORC-based CHP systems, wherever Earth heat is readily available. Geothermal sources are typically available with temperatures in the range of 110-180°C (Arvay *et al.*, 2011), but can also reach up to 300°C (Quoilin, 2011). As previously mentioned, this is within the operating range of commercially available ORC engines and geothermal sources with temperatures as low as 74°C can be utilized (although efficiency is low at such low temperatures).

A setback concerning geothermal systems is the high cost of drilling. In order to attain higher source temperatures, a geothermal system would generally require drilling of deep boreholes for the production and injection wells which, according Quoilin (2011), can reach up to 70% of the total investment for a geothermal ORC plant. Typically, a fluid (e.g. brine) is circulated through the production well (heat source) and injection well (heat sink), which in turn requires high pump power consumption. For low-temperature ORC plants this consumption can account for 30-50% and more of the system's electrical output (Quoilin, 2011).

ORC systems designed for geothermal applications have been developed by Ormat Technologies. In most cases, the fluid circulated through the production and injection wells is separated into a stream of steam, fed to the boiler of the ORC engine, and a stream of brine in a dedicated separator (Kaplan, 2007). The condensate is afterwards mixed with the separated brine to provide preheating of the organic fluid fed to the boiler in order to increase the thermodynamic efficiency of the cycle. Figure 13 shows

### Integration of Renewable Energy in Refrigerated Warehouses

Figure 13. Configuration of a geothermally driven ORC engine (Adapted from Kaplan, 2007)



a configuration with an additional heat exchanger (recuperator) which is applicable when the expansion in the turbine is done in the dry superheated zone and the expanded vapour contains heat which has to be extracted prior to condensation (Kaplan, 2007).

### Biogas-Fueled CHP Systems

The heat for driving a CHP system can be provided by combustion of biofuels (solid, liquid and gaseous), as shown in Table 4. In fact, most of the installed CHP systems employing ORC engines use biofuels as an energy source (Quoilin, 2011). An important advantage of biofuels over other renewables is reliability, as the resource is generally non-intermittent and energy production is easier to control. One of the most important considerations for efficient utilization of biofuels is the availability of biomass feedstock in close proximity to the CHP plant (U.S. Environmental Protection Agency, 2007).

Residual biomass, as opposed to biomass derived from energy crops, can be derived from various sources, among which wood wastes, crop residues, manure biogas, wastewater treatment biogas, municipal solid waste, food processing residues, etc. (U.S. Environmental Protection Agency, 2007). Combustion of biogas, derived via anaerobic digesters from biodegradable waste or from wastewater treatment facilities, is suitable for CHP systems of cold storage facilities. In particular, this can be beneficial for refrigerated warehouses of (or near) large food processing plants. Common food-processing wastes are fruit pits, cheese whey and meat processing residues, but these can be difficult to utilize as a fuel source because of the varying characteristics and properties of different waste streams. Hence, such wastes are most often disposed of as industrial wastewater and discharged to a local wastewater treatment plant (U.S. Environmental Protection Agency, 2007).

Food and other biodegradable wastes, composed of organic material, are subject to anaerobic decomposition of the organic matter and produce biogas with high methane ( $\text{CH}_4$ ) content of 45-70% (Rasi, 2009). Methane yields of selected feedstock from the food and other industries are reported by Rutz *et*

### Integration of Renewable Energy in Refrigerated Warehouses

*al.* (2009). Methane, which is the primary ingredient of natural gas, has high heat of combustion and substantial global warming potential (GWP). Thus, its capture and utilization in waste-to-energy systems is stimulated by many countries, some of which have put in place (or are planning to adopt) climate change mitigation policy instruments for that purpose. According to Eriksson (2010), the energy content of biogas can be expected in the range of 4.5-8.5 kWh/Nm<sup>3</sup>, while pure methane has an energy content of 9.81 kWh/Nm<sup>3</sup>. Through appropriate upgrade processes biogas can be converted to biomethane with methane content of about 90% (Rasi, 2009).

As indicated in Table 4, biofuels can be used as a heat source for various CHP prime movers. In the case of biogas, a gas turbine engine is especially suitable, as biogas can directly be fed to the combustion chamber of the engine. A disadvantage of biogas-driven CHP systems is the high capital and maintenance costs, along with the system complexity due to the need for involvement of appropriate equipment for conversion of biogas and pre-processing of the produced fuel in order to meet engine requirements. More information on biogas conversion is published by Hillen *et al.* (2010), Krich *et al.* (2005), Rutz *et al.* (2012) and the U.S. Environmental Protection Agency (2007).

The high capital and maintenance costs can lead to long payback periods if no government incentives are available. A feasibility study of biogas-fuelled CHP systems for meat processing facilities in Australia indicates a payback period in the range of 9.2-13.4 years. The financial benefits from savings of CO<sub>2</sub> emission permits to reduce the payback period for such systems to 7-9.2 years (McPhail & Rossington, 2010). Table 5 details typical performance parameters of biogas-fuelled CHP systems with different prime movers, while Table 6 shows estimates for the capital and operating costs associated with biomethane production, based on a study of Krich *et al.* (2005) about the production and use of biomethane from dairy waste.

The waste heat of the flue gases, which exit the CHP system at rather high temperatures of 80-550°C (Rutz *et al.*, 2012), can be utilized as heat source for a thermally driven refrigeration system. Suamir & Tassou (2011) evaluated the performance of an integrated system combining biogas-fuelled trigeneration and CO<sub>2</sub> refrigeration, designed to supply supermarkets with heating, cooling and electrical power. The today's technology level of such systems still requires relatively long payback periods. Waste heat of the primary system can also be used for additional power generation through a heat engine operating at lower temperatures (e.g. an ORC engine). Rutz *et al.* (2012) estimated that waste heat from a CHP plant with 1 MW electrical capacity can be used for an ORC engine to generate 7-10% (0.07-0.1 MW) additional power, thereby increasing the efficiency of the system by 45%. The CHP system can directly

Table 5. Prime movers for biogas-fuelled CHP systems (Adapted from U.S. Environmental Protection Agency, 2007)

	Gas Turbine	Microturbine	Reciprocating Engine	Steam Turbine	Stirling Engine	Fuel Cell
Capacity	0.5-40 MW	0.03-0.25 MW	< 5MW	0.05-250 MW	< 0.2 MW	< 1 MW
Field experience	Extensive	Extensive	Extensive	Extensive	Limited	Some
Electric efficiency based on HHV	22-36%	22-30%	22-45%	5-30%	5-45%	30-63%
Installed cost of CHP system (\$/W)	\$0.7 -2/W	\$1.1-2/W	\$0.8-1.5/W	\$0.35-0.75/W (w/o boiler)	\$1-10/W	\$3-5/W
O&M costs (\$/MWh)	\$6-11/ MWh	\$8-20/ MWh	\$8-25/ MWh	< \$4/MWh	~\$10/MWh	\$10-40/ MWh



### Integration of Renewable Energy in Refrigerated Warehouses

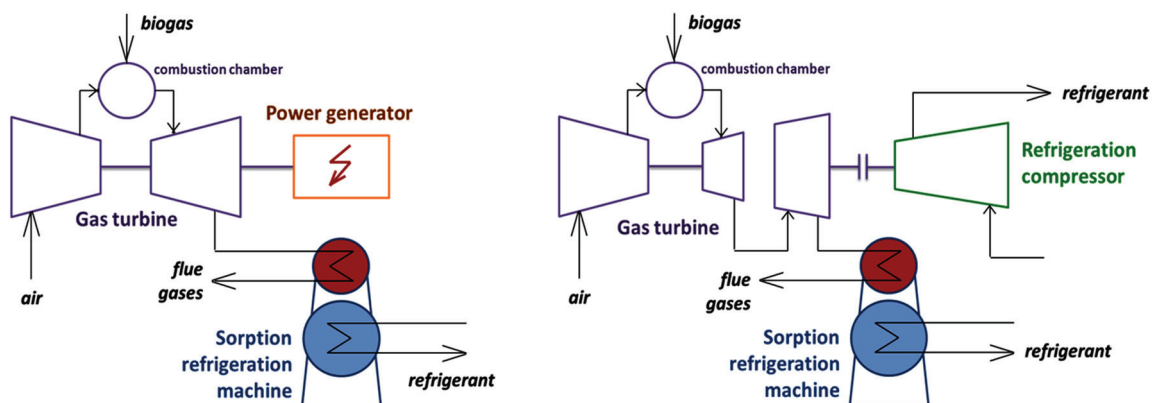
Table 6. Indicative cost ranges for biomethane production equipment (Adapted from Krich et al., 2005)

Equipment	Cost
<b>Anaerobic digester</b>	
Capital cost	\$88-164 per 1000 m <sup>3</sup>
Operating cost	\$17-21 per 1000 m <sup>3</sup>
<b>Biomethane upgrading plant</b>	
Capital cost	\$55-110 per 1000 m <sup>3</sup>
Operating cost	\$130-240 per 1000 m <sup>3</sup>
<b>Biomethane storage</b>	\$0-100 per 1000 m <sup>3</sup>
<b>Biomethane transport</b>	\$0-32 per 1000 m <sup>3</sup>

be used to mechanically drive the compressor of a vapour-compression refrigeration system, while the waste heat could drive a sorption refrigeration system (ASHRAE, 2008). Figure 14 shows simplified schematics of two possible configurations of trigeneration systems driven by a gas turbine.

A number of refrigerated warehouses around the world feature CHP systems fuelled by on-site produced biogas. For instance, the Cannington Cold Stores' Bridgwater site in the United Kingdom features a system with anaerobic digestion tanks and gas holders for on-site biogas production and storage (Figure 15). Biogas is produced from various food wastes originating from the 45,000 m<sup>3</sup> cold store, which provides ambient, chilled and frozen storage down to -25°C ("Cannington Cold Stores", n.d.). The produced biogas is used for heat and power generation via an on-site CHP system. Electricity generated by the CHP system is used to power the cold store and surplus electricity is fed to the utility grid under the Renewable Obligations scheme established in the United Kingdom. Waste heat from the CHP system is fed to the digesters to run the biogas generation process ("Cannington Cold Stores", n.d.). According to Kirk Group (2014), the total digestion volume of the facility is expected to reach 18,000 m<sup>3</sup>, while the generating capacity is expected to exceed 3.3 MW. Another example of a biogas production plant, using food wastes in the United Kingdom, is the Premier Foods' RF Brookes ready-meal factory at Rogerstone, Wales. The plant is estimated to generate 1.4 million m<sup>3</sup> of biogas with an energy content

Figure 14. Schematics of two possible configurations of biogas-fuelled trigeneration systems



### **Integration of Renewable Energy in Refrigerated Warehouses**

*Figure 15. Biogas production plant at the Cannington Cold Stores site. (© 2014, Kirk Group. Used with permission).*



of about 8.4 MWh, which is fed to a CHP system, thereby displacing 10% of the factory's fossil-fuel consumption ("Serving up food-factory waste", 2011).

## **INTEGRATION OF RENEWABLES INVOLVING THERMAL ENERGY STORAGE**

Integration of solar, wind and other distributed renewable energy sources in the power grid can be challenging, especially for traditional centralized grids with top-down structure. This is caused by the mismatch of supply and demand of energy, as total generation has to match total consumption in the grid at any moment. Grid balancing problems are common for both developed and developing economies worldwide. Peak summer loads because of the high energy demand for air-conditioning have become a typical problem for the U.S. power grid, while in Europe, which possesses a higher share of RES in its power supply system, the problem with the intermittency of renewable sources is even more pronounced.

The development of "smart grids" involves transition from the traditional top-down approach of power supply to a more distributed and flexible electricity supply and distribution system. Within this framework, industrial cold storage facilities can become a more active player within the grid by either selling excessive on-site generated electricity or by improving the power grid balance through smart temperature control, involvement of TES and energy management, thereby providing substantial economic benefits to the cold store operator (Fikiin, 2012a).

### **Thermal Energy Storage for Cold Accumulation**

Embedding TES systems as part of the cold-store refrigeration plants is a quite logical and intuitive measure, employed for years by the cold chain operators to profit from the cheaper electricity tariffs

### Integration of Renewable Energy in Refrigerated Warehouses

at the low-consumption periods. Simultaneously, TES appears to be a powerful tool for increasing the RES share in the cold storage sector by accumulating the excessive renewable energy, generated on-site, unless it is sold to the electricity grid (Fikiin, 2012a, b).

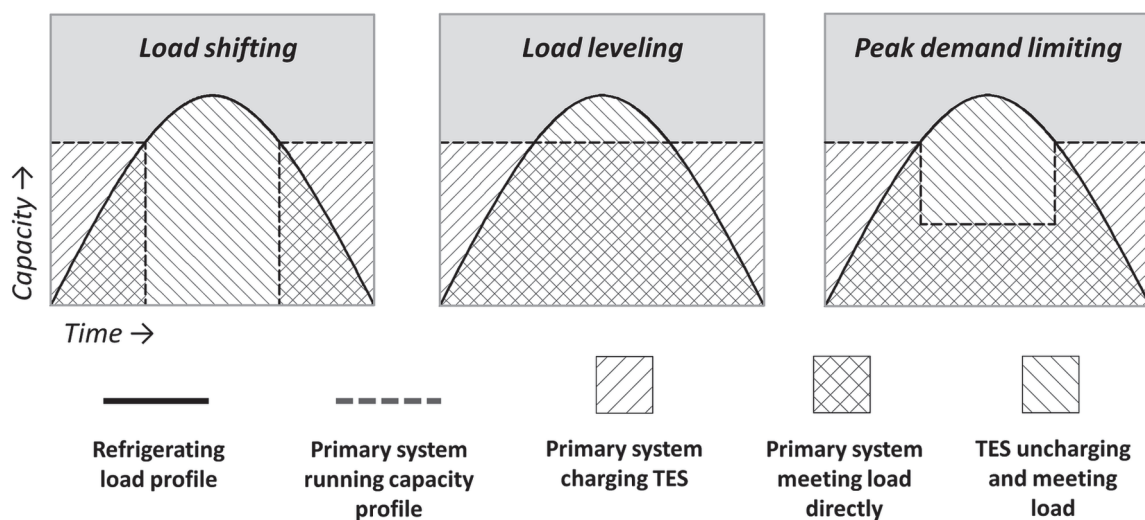
In fact, TES does not reduce (and might even increase) the overall energy consumption, but it distributes the loads during time in a much more efficient way. The main benefits for the store operator can be summarised as follows (Fikiin, 2012b; ASHRAE, 2008):

- Overall energy expenditures of the facility are lower;
- Peak capacity is reduced, which brings down the investment and the equipment size;
- Plant operation and maintenance are optimized, because when the refrigeration plant operates with large load variations, especially at capacities much lower than the designed maximum capacity (i) its efficiency drops substantially, (ii) control becomes more complicated, and (iii) some plant components may experience technical problems to cope with these variations.

Figure 16 gives a simplified example of peak demand reduction strategies when using TES. A TES system typically serves as a thermal buffer between the primary refrigeration circuit and a secondary circuit which supplies cold by pumping secondary refrigerant to air coolers placed in the refrigerated rooms of the store. The TES systems accumulate in tanks or special vessels the superfluous cold produced when running the primary circuit, thereby cooling the secondary refrigerant even when the compressors are switched off. This type of thermal storage is often referred to as “active” storage.

Comprehensive information on TES systems and their various benefits can be found in relevant literature (ASHRAE, 2008; Stoecker, 1998). TES systems can be classified in accordance with: (i) type of thermal storage medium, (ii) whether they store primarily sensible or latent heat, or (iii) the way the storage medium is used (ASHRAE, 2008). Thermal storage media may consist of water, aqueous solutions, pure or multicomponent liquids (e.g. containing glycols and alcohols), ice and phase-change materials (PCM),

Figure 16. Charging and discharging strategies for TES to meet peak refrigeration loads (Adapted from ASHRAE, 1993)



### Integration of Renewable Energy in Refrigerated Warehouses

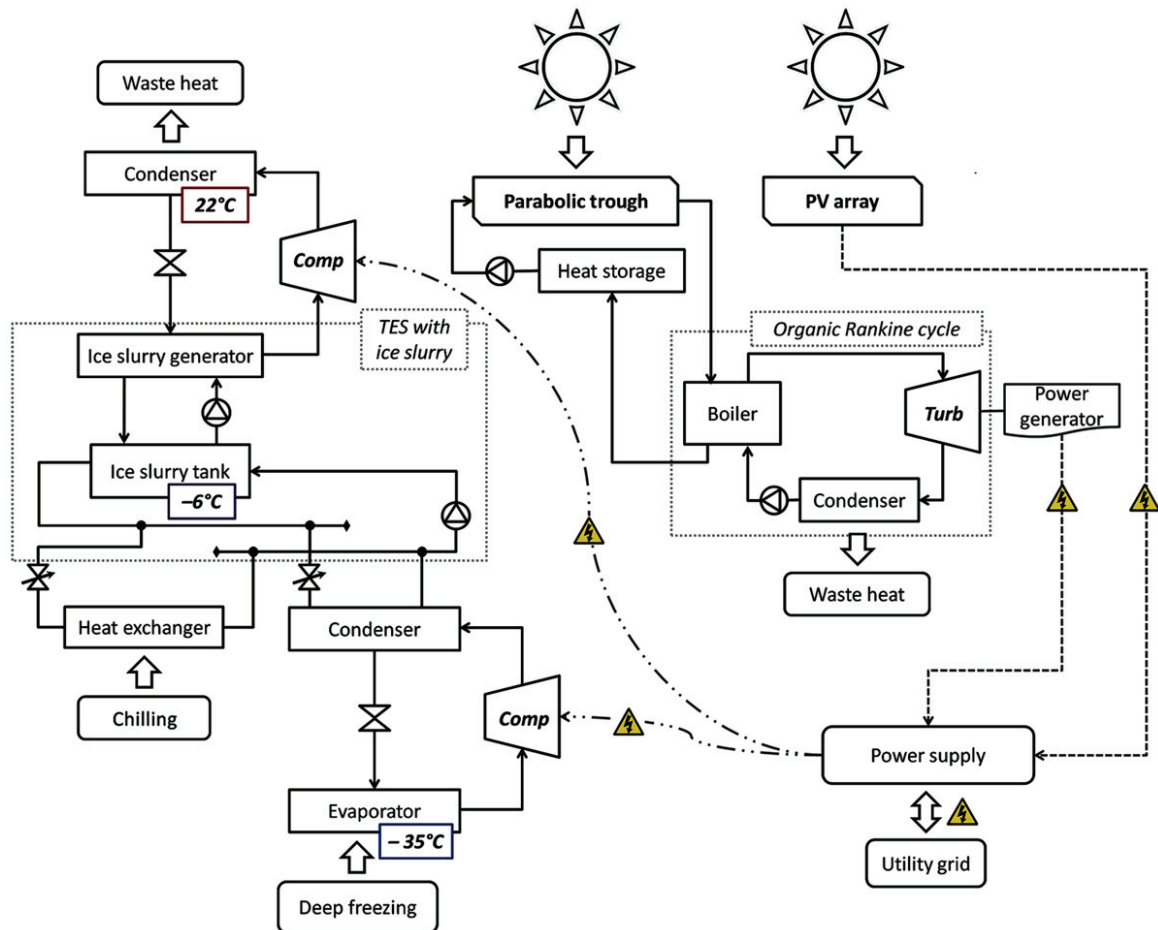
along with microcrystalline ice slurries, PCM slurries, etc. For example, Fikiin, Kaloyanov, Filatova, & Sokolov (2002) analysed a number of refrigeration systems and technologies involving ice-slurry-based TES for different industrial scenarios. Another useful review has been published by Tassou *et al.* (2005).

There are practically unlimited opportunities and numerous engineering solutions for integrating renewable energy in TES systems and cold accumulating facilities of refrigerated warehouses. Figure 17 illustrates a possible arrangement of such a refrigeration plant employing ice-slurry and powered by a solar-driven ORC engine.

### Temperature Control for Passive Thermal Energy Storage

Temperature is generally considered as the “single most important factor determining the food quality and safety”. This definition means that a lot of other process parameters or storage conditions may more or less influence upon the food product in different industrial situations, but temperature is the

Figure 17. Possible arrangement of a solar powered refrigeration plant using ice slurry (Adapted from Van Bael, 1996; Fikiin *et al.*, 2002)



### Integration of Renewable Energy in Refrigerated Warehouses

only physical value whose importance is always enormous. Hence, proper temperature control is the prime simple receipt for the success of every food processor, store operator and retailer (Fikiin, 2003). The temperature-controlled cold supply chain for refrigerated processing, storage, distribution, retail and household handling of foods is therefore of paramount importance for guaranteeing safety, quality, wholesomeness and extended shelf-life of perishable commodities (Fikiin, 2003; Cleland, 2010).

From the viewpoint of product safety and quality, the “golden rule” is that storage temperature must be maintained as constant as possible. In that context, numerous product-specific data for the practical storage life of different chilled and frozen commodities kept at the well known constant storage temperatures are published in the specialized literature (ASHRAE, 2014; Fikiin, 2003). However, as Table 7 implies, the “golden rules” and strategies for energy savings might often contradict safety and quality related requirements. For instance, the so-called “passive” thermal energy storage involves artificial temperature fluctuations to accumulate cold in the refrigerated products, when excessive and cheap energy is available, and to release this energy at the time of peak loads, when the energy demand is higher (Altwies & Reindl, 1999; Van der Sluis, 2008). Such approaches are very intuitive and proven in real practice for many years. The need for additional investment to build up “active” TES systems is thus avoided.

Recent advancements in information technologies and automatics make it possible to implement sophisticated temperature control strategies for intelligent energy use. Such an intelligent approach could be illustrated by a comparatively simple strategy, called “Night Wind”, investigated under EU’s FP6 Project No. 020045 “Grid Architecture for Wind Power Production with Energy Storage through Load Shifting in Refrigerated Warehouses” (Van der Sluis, 2008). The “Night Wind” strategy combines the advantages of using a passive TES principle and a way to involve renewable wind energy when meeting the electricity demand of cold stores on a local, regional or Europe-wide level. As discussed further in this section, similar strategies have been applied outside of Europe as well.

Table 7. Electricity saving strategies for refrigerated storage (Estrada-Flores, 2010)

Electricity Saving Strategies	Temperature-Related Heuristics For Quality Preservation
<b>For Frozen Products</b>	
<ul style="list-style-type: none"> <li>• Peak avoidance techniques</li> <li>• Sub-cooling of the warehouse during weekends</li> <li>• Intelligent matching of load (variable and fixed compressor’s capacity)</li> <li>• Adaptive defrost</li> </ul>	<ul style="list-style-type: none"> <li>• Peak avoidance and sub-cooling techniques should maintain product temperatures within <math>-8</math> and <math>-25^{\circ}\text{C}</math></li> </ul>
<b>For Chilled Products (Dedicated Storage)</b>	
<ul style="list-style-type: none"> <li>• Peak avoidance techniques (see heuristics)</li> <li>• Intelligent matching of loads</li> </ul>	<ul style="list-style-type: none"> <li>• Sub-cooling to temperatures below <math>0^{\circ}\text{C}</math> is not recommended for horticultural products (or others susceptible to freezing damage)</li> <li>• Sub-cooling to <math>-2^{\circ}\text{C}</math> can be well tolerated by some dairy products (e.g. milk, butter, cheddar cheese)</li> </ul>
<b>For Controlled Atmosphere storage</b>	
<ul style="list-style-type: none"> <li>• Increasing evaporation temperature above the recommended storage temperature is a possibility (see heuristics)</li> </ul>	<ul style="list-style-type: none"> <li>• Tolerance of commodities to temperatures above the recommended storage temperature needs to be investigated experimentally. No temperature tolerance guidelines have been fully established for controlled atmosphere storage</li> </ul>



## **Integration of Renewable Energy in Refrigerated Warehouses**

### The “Night Wind” Concept

Distributed renewable energy resources (such as wind and solar energy) have a substantial potential for energy supplies and reducing CO<sub>2</sub> emissions but have been difficult to integrate so far because of their intermittent contribution. The integration of wind power into the nationwide and transnational energy supply systems becomes more complicated with increasing the production capacity of installed wind turbines, because of the mismatch of supply and demand of energy. The wind energy is generated at random times, whereas the energy use pattern shows distinct demand peaks during day time and office hours, and low consumption during the night. Refrigerated warehouses are constant power consumers (day and night), where electricity is converted by the refrigeration plant into thermal energy. The use of a refrigerated warehouse for storing renewable wind energy affords economic benefits resulting from the cost difference between low and peak-hour electricity tariffs and permits to offset undesirable demand peaks in the electrical grid (Van der Sluis, 2008; Fikiin, 2011; Fikiin, van der Sluis, Paraskova, Iserliyska, & Tsokov, 2009, 2010). Energy is stored by producing more cold than necessary (thereby refrigerating the products below the prescribed temperatures), while turning off the refrigeration plant releases virtual energy matching the difference between the average and the zero cold store demands, thus letting foods warm up back to the recommended temperatures of storage. For example, if the temperature of stored frozen products throughout the European Union is permitted to vary by 1 °C only, all refrigerated warehouses can act as a giant battery on the grid – they could store twice the EU’s wind power production, as estimated for 2010 by Van der Sluis (2008). Refrigerated foods themselves are thereby used for passive TES as accumulators of cold (Fikiin *et al.*, 2009; Fikiin, 2012c). In particular, frozen foods are thus employed as a phase-change material (Fikiin, 2011, 2014). While balancing wind power production by fossil fuel power generation is inefficient, such balancing by refrigerated warehouse load management is a sustainable (environmentally friendly and cost effective) alternative with reduced running costs for the cold chain operators (Van der Sluis, 2008; Butler, 2007; Fikiin, 2011).

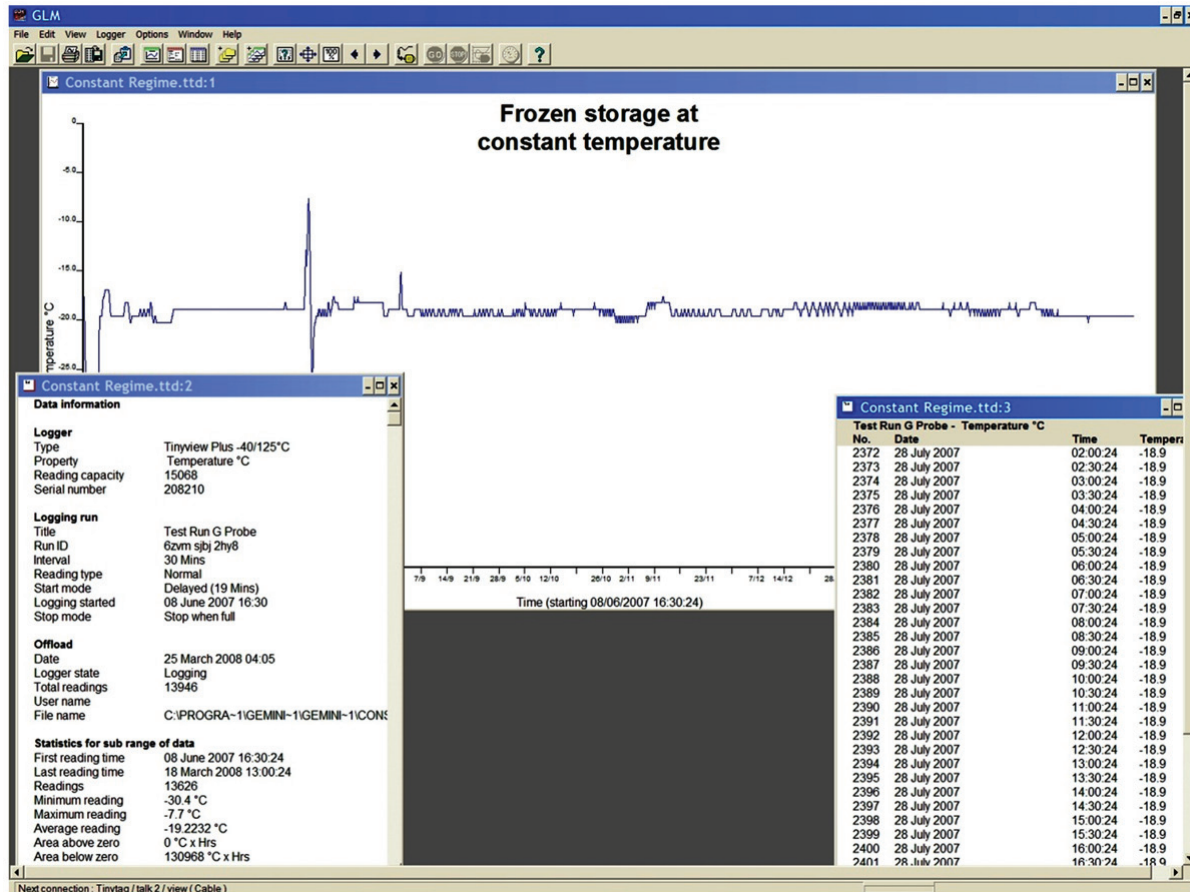
### Quality Attributes of Frozen Foods Undergoing Temperature Fluctuations (Freeze-Thaw Cycles)

Special attention is to be paid to the refrigerated food quality as affected by the “Night Wind” technology. For that purpose, quality attributes of selected frozen foods undergoing temperature fluctuations (freeze-thaw cycles) have been investigated. Parallel tests have been conducted with 10 different food samples of identical type, shape and size, stored during 8 months at constant and variable temperature regimes (Fikiin, 2011; Fikiin *et al.*, 2009, 2010). The samples – meat (bacon), fish (smoked Mackerel fillet), bakeries (fruit pie), fruit (strawberries), vegetables (tomatoes, melons and peppers), potatoes (blanched/semi-grilled French fries) and ice cream have been wrapped in plastic bags and boxes, evacuated and frozen at a constant air temperature of –19 °C as well as at a variable temperature (with day-night cycles) ranging from –16/–18 °C down to –26/–28 °C, as shown in Figure 18 and Figure 19 (Fikiin, 2011; Fikiin *et al.*, 2009, 2010).

After 3 days, and 2, 4, 6 and 8 months of frozen storage, the samples have been thawed in air ambience up to a temperature in the product centre of 20–22 °C. Thus, a number of quality attributes have periodically been evaluated – texture (by penetrometric measurements), colour (by the method of Gardner) and drip losses. Sensory evaluation has also been carried out (with the aid of a taste panel) to estimate the

### Integration of Renewable Energy in Refrigerated Warehouses

Figure 18. Frozen storage at constant temperature (classical)



product appearance, colour, flavour and consistency. Data obtained have been summarized in the form of tables, graphs and predictive equations (Fikiin, 2011; Fikiin *et al.*, 2009, 2010).

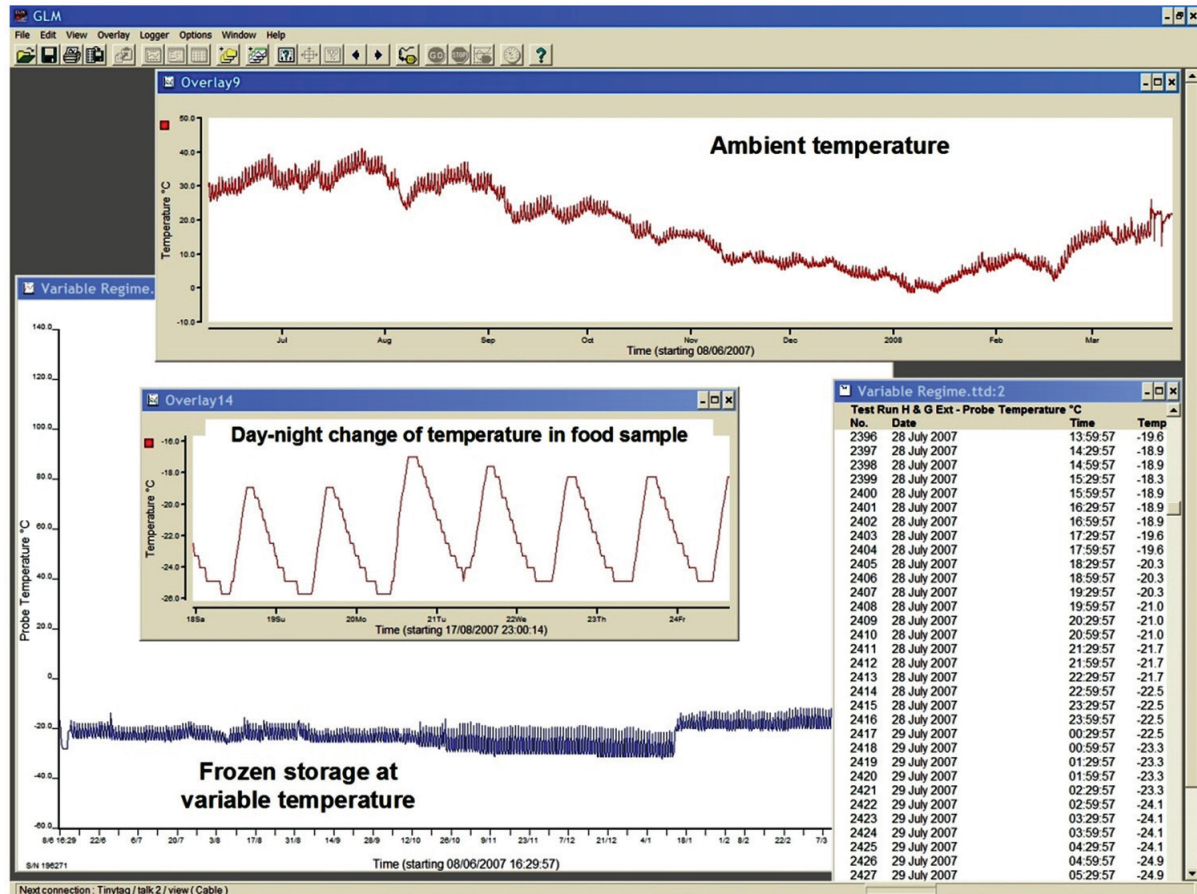
This study revealed that the quality of frozen products, subject to fluctuations of storage temperature, is generally acceptable but, as expected, inferior in comparison with food maintained at a constant temperature (in compliance with the established food refrigeration standards and good practices). However, for many products this quality decay is rather negligible and can be offset by the obvious economic and sustainability-related advantages of the “Night Wind” technology (Fikiin, 2011; Fikiin *et al.*, 2009, 2010). In that context, potatoes (French fries) appeared to be the most robust “Night Wind friendly” product (Fikiin, 2011; Fikiin *et al.*, 2009, 2010).

### Decision Support and Automated Control

The “Night Wind” concept needs optimal strategies for fine control of the cold store operation, based on economic criteria, e.g. balance between the instantaneous wind energy production and actual electricity demand, predicted dynamic/stochastic variations of electricity tariffs on the stock market, etc., along with engineering and food quality requirements. For that purpose, a control system (Figure 20) has been

## Integration of Renewable Energy in Refrigerated Warehouses

Figure 19. Frozen storage at variable temperature (Night Wind)



created to manage in real time wind power integration, depending on the store's refrigeration demand, the intermittent availability of wind energy, the variations of electricity prices as per a stepwise subscription plan or in a stochastic manner on the stock market, and other factors (Van der Sluis, 2008; Fikiin, 2011).

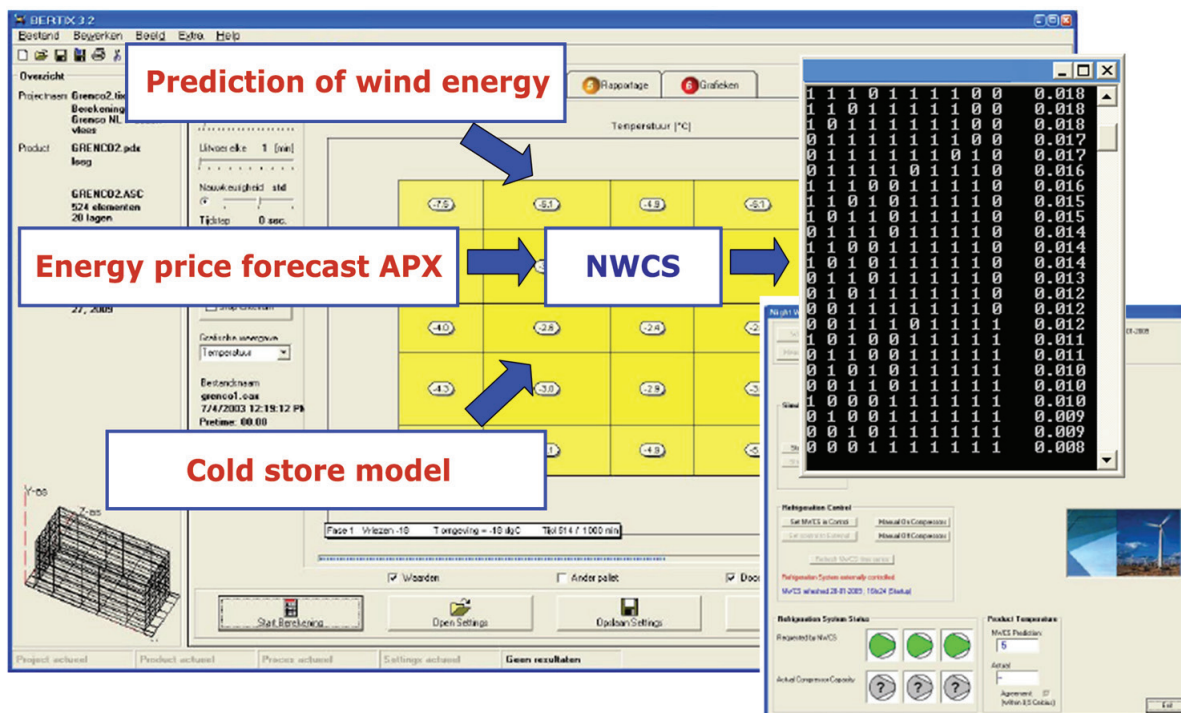
The control system can serve: (i) as a decision-support information system to assist the cold chain operator when taking decisions on the most profitable pattern of energy use, or (ii) as an expert system embedded in the hardware and software for fully automated control of the store.

### Economic Benefit and Precautions

The "Night Wind" temperature control strategy has been demonstrated at the store of Partner Logistics BV at Bergen op Zoom, the Netherlands – one of the largest frozen food stores in Europe (for 680,000 pallets). This refrigerated warehouse stores basically French fries, whose quality remains almost the same after daily temperature fluctuations and freeze-thaw cycles. Van der Sluis (2008) reported a very substantial real profit from implementing the "Night Wind" technology at this facility. Other pilot projects following the concept behind "Night wind" have also been started. Curry (2010) reports application in a 155,742 m<sup>3</sup> refrigerated warehouse in Cuxhaven, Germany used to store frozen fish at -20°C.

### Integration of Renewable Energy in Refrigerated Warehouses

Figure 20. The “Night Wind” control system (Adapted from Van der Sluis, 2008)



Another example is the SnoTemp Cold Storage facility in Albany, Oregon used for storing blueberries (Scruggs, 2013). The EU-funded “e-harbours” project has also examined this strategy for cold stores in the Antwerp and Hamburg harbours. An interactive simulation which visualizes the concept is available online at: <http://eharbours.eu/simulation/>.

Implementing the “Night Wind” technology for passive TES should be made with extremely high attention, care, due diligence and compliance with the established food standards and regulations. Small inaccuracies might badly damage the stored produce. The best approach is to seek professional advice of competent food technologists, food refrigeration experts or to approach directly the “Night Wind” coordinator (<http://www.nightwind.eu>). Many delicate products are not at all suitable to endure temperature fluctuations, so that a careful and detailed in-situ examination of each specific product is needed before any dangerous industrial exercises with large quantities of expensive produce.

## POLICY INSTRUMENTS IN SUPPORT OF RENEWABLE ENERGY INTEGRATION

Policy instruments are a type of leverage that governments and other public authorities often utilize to improve the competitiveness of renewable energy developments, as the latter are often capital intensive and require some form of support in order to become economically efficient. Cold store operators can benefit from such policy instruments when integrating renewable energy sources in their energy supply. The most common policies in support of renewable energy developments are described below, including examples of implementation of such policies in some countries. REN21 (2013) reports that, as of early



### Integration of Renewable Energy in Refrigerated Warehouses

2013, policy instruments in support of renewable energy are in place in 127 countries worldwide. A summary of different types of policies enacted by some of the countries is given in Table 8 (where the acronyms in the headers denote different policy instruments described further in this section).

Detailed up-to-date information on active policies in different countries can be found online at: <http://www.res-legal.eu/> (for the EU), <http://www.dsireusa.org/> (for the USA), and <http://www.iea.org/policiesandmeasures/renewableenergy/> (worldwide).

## Regulatory Policies

### Feed-In Tariffs

Feed-in tariff (FIT) schemes provide renewable energy producers with long-term agreements, usually with duration of 10-25 years, which typically involve guaranteed access to the power grid and oblige electric utilities to purchase electricity, generated by eligible renewable sources, at specified prices for every kilowatt-hour (kWh). The price can depend on type of technology, project location and size, among others, but can also be bound to decline over time, in track with expected reductions in the cost of renewable energy technologies. Feed-in tariff schemes may also be linked to streamlined administrative procedures, which reduce bureaucratic overhead, minimize project costs and accelerate the pace of project development (Couture, Cory, Kreycik, & Williams, 2010). FITs can be designed with a fixed tariff level or as a premium over the prevailing market price of electricity.

Table 8. Renewable energy support policies adopted by various countries – nationwide (●); at a state or provincial level (○) (Adapted from REN21, 2013)

Country	FIT	NM	RPS	REC	FI	PT	Country	FIT	NM	RPS	REC	FI	PT
Australia	○			●	●		Japan	●	●	●	●	●	
Brazil		●			●	●	Jordan	●	●			●	●
Bulgaria	●				●		Kazakhstan	●			●		
Canada	○	○	○		●	●	Kenya	●				●	
China	●		●		●	●	Mexico		●			●	●
Denmark	●	●		●	●	●	Nepal					●	●
Egypt		●			●	●	Netherlands	●	●		●	●	
Finland	●			●	●		Philippines	●	●	●		●	●
France	●			●	●	●	Russia					●	
Germany	●				●		South Korea		●	●	●	●	
Greece	●				●		South Africa					●	●
India	●	●	●	●	●	●	Spain	●	●			●	
Indonesia	●		●		●	●	Sweden			●	●	●	
Israel	●		●		●	●	United Kingdom	●		●	●	●	
Italy	●	●	●	●	●	●	United States	○	○	○	○	●	●



### **Integration of Renewable Energy in Refrigerated Warehouses**

The feed-in tariff is the most widely adopted policy instrument for supporting renewable energy developments and, according to Couture *et al.* (2010), has promoted approximately 75% of global PV and 45% of global wind deployment. Historically feed-in tariffs are considered a German model and have been the driving force behind the sustained development of renewable energy projects in the European Union, where this mechanism has been applied for about two decades, but has more recently spread to other regions, including North America, Australia and Southeast Asia.

In Germany feed-in tariffs apply to various technologies, e.g. €48.7/MWh for onshore wind developments, €110.2-159.2/MWh for solar systems, €250/MWh for geothermal systems and €60-143/MWh for biomethane, with various depressions of tariffs and additional premiums applicable (KPMG International, 2013). In France feed-in tariffs for onshore wind developments amount to €82/MWh for the first 10 years and the same or a reduced rate for the next 5 years, while tariffs for solar PV systems vary in the range of €172.7-315.9/MWh, depending on the type and size of the power plant, €200/MWh for geothermal systems and €81.2-133.7/MWh for biogas (KPMG International, 2013). Feed-in tariff policies in the United States vary according to state. According to the U.S. Energy Information Administration (2013), state-level programs are established in California, Hawaii, Maine, Oregon, Rhode Island, Vermont and Washington, while various programs have been established independently by different utilities in some of the states, including Florida, Georgia, Indiana, Kentucky, Mississippi, New York, North Carolina, Texas, Virginia and others.

### **Net Metering**

Net metering (NM) is a service to power consumers that are also power producers, under which electricity generated on-site and fed to the utility grid is used to offset electricity provided to the consumer by the utility during the applicable billing period. This is similar to the feed-in tariff mechanism, but the significant difference is that in a net metering program electricity fed to the utility grid is compensated at the regular retail rate at which the utility sells power to the consumer, i.e. the equivalent of subtracting the amount of electricity (kWh) generated on-site and fed to the grid from the amount (kWh) consumed from the grid and paying the remaining electricity to the utility at normal retail prices. The feed-in tariff scheme may therefore be more beneficial to a RES producer.

### **Renewable Portfolio Standards and Renewable Energy Certificates**

Quota obligations, also referred to as renewable portfolio standards (RPS), require or encourage electricity producers within a given jurisdiction to supply a certain minimum share of their electricity from designated renewable resources (U.S. Energy Information Administration, 2012). This regulatory mechanism is typically imposed on electric utilities or producers, with a certain penalty being imposed in case of failure to comply. To facilitate compliance, often RPS schemes are accompanied by a renewable energy certificates (RECs) program.

RECs are tradable credits (usually in the form of electronic records) which represent the value of electricity produced from renewable sources not connected to the grid of the respective utility (Van der Linden *et al.*, 2005). Such programs permit electric utilities or producers, unable to meet their RPS obligations, to buy RECs from other suppliers, even when there is no physical connection (i.e. power grid) between the respective entities. Because the possession of RECs can serve for compliance and

### **Integration of Renewable Energy in Refrigerated Warehouses**

avoidance of penalties, RECs attain monetary value and can be traded like other commodities, i.e. they can be purchased directly from the renewable energy producer or from intermediaries (Van der Linden *et al.*, 2005). The RPS and RECs systems are also related to the feed-in tariff system and these are sometimes used in combination.

REN21 (2013) reports that renewable portfolio standards are enacted at the national level in 22 countries, as well as in 54 states or provinces in the United States, Canada, and India. An RPS system, known as Renewable Obligations scheme, is established in the United Kingdom, whereby renewable power producers receive tradable renewable obligation certificates, i.e. RECs, the amount of which depends on technological maturity and *LCOE*. There is a penalty for non-compliance to the RPS scheme which amounted to £42.02/MWh as of 2013-2014 (KPMG International, 2013). In China a 15% renewable quota is imposed on utilities, while Norway and Sweden have established a common green certificate (i.e. RECs) market (REN21, 2013). According to the U.S. Energy Information Administration (2012), most of the states in the USA have renewable portfolio standards, among them California which requires electric utilities to derive 33% of their retail sales from eligible renewable energy resources by 2020, with an interim target of 25% by the end of 2016.

### **Fiscal Incentives**

Governments often provide financial incentives, in the form of subsidies, grants, rebates and loans, in order to reduce or offset the installed cost incurred by the investor in a renewable energy project. Grant programs usually provide, on a competitive basis, one-time lump-sum payments that are not repayable and are often based on a percentage of the total investment costs. Rebates provide a refund or discount off the initial cost of the project, often based on the installed capacity of a system, e.g. \$/kW, and are generally acquired through an application process (Lantz & Dorris, 2009). Another support mechanism is soft loans, involving below-market interest rates among other benefits, provided to RES developers. Most countries use at least some of the aforementioned mechanisms to promote renewable energy developments. For instance, in the United States various grant and loan programs are applied at the federal level, while many of the states have their own rebate program.

Tax incentives in the form of tax deductions or tax credits are another popular mechanism. Tax incentives can be based on the amount of investment or production and may include: exemption of investments in renewable energy projects from income or corporate taxes, exemption of RES from energy taxes, tax refunds or lower VAT rates for renewable electricity and other stimuli (Van der Linden *et al.*, 2005). Tax incentives are similar to rebate programs, but the main difference is that they only reduce tax liability and therefore have a less direct impact. Tax incentives are a widespread policy adopted by many governments. For instance, a number of tax incentives related to renewable energy are available in China, including reductions in corporate income taxes and VAT (KPMG International, 2013). In the USA investment and production tax credits are enacted at the federal level. According to the North Carolina State University (2014), as of 2013 renewable electricity production tax credits vary in the range of \$11-23/MWh, depending on the renewable source and generally apply to the first ten years of operation, while investment tax credits amount to 30% of the investment costs for solar, fuel cell and small wind installations and 10% for geothermal, microturbine and CHP installations, with limitations on maximum amount and system size.

### **Integration of Renewable Energy in Refrigerated Warehouses**

Another less common incentive mechanism is green marketing whereby individual power consumers voluntarily pay a premium on the electricity bill to promote renewable electricity, which is subsequently at least to some degree paid to the RES producer. The scope and effect of this policy has been until now much more limited.

### **Public Competitive Bidding**

Public competitive bidding, also referred to as public tendering (PT) or public auction, is a procurement mechanism whereby public authorities solicit bids for a given amount of renewable energy supply or capacity and the contract is awarded to the most competitive bid, but typically at prices above standard market levels (REN21, 2013). Electric utilities are hence often obliged to purchase the electricity at the price proposed by the winning bids and are sometimes supported by a government fund (Van der Linden *et al.*, 2005). Separate auctions can be carried out for different RES technologies. This mechanism has been used in some countries, including the United States, United Kingdom, Ireland, France and China (Van der Linden *et al.*, 2005).

## **POLICY CONTEXT AND POTENTIAL FOR FUTURE RESEARCH**

As stated by the UN Secretary-General “New and renewable sources of energy stand at the centre of global efforts to induce a paradigm shift towards green economies, poverty eradication and ultimately sustainable development” (Food and Agriculture Organization of the United Nations, 2011). Renewable energy can be used throughout the food sector either directly to generate energy on-site or indirectly by integrating this energy into the existing conventional energy supply system. Renewable energy sources tend to be widely dispersed throughout agricultural areas. Reliable and affordable energy supply is an essential component for sustainable development (Food and Agriculture Organization of the United Nations, 2011, 2012; United Nations, 2013; European Strategic Energy Technology Plan, 2010).

Wherever good renewable energy resources are available, farmers, fishermen, food processing and preservation businesses have various opportunities to install equipment for generating wind power, solar power, micro-hydropower, etc. In the future, it may also be possible to obtain electricity from sea and ocean resources. Solar thermal, biomass and geothermal resources generated from decentralized facilities can serve for both heating and cooling. The IPCC report “*Renewable Energy and Climate Change Mitigation*” (Intergovernmental Panel on Climate Change, 2011) assesses in more detail each of these technologies and analyses their integration into existing and future energy supply systems. Issues concerning sustainable development, costs and potential revenues and supporting policies are also considered in this report (Intergovernmental Panel on Climate Change, 2011; Food and Agriculture Organization of the United Nations, 2011).

The worldwide market for industrial refrigerated storage of food, beverages and pharmaceuticals is large and constantly growing. Conventional refrigeration plants deliver temperatures in the range of  $-50^{\circ}\text{C}$  to  $20^{\circ}\text{C}$ , while the refrigeration capacity of most plants commonly varies in the range of hundreds of kW to dozens of MWs. Large electrically-driven vapour-compression refrigeration machines supply cold to a distribution network and operate with a *COP* ranging, most often, from 3 to 6 as a function of the required refrigerating temperature and other working conditions. Large cooling towers are usually employed to dissipate condenser heat to the environment. Industrial installations, using heat from

### ***Integration of Renewable Energy in Refrigerated Warehouses***

waste processes and RES to operate thermally-driven refrigeration equipment, become competitive with the vapour-compression systems in areas where the electricity supply is unstable. For example, solar thermally-driven refrigeration systems might employ roof- or ground-mounted, low- and medium-temperature solar collectors but very few industrial systems have been implemented and studied so far. The rising price of electricity increases the interest in solar refrigeration whose capital cost is still relatively high and prevents a wider market uptake. Further research on equipment simplification, unification and cheapening is thus critically important (European Solar Thermal Technology Platform, 2008; European Technology Platform on Renewable Heating and Cooling, 2014).

Developing of knowledge-based energy and resource management systems for improved efficiency through sharing resources (e.g. plants, conventional and RES energy, water, residues and recycled materials) and integrating multiple production units of a single company or multiple companies on a single industrial production site also represents a rather challenging research trend of multidisciplinary and cross-sectional nature (Sustainable Process Industry through Resource and Energy Efficiency, 2013). Making the cold storage sector a key player in this cross-sectorial interaction and elaborating adequate expert systems for smart automated control of refrigerated warehouses in accordance with such criteria can thus revolutionise the sector, thereby contributing to building a resource-efficient and highly sustainable economy of the future.

## **CONCLUSION**

The opportunity for RES integration in the energy supply of cold storage facilities has often been overlooked so far, because of credible concerns over technical and economic performance, but also due to the lack of sufficient knowledge on the various engineering solutions to the problem. Although extensive information on RES applications and research for heating and power generation is available and easily accessible, studies concerning refrigeration systems are still scarce, while relevant information is fragmentary and dispersed. In order to bridge this gap, the present chapter provides a broad, albeit not entirely exhaustive, review of recent developments and ongoing research on state-of-the-art technologies for RES utilization in industrial refrigeration plants, with a particular focus on refrigerated warehouses for storage of perishable food commodities.

Presently, the RES use for on-site power generation, especially through solar PV systems, appears to have gained more ground than RES-powered thermally driven refrigeration systems, as far as large refrigerated warehouses are concerned. There is significant progress in the application of roof-mounted PV systems, due to their easy implantation and substantial government incentives. Whilst on-site wind turbines and wind parks are still rare, in a smart grid context, the proposed “Night Wind” strategy can substantially benefit both cold store operators and electric utilities.

Solar, geothermal and biogas-driven CHP and trigeneration systems are still uncommon, but recent developments and research show promising trends. Solar-driven Stirling engines are actively investigated and developed by several companies, while development of the organic Rankine cycle technology affords encouraging prospects for low-temperature solar and geothermal applications. CHP and trigeneration systems driven by biogas present a valuable opportunity for food-processing factories which generate large amounts of food wastes. Thermally driven refrigeration systems need further improvements in order to become technically feasible and competitive for large refrigerated facilities, but the number of pilot and research projects is growing. In general, further research is required to make RES-powered systems

### **Integration of Renewable Energy in Refrigerated Warehouses**

(which are currently viable for small-scale air-conditioning and cooling applications) competitive for larger refrigeration capacities as well. In the medium term, building up of experience and increased number of market actors should significantly enhance the technical and economic performance of the aforementioned technologies.

RES-related projects are often hardly plausible to cold store operators, because of the difficulties associated with technical implementation and high initial investments. In addition, such projects need a pro-active and/or interactive approach towards the energy supply system, require increased organizational efforts and thus demand greater resulting involvement of the cold store operator. Hence, it might appear to be more comfortable for the operator just to count on its traditional role of passive electricity consumer from the utility grid, especially in the short term. Nevertheless, RES integration is a paramount trend for sustainable growth of the cold storage sector around the globe. The RES attractiveness constantly increases because of the escalating costs of conventional energy resources. While the capital costs for initial investment in RES technologies are comparatively high, the renewable resources are practically free in most cases, i.e. the running costs are marginal. The selection of the most appropriate RES technology for a particular industrial scenario should be based on (i) a thorough evaluation of resource potential of the concrete site, (ii) dynamic modelling and simulation, along with a comprehensive life cycle analysis of the concerned RES system, and (iii) a survey of local government policies and incentives. Furthermore, knowledge-based optimisation and accurate energy management are indispensable to ensure that the RES system is operated in the most efficient manner.

### **ACKNOWLEDGMENT**

Part of this survey has been performed within the EU Projects NIGHT WIND (*Grid Architecture for Wind Power Production with Energy Storage through Load Shifting in Refrigerated Warehouses*, No. SES6-020045) and ICE-E (*Improving Cold Storage Equipment in Europe*, No. IEE/09/849/SI2.558301) whose support is gratefully acknowledged. The authors would also like to thank Richard Tracy, Vice President of the Global Cold Chain Alliance, and Ron Vallort, ASHRAE President (2004-2005), for their kind assistance.

### **REFERENCES**

- Altwies, J. E., & Reindl, D. T. (1999). Passive thermal energy storage in refrigerated warehouses. In *Proceedings of the 20th IIR International Congress of Refrigeration*. Sydney, Australia.
- Arvay, P., Muller, M., Ramdeen, V., & Cunningham, G. (2011). Economic implementation of the organic Rankine cycle in industry. In *ACEEE Summer Study on Energy Efficiency in Industry*. Washington, D.C.: American Council for an Energy-Efficient Economy.
- ASHRAE. (1993). *Design guide for cool thermal storage*. Atlanta, GA: ASHRAE.
- ASHRAE. (2008). *ASHRAE Handbook: HVAC systems and equipment*. Atlanta, GA: ASHRAE.
- ASHRAE. (2009). *ASHRAE Handbook: Fundamentals*. Atlanta, GA: ASHRAE.



### **Integration of Renewable Energy in Refrigerated Warehouses**

ASHRAE. (2014). *ASHRAE Handbook: Refrigeration*. Atlanta, GA: ASHRAE.

Aye, L., Sepulveda, C., Merino, G., & Canumir, J. (2012). Evaluation of a solar refrigeration system for field storage of blueberries in Biobío Region. In *Proceedings of the Australian Solar Energy Society 50th Annual Conference*. Melbourne, Australia: Australian Solar Energy Society.

Bennett, P. (2014, May 21). *Aldi completes 1.5MW solar array at multi-million pound cold store and distribution centre*. Retrieved from Solar Power Portal: [http://www.solarpowerportal.co.uk/news/aldi\\_completes\\_1.5mw\\_solar\\_array\\_at\\_multi\\_million\\_pound\\_cold\\_store\\_and\\_2356](http://www.solarpowerportal.co.uk/news/aldi_completes_1.5mw_solar_array_at_multi_million_pound_cold_store_and_2356)

Briley, G. (2004). A history of refrigeration. *ASHRAE Journal*, 46(11), S31–S34.

Butler, D. (2007, February 7). Fridges could save power for a rainy day. *NATNews*. doi:10.1038/news070205-9

*California Green Designs completes largest commercial solar installation in Los Angeles*. (2011, May 17). Retrieved December 1, 2014, from PRLog Web site: <http://www.prlog.org/11495852-california-green-designs-completes-largest-commercial-solar-installation-in-los-angeles.html>

*Cannington Cold Stores: Biogas CHP delivers green energy solution for cold storage*. (n.d.). Retrieved December 1, 2014, from Cogenco Web site: [http://www.cogenco.com/uk-cogenco/ressources/documents/1/44419,Cannington-Cold-Stores\\_Cogenco.pdf](http://www.cogenco.com/uk-cogenco/ressources/documents/1/44419,Cannington-Cold-Stores_Cogenco.pdf)

Cleland, D. J. (2010). Temperature control and energy efficiency in cold storage. In *1st IIR Conference on Sustainability and the Cold Chain*, Cambridge, UK.

*ICE Cold Storage cuts energy costs 75% with solar power*. (2009, March 20). Retrieved July 21, 2014, from Environmental Leader Web site: <http://www.environmentalleader.com/2009/03/20/ice-cold-storage-cuts-energy-costs-75-with-solar-power/>.

Coulomb, D. (2006, November). *Statement given by Didier Coulomb, Director of the International Institute of Refrigeration*. Paris, France: International Institute of Refrigeration. Retrieved from: [http://www.un.org/webcast/unfccc/2006/statements/061117iir\\_e.pdf](http://www.un.org/webcast/unfccc/2006/statements/061117iir_e.pdf)

Couture, T., Cory, K., Kreycik, C., & Williams, E. (2010). *A policymaker's guide to feed-in tariff policy design*. Golden, CO: National Renewable Energy Laboratory. doi:10.2172/984987

Curry, A. (2010, April 2). *Frozen fish help reel in Germany's wind power*. Retrieved from National Geographic News: <http://news.nationalgeographic.com/news/2010/04/100402-frozen-fish-wind-power/>

*DelSolar completes US Foodservice solar installation*. (2011, July 14). Retrieved December 1, 2014, from Refrigerated Transporter: <http://refrigeratedtransporter.com/foodservice/delsolar-completes-us-foodservice-solar-installation>

Döll, J., Bentaher, H., & Morgenstern, A. (2014). First results of a pilot installation of a solar thermally driven cold store. *International Journal of Refrigeration*, 39, 77–85. doi:10.1016/j.ijrefrig.2013.11.010

EDF Renewable Energy. (2009, April 3). *enXco dedicates 1.8 MW (DC) solar project at Hall's Warehouse Corp*. Retrieved December 1, 2014, from: [http://www.edf-re.com/about/press/enxco\\_dedicates\\_1.8\\_mw\\_dc\\_solar\\_project\\_at\\_halls\\_warehouse\\_corp/](http://www.edf-re.com/about/press/enxco_dedicates_1.8_mw_dc_solar_project_at_halls_warehouse_corp/)

**Integration of Renewable Energy in Refrigerated Warehouses**

Epstein. (2013). *Testa Produce*. Retrieved July 21, 2014, from: [http://www.epsteinglobal.com/Projects/war\\_dist\\_6.html](http://www.epsteinglobal.com/Projects/war_dist_6.html)

Eriksson, O. (2010). Environmental technology assessment of natural gas compared to biogas. In P. Potocnik (Ed.), *Natural Gas* (pp. 127–146). InTech; Available from <http://www.intechopen.com/books/natural-gas/environmental-technology-assessment-of-natural-gascompared-to-biogas> doi:10.5772/9837

Estrada-Flores, S. (2010). Achieving temperature control and energy efficiency in the cold chain. In *Proceedings of the 1st IIR International Cold Chain Conference*, Cambridge, UK.

European Solar Thermal Technology Platform. (2008). *Solar heating and cooling for a sustainable energy future in Europe*. Retrieved from: [http://www.estif.org/fileadmin/estif/content/projects/downloads/European\\_Solar\\_Thermal\\_Technology\\_Platform\\_SRA\\_RevisedVersion.pdf](http://www.estif.org/fileadmin/estif/content/projects/downloads/European_Solar_Thermal_Technology_Platform_SRA_RevisedVersion.pdf)

European Strategic Energy Technology Plan. (2010). *Towards a low-carbon future*. Luxembourg: Publications Office of the European Union. Retrieved from: [http://ec.europa.eu/energy/publications/doc/2010\\_setplan\\_brochure.pdf](http://ec.europa.eu/energy/publications/doc/2010_setplan_brochure.pdf)

European Technology Platform on Renewable Heating and Cooling. (2014). *Common implementation roadmap for renewable heating and cooling technologies*. Retrieved from: [http://www.rhc-platform.org/fileadmin/Publications/RHC\\_Common\\_Roadmap.pdf](http://www.rhc-platform.org/fileadmin/Publications/RHC_Common_Roadmap.pdf)

Fikiin, K., van der Sluis, S., Paraskova, P., Iserliyska, D., & Tsokov, L. (2009). A sustainable cold chain technology for storing renewable energy in refrigerated warehouses and its implications on food quality. In *Proceedings of the EFFoST Conference “New Challenges in Food Preservation”*. Budapest, Hungary.

Fikiin, K. A. (2003). *Novelties of Food Freezing Research in Europe and Beyond. Flair-Flow Europe Synthetic Brochure for SMEs, 10*. Paris, France: Institut National de la Recherche Agronomique.

Fikiin, K. A. (2011). Refrigerated warehousing as a smart tool to store renewable energy for improving the food chain and power supply sustainability. In *Proceedings of the 6th International CIGR Technical Symposium “Towards a Sustainable Food Chain”*. Nantes, France.

Fikiin, K. A. (2012a). *Integration of renewable energy in the cold storage sector. Info Pack 11 of the EU Project ‘Improving the Cold Storage Equipment in Europe (ICE-E)’*. Available from <http://www.khlim-inet.be/drupalice/case-studies#infopacks>

Fikiin, K. A. (2012b). *Thermal energy storage. Info Pack 10 of the EU Project ‘Improving the Cold Storage Equipment in Europe (ICE-E)’*. Available from <http://www.khlim-inet.be/drupalice/case-studies#infopacks>

Fikiin, K. A. (2012c). Temperature control strategies for smarter energy use. Info Pack 17 of the EU Project ‘Improving the Cold Storage Equipment in Europe (ICE-E)’. Available from <http://www.khlim-inet.be/drupalice/case-studies#infopacks>

Fikiin, K. A. (2014). Integration of renewable energy and smart temperature control strategies in refrigerated warehouses for a more sustainable food cold chain. In *Proceedings of the 7th Central European Congress on Food (CEFood 2014)*. Ohrid, FYR Macedonia, BA-157.

### **Integration of Renewable Energy in Refrigerated Warehouses**

Fikiin, K. A., Kaloyanov, N. G., Filatova, T. A., & Sokolov, V. N. (2002). Fine-crystalline ice slurries as a basis of advanced industrial technologies: State of the art and future prospects. [in Russian]. *Refrigeration Business (Moscow)*, 7, 4–11.

Fikiin, K. A., van der Sluis, S., Paraskova, P., Iserliyska, D., & Tsokov, L. (2010). Sustainability enhancement of refrigerated warehousing by using frozen foods as a phase-change material to store renewable energy. In *Proceedings of the 9th IIR Conference on Phase-Change Materials and Slurries for Refrigeration and Air Conditioning*. Sofia, Bulgaria.

Food and Agriculture Organization of the United Nations. (2011). *Energy-smart food for people and climate*, Issue Paper. Retrieved from: <http://www.fao.org/docrep/014/i2454e/i2454e00.pdf>

Food and Agriculture Organization of the United Nations. (2012). *Energy-smart food at FAO: An overview*. Retrieved from: <http://www.fao.org/docrep/015/an913e/an913e.pdf>

Food Bank of Contra Costa and Solano. (n.d.). *Solar panels*. Retrieved July 21, 2014, from: <http://www.foodbankccs.org/about/green-initiatives/solar-panels.html>

U. S. Foods. (2011, April 13). *U.S. Foodservice-San Francisco activates largest solar panel system in Alameda County to power warehouse*. Retrieved December 1, 2014, from: <http://www.usfoods.com/about-us/media/news-releases/2011/u-s--foodservice-san-francisco-activates-largest-solar-panel-sys.html>

U. S. Foods. (2011, July 13). *U.S. Foodservice-Los Angeles activates one of the largest solar panel systems in Southern California to power warehouse*. Retrieved December 1, 2014, from: <http://www.usfoods.com/about-us/media/news-releases/2011/u-s--foodservice-los-angeles-activates-one-of-the-largest-solar-.html>

U. S. Foods. (2011, November 16). *US Foods activates solar panel system to power distribution center in Phoenix*. Retrieved December 1, 2014, from: <http://www.usfoods.com/about-us/media/news-releases/2011/us-foods-activates-solar-panel-system-to-power-distribution-cent.html>

Grover, S. (2011, June 28). *Green roof covers wind- and solar-powered produce warehouse*. Retrieved July 21, 2014, from TreeHugger Web site: <http://www.treehugger.com/corporate-responsibility/green-roof-covers-wind-and-solar-powered-produce-warehouse.html>

HelioSage. (n.d.). *Merchants Terminal Corporation: Changing the energy management game with one of Maryland's largest solar arrays*. Retrieved December 1, 2014, from: <http://heliosage.com/detail/merchants-terminal-corporation/>

Henningsen Cold Storage Co. (2010, May 5). *Solar Nation installs 200 kilowatt solar-electric system on the Henningsen Cold Storage Co. facility located in Portland, OR*. Retrieved July 21, 2014, from: [http://www.henningsen.com/mediaroom\\_solarnation.html](http://www.henningsen.com/mediaroom_solarnation.html)

Hillen, F., Wall, G., Schulze, M., & Chvatal, S. (2010). *User manual on the biogas conversion through CHP*. Retrieved from: <http://ec.europa.eu/energy/renewables/bioenergy/doc/anaerobic/d21.pdf>

Holdmann, G. (2008). *The Chena Hot Springs 400 kW geothermal power plant* [PDF document]. Retrieved from: [http://apps1.eere.energy.gov/tribalenergy/pdfs/geo07\\_chena.pdf](http://apps1.eere.energy.gov/tribalenergy/pdfs/geo07_chena.pdf)

Holt Logistics Corp. (2014). *Riverside Renewable Energy*. Retrieved July 21, 2014, from: <http://www.holtlogistics.com/riverside-renewable-energy>

### Integration of Renewable Energy in Refrigerated Warehouses

- Infante Ferreira, C., & Kim, D. (2014). Techno-economic review of solar cooling technologies based on location-specific data. *International Journal of Refrigeration*, 39, 23–37. doi:10.1016/j.ijrefrig.2013.09.033
- Intergovernmental Panel on Climate Change. (2011). *Special report on renewable energy and climate change mitigation*. Retrieved from: [http://srren.ipcc-wg3.de/report/IPCC\\_SRREN\\_Full\\_Report.pdf](http://srren.ipcc-wg3.de/report/IPCC_SRREN_Full_Report.pdf)
- Intergovernmental Panel on Climate Change. (2014). *Climate change 2014: Mitigation of climate change*. Cambridge, United Kingdom: Cambridge University Press.
- International Energy Agency. (2007). *Renewables in global energy supply*. Paris, France: International Energy Agency.
- International Institute of Refrigeration. (2007). *Refrigeration drives sustainable development*. Paris, France: International Institute of Refrigeration. Retrieved from: [http://www.iifir.org/userfiles/file/\\_Backup/Dossiers\\_Exclusifs/RDSD\\_EN.pdf](http://www.iifir.org/userfiles/file/_Backup/Dossiers_Exclusifs/RDSD_EN.pdf)
- International Institute of Refrigeration. (2015, in press). *Role of Refrigeration in Worldwide Economy (Info Note)*. Paris, France: International Institute of Refrigeration.
- Kalogirou, S. (2009). *Solar energy engineering: processes and systems*. Burlington, MA: Academic Press.
- Kaplan, U. (2007). Advanced organic Rankine cycles in binary geothermal power plants. In *Proceedings of the 20th World Energy Congress*. Rome, Italy: World Energy Council.
- Kim, D., & Infante Ferreira, C. (2008). Solar refrigeration options – A state-of-the-art review. *International Journal of Refrigeration*, 31(1), 3–15. doi:10.1016/j.ijrefrig.2007.07.011
- Kirk Group. (2014, May 20). *Anaerobic digestion success for a UK food waste plant*. Retrieved July 25, 2014, from: <https://kirkenviro.wordpress.com/2014/05/20/anaerobic-digestion-success-for-a-uk-food-waste-plant/>
- Klein, S., & Reindl, D. (2005). Solar refrigeration. *ASHRAE Journal*, 47(9), S26–S30.
- KPMG International. (2013). *Taxes and incentives for renewable energy*. Retrieved from: <https://www.kpmg.com/Global/en/IssuesAndInsights/ArticlesPublications/taxes-and-incentives-for-renewable-energy/Documents/taxes-and-incentives-for-renewable-energy-2013.pdf>
- Krich, K., Augenstein, D., Batmale, J., Benemann, J., Rutledge, B., & Salour, D. (2005). *Biomethane from dairy waste: A sourcebook for the production and use of renewable natural gas in California*. Retrieved from: <https://www.americanbiogascouncil.org/pdf/biomethaneFromDairyWaste.pdf>
- Lantz, E., & Dorris, E. (2009). *State clean energy practices: Renewable energy rebates*. Golden, CO: National Renewable Energy Laboratory. doi:10.2172/950149
- Lazzarin, R. (2014). Solar cooling: PV or thermal? A thermodynamic and economical analysis. *International Journal of Refrigeration*, 39, 38–47. doi:10.1016/j.ijrefrig.2013.05.012
- Lewis, J., Chaer, I., & Tassou, S. (2007). *Reviews of alternative refrigeration technologies*. London, United Kingdom: Brunel University.

### **Integration of Renewable Energy in Refrigerated Warehouses**

McPhail, N., & Rossington, D. (2010). *The use of abattoir waste heat for absorption refrigeration*. Sidney, Australia: Meat & Livestock Australia Limited.

Milk, B. (n.d.) *Here comes the Sun*. Retrieved December 1, 2014, from Global Cold Chain Alliance Web site: <http://www.gcca.org/cold-facts/here-comes-the-sun/>

Müller-Steinhagen, H., & Trieb, F. (2004). Concentrating solar power: A review of the technology. *Ingenia*, 18, 43–50.

North Carolina State University. (2014). *Database of state incentives for renewables and efficiency*. Available from <http://www.dsireusa.org/>

Norwood, Z. (2011). *A better steam engine: Designing a distributed concentrating solar combined heat and power*. (Doctoral dissertation). Retrieved from eScholarship, UC Berkeley Electronic Theses and Dissertations.

Norwood, Z., & Kammen, D. (2012). Life cycle analysis of distributed concentrating solar combined heat and power: Economics, global warming potential and water. *Environmental Research Letters*, 7(4), 044016. doi:10.1088/1748-9326/7/4/044016

Obersteiner, C., Weißensteiner, L., Haas, R., Erge, T., Sauer, C., & Sothmann, D. . . . Tambjerg, L. (2008). *Market potentials, trends and marketing options for distributed generation in Europe*. Retrieved from: [http://www.iee-massig.eu/papers\\_public/MASSIG\\_Deliverable2.1\\_Market\\_Potentials\\_and\\_Trends.pdf](http://www.iee-massig.eu/papers_public/MASSIG_Deliverable2.1_Market_Potentials_and_Trends.pdf)

Podesser, E., Ghirlando, R., Nunez, T., Jaradat, M., Krause, M., Heinzen, R., . . . del Cano, J. (2010). *State of the art – Survey on new solar cooling developments*. Retrieved from: [http://archive.iea-shc.org/publications/downloads/IEA-Task38-Report\\_C1\\_final2.pdf](http://archive.iea-shc.org/publications/downloads/IEA-Task38-Report_C1_final2.pdf)

Podmolik, M. E. (2011, July 11). Keeping track of everything from blueberries to a \$20 million green building. *Chicago Tribune*. Retrieved from: <http://articles.chicagotribune.com/2011/jul/11>

Pridasawas, W. (2006). *Solar-driven refrigeration systems with focus on the ejector cycle*. (Doctoral dissertation). Retrieved from DiVA portal.

Quoilin, S. (2011). *Sustainable energy conversion through the use of organic Rankine cycles for waste heat recovery and solar applications*. (Doctoral dissertation). Retrieved from BICTEL/e - ULg Liège. (ULgetd-10032011-002906).

Rasi, S. (2009). *Biogas composition and upgrading to biomethane*. (Doctoral dissertation). Retrieved from Jyväskylä University Digital Archive. (URN:ISBN:978-951-39-3618-1).

REN21. (2013). *Renewables 2013 global status report*. Paris, France: REN21.

Royal Academy of Engineering. (2014). *Wind energy: Implications of large-scale deployment on the GB electricity system*. London, United Kingdom: Royal Academy of Engineering.

Rutz, D., Mergner, R., & Janssen, R. (2012). *Sustainable heat use of biogas plants*. Munich, Germany: WIP Renewable Energies.

Scruggs, K. P. (2013, June). Blueberries help store wind energy. *Consumer's Electric Ruralite Magazine*, 4-5.



### Integration of Renewable Energy in Refrigerated Warehouses

*Serving up food-factory waste for AD.* (2011, July 5). Retrieved July 25, 2014, from The Grocery Trader Web site: <http://grocerytrader.co.uk/?p=10173>

Siemens AG (2014). *Organic Rankine cycle technology.* Retrieved July 29, 2014, from: <http://www.energy.siemens.com/hq/en/fossil-power-generation/steam-turbines/orc.htm>

REC Solar. (2014, March 24). *How solar reduced a California farm's electric bill by 75%.* Retrieved July 21, 2014, from: <http://blog.recsolar.com/2014/03/how-solar-reduced-a-california-farms-electric-bill-by-75/>

Stoecker, W. (1998). *Industrial Refrigeration Handbook* (pp. 559–565). Digital Engineering Library: McGraw-Hill.

Suamir, I., & Tassou, S. (2011). Performance evaluation of integrated trigeneration and CO<sub>2</sub> refrigeration systems. In *Proceedings of the 2nd European Conference on Polygeneration*, Tarragona, Spain: Universitat Rovira i Virgili.

Sustainable Process Industry through Resource and Energy Efficiency. (2013). *SPIRE Roadmap.* Retrieved from: <http://www.spire2030.eu>

Tassou, S., Bellas, J., Chaer, I., Davies, T., Behnert, T., Wang, M.-J., & Goldstein, V. (2005). Present and future applications. In M. Kauffeld, M. Kawaji, & P. W. Egolf (Eds.), *Handbook on Ice Slurries – Fundamentals and Engineering* (pp. 251–271). Paris, France: International Institute of Refrigeration.

Tegen, S., Lantz, E., Hand, M., Maples, B., Smith, A., & Schwabe, P. (2013). *2011 cost of wind energy review.* Golden, CO: National Renewable Energy Laboratory. doi:10.2172/1072784

*Tony's Goes Green.* (n.d.). Retrieved December 1, 2014, from Tony's Fine Foods Web site: <http://www.tonysfinefoods.com/index.cfm/tonys-tradition/tonys-goes-green/>

*UN Secretary-General calls for greater investment and commitment to meet Sustainable Energy for All targets, tackle energy poverty and climate change.* (2014, June 6). Retrieved July 31, 2014, from Sustainable Energy for All Initiative Web site: <http://www.se4all.org/2014/06/05/un-secretary-general-calls-greater-investment-commitment-meet-sustainable-energy-targets-tackle-energy-poverty-climate-change/>

United Nations. (2013). *World economic and social survey 2013: Sustainable development challenges.* Retrieved from: [http://www.un.org/en/development/desa/policy/wess/wess\\_current/wess2013/WESS2013.pdf](http://www.un.org/en/development/desa/policy/wess/wess_current/wess2013/WESS2013.pdf)

U.S. Department of Energy. (2012). *SunShot vision study.* Retrieved from: <http://energy.gov/eere/sunshot/downloads/sunshot-vision-study-february-2012-book-sunshot-energy-efficiency-renewable>

U.S. Energy Information Administration. (2012, February 3). *Most states have renewable portfolio standards.* Retrieved August 2, 2014, from: <http://www.eia.gov/todayinenergy/detail.cfm?id=4850>

U.S. Energy Information Administration. (2013, May 30). *Feed-in tariffs and similar programs.* Retrieved August 2, 2014, from: [http://www.eia.gov/electricity/policies/provider\\_programs.cfm](http://www.eia.gov/electricity/policies/provider_programs.cfm)

U.S. Environmental Protection Agency. (2007). *Biomass combined heat and power catalog of technologies.* Retrieved from: [http://www.epa.gov/chp/documents/biomass\\_chp\\_catalog.pdf](http://www.epa.gov/chp/documents/biomass_chp_catalog.pdf)

### **Integration of Renewable Energy in Refrigerated Warehouses**

Van Bael, J. (1996). FLO-ICE as a carrier for cold. *CADDET Energy Efficiency Newsletter*, 4.

Van der Linden, N., Uytterlinde, M., Vrolijk, C., Nilsson, L., Khan, J., & Astrand, K. ... Wisser, R. (2005). Review of international experience with renewable energy obligation support mechanisms. Berkeley, CA: Lawrence Berkeley National Laboratory.

Van der Sluis, S. (2008). *Cold storage of wind energy – Night Wind*. Paper presented at the 4th International Congress for South-Eastern Europe ‘Energy Efficiency and Renewable Energy Sources’, Sofia, Bulgaria.

Vasilescu, C., & Infante Ferreira, C. (2014). Solar driven double-effect absorption cycles for sub-zero temperatures. *International Journal of Refrigeration*, 39, 86–94. doi:10.1016/j.ijrefrig.2013.09.034

Walmart Corp. (2014). *Walmart’s renewable energy commitment*. Retrieved July 21, 2014, from: <http://corporate.walmart.com/global-responsibility/environment-sustainability/energy>

*Walmart unveils industrial wind turbine at California distribution center*. (2012, August 16). Retrieved July 21, 2014, from Green Retail Decisions Web site: <http://www.greenretaildecisions.com/news/2012/08/16/walmart-unveils-industrial-wind-turbine-at-california-dc->

Wang, K., & Vineyard, E. (2011). Adsorption refrigeration. *ASHRAE Journal*, 53(9), 14–24.

Weber, C., Berger, M., Mehling, F., Heinrich, A., & Nunez, T. (2014). Solar cooling with water-ammonia absorption chillers and concentrating solar collector - Operational experience. *International Journal of Refrigeration*, 39, 57–76. doi:10.1016/j.ijrefrig.2013.08.022

Weiss, W., & Rommel, M. (Eds.). (2008). *Process Heat Collectors*. Gleisdorf, Austria: AEE INTEC; Available from <http://aee-intec.at/0uploads/dateien560.pdf>

Wirsol. (2013, August 15). *8.1 Megawatts: Europe’s largest solar roof plant goes online near Mannheim*. Retrieved December 1, 2014, from: <http://us.wirsol.com/references-us/references-agriculture-commercial-and-industrial-rooftops/>

Yearsley Group. (2012, September 5). *Yearsley Group £3.5 million investment in renewable energy*. Retrieved July 21, 2014, from: <http://yearsleyfood.co.uk/news-and-media/yearsley-group-3-million-investment-in-renewable-energy>

## **KEY TERMS AND DEFINITIONS**

**Cold Accumulation:** Preliminary cooling or freezing of a thermal energy storage medium with the aim of shifting refrigeration loads and permitting more efficient operation of the refrigeration system and/or more beneficial energy consumption patterns.

**Cold Storage:** Storage of perishable commodities (e.g. food, pharmaceuticals and biomaterials) in a refrigerated environment, thereby preserving their natural qualities for extended periods of time.

**Cold Store (Refrigerated Warehouse):** Industrial facility for refrigerated storage of foods or other biomaterials in chilled or frozen state.

### *Integration of Renewable Energy in Refrigerated Warehouses*

**Distributed Generation:** Decentralized generation of electricity, involving small-scale power generation systems located at the site of consumption, often allowing the consumer to act as a producer of electricity within the power supply system.

**Passive Thermal Energy Storage:** Strategy for shifting the energy demand of a refrigeration system by allowing temperature fluctuations in the refrigerated warehouse thereby accumulating cold in the stored products and/or the cold store construction.

**Policy Instrument:** Leverage mechanism used by public authorities to stimulate certain developments (e.g. investments in renewable energy projects) in order to overcome existing barriers and achieve predefined objectives, such as increased share of renewable energy in the energy supply mix.

**Renewable Source:** Energy resource which is non-depletable in a reasonable time frame, because it can be replenished in a relatively short period through naturally recurring processes.

**Smart Grid:** Electrical grid with advanced infrastructure, incorporating sophisticated information technology and control mechanisms, to balance the generation, distribution and consumption of electricity in the most sustainable, efficient, reliable and economic manner.

**Sustainable Development:** Societal development which provides the mankind with the capability of maintaining acceptable living standards without causing severe harm to the native environment and irreversible exhaustion of the natural resources available to the present and future generations.

**Trigeneration:** Simultaneous production of electricity, heating and refrigerating output, where residual heat of a cogeneration (CHP) plant is used to run a thermally driven refrigeration system.

*This research was previously published in the Handbook of Research on Advances and Applications in Refrigeration Systems and Technologies edited by Pedro Dinis Gaspar and Pedro Dinho da Silva, pages 803-853, copyright year 2015 by Engineering Science Reference (an imprint of IGI Global).*

## Integration of Renewable Energy in Refrigerated Warehouses

### APPENDIX

Table 9. Nomenclature

$a_1, a_2$	Temperature dependent heat loss coefficients of the solar collector
$A_s$	Surface area of the solar collector [m <sup>2</sup> ]
CRF	Capital recovery factor
$E_R$	Capacity of the renewable energy source [W]
$E_S$	Input capacity required by / supplied to the refrigeration unit [W]
FC	Fuel costs per unit of energy input
FLH	Number of annual equivalent full-load hours
I	Total investment costs, including initial costs, construction costs and decommissioning costs
$I_\beta$	Solar irradiance [W.m <sup>-2</sup> ]
$L_T$	Project duration / operational lifetime of the system [years]
OM	Net annual operation and maintenance costs
$P_G$	Generated electrical power [W]
$P_P$	Power capacity of circulation pumps [W]
$P_S$	Required input power capacity [W]
$Q_A$	Waste heat rejected to the heat sink / ambience [W]
$Q_C$	Waste heat of the refrigeration cycle rejected at the condenser [W]
$Q_E$	Refrigerating capacity [W]
$Q_R$	Utilized residual heat of the CHP system [W]
$Q_S$	Supplied input heat capacity [W]
$Q_{sol}$	Heat supplied to the heated substance by solar collectors [W]
r	Weighted average cost of capital
$T_A$	Ambient air temperature / heat sink temperature [K]
$T_L$	Temperature of the refrigerated space [K]
$T_{Ref}$	Reference temperature at which the reference efficiency $\eta_{PV,R}$ is evaluated [K]
$U_L$	Overall heat loss coefficient of the PV cell [W.m <sup>-2</sup> .K <sup>-1</sup> ]
W	Mechanical work output of the heat engine [W]
$\alpha_r$	Anticipated fraction of the Carnot efficiency that a refrigeration cycle is expected to achieve
$\beta$	Temperature coefficient of the PV cell [K <sup>-1</sup> ]
$\eta_0$	Zero-loss efficiency of the solar collector
$\eta_{C,rc}$	Carnot efficiency of the refrigeration cycle
$\eta_{CHP}$	Overall efficiency of the CHP system
$\eta_{el,CHP}$	Electrical efficiency of the CHP system
$\eta_{es}$	Energy conversion efficiency of the energy supply system
$\eta_{hd}$	Efficiency of the heat distribution system
$\eta_{he}$	Thermal efficiency of the heat engine

continued on following page

### Integration of Renewable Energy in Refrigerated Warehouses

Table 9. Continued

$\eta_{pg}$	Efficiency of the power generator
$\eta_{pv}$	Efficiency of the PV module
$\eta_{pv,R}$	Reference efficiency of the PV module
$\eta_{sc}$	Efficiency of the solar collector
$\eta_{th,CHP}$	Thermal efficiency of the CHP system
$\tau\alpha$	Product of glass transmissivity and cell absorptance

Table 10. Acronyms

CHP	Combined Heat and Power
COP	Coefficient of Performance
CSP	Concentrated Solar Power
DGNB	Deutsche Gesellschaft für Nachhaltiges Bauen
EMS	Energy Management System
FI	Fiscal Incentive
FIT	Feed-In Tariff
GAX	Generator-Absorber-Heat Exchanger
GWP	Global Warming Potential
HAWT	Horizontal-Axis Wind Turbine
IPCC	Intergovernmental Panel on Climate Change
LCA	Life Cycle Analysis
LCOE	Levelized Cost Of Energy
LEED	Leadership in Energy and Environmental Design
NM	Net Metering
ORC	Organic Rankine Cycle
OSE	Overall System Efficiency
O&M	Operation and Maintenance
PCM	Phase-Change Material
PPA	Power Purchasing Agreement
PT	Public Tendering
PV	PhotoVoltaic
R&D	Research and Development
REC	Renewable Energy Certificate
RES	Renewable Energy Source
RPS	Renewable Portfolio Standard
TES	Thermal Energy Storage
UN	United Nations
VAT	Value Added Tax
VAWT	Vertical-Axis Wind Turbine



Published in the United States of America by

IGI Global  
Information Science Reference (an imprint of IGI Global)  
701 E. Chocolate Avenue  
Hershey PA, USA 17033  
Tel: 717-533-8845  
Fax: 717-533-8661  
E-mail: [cust@igi-global.com](mailto:cust@igi-global.com)  
Web site: <http://www.igi-global.com>

Copyright © 2018 by IGI Global. All rights reserved. No part of this publication may be reproduced, stored or distributed in any form or by any means, electronic or mechanical, including photocopying, without written permission from the publisher. Product or company names used in this set are for identification purposes only. Inclusion of the names of the products or companies does not indicate a claim of ownership by IGI Global of the trademark or registered trademark.

Library of Congress Cataloging-in-Publication Data

Names: Information Resources Management Association, editor.

Title: Sustainable development : concepts, methodologies, tools, and applications / Information Resources Management Association, editor.

Description: Hershey, PA : Information Science Reference, [2018] | Includes index.

Identifiers: LCCN 2017023176 | ISBN 9781522538172 (hardcover) | ISBN 9781522538189 (ebook)

Subjects: LCSH: Sustainable development.

Classification: LCC HC79.E5 S861867 2018 | DDC 338.9/27--dc23 LC record available at <https://lcn.loc.gov/2017023176>

British Cataloguing in Publication Data

A Cataloguing in Publication record for this book is available from the British Library.

All work contributed to this book is new, previously-unpublished material. The views expressed in this book are those of the authors, but not necessarily of the publisher.

For electronic access to this publication, please contact: [eresources@igi-global.com](mailto:eresources@igi-global.com).

### III. SUMMARY OF RESULTS AND CONCLUSION

#### III.1 Contributing developments

As already pointed out, the cold chain is a powerful means to combat carbon emissions caused by food losses. Simultaneously, as detailed in Section I, extending the cold chain has obvious implications for the environment and climate. The series of actions and equipment, applied to maintain products within a specified low-temperature range from their harvest/production to the consumption, are a source of direct and indirect greenhouse gas emissions, which must be mitigated or eliminated. The carbon-neutral and sustainability-enhancing means and strategies include: (i) objective and accurate description, understanding and evaluation of underlying physical phenomena both qualitatively and quantitatively, (ii) optimisation and proper design of cold-chain processes and systems for energy efficiency and environmental friendliness, (iii) knowledge-based management strategies for intelligent and economical energy use, and (iv) inventing innovative cold-chain processes and equipment, which improve the state of play in an incremental or radical manner. In this context, the following scientific results, particular contributions and technology advancements, presented in the framework of this VAE doctorate, can be summarised:

✿ A **rigorous mathematical description** is proposed for the unsteady-state heat transfer in arbitrarily shaped moisture-containing solid media, such as food systems, undergoing isothermal or non-isothermal phase transitions. It is demonstrated that the integral enthalpic formulation is always valid for all studied frozen and unfrozen regions, along with the phase-change interface, while the differential formulation is strictly applicable for gradual non-isothermal phase transformations or lack of phase changes. The classical Stefan problem with isothermal phase change and sharp moving boundary is interpreted as an isolated case of the overall enthalpy formulation for nonlinear heat conduction in the whole studied fixed domain experiencing gradual phase change within a temperature range. It is demonstrated how the enthalpy and Kirchhoff transforms permit to handle the non-linearities of the governing energy conservation equation by converting the equivalent specific heat capacity method to smart fixed-domain formulations involving relationships between enthalpy, temperature, Kirchhoff function and thermal diffusivity. Several enthalpy methods for solving highly non-linear heat transfer problems are thus featured as a methodological platform for sustainability-improving heat transfer analysis and relevant engineering solutions for various industrial scenarios.

- ❄ An **improved finite-difference enthalpy method** is introduced and validated for the first time in food refrigeration to solve unsteady and non-linear heat transfer problems involving chilling and freezing (heating and thawing) by fixed-grid numerical techniques. The method incorporates all non-linearities, caused by temperature-dependent thermophysical characteristics, in a single relationship between the volumetric specific enthalpy and the Kirchhoff function. This approach avoids the need for iteration cycles to evaluate the thermophysical characteristics and heat transfer coefficients at each time step, as well as averaging the thermal conductivity at every spatial increment. The suggested enthalpy-Kirchhoff transform quasi-linearisation permits larger time steps, less time-consuming numerical solutions and eliminates detrimental computational phenomena (such as latent heat peak '*jumping*' and stable oscillations), typical for the equivalent heat specific heat capacity formulation used conventionally for non-linear heat transfer problems in fixed-domains. The direct handling of the unsteady-state enthalpy fields facilitates substantially the energy analysis and resulting sustainability assessment of the investigated refrigeration processes and systems.
  
- ❄ An **innovative finite-element numerical model** is elaborated for the phase-change heat transfer during freezing or thawing of arbitrarily shaped foods by using the aforementioned combined enthalpy and Kirchhoff transform method. Smart change of variables in the highly non-linear unsteady-state 3D heat conduction problem is performed, so that a sole relationship between the volumetric specific enthalpy and the Kirchhoff function becomes incorporative of all non-linearities resulting from the temperature-dependent thermophysical properties. This reformulation provides an efficient finite-element numerical solution, free from the risk for missing the peak of apparent specific heat capacity and/or the abrupt change of thermal conductivity. Linearising the governing equation leads to constant finite element matrices to be calculated only once. The recommended solution strategy is far more economical, in terms of computational resources, than the conventional finite-element algorithms based on the untransformed non-linear Fourier equation or on an enthalpy-based reformulation only. The multi-optional finite-element code developed is validated by freezing experiments with Karlsruhe food simulator. (The outlined achievement is distinguished with the *Superior Paper Award 2001* of the *American Society of Agricultural and Biological Engineers – ASABE*).

- ❄ **Original unified predictive equations** are presented for the thermophysical properties (specific heat capacity, thermal conductivity and density), enthalpy and Kirchhoff variable of chilled and frozen foods. Multicomponent aqueous food materials are analysed as two-phase and two-component systems of water and dry matter (exhibited by three fractions of dry substance, water and ice below the initial freezing temperature). Each studied property is featured as a function of moisture content and temperature. Both intrinsic and equivalent specific heat capacities are afforded to account for the latent heat effect wherever necessary. A number of useful relationships between enthalpy and temperature, Kirchhoff variable and temperature, and enthalpy and Kirchhoff function are derived and reported for the first time in the scientific literature. The proposed formulae have a large scope of applications and cover virtually all industrially processed food materials, except those consisting mainly of fats. The equations' reliability and accuracy are proven by comparison with past authors' results, as well as through long-term computational experience of independent researchers (food scientists and technologists, refrigeration equipment designers, mathematical and computer modellers). The set of correlations reported are recognised, cited and often mentioned among the classical reference sources in both research articles and monographs or handbooks on food engineering, food preservation or on physical and engineering properties of foods.
- ❄ **A novel principle for chilling and freezing of foods by hydrofluidisation** is launched and pioneered in food refrigeration industry. The method uses unfreezable liquids or two-phase microcrystalline ice suspensions as fluidising agents to create a highly turbulent hydrofluidised bed of refrigerating medium and moving products. Strong tubulisation, along with thawing of minute ice particles on the product surface, ensure enhanced heat transfer, high chilling or freezing rates, great throughput, short processing times and fine-grain crystal structure inside frozen foods. The refrigerating medium temperature can be maintained by a single-stage refrigerating machine with higher COP and nearly twice lower CAPEX and OPEX than the conventional air fluidisation and air-blast freezing with two-stage machines, thereby halving the resulting carbon emissions. The notion, concept and term '*hydrofluidisation*' are introduced for the first time in the scientific literature as a starting point for an eponymous research trend in food engineering around the world. Suitable compositions of aqueous refrigerating media are formulated to serve as hydrofluidising agents and predictive equations are established for their thermophysical and rheological properties.

❁ A number of **sustainability-enhancing technologies, smart engineering solutions and control strategies for integration of renewable energy** (solar, wind, geothermal, biogas, etc.) in the cold chain and more specifically in refrigerated warehousing are featured, classified and evaluated. A **demand-response strategy (named ‘Night Wind’)** for managing the storage of renewable energy by smart load shifting in refrigerated warehouses is investigated. The existing mismatch between the power demand and supply is balanced by permitting the temperature of stored frozen products to vary within a small temperature range, thereby turning the warehouses to a powerful ‘*virtual battery*’ on the grid, capable of decarbonising both the electricity supply and food refrigeration facilities. The frozen produce itself serves as a phase-change medium for latent thermal energy storage, while the cold chain operator is converted from a simple energy user to an interactive actor on the energy marketplace. The effect of the ‘*Night Wind*’ control mode on the refrigerated food quality is examined experimentally, as affected by temperature fluctuations and freeze-thaw cycles, so that ‘*Night Wind*’ tolerable or friendly products are identified accordingly.

### III.2 Technology outlook and research trends

Although food refrigeration is deemed a traditional and relatively conservative sector, discoveries, inventions and R&D success stories in the low-temperature technologies are extensively taking place within all areas of the cold-chain innovation ecosystem (Figure 3.1).

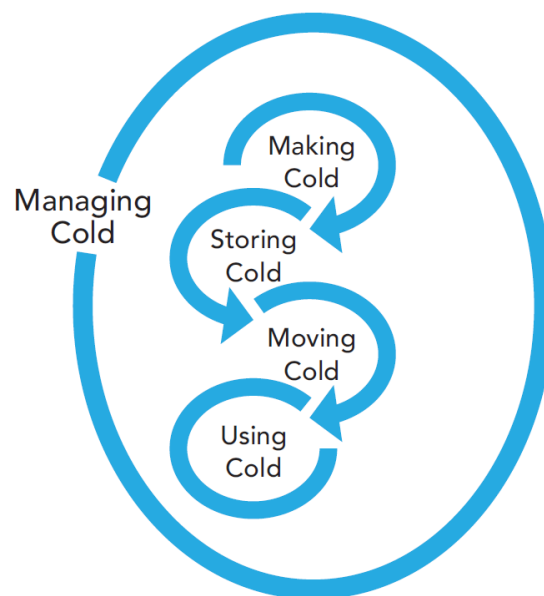


**Figure 3.1.** Systemic approach to the cold chain innovations.<sup>1</sup>

<sup>1</sup> Peters et al. (2018). Clean cooling landscape assessment. <https://rb.gy/bcv29>



In particular, a number of remarkable R&D trends can be outlined, as follows:

- ☑ In the **cold production by known technologies**, the so-called ‘*clean cooling*’ concept foresees the complete transition from fluorinated to natural refrigerants (e.g. CO<sub>2</sub>, ammonia, hydrocarbons, water or air). The use of fluorinated refrigerants can only be regarded as a short-term expedient measure to address urgent exigencies, with a clear plan for transitioning to naturals as quickly as possible.
- ☑ The **cold production by new physical principles** includes a broad range of innovative technologies under investigation, as illustrated in Figure 3.2. Alternative physical principles of generating cold can phase out harmful refrigerants (with a GWP several thousand times higher than that of CO<sub>2</sub>), thereby eliminating entirely the direct greenhouse gas emissions.

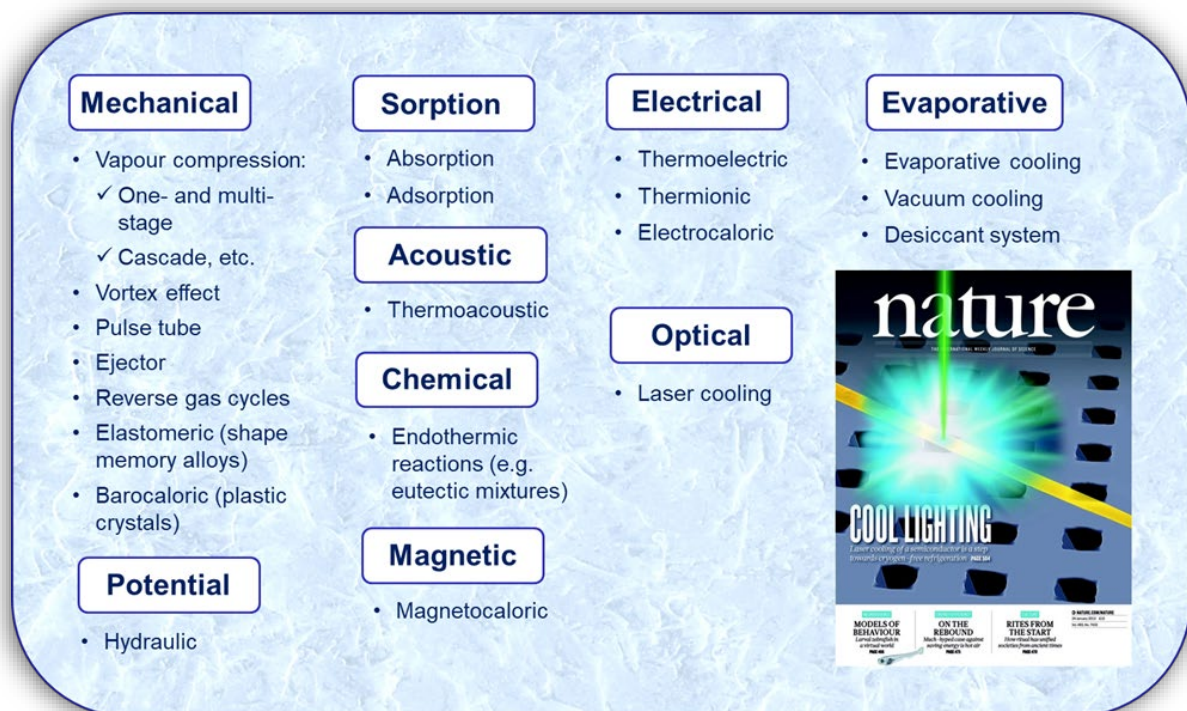


**Figure 3.2.** Principles and methods for production of artificial cold.

Unconventional zero-direct-emission solid-state refrigeration principles (thermoelectric, magnetocaloric, electrocaloric, elastomeric or barocaloric) are currently in the spotlight and being actively investigated (e.g., by the new IIR working group on Solid-State Cooling and Heating<sup>2</sup>). The recently launched method of ionocaloric refrigeration attracts attention as well.<sup>3</sup>

<sup>2</sup> IIR (2022). Working group: Solid-State Cooling and Heating. <https://iifiir.org/en/working-group-solid-state-heating-and-cooling>

<sup>3</sup> Mark Wilson R. (2023). Ionocaloric refrigeration makes its debut. *Physics Today*. <https://doi.org/10.1063/PT.6.1.20230201a>

- ☑ The **cold application to food processing and preservation** comprises a number of novel, emerging or still uncommon refrigeration techniques – partial freezing (superchilling), hydro-fluidisation, supercooling, dehydrofreezing, pressure-assisted and pressure-shift freezing, freezing under electromagnetic disturbances (static electric field, microwave- and radiofrequency-aided freezing, oscillating magnetic field for cells alive system, magnetic resonance freezing and pulsed electric field), ultrasound-assisted freezing, freezing with ice nucleation proteins, heat transfer enhancement by nanoparticles, etc. Isochoric low-temperature pressure-aided supercooling was recently widely publicised and advertised worldwide (under the name ‘*isochoric freezing*’) as a ground-breaking and game-changing technology. The method has been advocated as a revolution in food preservation, a panacea for most problems of food storage or a breakthrough solution to both energy- and quality-related problems of global frozen food industry.<sup>4</sup> However, we have revealed and informed the scientific community and cold-chain professionals that part of the associated claims (e.g., enormous energy savings) are unsupported and greatly exaggerated.<sup>5,6,7</sup>
  
- ☑ Enabling cold chain by **renewable, hybrid energy-conversion technologies and relevant R&D topics**, such as (i) up to 100% renewable carbon-neutral refrigeration for cold-chain applications; (ii) combined cooling, heat and power generation; (iii) energy mapping of industrial food refrigeration capacities and associated power expenditure; (iii) employing the cold supply chain for perishable commodities as an energy distributing network; (iv) cold-to-power solutions along the LNG or liquid H<sub>2</sub> supply networks (e.g., use of cold from LNG regasification); (v) industrial food refrigeration with low-temperature thermal energy storage and power grid balancing by phase-change materials and slurries; (vi) ‘*passive*’ or ‘*active*’ energy storage in large refrigerated facilities serving as virtual or Carnot batteries; (vii) energy-efficient operations and logistics along the cold supply chain; (viii) cold-chain digitalisation (e.g., via Internet of things or artificial intelligence); and (ix) smart interoperability between power grids and cold-chain networks for achieving a flexible and low-carbon energy system.

---

<sup>4</sup> Perelmutter, S. (2021). How isochoric freezing could drastically reduce carbon emissions. <https://rb.gy/7wrh1>

<sup>5</sup> Fikiin, K., Akterian, S. (2022). A lauded refrigeration technique and resource-efficiency of frozen food industry. *Trends Food Sci. Technol.*, 128: 185-187, <https://doi.org/10.1016/j.tifs.2022.05.008>

<sup>6</sup> Fikiin, K., Akterian, S., Le Bail, A., Carson, J., Eikevik, T.M. (2023). ‘*Isochoric freezing*’: Ambitions and reality, *J. Food Eng.*, <https://doi.org/10.1016/j.jfoodeng.2023.111460>

<sup>7</sup> IIR News (2023). Is an ‘*isochoric freezing*’ revolution really in the offing? <https://rb.gy/9nx5o>

To date, no competitive alternatives to refrigeration have been discovered when maintaining the nutritional resources of the planet, as it is the gentlest long-term preservation method for maximal retention of their bioactive compounds and valuable nutrients. All other post-harvest or post-mortem food preservation techniques (e.g., thermal and non-thermal processing – sterilisation, pasteurisation, drying, curing, smoking, ohmic heating, pulsed electrical field, irradiation, pressure processing, salting, sugaring, chemicals, etc.) may complement food refrigeration, but cannot entirely replace it to achieve the same product quality and shelf-life. To provide safe and wholesome perishables, the continuous and ubiquitous impact of low temperatures must be ensured throughout the entire supply chain from producers to consumers. Thus, the food chains around the world most often manifest themselves as cold chains.

Considered as an industrial sector, refrigerated processing, storage and distribution play the dual role of a reductant of food-lose-caused carbon emissions and one of the major contributors to ozone depletion, global warming and resulting climate changes. The latter raises a widespread public concern, so that research endeavours towards the cold chain resilience and sustainability are intensively ongoing at a global scale.

There is a pressing need for reliable means for knowledge-based analysis and design of efficient and affordable cold chains, as well as for enhancing the environmental friendliness and climate neutrality of food refrigeration industry. Accordingly, the present VAE thesis attempted to face part of these challenges by delivering several modest author's contributions to heat transfer modelling, cold-chain processes and relevant engineering systems.

## Annex I

### LIST OF PUBLICATIONS (Journal Articles and Book Chapters) underlying the present VAE thesis

1. **Fikiin K.A. (1998)**. Some general principles in modelling of unsteady heat transfer in two-phase multicomponent aqueous food systems for product quality improvement. In *Food Quality Modelling*, Eds.: B.M. Nicolai and J. De Baerdemaeker, Office for Official Publications of the European Communities, Luxembourg, pp. 179-186, <https://rb.gy/uonw4>
2. **Fikiin K.A. (1996)**. Generalised numerical modelling of unsteady heat transfer during cooling and freezing using an improved enthalpy method and quasi-one-dimensional formulation. *International Journal of Refrigeration*, Vol. 19, No. 2, pp. 132-140, [https://doi.org/10.1016/0140-7007\(95\)00055-0](https://doi.org/10.1016/0140-7007(95)00055-0)
3. **Scheerlinck N., Verboven P., Fikiin K.A., De Baerdemaeker J. and Nicolai B.M. (2001)**. Finite-element computation of unsteady phase change heat transfer during freezing or thawing of food using a combined enthalpy and Kirchhoff transform method. *Transactions of the American Society of Agricultural Engineers*, Vol. 44, No. 2, pp. 429-438, <https://doi.org/10.13031/2013.4671>
4. **Fikiin K.A. and Fikiin A.G. (1999)**. Predictive equations for thermophysical properties and enthalpy during cooling and freezing of food materials. *Journal of Food Engineering*, Vol. 40, No. 1-2, pp. 1-6, [https://doi.org/10.1016/S0260-8774\(99\)00026-6](https://doi.org/10.1016/S0260-8774(99)00026-6)
5. **Fikiin K.A., Wang Ming-Jian, Kauffeld M. and Hansen T.M. (2005)**. Direct contact chilling and freezing of foods in ice slurries – Chapter 9, In *Handbook on Ice Slurries – Fundamentals and Engineering*, Eds.: M. Kauffeld, M. Kawaji and P.W. Egolf, International Institute of Refrigeration, pp. 251-271, <https://iifir.org/en/fridoc/4122>
6. **Fikiin K.A. and Stankov B.N. (2018)**. Integration of renewable energy in refrigerated warehouses – Chapter 33, In *Sustainable Development: Concepts, Methodologies, Tools, and Applications*, IGI Global, Pennsylvania, USA, pp. 721-770, <https://doi.org/10.4018/978-1-5225-3817-2.ch033>

---

**Titre : Analyse thermophysique et solutions d'ingénierie vers la durabilité de la chaîne du froid**

**Mots clés :** industrie alimentaire, chaîne du froid, réfrigération, congélation, énergie, durabilité

**Résumé :** La thèse met l'accent sur le froid alimentaire et la chaîne du froid pour les bioproduits périssables. Le travail porte sur des modèles mathématiques innovants du transfert de chaleur non-stationnaire pendant la réfrigération et congélation des aliments et des systèmes aqueux de diverses configurations. L'attention est portée sur méthodes enthalpiques et transformées de variables pour résoudre des problèmes de transfert de chaleur non-linéaires par des techniques numériques. Une méthode améliorée d'enthalpie et de transformation de Kirchhoff est introduite pour le scénario le plus courant des changements de phase graduels et non-isothermes. Equations prédictives pour les caractéristiques thermophysiques sont établies pour des aliments congelés et non-congelés et reconnu internationalement. Une nouvelle méthode d'"hydrofluidisation" est lancée pour réunir

les avantages des techniques de fluidisation de l'air et de congélation par immersion (en utilisant des liquides non-congelables ou des coulis de glace biphasiques comme milieux refroidissants et agents de fluidisation). Solutions techniques de pointe pour la collecte et conversion de l'énergie, intégrant de multiples sources renouvelables dans l'entreposage frigorifique, sont conceptualisées. Une stratégie de réponse à la demande est testée pour le stockage "*passif*" de l'énergie renouvelable dans les entrepôts frigorifiques afin d'agir comme des "*batteries virtuelles*" pour l'écrêtement des pointes de consommation, et pour l'équilibrage et la décarbonisation du réseau électrique, en tenant également compte de l'effet des fluctuations de température et des cycles de congélation-décongélation sur la qualité du produit final.

---

**Title : Thermophysical analysis and engineering solutions towards cold chain sustainability**

**Keywords :** food industry, cold chain, chilling, freezing, energy, sustainability

**Abstract :** The thesis spotlights food refrigeration and cold chain for foods and perishable bioproducts. The work addresses innovative mathematical models, simulation and optimisation of unsteady-state heat transfer during chilling and freezing (warming and thawing) of foods and moisture-containing systems of various configurations. Attention is paid to enthalpy methods and variables' transforms for solving highly non-linear heat transfer problems by numerical techniques. An improved enthalpy and Kirchhoff transform method is firstly introduced for the most common food refrigeration scenario of gradual non-isothermal phase changes. Predictive equations for the thermophysical characteristics, enthalpy and Kirchhoff function are established for unfrozen and frozen foods, which received an international recognition.

A novel chilling and freezing method, named '*hydrofluidisation*', is launched to bring together the advantages of both air fluidisation and immersion food freezing techniques by using unfreezable liquids or two-phase ice slurries as refrigerating media and fluidising agents. State-of-the-art engineering solutions for energy harvesting and conversion, enabling proper integration of multiple renewable energy sources in the refrigerated warehousing of foods, are conceptualised and systematised. A demand response strategy is tested for '*passive*' storage of renewable energy in refrigerated warehouses to serve as '*virtual batteries*' for power peak '*shaving*', and electrical grid balancing and decarbonising, taking also into account the effect of temperature fluctuations and freeze-thaw cycles on the end product quality.